

SRP54 mutations induce Congenital
Neutropenia via dominant-negative effects
on *XBP1* splicing

Inauguraldissertation
zur
Erlangung der Würde eines Doktors der Philosophie
vorgelegt der
Philosophisch-Naturwissenschaftlichen Fakultät
der Universität Basel

von
Christoph Schürch
2023

Genehmigt von der Philosophisch-Naturwissenschaftlichen Fakultät auf
Antrag von

Prof. Dr. Claudia Lengerke

Prof. Dr. Markus Affolter

Prof. Dr. Christian Mosimann

Basel, den 30.03.2021

Prof. Dr. Marcel Mayor
Dekan der Philosophisch-
Naturwissenschaftlichen Fakultät

Table of Contents

ACKNOWLEDGMENTS.....	7
SUMMARY	9
1 INTRODUCTION.....	11
1.1 HEMATOPOIESIS.....	11
1.1.1 <i>Primitive Hematopoiesis</i>	12
1.1.2 <i>Definitive Hematopoiesis</i>	12
1.1.3 <i>Models of the Hematopoietic Landscape</i>	13
1.1.4 <i>Genetic Control of Hematopoiesis</i>	16
1.2 GRANULOPOIESIS	17
1.2.1 <i>Neutrophil Homeostasis and Trafficking</i>	18
1.2.2 <i>Heterogeneity of Neutrophils</i>	20
1.2.3 <i>Pathogen Killing by Neutrophils</i>	20
1.2.4 <i>NETosis</i>	22
1.2.5 <i>Neutrophils as Modulators of Inflammation</i>	23
1.3 DISORDERS OF THE BLOOD	26
1.3.1 <i>Cancerous Blood Disorders</i>	26
1.3.2 <i>Non-Cancerous Blood Disorders - Immunodeficiencies</i>	28
1.3.3 <i>Severe Congenital Neutropenia</i>	29
1.3.4 <i>Shwachman-Diamond Syndrome (SDS)</i>	32
1.4 THE ZEBRAFISH AS A MODEL ORGANISM.....	35
1.4.1 <i>Modeling Hematopoietic Disorders in Zebrafish</i>	35
1.5 PROTEIN EXPORT AND SIGNAL RECOGNITION PARTICLE.....	53
1.5.1 <i>SRP54 Deficiencies</i>	54
1.5.2 <i>Endoplasmic Reticulum Stress and Unfolded Protein Response</i>	55
1.6 AIM OF THIS THESIS	59
2 RESULTS.....	61
2.1 <i>SRP54</i> MUTATIONS INDUCE CONGENITAL NEUTROPENIA VIA DOMINANT-NEGATIVE EFFECTS ON <i>XBP1</i> SPLICING	61
2.2 ADDITIONAL DATA: SINGLE CELL RNA SEQUENCING OF <i>SRP54</i> MUTANT ZEBRAFISH	103
2.2.1 <i>Experimental Setup</i>	103
2.2.2 <i>Quality Control</i>	104
2.2.3 <i>Results – Additional Data</i>	106
2.2.3.1 Sorted Cells are not Exclusively Neutrophils.....	106
2.2.3.2 Several Genes are Found Differentially Expressed in <i>srp54</i> Mutant Cells	108
2.2.3.3 qRT-PCR Confirms Hits of the scRNA-seq.....	109
2.2.3.4 DE Analysis of the Neutrophil Cluster Reveals Lineage-Specific Candidate Genes	110
2.2.4 <i>Material and Methods – Additional Data</i>	111
2.2.4.1 Zebrafish Husbandry and Genetic Strains.....	111
2.2.4.2 Single Cell Sorting.....	112
2.2.4.3 Reverse Transcription and Library Preparation.....	112
2.2.4.4 qRT-PCR.....	112
3 DISCUSSION.....	115
4 CONTRIBUTION TO PUBLICATIONS	123
4.1 REGULATION OF GLIOMA CELL INVASION BY 3Q26 GENE PRODUCTS PIK3CA, SOX2 AND OPA1	123
4.1.1 <i>Summary</i>	123
4.1.2 <i>Contribution</i>	124
4.2 ONCOGENIC KRAS ^{G12D} CAUSES MYELOPROLIFERATION VIA NLRP3 INFLAMMASOME ACTIVATION	126
4.2.1 <i>Summary</i>	126
4.2.2 <i>Contribution</i>	127
4.4 TARGETING CHRONIC NFAT ACTIVATION WITH CALCINEURIN INHIBITORS IN DIFFUSE LARGE B-CELL LYMPHOMA	129
4.4.1 <i>Summary</i>	129

4.4.2 Contribution	131
REFERENCES	133
LIST OF GENES AND ABBREVIATIONS.....	153
APPENDIX	157
CURRICULUM VITAE	157

Acknowledgments

I would like to thank everyone who helped, guided or assisted me on my PhD journey. The following people were especially important for me during my PhD and without them, I would not be where I am now:

Claudia, thank you very much for giving me the opportunity to start my scientific career in your lab as a master student and guiding me through my PhD. Although you had to deal with a lot of stress in the last years, including a move to Tübingen, you were always there for me when I needed your advice, your supervision or your opinion. And what I especially admired, because it is not taken for granted, is that despite being so busy, you still took time to also talk about life outside of the lab and to have a chat.

Martina, you were there from the very first moment I joined the lab to the day I am going to hand in my thesis. During all this time, you were the first one to help me, to support me and to share your expertise with me. And next to all the help you gave me, we also shared tons of laughs and chats and I for sure gained a very good friend in you. So, you can look forward to feeding my cat from now on when I will be on holidays ;)

A thank you also goes to my colleagues and friends in the lab, especially:

Pauline and **Joëlle**, thank you for all the good times in the past 4 years. We shared many great moments inside and outside the lab, and you were always extremely helpful when I needed you.

Marlon, **Alain**, **Elsa** and **Henrik**, all of you brought new blood and life to our lab and I always enjoyed your company. If at a Mario Kart race, a brunch or at a party, it was always fun. And I especially thank Marlon for taking the time to proof-read this thesis.

And **Thorsten**, thank you for sharing your expertise with me and for your help.

Markus and **Christian**, thank you for being a part of my PhD committee and for providing me with very helpful input and advice during my committee meetings. I remember being quite a bit lost during my first PhD year, until my first committee meeting, where you helped me to get back on track and made me focus on the right topics.

Und schlussendlich no s gröschte Dankeschön an mini Familie: Mini Schweschtere **Fabienne** und **Madeleine**, Danke für all die super Ziite wo mir zämme erläbt hei und dass dirs immer mit mir uusghalte heit ;) Und natürlich mini **Eltère**, merci für alles wo dir für mi gmacht heit...ohni euch wär ich niemols dört woni jetz bi.

Finalment, també volia donar-te les gràcies a tu, **Maria Riera**. Gràcies per ser-hi des del primer a l'últim dia del meu PhD. Gràcies per sempre escoltar els meus problemes i preocupacions. Gràcies per fer-me companyia al laboratorì quan havia de treballar al cap de setmana. Gràcies per inclús acompanyar-me en viatges de feina. Gràcies per ajudar-me quan et necessitava... que era ben sovint. Gràcies per donar-me forces en moments i situacions difícils.

Gràcies per ser com ets. Sense tu no hagués pogut fer aquesta tesis.

Summary

Heterozygous *de novo* missense variants of *SRP54* were recently identified in patients presenting with Congenital Neutropenia (CN) or its syndromic form Shwachman-Diamond Syndrome (SDS).¹ Ever since its discovery as a driver of CN and SDS, *SRP54* has been increasingly studied in the context of disease and is nowadays considered the second most common cause of CN.^{2,3} Despite its hitherto unknown prevalence, the molecular mechanisms leading to the development of the disease are still largely unknown and patient treatments are far from specific.

In this thesis, I aimed to investigate the underlying mechanisms and processes contributing to the pathophysiology of *SRP54* deficiencies. To follow this aim, I characterized and established a transgenic *srp54* KO zebrafish as the first *in vivo* model of *srp54*-driven disease. Interestingly, *srp54*^{-/-} zebrafish show early embryonic mortality and suffer from severe neutropenia and developmental defects affecting multiple organs. *srp54*^{+/-} zebrafish on the other hand are viable and only display mild neutropenia and no overt other defects. However, when injecting *srp54*^{+/-} fish with human mRNA of three mutated *SRP54* variants (T115A, T117Δ and G226E) identified in patients, the neutropenia intensified, and pancreatic defects developed – a phenotype accurately mimicking the characteristics of SDS patients. Of note, the induced phenotypes showed mutation-specific differences, indicating that different *SRP54* lesions exert unique dominant-negative effects on the functionality of the residual wildtype *SRP54* protein. Consistent with these findings, overexpression of *SRP54* missense variants in human promyelocytic HL60 cells as well as in healthy CD34⁺ cord blood cells impaired granulocytic maturation.

Mechanistically, we found that *SRP54* defects significantly reduce the efficiency of the unconventional splicing of the transcription factor X-box binding protein 1 (*XBP1*), which is one of the major regulators of the unfolded protein response (UPR). Vice-versa, *xbp1* morphant zebrafish recapitulate phenotypes observed in *srp54* mutant fish, and the injection of spliced *xbp1* but not unspliced *xbp1* rescues the neutropenia in *srp54*^{+/-} embryos.

In order to identify additional mechanisms contributing to the pathophysiology of *SRP54* deficient patients, we performed single cell RNA sequencing of *srp54*-mutated zebrafish. Sequencing analysis revealed several differentially expressed genes with most of them converging on the major signaling branches of the UPR, indicating the cell's efforts to circumvent the impaired *XBP1* activity aiming to alleviate unresolved ER-stress.

1 Introduction

1.1 Hematopoiesis

1 trillion – this is the incredible amount of blood cells produced every day by our body.⁴⁻⁶ Impressively, the vast majority of this immense number of cells is derived from one single tissue: the bone marrow (BM). The BM is one of the largest organs of the human body and the home of the so-called hematopoietic stem cells (HSCs). HSCs are the most primitive cells of the whole blood system, harboring the potential to ultimately give rise to every single mature blood cell type. Thus, they are considered the most important players of hematopoiesis – the production of blood.⁷

First theories that the mammalian blood system is structured in a hierarchical way with HSCs at the top already emerged during the 19th century, when the German pathologist Franz Ernst Neumann described a “lymphoid marrow cell”, which was able to self-regenerate and form erythropoiesis.⁸ More than 50 years later, Neumann published an updated and extended version of his theory of hematopoiesis, which was further supported by the Russian-American Scientist Alexander A. Maximov, who postulated that a lymphocyte-like cell acts as a common progenitor seeding appropriate hematopoietic tissues.^{9,10}

These early theories about hierarchically structured hematopoiesis rapidly gained acceptance in the scientific field and eventually led the way for transplantation assays. The first documented BM transfusions date back to the early 20th century, with the procedure becoming widely used to treat patients suffering from marrow aplasia.⁷ This period of first in-human transfusion assays ultimately peaked in 1957, when E. Donnall Thomas performed the first allogeneic BM transplantation including irradiation and chemotherapy followed by intravenous infusion of BM cells from a healthy donor – a milestone in the history of BM transplantation.¹¹ Despite rapid advances in theoretical understanding of hematopoiesis and transplantation, it wasn't until the 1960's, when Ernest McCulloch and James Till managed to experimentally demonstrate the multilineage potential of HSCs by observing myeloid colonies in the spleen of irradiated mice after transplantation of BM cells.¹²⁻¹⁴

The hierarchical structure of hematopoiesis with BM-resident HSCs at the top is nowadays widely accepted and describes adult blood production. However, the process of hematopoiesis is subject of significant spatiotemporal changes during development and is thus divided into two different waves: The primitive wave of hematopoiesis and the definitive wave of hematopoiesis.¹⁵

1.1.1 Primitive Hematopoiesis

Primitive hematopoiesis, defined as the initial wave of blood cell production, is tightly restricted in time and space. Its primary output are primitive erythroid cells, which facilitate tissue oxygenation of the rapidly growing embryo.¹⁶ These primitive erythrocytes are produced in the blood islands of the yolk sac at embryonic day E7.25 in mice and, compared to definitive red blood cells, harbor unique characteristics, such as increased size, presence of a nucleus and elevated oxygen carrying potential.¹⁷⁻¹⁹ Despite being intensively studied for decades, the emergence of primitive erythrocytes is still highly controversial. This controversy is based on the observation that endothelial and blood cells both originate from a mass of cells derived from the primitive streak mesoderm.²⁰ Due to their common origin and the temporally parallel emergence of first primitive erythrocytes and blood vessels during embryogenesis, the theory of the existence of a bipotential clonal precursor – the hemangioblast – increasingly gained attention.^{15,17} Despite successful demonstration of the bipotential of single-cell-derived colonies *in vitro* and the discovery of hemangioblasts in zebrafish and drosophila,²¹⁻²⁴ its existence in higher vertebrates still could not be ultimately proven in *in vivo* models.

In addition to the initially described erythroid potential, several studies revealed that the hemangioblast also harbors the potential to give rise to primitive megakaryocytes and macrophages, hence adding a hitherto unknown myeloid component to the first wave of hematopoiesis.^{25,26}

1.1.2 Definitive Hematopoiesis

Definitive hematopoietic cells are hallmarked by being derived from HSCs. However, already before the emergence of the first HSCs, a wave of blood cell production giving rise to several cell types, which are phenotypically inseparable from definitive blood cells, is observable. Importantly, this first, HSC-independent wave of definitive hematopoiesis exclusively produces erythroid and myeloid cells and develops from a yolk sac resident pool of progenitor cells, named erythro-myeloid progenitors (EMPs).²⁷⁻³¹

The term EMP implies that these progenitors lack lymphoid potential. However, similar to erythroid and myeloid lineage cells, lymphoid lineage cells are present in the yolk sac before the onset of HSC-dependent hematopoiesis. The existence of these yolk sac derived lymphoid cells is still poorly understood, but evidence suggests that they originate from a rare pool of progenitor cells, distinct from EMPs.^{32,33}

Eventually, at mouse embryonic day E10.5, the first HSCs emerge in the aorta-gonad-mesonephros (AGM) region.^{28,34} Similar to primitive hematopoietic cells, HSCs are closely

related to the endothelium. However, rather than originating from a clonal progenitor, they directly emerge from the ventral wall of the dorsal aorta by a unique type of cell behavior – the endothelial-to-hematopoietic transition (EHT). Importantly, EHT does not involve asymmetric cell division. The process starts with budding of an endothelial cell from the aorta into the sub-aortic space, where the cell subsequently rounds up and acquires hematopoietic signatures.^{35,36} These newly born HSCs then enter circulation and seed the fetal liver, where they undergo massive expansion. By day E16.5, they finally start to colonize the BM, where they reside, self-renew and supply the mammalian body with new blood cells throughout adulthood.¹⁷

1.1.3 Models of the Hematopoietic Landscape

HSCs are the starting point of the generation of the highly complex and diverse adult blood system. Thus, they combine the essential tasks of supplying the body with adequate numbers of mature blood cells, whilst assuring to not exhaust in numbers – a trade-off HSCs manage to perform due to their ability to either self-renew or to undergo asymmetric cell division. By self-renewing, HSCs rapidly expand in numbers, which is of importance during development or after injury-caused stem cell exhaustion. By undergoing asymmetric cell division, they give rise to an HSC-like daughter cell and a more differentiated progenitor, thereby opening the gate for the establishment of the hematopoietic system.^{37,38} With each round of differentiation, HSCs progressively lose their self-renewal capacity, whilst becoming more and more committed. The loss of self-renewal ability already during the first rounds of differentiation subdivides the HSC pool into two distinct populations: Long-term HSCs (LT-HSCs) and short-term HSCs (ST-HSCs) (**Figure 1**). These populations mainly differ in their ability to support the reconstitution of the blood system of irradiated hosts after transplantation life-long (LT-HSCs) or only for temporally restricted time periods (ST-HSCs).^{39,40} Subsequently, ST-HSCs transition into so-called multipotent progenitors (MPPs), which are not able to self-renew anymore (**Figure 1**). At the MPP stage, the first steps of lineage-restriction occur, giving rise to either common lymphoid progenitors (CLPs) or common myeloid progenitors (CMPs).⁴¹⁻⁴³ CMPs further differentiate to either Megakaryocyte-Erythroid-Progenitors (MEPs) or Granulocyte-Monocyte-Progenitors (GMPs) (**Figure 1**). Whilst MEPs are the source of erythrocytes and megakaryocytes, GMPs give rise to the granulocytic lineages including neutrophils, basophils and eosinophils and also generate monocytes, which eventually differentiate into macrophages. CLPs on the other hand are responsible for the production of B-lymphocytes, T-lymphocytes and Natural Killer (NK) cells (**Figure 1**).⁴⁴

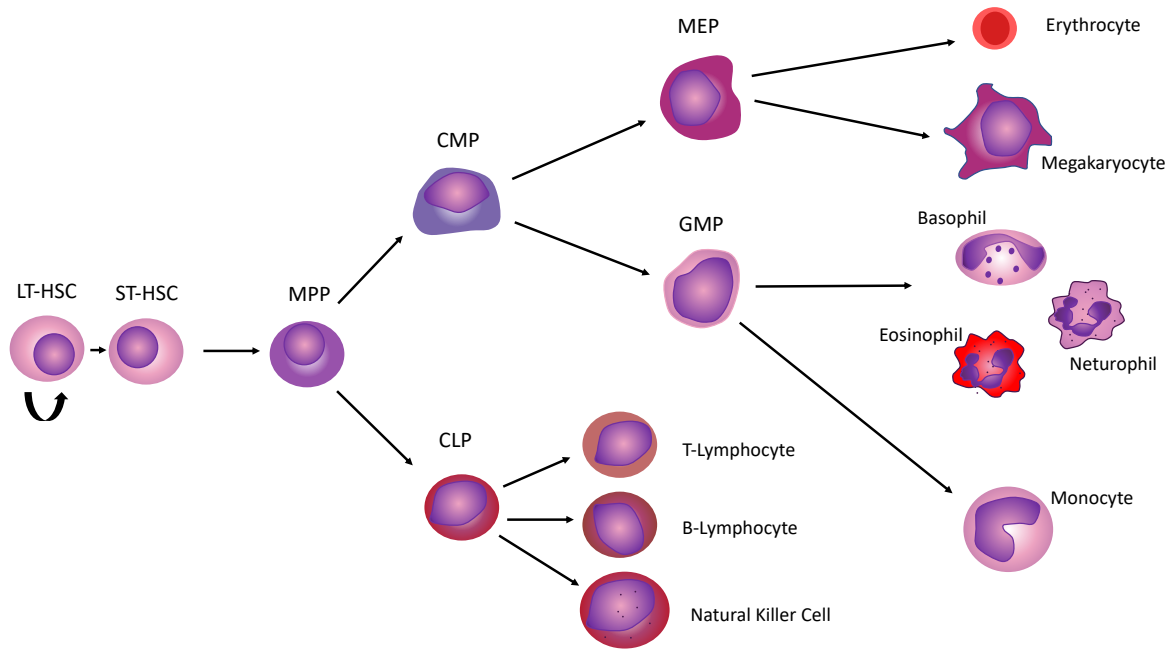


Figure 1: Classical model of hematopoiesis. LT-HSCs differentiate stepwise towards more committed progenitor cells. LT-HSC = Long-Term Hematopoietic Stem Cell, ST-HSC = Short-Term Hematopoietic Stem Cell, MPP = Multipotent Progenitor, CMP = Common Myeloid Progenitor, MEP = Megakaryocyte Erythrocyte Progenitor, GMP = Granulocyte Monocyte Progenitor, CLP = Common Lymphoid Progenitor. Adapted from Cheng et al.⁴⁵

This classical model of hematopoiesis has been widely accepted ever since Irving L. Weissman and his colleagues introduced it more than 20 years ago.^{44,46} However, recent technological advantages, especially on single-cell levels, allowed for more detailed analyses and led to the refinement of Weissman’s hierarchical model.⁴⁷⁻⁵⁰ In detail, the integration of flow cytometric, transcriptomic and functional data at single cell resolution revealed that the restriction of HSCs to a certain hematopoietic lineage does not occur in a step-wise fashion as hitherto assumed, but rather represents a continuous acquisition of different gene expression modules. These modules prime the cells towards a defined axis of differentiation without passing through distinct hierarchical progenitor populations. To adequately describe the pool of such pre-primed HSCs, Velten et al. introduced the term “Continuum of Low primed Undifferentiated Hematopoietic Stem – and Progenitor Cells” (CLOUD-HSPCs).⁴⁷ Already at early timepoints, CLOUD-HSPCs acquire lineage biases of multiple different branches, which work in a combinatorial way to prime the HSCPs towards a certain hematopoietic axis. This priming process however is not absolute, and changes in the acquired gene expression modules can overcome the barrier to eventually redirect a cell to differentiate along another hematopoietic axis. These new insights into hematopoiesis evoked the need for a revised hematopoietic landscape. In this landscape, differentiation is

no longer represented as a tree-like hierarchy from multipotency to unipotency, but rather as a probability map, comprising the most likely transition axes of HSPCs (**Figure 2**).^{47,51} In this revised model, first lineage specifications prime CLOUD-HSPCs independently towards megakaryocyte or erythrocyte potential (**Figure 2**).^{47,52-54} The second evident specification branch gives rise to myeloid and lymphoid cells. Unlike in the classical model however, early progenitors of this axis retain their pluripotential and cannot be separated according to their exclusive myeloid or lymphoid potential into CMPs and CLPs. Thus, the term Lymphoid Myeloid Primed Progenitors (LMPPs) was introduced to describe this population, which via the acquisition of distinct gene expression modules can give rise to all granulocytic and lymphoid cells.⁴⁸ Interestingly, data suggests the emergence of a parallel branch of myeloid primed progenitors directly from the pool of CLOUD-HSPCs, which exclusively gives rise to monocytes, but also harbors the potential to be re-directed towards granulocytic fate (**Figure 2**).⁴⁷

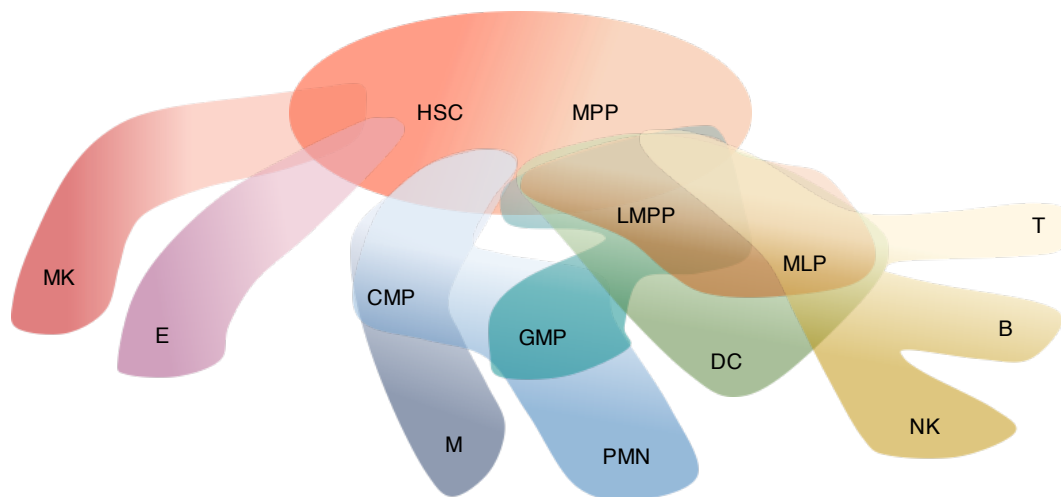


Figure 2: Revised model of hematopoiesis with continuous transitions rather than stepwise differentiation. Each colored path indicates a differentiation axis. The overlap of the different paths indicates the non-absolute fate decision, which arise from the acquisition of gene expression modules priming the cells towards a certain lineage. HSC = Hematopoietic Stem Cell, MPP = Multipotent Progenitor, MK = Megakaryocyte, E = Erythrocyte, CMP = Common Myeloid Progenitor, M = Monocyte, GMP = Granulocyte Monocyte Progenitor, PMN = Polymorphonuclear leukocytes, LMPP = Lymphoid Myeloid Primed Progenitor, MLP = Multilymphoid Progenitor, DC = Dendritic Cell, T = T-cell, B = B-cell, NK = Natural Killer Cell. Adapted from Scala et al.⁵¹

1.1.4 Genetic Control of Hematopoiesis

Hematopoiesis is a highly complex process, which needs to be tightly regulated in order to ensure adequate supply of the body with mature blood cells. As hematopoiesis occurs in distinct waves (see chapter 1.1.1 and 1.1.2), the underlying genetic program changes during development, what complicates its investigation. In the late 1990s and the early 2000s however, the idea to model hematopoiesis using the zebrafish increasingly gained attention, allowing direct visualization of processes and genetic programs involved in blood production, especially during early embryonic development. This new approach, facilitated by the possibility to perform large-scale genetic screens in zebrafish,⁵⁵⁻⁵⁸ eventually led to major advances in unraveling the mechanisms of hematopoiesis and enabled the discovery of a plethora of novel genes responsible for the control of our blood system.^{15,16,59,60}

The first major regulators of hematopoiesis arise in association with the induction of the hemangioblast. Studies revealed that the interplay of the transcription factors SCL/TAL1, GATA1, LMO2, FLI1 and ETSRP is crucial for this process.^{15,61-66} Later during primitive hematopoiesis, the first fate decisions of the hemangioblast are driven by the erythroid and myeloid master regulators GATA1 and PU1, respectively. These two transcription factors were shown to interact physically and compete for target genes, thereby exhibiting a cross-inhibitory relationship.^{67,68}

The differences of the primitive and the definitive wave of hematopoiesis are not only of temporal and spatial nature, but also include a functional component, with a completely new genetic program taking over. The most critical regulator of the emergence of the first HSCs is RUNX1. Although involved in primitive erythropoiesis, RUNX1 was shown to be dispensable and non-essential for primitive hematopoiesis.⁶⁹⁻⁷¹ However, lack of RUNX1 leads to the absence of HSCs during definitive hematopoiesis and evidence demonstrates its involvement in EHT.^{35,72,73} A second, extensively studied master regulator of definitive hematopoiesis is C-MYB, which was shown to be essential for HSC proliferation and differentiation. Accordingly, knock-down of *C-MYB* leads to the absence of definitive blood cells.^{15,74} Moreover, a complex network of signaling pathways, including WNT-, NOTCH-, BMP-4-, VEGF-, SCF- or Hedgehog-signaling, contributes to HSC homeostasis.⁷⁵⁻⁷⁷ Of high importance for the interplay of these pathways is the microenvironment of the BM, which provides the residing HSCs with the respective cues.¹⁵

1.2 Granulopoiesis

Granulopoiesis describes the process of the production of the three different types of granulocytes: neutrophils, eosinophils and basophils.⁷⁸ As a result of the recent revision of the hematopoietic landscape, away from a hierarchical structure with distinct stages of differentiation towards a continuous model, also the understanding of granulopoiesis changed substantially. Nonetheless, granulopoiesis in general is divided into two parts. The first part, termed neutrophil lineage determination, encompasses the process of an HSC to acquire granulocyte specific gene expression modules, until it reaches the point of unipotency, where its determination towards the granulocytic lineages cannot be changed anymore.⁷⁹ This first unipotent progenitor of granulopoiesis is the myeloblast (MB), which is commonly referred to as the first recognizable cell of the neutrophil lineage. The second part, called committed granulopoiesis, then describes the commitment of MBs to become mature polymorphonuclear leukocytes (PMNs) (Figure 3). The transition from MBs to PMNs is associated with continuous granulation of the differentiating cells and includes several, phenotypically distinct cell types. In a first step, MBs transform into promyelocytes (PMs), which are characterized by their high abundance of azurophilic granules. PMs then differentiate into myelocytes (MCs) (Figure 3). This differentiation step is associated with a switch from azurophilic granules to predominantly specific granules. In a next step of maturation, MCs transform into metamyelocytes (MMs) and later into band cells (BCs) (Figure 3), accompanied by a deformation of the nucleus to a kidney-like and then band-like shape, respectively. Ultimately, the nuclei of the BCs start to segment, and tertiary granules are formed, thereby giving rise to the terminally differentiated PMNs (Figure 3).⁷⁸⁻⁸¹

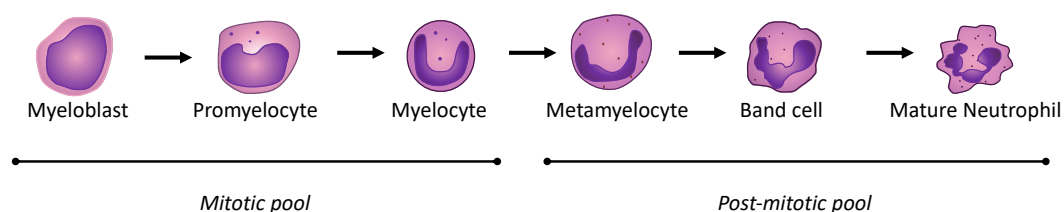


Figure 3: Committed granulopoiesis. Myeloblasts are the first unipotent cells of granulopoiesis and undergo several differentiation steps until they reach their mature form. The process of committed granulopoiesis is associated with continuous granulation and separates the differentiating cells into a mitotic and a post-mitotic pool. Adapted from Schürch et al.⁸²

Traditionally, the granulocytic cell populations in the BM are divided into three pools according to their proliferation and differentiation status.^{78,80} (1) The so-called stem cell pool, which includes all pluripotent progenitors, ranging from HSCs to primed granulocytic cell populations such as GMPs; (2) the mitotic pool, which comprises committed progenitors undergoing proliferation and differentiation (MBs, PMs and MCs); and (3) the post-mitotic pool, which consists of non-proliferating cells (MMs, BCs and PMNs) (**Figure 3**).^{78,80}

The master regulator of granulopoiesis is granulocyte-colony stimulating factor (G-CSF). It acts throughout the entire process of granulocyte formation, as shown by the expression of its receptor G-CSFR from myeloid progenitors to mature neutrophils, by controlling proliferation, survival and differentiation.⁸³ However, despite being universally expressed, mouse models demonstrated that G-CSF knock-out (KO) does not lead to a complete abolishment of granulopoiesis.⁸⁴⁻⁸⁶ This indicates that other factors, such as granulocyte-macrophage-colony stimulating factor (GM-CSF), Kit-ligand (KITL) or Interleukin-6 (IL-6) may play compensatory roles and partially take over the functions of G-CSF.^{84,87} Due to the numerous steps from HSCs to terminally matured PMNs, the transcriptome of granulocytic cells is continuously changing. The major transcription factors governing granulopoiesis are RUNX1, PU1, C/EBP- α , C/EBP- ϵ and GFI-1, whose individual KOs in animal models lead to severe granulocytic defects.^{68,88-92} Whilst low levels of PU1 were found to be beneficial for the differentiation of GMPs towards neutrophil fate, C/EBP- α was shown to be essential for the transition from CMPs to GMPs. RUNX1 as a master regulator of hematopoiesis is upstream of PU1 and C/EBP- α and affects their expression levels.⁸⁸ Later during granulopoiesis, at the PM stage, GFI-1 then supports the transition to the MC stage, where C/EBP- α is again involved and contributes to the termination of proliferation. Once granulopoiesis enters the post-mitotic stage, C/EBP- ϵ is necessary and coordinates terminal neutrophil differentiation.⁷⁹ In addition to the herein described master regulators of granulopoiesis, numerous other transcription factors and cytokines are involved in the production of neutrophils and cooperate to form a highly dynamic network, which ensures that the body is adequately supplied with PMNs.⁹³

1.2.1 Neutrophil Homeostasis and Trafficking

Once neutrophils reach maturity in the BM, they are able to enter circulation, eventually seed different tissues and at the end of their life-cycle get cleared by macrophages.⁹⁴ Interestingly, during homeostatic conditions, only approximately 1% of all neutrophils are actively circulating, while most of them are residing inside the BM.⁹⁵ In response to inflammatory stimuli such as infection however, neutrophil numbers in the periphery are rapidly increasing.

This indicates that neutrophil homeostasis and their release from the BM are tightly regulated, but highly flexible processes. The major players involved in neutrophil homeostasis are G-CSF and the two chemokine receptors CXCR2 and CXCR4.^{95,96} Whilst G-CSF, next to its role as a master-regulator of granulopoiesis, was shown to stimulate the release of neutrophils from the BM by upregulating CXCR2 ligands,⁹⁷ the interaction of CXCL12 and its receptor CXCR4 was demonstrated to support BM retention. Accordingly, G-CSF acts as a negative regulator of CXCL12 and CXCR4 expression.⁹⁸

Once in circulation, neutrophils, who are regarded as the first line of defense of the innate immunity, can be recruited to sites of infection or damage, where they exhibit their function. The process of neutrophil extravasation from the blood into inflamed tissues includes several steps and is called the leukocyte adhesion cascade (**Figure 4**).^{99,100} In a first step, E-, P- and L-selectins, expressed on inflammation-proximal endothelial cells, function as brakes, which slow down neutrophils in the blood stream. The weak selectin-mediated interactions result in a slow, rolling-like movement of neutrophils (**Figure 4**). During rolling, neutrophils get activated by chemokines and eventually adhere firmly to the endothelial cell surface through integrin-mediated binding (**Figure 4**).⁹⁹ After firm adhesion, neutrophils move slowly over the endothelial layer in a process termed crawling, until they reach a site appropriate for transendothelial migration (**Figure 4**).¹⁰¹ Transmigration is controlled by several adhesion and signaling molecules and either occurs in a paracellular or transcellular way.⁹⁹

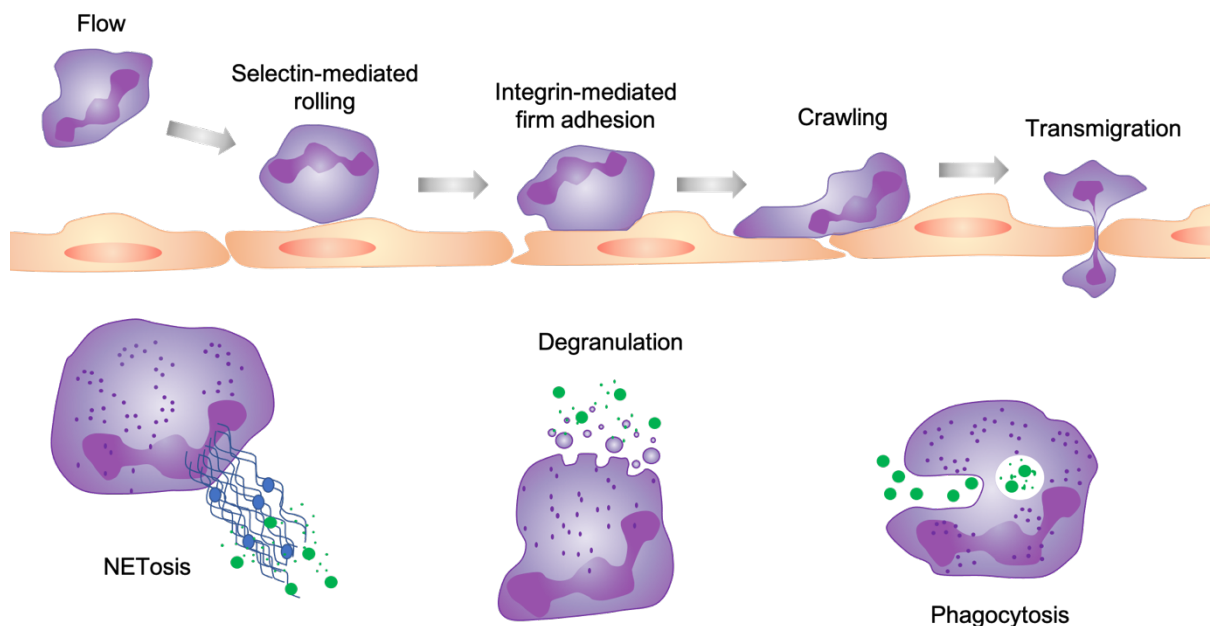


Figure 4: Overview of the leukocyte adhesion cascade and the different cytotoxic functions of neutrophils.

Top: Leukocyte adhesion cascade. Bottom left: NETosis. Bottom middle: Degranulation, Bottom right: Phagocytosis.

Adapted from Ley et al.¹⁰⁰ and from Rosales et al.⁹⁴

1.2.2 Heterogeneity of Neutrophils

Neutrophils are the most abundant leukocytes in the mammalian body. Since they are short-lived with a half-life of 6-8 h, a constant turnover is necessary and in humans up to 10^{11} new neutrophils have to be produced daily.¹⁰² Their short lifespan often used to be regarded as a roadblock for diversity and led to the assumption that neutrophils are a homogeneous cell population. However, recent technological advantages enabled the identification of variable sub-populations of neutrophils. A major contributor to this hitherto unknown heterogeneity is neutrophil aging in the blood.^{94,103} Neutrophil aging describes the functional and phenotypic changes of neutrophils over time, after they are released into circulation. Amongst others, these changes include the regulation of cell surface markers and ligands, such as L-selectin, CD11b or CXCR4, as well as the hypersegmentation of the nucleus.¹⁰³ Concerning the functional relevance of neutrophil aging, numerous aspects are still unknown. While several experiments demonstrate enhanced anti-inflammatory activity of aged neutrophils,¹⁰⁴ others are more likely to support the blunting of neutrophil function with age.^{105,106} Importantly, neutrophil aging is a diurnal process and follows the same pattern every day. The underlying reason for these diurnal changes is the tight coupling of neutrophil homeostasis to the circadian rhythm of the host. In mice for example, neutrophil release from the BM mainly occurs during their active phase in the early morning, and after aging in circulation, neutrophils eventually get cleared into different tissues, reaching a nadir around midnight.¹⁰⁷ Accordingly, the circadian fluctuations of neutrophil numbers and their diurnal functional changes suggest an adaptive relationship between the immune system and the variable daily demands of the body during active and resting phases.¹⁰³

1.2.3 Pathogen Killing by Neutrophils

Neutrophils are primarily known for their functions during inflammation and host defense. After they get activated by pro-inflammatory stimuli in a multistep process, which begins during the leukocyte adhesion cascade and later continues in the inflammatory tissue site, neutrophils gain the ability to exert their anti-inflammatory functions (**Figure 4**).¹⁰⁸ A prerequisite for neutrophils to act as primary immune cells of the body, is their capability to recognize pathogens – a process requiring numerous receptors, which can be divided into partially overlapping classes.

The first class of receptors are pattern-recognition receptors (PRRs), a class of receptors broadly found on immune cells.¹⁰⁸ Via their PRRs, neutrophils recognize pathogen-associated molecular patterns (PAMPs) and damage-associated molecular patterns (DAMPs), highlighting their roles in both, microbial infection as well as sterile inflammation. The most

common endocytic PRRs on neutrophils are c-type lectin receptors. However, PRRs that do not lead directly to phagocytosis, but rather prime and prepare them for activation by other stimuli are also found on neutrophils. The major type of these nonphagocytic PRRs are TLRs.¹⁰⁸

The second class of neutrophil receptors are G-protein coupled receptors (GPCRs), whose main function is to guide neutrophil migration. The primary GPCRs expressed on neutrophils are chemoattractant-receptors, chemokine-receptors or formyl-peptide receptors sensing bacteria or tissue injuries.^{109,110}

A third class of receptors comprises all cytokine receptors expressed on neutrophils, including type 1 and type 2 cytokine receptors as well as TNF-receptors. Generally, cytokine receptors are known to contribute significantly to intercellular communication thereby regulating neutrophil functions.¹¹¹

Finally, the last class of neutrophil receptors are opsonin receptors. Fc γ – and complement receptors are the main members of this class and their co-stimulation triggers the engulfment of IgG-opsonized particles and further activates the neutrophil's killing mechanisms.¹¹²

The interplay of all of these four classes of receptors eventually determines the magnitude of neutrophil activation and shapes the neutrophil's response to adequately exert its function.

Once neutrophils are activated as a result of pathogen recognition, they initiate phagocytosis (**Figure 4**). Thereby they engulf opsonized particles or microbes in a rapid process highly dependent on Fc γ – or complement receptors and internalize them in phagocytic vacuoles (**Figure 4**).^{113,114} These phagocytic vacuoles then undergo phagosomal maturation, a process involving multiple fusion and fission events, to acquire the components necessary for the killing of the internalized particles.¹¹⁵ A major source of antimicrobial peptides and proteins are the granules of neutrophils, which fuse with phagocytic vacuoles in a process called degranulation or exocytosis.^{116,117} Three different types of granules are sequentially formed during granulopoiesis (See chapter 1.2) and characterized by their specific composition. The primary granules, also known as azurophilic granules, are hallmarked by the presence of myeloperoxidase (MPO), but also contain other antimicrobial constituents, such as α -defensins.¹¹⁸ The secondary granules, termed specific granules, are peroxidase-negative and due to their large size harbor a rich arsenal of antimicrobial substances, including lactoferrin or lysozyme. In contrast, the tertiary granules, called gelatinase granules, are smaller and only contain few proteolytic or bactericidal peptides and proteins.¹¹⁹ They mainly serve as a reservoir for enzymes and receptors essential during the leukocyte adhesion cascade rather than actively contributing to the antimicrobial function of neutrophils.¹¹⁷ In addition to these three types of granules, also secretory vesicles are essential contributors to the neutrophilic

ability to recognize and kill pathogens.¹²⁰ Importantly, however, secretory vesicles do not contain intravesicular effectors, but refurbish the surface of neutrophils with receptors upon exocytosis.^{121,122} Of note, after activation, neutrophils can also initiate degranulation independent of phagocytosis. In this case, the granules fuse with the plasma membrane rather than with the phagosomal membrane and release their cytotoxic content directly into the environment (**Figure 4**).¹²³ Taken together, the heterogeneity of their granules enables neutrophils to differentially respond to variable pro-inflammatory stimuli and to adapt their functions to the microenvironmental needs.

Co-incident with the phagocytosis of opsonized particles, neutrophils undergo a process called respiratory or oxidative burst. This process is associated with a rapid increase in the neutrophils' oxygen consumption and eventually results in the release of reactive oxygen species (ROS) to support the killing of pathogens.¹⁰⁸ In detail, the incorporation of pro-inflammatory stimuli leads to the assembly of the NADPH-oxidase complex, which in turn catalyzes the electron transfer from cytosolic NADPH to oxygen, which has been accumulated during the respiratory burst.^{124,125} Thereby, superoxide (O_2^-) is produced, which in a dismutation reaction gives rise to hydrogen peroxide (H_2O_2). Superoxide as well as hydrogen peroxide themselves act microbicidal, but they also react in a chain-like manner to give rise to further ROS. Inside the phagosomes for example, hydrogen peroxide reacts with chloride in an MPO dependent process leading to the generation of hypochlorous acid (HOCl).¹²⁵ In addition to the antimicrobial peptides and proteins of granules, the ROS produced as a result of the respiratory burst further increase the magnitude and the manifoldness of the pathogen-killing function of neutrophils.

1.2.4 NETosis

In the early 2000s, Zychlinsky and colleagues discovered a novel way by which neutrophils are able to kill pathogens.¹²⁶ For the first time, they observed neutrophils releasing chromatin fibers and a mixture of granule proteins, which together serve as an extracellular trap to effectively catch and kill microbes (**Figure 4**).¹²⁶ The formation of such neutrophil extracellular traps (NETs) is the main characteristic of a cell death pathway called NETosis, which is morphologically different from apoptosis and necrosis and does not lead to phagocytosis but induces degradation of the NETting neutrophil by nucleases and proteases.^{108,127} Recently however, evidence suggested that NET formation may also occur as so-called vital NETosis, a process not necessarily resulting in neutrophil lysis.¹²⁸

A prerequisite for NETosis is the activation of the neutrophil. Once activated, several intracellular stimuli, such as differential calcium concentrations, ROS production or activation

of kinase signaling cascades, are necessary for the onset of NET formation.¹²⁹ The initiation of NETosis is associated with increased neutrophil cell spreading and extracellular matrix adhesion followed by the shedding of plasma membrane vesicles.¹³⁰ A variety of functions has been assigned to these vesicles and their content, including promoting thrombosis, inhibiting bacterial growth, exerting antimicrobial effects and dampening inflammation.¹²⁹ However, their exact roles still require further investigation and are not ultimately resolved yet. In a next step during NETosis, several histone posttranslational modifications trigger chromatin decompensation. The best-characterized histone modifications are acetylation, citrullination and histone cleavage by serine proteases. Especially citrullination via the enzyme PAD4 is believed to be a critical step during NET formation.^{130,131} However, numerous studies contradict this statement by demonstrating PAD4-independent NETosis.^{132,133} Potentially, PAD4-mediated citrullination thus might also just act as a modifier of NET function – a hypothesis supported by the enhanced ability of NETs to signal via TLR4 upon citrullination.¹³⁴ Similar to the shedding of microvesicles, also the decondensation of the chromatin still remains a matter of debate and needs further investigation.

After chromatin decompensation, the nuclear lamin meshwork undergoes dramatic changes and the nuclear envelope eventually permeabilizes and ruptures, allowing the chromatin to enter the cytosol.^{130,135} Subsequently, the cytoskeleton and membranous organelles such as mitochondria, granules and vesicles are subjects of major remodeling, which supports the release of antimicrobial agents and forces the plasma membrane to destabilize.¹³⁵ The destabilization of the plasma membrane leads to a continuous increase in permeability until the membrane eventually ruptures and enables the release of chromatin and its associated granule proteins.¹³⁰ A potential mechanism driving the rupture of the plasma membrane is the entropic swelling of the decompensated chromatin and the thereby evolving mechanical pressure on the membrane.¹³⁶ However, as many aspects of NETosis, this hypothesis requires further investigation.

1.2.5 Neutrophils as Modulators of Inflammation

Traditionally, neutrophils are known for their antimicrobial activities. However, during the last decades, also the immunomodulatory function of neutrophils was increasingly studied, which led to the discovery of a wide variety of hitherto unknown interactions with other immune cells. These interactions might either be direct cell-to-cell contacts mediated by the expression of various receptors on the neutrophil's cell surface, or secretory signals, such as neutrophilic cytokines or other effectors.¹⁰⁸

The most fundamental modulatory function of neutrophils affects the hematopoietic stem cell niche. Zebrafish experiments demonstrated that already during embryogenesis, primitive neutrophils are shaping the microenvironment of HSCs and contribute to the determination of HSC fate.¹³⁷ Later during development, neutrophils play a pivotal role in regulating the definitive HSC niche. Within mammalian BM for example, neutrophils were shown to stimulate HSC proliferation via ROS production upon acute infection of inflammation.¹³⁸ Moreover, another study provided evidence that neutrophilic prostaglandin E2 secretion in the BM serves as a stimulator of osteoblastic activity to eventually counteract HSC mobilization during stress situations.¹³⁹ Especially interesting from a medical point of view is the ability of neutrophils to mediate tissue repair. Specifically, within the BM, neutrophils are able to drive sinusoidal regeneration after chemo – or radiotherapy prior to hematopoietic stem cell transplantations (HSCT). Hence, further investigation of their function will provide detailed insights into the reconstitution of the BM niche after HSCT and might unveil novel therapeutic targets to minimize radiation-associated tissue damage.^{140,141}

Importantly, not only HSCs are targets of the immunomodulatory functions of neutrophils. As one of the first immune cell types to arrive at sites of infection, neutrophils shape the microenvironment and contribute to the initiation and the regulation of the immune response. By secreting a wide range of different cytokines, they interact with macrophages, dendritic cells (DCs), NK cells as well as B - and T-lymphocytes. The neutrophil-macrophage interaction is substantially supporting the inflammatory response, since neutrophil-derived secreted chemokines and granules stimulate monocyte and macrophage recruitment to inflammation sites and enhance their anti-microbial activity, respectively.¹⁴²⁻¹⁴⁴ Once inflammation resolves, macrophages take up apoptotic neutrophils, what leads to a reshuffling of the pool of macrophage-secreted cytokines in a way that promotes tissue repair and downregulates granulopoiesis by decreasing G-CSF production.^{108,145}

Compared to the well-studied neutrophil-macrophage relationship, the interaction of neutrophils with DCs and NK cells is still only rudimentarily understood. However, evidence suggests that these three cell types engage in a positive feedback loop in which neutrophil-DC interaction stimulates NK cells to produce IFN- γ , which in turn further activates and primes neutrophils. Contradictory to this observation, neutrophils were also shown to directly interact with NK cells, without the involvement of dendritic cells.^{146,147}

A rather unexpected crosstalk discovered during the last decades, is the crosstalk between neutrophils and lymphocytes. The neutrophil-lymphocyte interaction is bi-directional, meaning that neutrophil-derived factors modulate lymphocyte function and vice versa. A prerequisite for the interaction of different cell types is their co-localization at distinct target

sites. In case of the neutrophil-lymphocyte interaction, this co-localization is triggered by the reciprocal secretion of neutrophil- or lymphocyte-derived chemoattractants, respectively.¹⁴⁸ Once both cell types are located in close proximity, several mechanisms, by which neutrophils communicate with lymphocytes take place.¹⁴⁹ These mechanisms range from the release of cytokines to stimulate Th1 cell differentiation to the secretion of factors modulating B-cell maturation and development.¹⁵⁰⁻¹⁵³ On the other hand, the major lymphocyte-derived modulator of neutrophil function is IFN- γ , whose secretion not only prolongs neutrophil life span, but also enhances their phagocytic capacity.¹⁵⁴ In addition, IFN- γ signaling was shown to confer the ability to present antigens on neutrophils, as demonstrated by the observation of major histocompatibility complex (MHC) class II antigens expressed on T-cell proximal neutrophils.¹⁵⁵⁻¹⁵⁷

Taken together, the diverse immunomodulatory functions of neutrophils once more prove that these cells are more than just a short-lived, transcriptionally inactive, homogeneous microbe-killing machinery. Their tasks range from HSC specification and BM regeneration to the regulation of the innate immune response and even include an important modulatory function in adaptive immunity.

1.3 Disorders of the Blood

Hematopoiesis is a highly complex multistep process, which is controlled by an immense network of regulating factors. Already smallest perturbations of this network might cause major disbalances, eventually leading to hematologic disorders. Mostly, these perturbations come in the form of genetic mutations affecting critical regulators of blood cell formation. Due to the faulty function of such mutated regulators, myeloid or lymphoid precursors start to proliferate and differentiate in an uncontrolled manner, eventually resulting in conditions hallmarked by pathologically abnormal blood counts.¹⁵⁸ However, not only quantitative abnormalities of blood cells are drivers of hematologic disorders. Mutations may also affect the functionality of terminally differentiated blood cells, rendering them unable to fulfill their tasks properly, disbalancing the immune system and potentially causing disease.¹⁵⁹

1.3.1 Cancerous Blood Disorders

In general, blood disorders can be divided into two classes: Malignant (cancerous) blood disorders and benign (non-cancerous) blood disorders. Due to their often severe progression and the difficulties associated with their treatment, a substantial part of hematologic research is addressing malignant blood disorders. Malignant blood disorders are very heterogeneous and are broadly sub-divided into acute and chronic leukemias, myelodysplastic syndromes (MDS), myeloproliferative neoplasms (MPN), Hodgkin's lymphoma (HL) and non-Hodgkin's lymphoma (NHL).¹⁶⁰ The first two of these sub-groups, acute and chronic leukemias, can be further categorized according to their myeloid or lymphoid origin. Amongst these different types of leukemias, almost one third of all clinical cases are acute myeloid leukemias (AML).¹⁶¹ AML is characterized by the uncontrolled proliferation and differentiation of a clonal population of myeloid blasts in the BM or the periphery, eventually leading to the accumulation of these blasts at the expense of normal hematopoiesis.¹⁶²⁻¹⁶⁴ The underlying causes for the development of AML can be either cytogenetic alterations or genetic mutations. Cytogenetically, several chromosomal-translocations, which result in the formation of chimeric fusion proteins have been found in AML-patients and were identified as drivers of the disease.^{165,166} Before technologic advances made novel sequencing approaches possible, such chromosomal translocations were thought to be solely responsible for almost 40% of all AML cases.¹⁶⁷ However, recent investigations revealed that the vast majority of AML-patients is carrying recurrent genetic mutations. When evidence of such mutations as drivers of AML emerged at the beginning of the 21st century, it was hypothesized that one chromosomal translocation or mutation alone is not sufficient to cause malignant transformation.¹⁶⁸⁻¹⁷⁰ In detail, this hypothesis, nowadays widely accepted as the

so-called “2-hit” model of leukemogenesis, postulates that a first mutation, termed “class 1 mutation”, confers a proliferative or survival advantage to the hematopoietic progenitor cell, whilst a second mutation, termed “class 2 mutation”, impairs differentiation, thereby causing the progenitor to accumulate in an uncontrolled manner and to outcompete and suppress normal hematopoiesis.¹⁷⁰ Despite still representing the basis of our understanding of leukemogenesis, the “2-hit” model has continuously been modified and refined over the past few years.¹⁷¹ One of the major modifications was the introduction of mutations that are able to cause clonal hematopoiesis of indeterminate potential (CHIP) – a recently discovered novel disease entity, which describes patients carrying somatic clonal mutations without showing any evidence of a hematologic neoplasm.¹⁷² Mutations in genes associated with CHIP, such as *DNMT3A*, *TET2* or *ASXL1*, are commonly acquired during aging, and predispose the carrier to an increased risk of subsequent diagnosis of myeloid or lymphoid neoplasia.^{172,173} Since CHIP mutations neither match the criteria of “class 1 mutations” nor of “class 2 mutations”, they are believed to be acquired before cooperating mutations that contribute to disease features occur.¹⁷²

The technological advantages in sequencing, especially the availability of next-generation sequencing, also substantially contributed to the treatment options for AML-patients. Whilst AML-patients used to be treated in a highly generalized and inefficient way, with a combination of chemo – and radiotherapy, potentially followed by stem cell transplantation, the understanding of the genetic landscape of AML nowadays allows for prognostic risk stratification according to the genetic background and enables the application of risk-tailored or even molecularly targeted treatment strategies.¹⁷⁴⁻¹⁷⁷

The chronic counterpart of AML is chronic myeloid leukemia (CML). Compared to AML, CML is a rare and very homogenous disorder. The cytogenetic hallmark of CML patients is the so-called Philadelphia chromosome – a reciprocal translocation between chromosomes 9 and 22, found in more than 90% of all CML cases.^{165,178} The result of this translocation is the generation of the BCR-ABL fusion protein, which harbors tyrosine kinase activity and leads to uncontrolled cell growth of predominantly mature granulocytes. Due to its homogenous genetic background, CML is highly successfully treated with tyrosine kinase inhibitors and compatible with a normal lifespan.¹⁷⁹

In contrast to AML and CML, acute (ALL) and chronic lymphoblastic leukemia (CLL) are of lymphoid origin. ALL is rarely found in adults, with 60% of its cases being children or adolescents under 20 years of age.^{180,181} CLL on the other hand, is the most abundant form of leukemia in adults.¹⁶¹ Whilst ALL usually affects premature B – and T-cells, CLL is characterized by the accumulation of mature B-cells in hematopoietic tissues.¹⁸² Similar to

AML, also the genetic landscape of lymphoblastic leukemias is increasingly understood and the treatment regimens are transforming from generalized to more personalized and targeted approaches.¹⁸²

Other malignant blood disorders arising from the lymphoid lineage are lymphomas – cancers of the lymphatic system. Lymphomas are divided into two subgroups called HL and NHL. While HLs describe all lymphomas arising from Reed/Sternberg cells,^{183,184} which are somatically mutated B-cells carrying rearranged Ig heavy and light chain genes and functioning as clonal tumor cells,^{185,186} NHLs comprise the remaining 90% of lymphomas.^{161,187}

In contrast to acute leukemias and lymphomas, MDS and MPN are compatible with normal lifespan and often start as benign diseases, before turning malignant. MDS is a clonal BM disease characterized by dysplasia of hematopoietic tissues, peripheral cytopenia and an elevated risk of leukemic transformation.^{188,189} MPN on the other hand is characterized by an overproduction of differentiated hematopoietic cells with most phenotypic driver mutations converging on JAK-STAT signaling.¹⁹⁰⁻¹⁹²

1.3.2 Non-Cancerous Blood Disorders - Immunodeficiencies

Defects of the immune system, such as quantitative and qualitative blood cell abnormalities often arise in association with malignant hematopoietic disorders, non-hematological conditions or therapeutic interventions.¹⁵⁹ If these blood cell abnormalities exceed certain threshold values and cause immunocompromisation, they are termed secondary immunodeficiencies (SID).^{193,194} However, in rare cases, defects compromising immunity may also occur as an isolated clinical problem without any causal relation to environmental effects. Such isolated forms of immune defects are categorized as primary immunodeficiencies (PIDs) and predominantly result from genetic lesions.^{195,196} In recent years, the field of PIDs was progressing rapidly due to technological advances, leading to the discovery of numerous novel mutations driving different forms of PIDs with more than 400 genetic disease-drivers being officially recognized today.¹⁹⁷

Usually, non-cancerous blood disorders, including immunodeficiencies, are referred to as benign blood disorders, since they may be resolved by therapy, may be asymptomatic or may not affect life expectancy. However, the denomination benign is highly misleading, as several non-cancerous blood disorders render the patients highly susceptible to recurrent infections and also substantially increase the risk for malignant transformation.^{196,198}

In this doctoral thesis I am focusing on neutropenia – an immunodeficiency characterized by reduced absolute numbers of neutrophils in blood circulation.¹⁹⁹ Since the absolute neutrophil

count (ANC) is highly variable according to age and ethnicity, the classification of the disease has to be adapted accordingly. In white adults, mild neutropenia is diagnosed if the ANC is ranging from 1000 – 1500/ μ l; moderate neutropenia if the ANC is in between 500 – 1000/ μ l and severe neutropenia if the ANC is below 500/ μ l.²⁰⁰⁻²⁰² In most cases, neutropenia is iatrogenic, for example as an adverse event during cytotoxic chemotherapy,²⁰³ but also viral infections or autoantibodies are known to induce the disease.²⁰¹ Only very rarely, neutropenia results from a genetic disposition and develops as a PID. Despite being rare, the group of congenital neutropenias (CNs) is very heterogenous. It includes isolated forms of neutropenia but also comprises syndromic disorders characterized by skeletal abnormalities, intellectual disabilities, skin hypopigmentation, pancreatic defects and many more (Table 1).^{201,204}

1.3.3 Severe Congenital Neutropenia

Severe congenital neutropenia (SCN) is the most common form of CN.²⁰⁴ It was described for the first time in 1956 by Rolf Kostmann as an autosomal recessive disease characterized by recurrent bacterial infections as a consequence of severe chronic neutropenia.²⁰⁵ Generally, SCN is characterized by impaired differentiation of granulocytic cells, most frequently at the promyelocyte-stage, resulting in elevated numbers of atypical promyelocytes at the expense of normal granulopoiesis.^{206,207} Often, already during the first months of life, patients suffer from a wide range of infections, such as otitis, pneumonia, gingivitis and skin infections.²⁰⁸ For a long time, the mortality of SCN was very high, with more than 80% of the patients dying from severe bacterial infections. However, the discovery and the clinical use of G-CSF, rendered possible mainly by the contribution of Karl Welte,^{209,210} significantly reduced the frequency of life-threatening infections and substantially increased ANCs in patients.²¹¹ Nowadays, the mortality of SCN patients treated with G-CSF is lower than 20%, with approximately half of these deaths resulting from sepsis or bacterial infections.²¹² The other half is attributed to non-hematologic phenotypes occurring in some of the many syndromic forms of SCN.²⁰⁷ An additional life-threatening risk associated with SCN is the increased probability of undergoing malignant transformation. In detail, studies revealed that the cumulative incidence of neutropenia patients on long-term G-CSF treatment to develop either AML or MDS is 21%, indicating the importance of addressing this issue when treating SCN.^{212,213}

In recent years, the genetic background of SCN has been increasingly revealed. Approximately 60% of all patients are carrying autosomal dominant mutations in the *ELANE* gene, which encodes neutrophil elastase (NE).^{214,215} NE, a serine protease, is found inside azurophilic granules of mature PMNs and upon release cleaves extracellular matrix

proteins.²¹⁵⁻²¹⁷ Considering the mode of action of *ELANE* mutations, relatively little is known. A major factor hampering the investigation of the disease mechanism is the failure of animal models to reproduce the phenotypes observed in patients. Hence, several hypotheses, whose correctness is still a matter of debate, have been proposed. Most of these hypotheses converge on two major potential mechanisms.²¹⁷ The first one states that mislocalization of mutated NE eventually causes a maturation arrest of granulocytic cells,^{215,218} whereas the second one proposes ER stress resulting from misfolded mutated NE to be the reason for hampered neutrophilic differentiation.²¹⁹⁻²²¹ Since there are data supporting both of these hypotheses, further investigations are needed to ultimately unveil the mechanism leading to the development of *ELANE*-associated SCNs.

Nowadays, more than 200 different mutations in the *ELANE* gene are known.²²² Of note, these mutations do not lead to SCN exclusively, but can also induce another type of congenital neutropenia termed cyclic neutropenia (CyN).^{214,216,217,223} CyN is a recurring severe neutropenia with a common periodicity of 21 days and an ANC < 200/ μ l.^{222,223} During these neutropenic periods, patients often suffer from mouth ulcers, fever and bacterial infections potentially resulting in gangrene, bacteremia or septic shocks.²²⁴ Similar to SCN, CyN patients are commonly treated with G-CSF. Of note, G-CSF treatment does not prevent cycling, but shortens the cycle length and thereby reduces the duration of the neutropenic nadir.^{216,217,224}

A big enigma of SCN and CyN is the fact that there is no genotype-phenotype correlation for *ELANE* mutations, with similar mutations being able to cause both of these types of neutropenia. Recent research suggests the presence of specific UPR inhibitors in CyN patients to be responsible for the overall milder phenotype, however further investigations are necessary to ultimately enable the phenotypic determination of *ELANE* mutations.^{225,226}

As a result of the technological advances in sequencing techniques in the 21st century, novel driver mutations were also identified in CN (**Table 1**).²⁰¹ In most cases, these novel mutations are associated with syndromic forms of CN. A mutated gene, which was increasingly linked to isolated SCN is *HAX1*. However, *HAX1* exists in two different isoforms, and only mutations exclusively affecting isoform A lead to isolated SCN, whilst mutations affecting both, isoform A and B, result in the development of a syndromic form of CN, which is characterized by neurological defects.^{200,227,228} Mechanistically, it is known that *HAX1* mutations govern the balance between proapoptotic and antiapoptotic signals thereby causing a maturation arrest at the promyelocytic stage.^{200,229} Nowadays, approximately 15% of all SCN cases are thought to result from *HAX1* mutations.²⁰⁰

Another genetic defect found to drive the development of CN without disturbing other organs, was affecting *GFI1*.²³⁰ Of note, next to the impairment of myeloid differentiation, *GFI1* mutations also interfere with other hematopoietic lineages, such as T and B lymphocytes or dendritic cells.²⁰⁰

Amongst the first mutated genes identified to cause CN was *G6PC3*.²³¹ However, patients carrying such mutations often also present with thrombocytopenia and a wide variety of extra-hematopoietic phenotypes including urogenital, endocrine and congenital heart defects, hearing loss, facial dysmorphia, failure to thrive and many more.²³²⁻²³⁶

This thesis is focusing on *SRP54* - a gene, which was only associated with CN approximately three years ago, but ever since was increasingly found mutated in patients presenting with neutropenia.^{1,2,237-239} In fact, evidence suggests that mutations in *SRP54* are the second most common cause of inherited neutropenia.³ Interestingly, despite being found in isolated SCN cases, a substantial part of *SRP54* mutations was identified in patients suffering from a syndromic form of neutropenia called Shwachman-Diamond Syndrome (SDS).^{1,2}

Table 1: Overview of mutated genes associated with CN and its syndromic forms (exclusive of SDS). Adapted and updated from Skokowa et al.²⁰⁷

Gene	Protein	Symptoms
<i>ELANE</i>	Neutrophil elastase	SCN, monocytosis, eosinophilia, malignant transformation
<i>ELANE</i>	Neutrophil elastase	CyN, malignant transformation
<i>HAX1</i>	HCSL1-associated protein X-1	SCN, malignant transformation
<i>GFI1</i>	Growth factor independent protein 1	SCN, lymphopenia
<i>G6PC3</i>	Glucose-6-phosphatase catalytic subunit 3	SCN, thrombocytopenia, malignant transformation, cardiac defects, hearing loss, urogenital malformations
<i>SRP54</i>	Signal recognition particle 54	SCN, malignant transformation
<i>GATA2</i>	GATA binding protein 2	CN, monocytopenia, aplastic anemia, NK and DC defects, malignant transformation, pulmonary dysfunction, warts
<i>TCIRG</i>	T cell immune regulator	SCN, hemangiomas
<i>CXCR4</i>	C-X-C motif chemokine receptor 4	CN, WHIM syndrome, B cell defects
<i>JAGN1</i>	Jagunal homolog 1	SCN, short stature, bone defects
<i>SLC37A4</i>	Solute carrier family 37 member 4	CN, hypoglycemia, pancreatitis, osteoporosis
<i>STK4</i>	Serine/threonine kinase 4	CN, monocytopenia, lymphopenia, warts, atrial septal defects

<i>CLPB</i>	Caseinolytic mitochondrial matrix peptidase chaperone subunit B	3-Methylglutaconic aciduria type VII, malignant transformation
<i>AP3B1</i>	Adaptor related protein complex 3 subunit beta 1	Hermansky-Pudlak syndrome 2, functional defects of NK and T cells, stunted growth, albinism
<i>LAMTOR2</i>	Late endosomal/lysosomal adaptor, MAPK and mTOR activator 2	p14 deficiency
<i>USB1</i>	U6 SnRNA biogenesis phosphodiesterase	Clericuzion type poikiloderma
<i>VPS45</i>	Vacuolar protein sorting 45 homolog	CN, BM fibrosis, progressive anemia, thrombocytopenia, splenomegaly, osteosclerosis, hearing loss, delayed development, nephromegaly
<i>VPS13B</i>	Vacuolar protein sorting 13 homolog B	Cohen syndrome
<i>CXCR2</i>	C-X-C motif chemokine receptor 2	CN, myelokathexis
<i>EIF2AK3</i>	Eukaryotic translation initiation factor 2-alpha kinase 3	Wolcott-Rallison syndrome
<i>LYST</i>	Lysosomal trafficking regulator	Chédiak-Higashi syndrome
<i>RAB27A</i>	Ras-related protein Rab-27A	Griscelli syndrome type 2
<i>AK2</i>	Adenylate kinase 2	Adenylate kinase 2 deficiency
<i>RMRP</i>	RNA component of mitochondrial RNA processing endoribonuclease	Cartilage-hair hypoplasia
<i>TCN2</i>	Transcobalamin 2	Transcobalamin 2 deficiency
<i>CSF3R</i>	Colony stimulating factor 3 receptor	SCN
<i>WAS</i>	Wiskott-Aldrich Syndrome protein	Wiskott-Aldrich Syndrome
<i>TAZ</i>	Tafazzin	Barth Syndrome
<i>CD40LG</i>	CD40 ligand	Hyper-IgM Syndrome type 1

1.3.4 Shwachman-Diamond Syndrome (SDS)

SDS was first described in 1961, when Nezelof and Watchi treated two patients suffering from pancreatic insufficiency and hematologic manifestations including neutropenia.²⁴⁰ Three years later, Harry Shwachman and Louis Diamond proclaimed the need for a new disease entity, as they characterized five additional patients showing similar phenotypes to the ones treated by Nezelof and Watchi.²⁴¹ In the following years, the clinical features of SDS became

increasingly studied and understood, leading to the addition of novel, hitherto unknown features to the scope of SDS. Nowadays, a plethora of phenotypes such as skeletal abnormalities as well as an increased risk for patients to develop MDS or AML are regarded as supplementary hallmarks of the disease and play an important role in the classification of SDS.^{242,243}

Since the phenotypes of SDS patients are highly variable, the treatment strategies are adapted according to the manifestations a patient is presenting. Whilst most patients do not essentially need G-CSF to alleviate the often intermittent neutropenia, some patients suffer from recurrent infections due to severe neutropenia and thus are dependent on G-CSF therapy.²⁴⁴ Once SDS is progressed and severe aplastic anemia develops or malignant transformation takes place, hematopoietic stem cell transplants remain the only treatment option.²⁴⁴ While pancreas insufficiency is usually treated by oral administration of pancreatic enzyme supplements, skeletal abnormalities require adequate calcium and vitamin D intake to ensure proper bone density.²⁴⁵

At the beginning of the 21st century, mutations in the gene *SBDS* were identified as the sole genetic cause of SDS.²⁴⁶⁻²⁴⁹ Shortly after its discovery as the driver of SDS, first reports demonstrated that the *SBDS* protein localizes to the nucleolus, where it associates with ribosomal RNA and plays a crucial role in Ribosome biogenesis.²⁵⁰⁻²⁵³ Moreover, it was shown that numerous cellular processes and functions were affected by defective *SBDS*, eventually leading to impaired DNA repair mechanisms, *mTORC1*-hyperactivation, increased *p53* and *Fas* signaling, upregulation of osteoprotegerin and vascular endothelial growth factor-A, as well as many other aberrations.²⁵⁴ Most of these observations potentially arise as a side-effect of hampered ribosomal maturation, however, evidence suggests an additional role for *SBDS* during cell proliferation and division.^{255,256} In detail, *SBDS* stabilizes the mitotic spindle, where it co-localizes with centromeres and microtubules. Consequently, SDS patients present with elevated numbers of multipolar spindles and increased genomic instability.²⁵⁵ These findings, assigning a role in cell division to *SBDS*, are especially striking, since they may explain the neutropenic phenotype of SDS patients.²⁵⁶

Although *SBDS* was initially thought to be the only molecular cause of SDS, it quickly became evident that only approximately 80-90% of all patients are mutated in *SBDS*, with the residual 10-20% remaining without known genetic background.^{254,257} Only four years ago, in 2017, first researchers managed to identify novel drivers of SDS (Table 2). By performing exome-sequencing of *SBDS*-negative SDS patients, laboratories in Toronto and Jerusalem described *DNAJC21*²⁵⁸ and *EFL1*²⁵⁹ mutations, respectively, as alternative causes of the disease. The finding of these two genes is rather unsurprising, since *DNAJC21*, similar to

SBDS, is involved in the maturation of the 60s subunit of the ribosome,²⁶⁰ and EFL1 even directly associates with SBDS, thereby forming a functional unit, mutually dependent on both of the involved proteins.^{254,261} Nowadays, *EFL1* mutations are widely accepted as drivers of SDS.²⁶² *DNAJC21* defects on the other hand were proposed to constitute a distinct, unique disease entity characterized by features overlapping with SDS and Dyskeratosis congenita.²⁶³ Very recently, a young boy presenting with the typical manifestations of SDS was demonstrated to carry a heterozygous missense variant in the *EIF6* gene.²⁶⁴ Interestingly, EIF6 is known as an inhibitor of ribosomal maturation, whose removal is catalyzed by the functional unit formed by SBDS and ELF1.²⁶¹ The direct involvement in the *SBDS* axis renders *EIF6* a potential novel driver of SDS, however, the identification of additional patients is necessary to strengthen this association.

The only gene causing SDS, which is not directly involved in ribosome biogenesis, is *SRP54*.^{1,2} Identified as *de novo* missense variants in 3 patients in 2017 by the laboratory of Seiamak Bahram in collaboration with our research group,¹ *SRP54* mutations were rapidly recognized as a novel cause of SDS.²⁵⁴ As mentioned above, however, *SRP54* lesions do not exclusively result in SDS, but can also manifest in the form of isolated SCN. Since this thesis focusses on the investigation of *SRP54* deficiencies, a separate section (1.5.1) is addressing the association of *SRP54*, SDS and SCN in more detail.

Table 2: Overview of mutated genes associated with SDS.

Gene	Protein	Protein Function
<i>SBDS</i> ²⁴⁶	Shwachman-Bodian-Diamond Syndrome protein	Interaction with EFL1 to trigger release of EIF6 to support 80S assembly; stabilization of the mitotic spindle
<i>DNAJC21</i> ²⁵⁸	DnaJ heat shock protein family (Hsp40) member C21	Association with ribosomal RNA and maturation of 60S subunit
<i>EFL1</i> ²⁵⁹	Elongation factor-like GTPase 1	Interaction with SBDS to trigger release of EIF6 to support 80S assembly
<i>EIF6</i> ²⁶⁴	Eukaryotic translation initiation factor 6	Regulatory inhibition of ribosomal maturation
<i>SRP54</i> ¹	Signal recognition particle 54	Subunit of the SRP, essential for protein secretion

1.4 The Zebrafish as a Model Organism

The zebrafish (*danio rerio*) has been used for research purposes since the middle of the 20th century.²⁶⁵ However, it was George Streisinger in 1981, who shed light on the immense potential of the zebrafish as a model organism, when he successfully produced homozygous clones on a large scale, thereby significantly facilitating genetic manipulations and analyses.²⁶⁶ Compared to other research animals, zebrafish harbor several advantages, including high fecundity, rapid extrauterine embryonal development or optical clarity. Importantly, they represent a particularly powerful model to study hematopoiesis, since the genetic factors involved in blood formation as well as the structure and function of hematopoietic cells are highly conserved with higher vertebrates.²⁶⁷ Thus, especially during the last 25 years, zebrafish has risen to become one of the most frequently used and most reliable models of hematopoiesis.²⁶⁷

1.4.1 Modeling Hematopoietic Disorders in Zebrafish

The following review broadly describes the genetic manipulations enabling zebrafish transgenesis and provides an overview of the existing zebrafish models of hematopoietic disorders. Martina Konantz and I are sharing the first authorship of this review.

Modeling hematopoietic disorders in zebrafish. Konantz M, Schürch C, Hanns P, Müller JS, Sauter L, Lengerke C. *Dis Model Mech.* 2019 Sep 6;12(9):dmm040360. doi: 10.1242/dmm.040360. PMID: 31519693; PMCID: PMC6765189.

AT A GLANCE

Modeling hematopoietic disorders in zebrafish

Martina Konantz^{1,*}, Christoph Schürch^{1,*}, Pauline Hanns¹, Joëlle S. Müller¹, Loïc Sauteur¹ and Claudia Lengerke^{1,2}

ABSTRACT

Zebrafish offer a powerful vertebrate model for studies of development and disease. The major advantages of this model include the possibilities of conducting reverse and forward genetic screens and of observing cellular processes by *in vivo* imaging of single cells. Moreover, pathways regulating blood development are highly conserved between zebrafish and mammals, and several discoveries made in fish were later translated to murine and human models. This review and accompanying poster provide an overview of zebrafish hematopoiesis and discuss

the existing zebrafish models of blood disorders, such as myeloid and lymphoid malignancies, bone marrow failure syndromes and immunodeficiencies, with a focus on how these models were generated and how they can be applied for translational research.

KEY WORDS: Disease models, Hematopoiesis, Blood disorders, Leukemia, Immunodeficiency, Bone marrow failure syndrome

¹Department of Biomedicine, University of Basel and University Hospital Basel, Basel 4031, Switzerland. ²Division of Hematology, University of Basel and University Hospital Basel, Basel 4031, Switzerland.
*These authors contributed equally to this work

‡Author for correspondence (martina.konantz@unibas.ch)

id M.K., 0000-0002-4319-3119; C.L., 0000-0001-5442-2805

This is an Open Access article distributed under the terms of the Creative Commons Attribution License (<https://creativecommons.org/licenses/by/4.0>), which permits unrestricted use, distribution and reproduction in any medium provided that the original work is properly attributed.

Introduction

Zebrafish (*Danio rerio*) are increasingly used to study mechanisms regulating vertebrate tissue development and disease pathogenesis. Since especially blood cell types and their regulation are highly conserved (Box 1), many mutated zebrafish orthologs of human blood-disease-related genes have been successfully phenocoped, and the number of disease models is increasing with the current genomic advances. Additionally, specific advantages of the zebrafish model include its external fertilization and rapid development as well as (embryonic) transparency, facilitating *in vivo* imaging and the performance of genetic and small-molecule screens (Box 2) (Bertrand and Traver, 2009; Davidson and Zon, 2004; Li et al.,

Modeling hematopoietic disorders in zebrafish

Martina Konantz, Christoph Schürch, Pauline Hanns, Joëlle S. Müller, Loïc Sauteur and Claudia Lengerke

Degree of conservation

Humans and zebrafish share 71% of the same genes, and 82% of disease-associated human genes are conserved in zebrafish (Horn et al., 2017).

Hematopoiesis in zebrafish

24 hpf: Definitive wave

5 dpf: Primitive

Definitive wave:

- Anterior lateral mesoderm
- Intermediate cell mass
- Posterior blood island
- Ventral wall of the dorsal aorta
- Caudal hematopoietic tissue
- Thymus
- Developing kidney

Myeloproliferative neoplasia

Classical MPNs are characterized by chronic, uncontrolled proliferation of erythroid, megakaryocytic or granulocytic cells, and can eventually lead to leukemia. Driver mutations in either *JAK2*, *MPL*, *CSF3R* or *CSF3R* cause the vast majority of MPNs.

Polycythemia vera: *JAK2*^{H595R} inhibits *IL3* requirement (human *JAK2*^{H595R})

Essential thrombocythemia: *CSF3R*-S454S and *CAUS*-S45S inhibit

Phenotype in zebrafish:

- Increased erythropoiesis
- Reduced erythropoiesis
- Spleen hyperplasia
- Knockdown of *Socs1* or *JAK2* inhibitor amplifies the effects of *JAK2*^{H595R} overexpression

Phenotype in zebrafish:

- Increased thrombopoiesis
- Increased platelet aggregation
- Reduced thrombopoiesis
- Reduced platelet aggregation
- Indicates the zebrafish as a relevant *in vivo* model for testing and screening of therapeutic compounds targeting mutant *JAK2*

Described in He et al., 2009*

Myeloid neoplasms

MPNs are a heterogeneous group of myeloid malignancies with peripheral blood cytopenia and abnormal hematopoiesis that can progress to AML. AML is a heterogeneous clonal disorder of hematopoietic progenitors caused by somatic mutations, fusion of genes due to translocations, inversions, deletions or activating point mutations.

ASXL1 disruption: *ASXL1* is a histone deacetylase that cooperates with *MPL* and *JAK2* in hematopoiesis.

NPM1-RUNX1 fusion: *NPM1* and *RUNX1* are both hematopoietic stem cell genes.

AML1-ETO fusion: *AML1* and *ETO* are both hematopoietic stem cell genes.

Phenotype in zebrafish:

- ~50% of *asxl1*^{-/-} fish develop MPN with increased erythropoiesis and anemia.
- Combined loss of *asxl1* and *runx1* leads to MPN (MPL) and AML (ETO).
- Required for HSPC survival via *Runx1*-mediated mitochondrial apoptosis
- AML in double-transgenic fish suggests synergism between *asxl1* and *runx1* mutations in the same progenitors
- Can be used for small-molecule screens to identify drugs that specifically rescue AML1/ETO-mediated effects

Described in Ghil et al., 2016*

Acute lymphoblastic leukemia

In T-ALL, immature T-cell progenitors infiltrate the BA. It affects both children and adults, whereas B-ALL is the most prevalent pediatric leukemia and the leading cause of childhood cancer-related deaths.

Phenotype in zebrafish:

- ~81% adult zebrafish develop T-ALL
- Similar progression to human T-ALL
- Clonal expansion of lymphocyte precursors
- First zebrafish cancer model, described in 2003
- Helped to elucidate the genetic basis of T-ALL: dissemination to T-ALL
- Observed the effect of *sh3* translocation upon MHC overexpression
- Identified MHC-ITD as T-ALL regulator
- Used for small-molecule screens to identify prognostic
- Used to identify *Lambdalis* as a novel potential therapeutic compound

Described in Langsdorf et al., 2003*

Blood toxicity

Blood cell toxicity is one of the most common drug side effects; current strategies rely on *in vitro* assays and xenotransplant *in vivo* mammalian models. Zebrafish can be used as a whole-animal model organism for high-throughput screening.

Control: 3D imaging of the area of interest, e.g. the CHT

Hemolytic anemia after treatment: Selection of *sdh* - analysis

Described in Ghil et al., 2016*

Bone marrow failure syndromes

Bone marrow failure syndromes are a heterogeneous group of rare disorders characterized by cytopenias and increased risk of leukemia.

Diamond-Blackfan anemia (DBA) (*rps24*^{-/-}): 5S6-like syndrome (*rps24*^{5S6} knockdown)

Phenotype in zebrafish:

- Severe anemia and reduced spleen
- Increased apoptosis
- Hematopoietic, skeletal and neural pathways affected
- Provides information about disease pathogenesis
- May be used in genetic screens to identify mutations that suppress the erythroid effect
- Screening for compounds that can rescue the hematopoietic phenotype

Described in Taylor et al., 2012**

Primary immunodeficiencies

PIDs feature impaired immunity and increased susceptibility to infections. More than 230 genes have been identified as being involved in PIDs, but the disease of many disorders is still unknown or poorly understood.

Wiskott-Aldrich syndrome: A rare X-linked recessive disease characterized by eczema, bleeding and recurrent autoinfections.

ZAP70-related SCD: A rare autosomal recessive disease characterized by severe combined immunodeficiency with T-cell lymphomas.

Phenotype in zebrafish:

- Monocyte mutants viable until at least 3 dpf
- Selective leukocyte recruitment to neurons
- Neutrophil phagocytosis increased mortality from bacterial infection
- Defective clearance of *E. coli* swarms due to deficient pseudopods
- Mimics human Wisk
- Allows the testing of mutator immune cell behavior
- Might be used for small-molecule screens

Described in Jones et al., 2013*

Hematopoietic stem cell

Myeloid precursor → Red blood cell, Platelet, Monocyte, Macrophage, Granulocytes (neutrophils, basophils, eosinophils)

Lymphoid precursor → T cell, NK cell, B cell

*For full references, please see accompanying article.
**Reproduced with permission and not published under the terms of the CC BY license of this article.
Abbreviations: aa, amino acid; AKT, protein kinase B; ALL, acute lymphoblastic leukemia; AML, acute myeloid leukemia; emil, additional sex combs-like; h, basic amino acid domain; BAX, BCL2-associated protein; BCL2, B cell lymphoma 2; BCL2L1, BCL2-like 1; BCL2L2, BCL2-like 2; BCL2L3, BCL2-like 3; BCL2L4, BCL2-like 4; BCL2L5, BCL2-like 5; BCL2L6, BCL2-like 6; BCL2L7, BCL2-like 7; BCL2L8, BCL2-like 8; BCL2L9, BCL2-like 9; BCL2L10, BCL2-like 10; BCL2L11, BCL2-like 11; BCL2L12, BCL2-like 12; BCL2L13, BCL2-like 13; BCL2L14, BCL2-like 14; BCL2L15, BCL2-like 15; BCL2L16, BCL2-like 16; BCL2L17, BCL2-like 17; BCL2L18, BCL2-like 18; BCL2L19, BCL2-like 19; BCL2L20, BCL2-like 20; BCL2L21, BCL2-like 21; BCL2L22, BCL2-like 22; BCL2L23, BCL2-like 23; BCL2L24, BCL2-like 24; BCL2L25, BCL2-like 25; BCL2L26, BCL2-like 26; BCL2L27, BCL2-like 27; BCL2L28, BCL2-like 28; BCL2L29, BCL2-like 29; BCL2L30, BCL2-like 30; BCL2L31, BCL2-like 31; BCL2L32, BCL2-like 32; BCL2L33, BCL2-like 33; BCL2L34, BCL2-like 34; BCL2L35, BCL2-like 35; BCL2L36, BCL2-like 36; BCL2L37, BCL2-like 37; BCL2L38, BCL2-like 38; BCL2L39, BCL2-like 39; BCL2L40, BCL2-like 40; BCL2L41, BCL2-like 41; BCL2L42, BCL2-like 42; BCL2L43, BCL2-like 43; BCL2L44, BCL2-like 44; BCL2L45, BCL2-like 45; BCL2L46, BCL2-like 46; BCL2L47, BCL2-like 47; BCL2L48, BCL2-like 48; BCL2L49, BCL2-like 49; BCL2L50, BCL2-like 50; BCL2L51, BCL2-like 51; BCL2L52, BCL2-like 52; BCL2L53, BCL2-like 53; BCL2L54, BCL2-like 54; BCL2L55, BCL2-like 55; BCL2L56, BCL2-like 56; BCL2L57, BCL2-like 57; BCL2L58, BCL2-like 58; BCL2L59, BCL2-like 59; BCL2L60, BCL2-like 60; BCL2L61, BCL2-like 61; BCL2L62, BCL2-like 62; BCL2L63, BCL2-like 63; BCL2L64, BCL2-like 64; BCL2L65, BCL2-like 65; BCL2L66, BCL2-like 66; BCL2L67, BCL2-like 67; BCL2L68, BCL2-like 68; BCL2L69, BCL2-like 69; BCL2L70, BCL2-like 70; BCL2L71, BCL2-like 71; BCL2L72, BCL2-like 72; BCL2L73, BCL2-like 73; BCL2L74, BCL2-like 74; BCL2L75, BCL2-like 75; BCL2L76, BCL2-like 76; BCL2L77, BCL2-like 77; BCL2L78, BCL2-like 78; BCL2L79, BCL2-like 79; BCL2L80, BCL2-like 80; BCL2L81, BCL2-like 81; BCL2L82, BCL2-like 82; BCL2L83, BCL2-like 83; BCL2L84, BCL2-like 84; BCL2L85, BCL2-like 85; BCL2L86, BCL2-like 86; BCL2L87, BCL2-like 87; BCL2L88, BCL2-like 88; BCL2L89, BCL2-like 89; BCL2L90, BCL2-like 90; BCL2L91, BCL2-like 91; BCL2L92, BCL2-like 92; BCL2L93, BCL2-like 93; BCL2L94, BCL2-like 94; BCL2L95, BCL2-like 95; BCL2L96, BCL2-like 96; BCL2L97, BCL2-like 97; BCL2L98, BCL2-like 98; BCL2L99, BCL2-like 99; BCL2L100, BCL2-like 100; BCL2L101, BCL2-like 101; BCL2L102, BCL2-like 102; BCL2L103, BCL2-like 103; BCL2L104, BCL2-like 104; BCL2L105, BCL2-like 105; BCL2L106, BCL2-like 106; BCL2L107, BCL2-like 107; BCL2L108, BCL2-like 108; BCL2L109, BCL2-like 109; BCL2L110, BCL2-like 110; BCL2L111, BCL2-like 111; BCL2L112, BCL2-like 112; BCL2L113, BCL2-like 113; BCL2L114, BCL2-like 114; BCL2L115, BCL2-like 115; BCL2L116, BCL2-like 116; BCL2L117, BCL2-like 117; BCL2L118, BCL2-like 118; BCL2L119, BCL2-like 119; BCL2L120, BCL2-like 120; BCL2L121, BCL2-like 121; BCL2L122, BCL2-like 122; BCL2L123, BCL2-like 123; BCL2L124, BCL2-like 124; BCL2L125, BCL2-like 125; BCL2L126, BCL2-like 126; BCL2L127, BCL2-like 127; BCL2L128, BCL2-like 128; BCL2L129, BCL2-like 129; BCL2L130, BCL2-like 130; BCL2L131, BCL2-like 131; BCL2L132, BCL2-like 132; BCL2L133, BCL2-like 133; BCL2L134, BCL2-like 134; BCL2L135, BCL2-like 135; BCL2L136, BCL2-like 136; BCL2L137, BCL2-like 137; BCL2L138, BCL2-like 138; BCL2L139, BCL2-like 139; BCL2L140, BCL2-like 140; BCL2L141, BCL2-like 141; BCL2L142, BCL2-like 142; BCL2L143, BCL2-like 143; BCL2L144, BCL2-like 144; BCL2L145, BCL2-like 145; BCL2L146, BCL2-like 146; BCL2L147, BCL2-like 147; BCL2L148, BCL2-like 148; BCL2L149, BCL2-like 149; BCL2L150, BCL2-like 150; BCL2L151, BCL2-like 151; BCL2L152, BCL2-like 152; BCL2L153, BCL2-like 153; BCL2L154, BCL2-like 154; BCL2L155, BCL2-like 155; BCL2L156, BCL2-like 156; BCL2L157, BCL2-like 157; BCL2L158, BCL2-like 158; BCL2L159, BCL2-like 159; BCL2L160, BCL2-like 160; BCL2L161, BCL2-like 161; BCL2L162, BCL2-like 162; BCL2L163, BCL2-like 163; BCL2L164, BCL2-like 164; BCL2L165, BCL2-like 165; BCL2L166, BCL2-like 166; BCL2L167, BCL2-like 167; BCL2L168, BCL2-like 168; BCL2L169, BCL2-like 169; BCL2L170, BCL2-like 170; BCL2L171, BCL2-like 171; BCL2L172, BCL2-like 172; BCL2L173, BCL2-like 173; BCL2L174, BCL2-like 174; BCL2L175, BCL2-like 175; BCL2L176, BCL2-like 176; BCL2L177, BCL2-like 177; BCL2L178, BCL2-like 178; BCL2L179, BCL2-like 179; BCL2L180, BCL2-like 180; BCL2L181, BCL2-like 181; BCL2L182, BCL2-like 182; BCL2L183, BCL2-like 183; BCL2L184, BCL2-like 184; BCL2L185, BCL2-like 185; BCL2L186, BCL2-like 186; BCL2L187, BCL2-like 187; BCL2L188, BCL2-like 188; BCL2L189, BCL2-like 189; BCL2L190, BCL2-like 190; BCL2L191, BCL2-like 191; BCL2L192, BCL2-like 192; BCL2L193, BCL2-like 193; BCL2L194, BCL2-like 194; BCL2L195, BCL2-like 195; BCL2L196, BCL2-like 196; BCL2L197, BCL2-like 197; BCL2L198, BCL2-like 198; BCL2L199, BCL2-like 199; BCL2L200, BCL2-like 200; BCL2L201, BCL2-like 201; BCL2L202, BCL2-like 202; BCL2L203, BCL2-like 203; BCL2L204, BCL2-like 204; BCL2L205, BCL2-like 205; BCL2L206, BCL2-like 206; BCL2L207, BCL2-like 207; BCL2L208, BCL2-like 208; BCL2L209, BCL2-like 209; BCL2L210, BCL2-like 210; BCL2L211, BCL2-like 211; BCL2L212, BCL2-like 212; BCL2L213, BCL2-like 213; BCL2L214, BCL2-like 214; BCL2L215, BCL2-like 215; BCL2L216, BCL2-like 216; BCL2L217, BCL2-like 217; BCL2L218, BCL2-like 218; BCL2L219, BCL2-like 219; BCL2L220, BCL2-like 220; BCL2L221, BCL2-like 221; BCL2L222, BCL2-like 222; BCL2L223, BCL2-like 223; BCL2L224, BCL2-like 224; BCL2L225, BCL2-like 225; BCL2L226, BCL2-like 226; BCL2L227, BCL2-like 227; BCL2L228, BCL2-like 228; BCL2L229, BCL2-like 229; BCL2L230, BCL2-like 230; BCL2L231, BCL2-like 231; BCL2L232, BCL2-like 232; BCL2L233, BCL2-like 233; BCL2L234, BCL2-like 234; BCL2L235, BCL2-like 235; BCL2L236, BCL2-like 236; BCL2L237, BCL2-like 237; BCL2L238, BCL2-like 238; BCL2L239, BCL2-like 239; BCL2L240, BCL2-like 240; BCL2L241, BCL2-like 241; BCL2L242, BCL2-like 242; BCL2L243, BCL2-like 243; BCL2L244, BCL2-like 244; BCL2L245, BCL2-like 245; BCL2L246, BCL2-like 246; BCL2L247, BCL2-like 247; BCL2L248, BCL2-like 248; BCL2L249, BCL2-like 249; BCL2L250, BCL2-like 250; BCL2L251, BCL2-like 251; BCL2L252, BCL2-like 252; BCL2L253, BCL2-like 253; BCL2L254, BCL2-like 254; BCL2L255, BCL2-like 255; BCL2L256, BCL2-like 256; BCL2L257, BCL2-like 257; BCL2L258, BCL2-like 258; BCL2L259, BCL2-like 259; BCL2L260, BCL2-like 260; BCL2L261, BCL2-like 261; BCL2L262, BCL2-like 262; BCL2L263, BCL2-like 263; BCL2L264, BCL2-like 264; BCL2L265, BCL2-like 265; BCL2L266, BCL2-like 266; BCL2L267, BCL2-like 267; BCL2L268, BCL2-like 268; BCL2L269, BCL2-like 269; BCL2L270, BCL2-like 270; BCL2L271, BCL2-like 271; BCL2L272, BCL2-like 272; BCL2L273, BCL2-like 273; BCL2L274, BCL2-like 274; BCL2L275, BCL2-like 275; BCL2L276, BCL2-like 276; BCL2L277, BCL2-like 277; BCL2L278, BCL2-like 278; BCL2L279, BCL2-like 279; BCL2L280, BCL2-like 280; BCL2L281, BCL2-like 281; BCL2L282, BCL2-like 282; BCL2L283, BCL2-like 283; BCL2L284, BCL2-like 284; BCL2L285, BCL2-like 285; BCL2L286, BCL2-like 286; BCL2L287, BCL2-like 287; BCL2L288, BCL2-like 288; BCL2L289, BCL2-like 289; BCL2L290, BCL2-like 290; BCL2L291, BCL2-like 291; BCL2L292, BCL2-like 292; BCL2L293, BCL2-like 293; BCL2L294, BCL2-like 294; BCL2L295, BCL2-like 295; BCL2L296, BCL2-like 296; BCL2L297, BCL2-like 297; BCL2L298, BCL2-like 298; BCL2L299, BCL2-like 299; BCL2L300, BCL2-like 300; BCL2L301, BCL2-like 301; BCL2L302, BCL2-like 302; BCL2L303, BCL2-like 303; BCL2L304, BCL2-like 304; BCL2L305, BCL2-like 305; BCL2L306, BCL2-like 306; BCL2L307, BCL2-like 307; BCL2L308, BCL2-like 308; BCL2L309, BCL2-like 309; BCL2L310, BCL2-like 310; BCL2L311, BCL2-like 311; BCL2L312, BCL2-like 312; BCL2L313, BCL2-like 313; BCL2L314, BCL2-like 314; BCL2L315, BCL2-like 315; BCL2L316, BCL2-like 316; BCL2L317, BCL2-like 317; BCL2L318, BCL2-like 318; BCL2L319, BCL2-like 319; BCL2L320, BCL2-like 320; BCL2L321, BCL2-like 321; BCL2L322, BCL2-like 322; BCL2L323, BCL2-like 323; BCL2L324, BCL2-like 324; BCL2L325, BCL2-like 325; BCL2L326, BCL2-like 326; BCL2L327, BCL2-like 327; BCL2L328, BCL2-like 328; BCL2L329, BCL2-like 329; BCL2L330, BCL2-like 330; BCL2L331, BCL2-like 331; BCL2L332, BCL2-like 332; BCL2L333, BCL2-like 333; BCL2L334, BCL2-like 334; BCL2L335, BCL2-like 335; BCL2L336, BCL2-like 336; BCL2L337, BCL2-like 337; BCL2L338, BCL2-like 338; BCL2L339, BCL2-like 339; BCL2L340, BCL2-like 340; BCL2L341, BCL2-like 341; BCL2L342, BCL2-like 342; BCL2L343, BCL2-like 343; BCL2L344, BCL2-like 344; BCL2L345, BCL2-like 345; BCL2L346, BCL2-like 346; BCL2L347, BCL2-like 347; BCL2L348, BCL2-like 348; BCL2L349, BCL2-like 349; BCL2L350, BCL2-like 350; BCL2L351, BCL2-like 351; BCL2L352, BCL2-like 352; BCL2L353, BCL2-like 353; BCL2L354, BCL2-like 354; BCL2L355, BCL2-like 355; BCL2L356, BCL2-like 356; BCL2L357, BCL2-like 357; BCL2L358, BCL2-like 358; BCL2L359, BCL2-like 359; BCL2L360, BCL2-like 360; BCL2L361, BCL2-like 361; BCL2L362, BCL2-like 362; BCL2L363, BCL2-like 363; BCL2L364, BCL2-like 364; BCL2L365, BCL2-like 365; BCL2L366, BCL2-like 366; BCL2L367, BCL2-like 367; BCL2L368, BCL2-like 368; BCL2L369, BCL2-like 369; BCL2L370, BCL2-like 370; BCL2L371, BCL2-like 371; BCL2L372, BCL2-like 372; BCL2L373, BCL2-like 373; BCL2L374, BCL2-like 374; BCL2L375, BCL2-like 375; BCL2L376, BCL2-like 376; BCL2L377, BCL2-like 377; BCL2L378, BCL2-like 378; BCL2L379, BCL2-like 379; BCL2L380, BCL2-like 380; BCL2L381, BCL2-like 381; BCL2L382, BCL2-like 382; BCL2L383, BCL2-like 383; BCL2L384, BCL2-like 384; BCL2L385, BCL2-like 385; BCL2L386, BCL2-like 386; BCL2L387, BCL2-like 387; BCL2L388, BCL2-like 388; BCL2L389, BCL2-like 389; BCL2L390, BCL2-like 390; BCL2L391, BCL2-like 391; BCL2L392, BCL2-like 392; BCL2L393, BCL2-like 393; BCL2L394, BCL2-like 394; BCL2L395, BCL2-like 395; BCL2L396, BCL2-like 396; BCL2L397, BCL2-like 397; BCL2L398, BCL2-like 398; BCL2L399, BCL2-like 399; BCL2L400, BCL2-like 400; BCL2L401, BCL2-like 401; BCL2L402, BCL2-like 402; BCL2L403, BCL2-like 403; BCL2L404, BCL2-like 404; BCL2L405, BCL2-like 405; BCL2L406, BCL2-like 406; BCL2L407, BCL2-like 407; BCL2L408, BCL2-like 408; BCL2L409, BCL2-like 409; BCL2L410, BCL2-like 410; BCL2L411, BCL2-like 411; BCL2L412, BCL2-like 412; BCL2L413, BCL2-like 413; BCL2L414, BCL2-like 414; BCL2L415, BCL2-like 415; BCL2L416, BCL2-like 416; BCL2L417, BCL2-like 417; BCL2L418, BCL2-like 418; BCL2L419, BCL2-like 419; BCL2L420, BCL2-like 420; BCL2L421, BCL2-like 421; BCL2L422, BCL2-like 422; BCL2L423, BCL2-like 423; BCL2L424, BCL2-like 424; BCL2L425, BCL2-like 425; BCL2L426, BCL2-like 426; BCL2L427, BCL2-like 427; BCL2L428, BCL2-like 428; BCL2L429, BCL2-like 429; BCL2L430, BCL2-like 430; BCL2L431, BCL2-like 431; BCL2L432, BCL2-like 432; BCL2L433, BCL2-like 433; BCL2L434, BCL2-like 434; BCL2L435, BCL2-like 435; BCL2L436, BCL2-like 436; BCL2L437, BCL2-like 437; BCL2L438, BCL2-like 438; BCL2L439, BCL2-like 439; BCL2L440, BCL2-like 440; BCL2L441, BCL2-like 441; BCL2L442, BCL2-like 442; BCL2L443, BCL2-like 443; BCL2L444, BCL2-like 444; BCL2L445, BCL2-like 445; BCL2L446, BCL2-like 446; BCL2L447, BCL2-like 447; BCL2L448, BCL2-like 448; BCL2L449, BCL2-like 449; BCL2L450, BCL2-like 450; BCL2L451, BCL2-like 451; BCL2L452, BCL2-like 452; BCL2L453, BCL2-like 453; BCL2L454, BCL2-like 454; BCL2L455, BCL2-like 455; BCL2L456, BCL2-like 456; BCL2L457, BCL2-like 457; BCL2L458, BCL2-like 458; BCL2L459, BCL2-like 459; BCL2L460, BCL2-like 460; BCL2L461, BCL2-like 461; BCL2L462, BCL2-like 462; BCL2L463, BCL2-like 463; BCL2L464, BCL2-like 464; BCL2L465, BCL2-like 465; BCL2L466, BCL2-like 466; BCL2L467, BCL2-like 467; BCL2L468, BCL2-like 468; BCL2L469, BCL2-like 469; BCL2L470, BCL2-like 470; BCL2L471, BCL2-like 471; BCL2L472, BCL2-like 472; BCL2L473, BCL2-like 473; BCL2L474, BCL2-like 474; BCL2L475, BCL2-like 475; BCL2L476, BCL2-like 476; BCL2L477, BCL2-like 477; BCL2L478, BCL2-like 478; BCL2L479, BCL2-like 479; BCL2L480, BCL2-like 480; BCL2L481, BCL2-like 481; BCL2L482, BCL2-like 482; BCL2L483, BCL2-like 483; BCL2L484, BCL2-like 484; BCL2L485, BCL2-like 485; BCL2L486, BCL2-like 486; BCL2L487, BCL2-like 487; BCL2L488, BCL2-like 488; BCL2L489, BCL2-like 489; BCL2L490, BCL2-like 490; BCL2L491, BCL2-like 491; BCL2L492, BCL2-like 492; BCL2L493, BCL2-like 493; BCL2L494, BCL2-like 494; BCL2L495, BCL2-like 495; BCL2L496, BCL2-like 496; BCL2L497, BCL2-like 497; BCL2L498, BCL2-like 498; BCL2L499, BCL2-like 499; BCL2L500, BCL2-like 500; BCL2L501, BCL2-like 501; BCL2L502, BCL2-like 502; BCL2L503, BCL2-like 503; BCL2L504, BCL2-like 504; BCL2L505, BCL2-like 505; BCL2L506, BCL2-like 506; BCL2L507, BCL2-like 507; BCL2L508, BCL2-like 508; BCL2L509, BCL2-like 509; BCL2L510, BCL2-like 510; BCL2L511, BCL2-like 51

Box 1. Hematopoietic development in zebrafish

As in other vertebrates, zebrafish hematopoiesis develops in sequential waves (Davidson and Zon, 2004). Primitive hematopoiesis starts at two anatomically separate mesodermal sites in the embryo: the intermediate cell mass, which contributes to the first circulating erythrocytes, and the rostral blood island, which gives rise to primitive macrophages and neutrophils (Detrich et al., 1995; Palis and Yoder, 2001). A second transient hematopoietic wave occurs from the posterior blood islands, where multipotent erythromyeloid progenitors are generated between 24 and 30 hpf (Bertrand et al., 2007, 2010b). Between 28 and 32 hpf, definitive hematopoietic stem/progenitor cells (HSPCs) start emerging from the ventral dorsal aorta – the equivalent of the mammalian aorta-gonad-mesonephros region (Bertrand et al., 2010a, 2010b; Kissa and Herbomel, 2010). These definitive HSPCs then migrate to and amplify in the caudal hematopoietic tissue (Bertrand et al., 2010a; Boisset et al., 2010) – a site equivalent to the fetal liver in mammals – before they subsequently colonize the thymus and the kidney marrow. The latter is the adult hematopoietic organ and sustains hematopoiesis throughout the zebrafish life span (Chen and Zon, 2009; Jin et al., 2007), and the thymus enables T-cell maturation.

2015; Palis and Yoder, 2001). Since the first publication of the zebrafish genome in 2002 and its modifications and expansions in 2013, the zebrafish reference genome sequence has enabled many new discoveries, for example, the positional cloning of genes from mutations affecting embryogenesis, behavior and cell physiology in both healthy tissues and during disease pathogenesis (Howe et al., 2013). This review and accompanying poster summarize the current available hematopoietic disease models (see also Table 1), describes how they were generated and highlights their benefits.

Blood development is tightly regulated by complex interactions between hematopoietic stem cells (HSCs) and the microenvironment, making *in vivo* investigations mandatory. For human cells, these require analyses in xenograft models. These are naturally limited by

incomplete interspecies protein cross-reactivity and the requirement for an immunosuppressed host animal to prevent graft rejection. Therefore, researchers have developed animal models for further *in vivo* assessment of genotype-phenotype relations in hematologic disorders. Here, we describe the currently available zebrafish models for hematopoietic disorders in more detail.

Myeloid neoplasms

Myeloid malignancies are chronic or acute clonal diseases arising from hematopoietic stem and progenitor cells (HSPCs) characterized by uncontrolled proliferation and/or differentiation blocks in myeloid cells. Chronic myeloid neoplasms such as myeloproliferative neoplasms (MPNs), myelodysplastic syndromes (MDS) or chronic myelomonocytic leukemia (CMML) all have an increased risk of transformation into acute myeloid leukemia (AML) (Lindsley, 2017). The genetic causes for myeloid neoplasms are highly variable, but primarily occur in transcription factors, epigenetic regulators, tumor suppressors, signaling pathway proteins or components of the spliceosome. Many of these genes are essential for zebrafish blood development and have been successfully modeled to understand the underlying disease mechanisms.

Myeloproliferative neoplasms

MPNs are classified into three subgroups – polycythemia vera (PV), essential thrombocythemia (ET) and primary myelofibrosis – all of which are accompanied by disease-related complications, such as thrombosis and hemorrhages, and mainly affect people above 50 years of age (Vainchenker and Kralovics, 2017). Driver mutations in either *JAK2*, *MPL*, *CALR* or *CSF3R* (full names of genes/proteins used in this article are shown in Box 3) occur in the vast majority of MPN patients. Although treatment strategies exist, resistance to drugs such as *JAK2* inhibitors remains a big challenge (Meyer, 2017).

A major defining genetic event in human MPN is a gain-of-function mutation (V617F) in the *JAK2* gene (Baxter et al., 2005;

Box 2. Methods, advantages and disadvantages for modeling hematological disorders in zebrafish**Methods**

- **Transient strategies: mRNA or cDNA injections for overexpression of target genes, morpholino oligonucleotide (MO) injection for downregulation.** MOs are nonionic DNA analogs in which the ribose moiety has been substituted with an MO ring. They are generally designed to be complementary to the translational start site or a specific splice site in the pre-mRNA of the target gene, preventing translation or splicing of the pre-mRNA by a steric blocking mechanism. The technique is based on injecting these modified oligonucleotides, which then prevent expression of the targeted gene (see also <https://www.gene-tools.com>). Recently, serious concerns have been raised as to the specificity of MO effects (Kok et al., 2015). However, adequately controlled MOs used according to specific guidelines should still be accepted as a generic loss-of-function approach in the absence of genetic evidence (Blum et al., 2015; Stainier et al., 2017).
- **Permanent strategies: transgene expression, which allows expression of human sequences or fusion reporters, and genome editing tools.** Zinc-finger nucleases (ZFNs) can be used for targeting a unique genomic locus. Transcription activator-like effector nucleases (TALENs) are suitable for knock-in strategies or for removing large spans of DNA to cause genomic deletions. TILLING (targeted induced local lesions in genomes) allows directed introduction of point mutations in a specific gene. The CRISPR (clustered regularly interspaced short palindromic repeats)/Cas9 system can cut at a specific location but also allows knock-ins or removal of existing genes/sequences (Phillips and Westerfield, 2014).

- **Xenotransplantation of human cancer cells** (Konantz et al., 2012; Parada-Kusz et al., 2018; Veinotte et al., 2014) to generate patient-derived xenograft models, which may allow targeted therapy development and disease outcome prediction (Bentley et al., 2015; Gacha-Garay et al., 2019).

Advantages

- High fecundity, small size and fast embryonic development, which make the zebrafish amenable for large-scale screens.
- *Ex utero* fertilization and development, which allows (genetic) manipulation at all developmental stages and analyses of phenotypes that would die *in utero* in mice.
- Transparency during development and in adult *casper* (White et al., 2008) or *tralnac* (Krauss et al., 2013; Lister et al., 1999) fish, which allows live imaging of hematopoietic cells.
- Conserved regulatory pathways, especially in hematopoiesis.

Disadvantages

- Duplicated genome with many single-nucleotide polymorphisms and insertion/deletion variations.
- Cold-blooded animal – evolutionarily far away from humans.
- Lack of certain organs (e.g. lung, breast).
- Lack of specific antibodies for experimental work.
- Fish are greatly influenced by their environment (temperature, density etc.).
- Different morphology of certain blood cells.
- Lack of a fully functioning adaptive immune system.

Table 1. Summary of zebrafish models for hematopoietic disorders

Disease	Mutant	Method	Mutant phenotype	References
Myeloid neoplasm				
Myeloproliferative neoplasms	<i>jak2a</i> ^{V581F} ; gain of function	mRNA injection	Increased erythropoiesis	Ma et al., 2009
	<i>CALR</i> -del5, <i>CALR</i> 5-ins5; mutated human <i>CALR</i>	mRNA injection	Increased thrombopoiesis	Lim et al., 2016
Myelodysplastic syndromes	<i>tet2</i> ^{mi/m} ; disruption of the catalytic domain of zebrafish <i>tet2</i>	Genome editing with ZFN	Dysplasia of myeloid progenitors and anemia with abnormal circulating erythrocytes	Gjini et al., 2015
	<i>asx1</i> ; loss of function	TALEN	Clonal expansion of mutated HSPCs	Gjini et al., 2019
	<i>sf3b1</i> ; loss of function	MO knockdown	Blocked maturation at late progenitor stage, leading to macrolytic-anemia-like phenotype	De La Garza et al., 2016
	<i>prpf8</i> (<i>cph</i> mutant); driver mutation	Isolated from a forward genetic screen	Impaired myeloid differentiation within early hematopoiesis	Keightley et al., 2013
	<i>hspa9b</i> (<i>crs</i> mutant)	Isolated from a forward genetic screen	Anemia, dysplasia, increased blood cell apoptosis and multi-lineage apoptosis	Craven et al., 2005
5q- syndrome and CML-like disease	<i>spi1</i> (<i>pu.1</i>) ^{G242G} ; loss of function	TILLING	Expansion of myeloid blasts in the KM and their accumulation in the PB	Sun et al., 2013
	<i>c-myb</i> ^{hyper} ; hyperactivation	Transgenic line	Abnormal granulocyte expansion	Liu et al., 2017; North et al., 2007
	<i>rps14</i>	MO knockdown, CRISPR/Cas9	Anemia phenotype due to a late-stage erythropoiesis defect	Ear et al., 2016; Payne et al., 2012
	<i>irf8</i>	TALENs	Enhanced output of myeloid progenitors	Zhao et al., 2018
Acute myeloid leukemia	<i>AML1-ETO</i> ; transient expression in zebrafish embryos	Transgenic expression of human gene	Accumulation of immature hematopoietic blast cells in the ICM and circulating erythroid cells, with dysplastic features	Kalev-Zylinska et al., 2002
	<i>zspi1-MYST3/NCOA2</i>	Transgenic expression of human fusion gene	Extensive invasion of kidneys by myeloid blast cells	Zhuravleva et al., 2008
	<i>zspi1-FLT3-ITD</i>	Transgenic expression of human fusion gene	High numbers of myeloid progenitors in the KM and excess of blasts with focal aggregation	He et al., 2014; Lu et al., 2016
	<i>zspi1-tel-jak2a</i>	Transgenic expression of zebrafish fusion oncogene	Elevated numbers of white blood cells and anemia	Onnebo et al., 2005; Onnebo et al., 2012
	<i>NUP98-HOXA9</i>	Transgenic expression of human fusion oncogene	Disrupted myeloid-erythroid balance with an increase in myeloid progenitors as well as in HSCs and a decrease in erythroid cells	Deveau et al., 2015; Forrester et al., 2011
	Inducible <i>AML1-ETO</i>	Heat-shock-inducible transgenic expression of human fusion gene	Upon induction this model results in morphological and transcriptional characteristics of human AML without causing vascular defects and early death during embryogenesis	Cunningham et al., 2012; Yeh et al., 2008; Yeh et al., 2009
	<i>n-Myc</i>	Heat-shock-inducible transgenic expression of murine gene	Temporal control of <i>n-Myc</i> expression promoted cell cycle progression and increased ratios of myeloid cells and their precursors while avoiding early embryonic death	Shen et al., 2013
	<i>kRAS</i> ^{G12D}	Heat-shock-inducible transgenic expression of human oncogene	Expansion of myeloid cell population in the KM	Le et al., 2007
	<i>hRAS</i> ^{V12G}	Transgenic expression controlled by Gal4-UAS binary system	Spatial expression of this human oncogene in endothelial cells induces hyperproliferation of hematopoietic cells in the CHT	Alghisi et al., 2013
	<i>stat5.1</i>	Site-directed mutagenesis	Increased numbers of early and late myeloid cells, erythrocytes and B cells	Lewis et al., 2006

Continued

Table 1. Continued

Disease	Mutant	Method	Mutant phenotype	References
Lymphoid neoplasms				
T-cell acute lymphoblastic leukemia	<i>rag2-mMyc</i>	Transgenic expression of murine <i>mMyc</i> oncogene	Hyperproliferation of lymphoid cells with accumulation and infiltration of immature T-cell blasts	Feng et al., 2007; Feng et al., 2010; Gutierrez et al., 2014a; Gutierrez et al., 2011; Langenau et al., 2005a; Langenau et al., 2005b; Langenau et al., 2003; Le et al., 2007; Lobbardi et al., 2017; Reynolds et al., 2014; Ridges et al., 2012
	<i>rag2-Myc-Notch^{ICD}</i>	Double-transgenic line	Faster T-ALL onset partially due to faster thymic hyperplasia development	Blackburn et al., 2012; Blackburn et al., 2014; Chen et al., 2007
B-cell acute lymphoblastic leukemia	<i>TEL-AML1</i>	Transgenic expression of human fusion oncogene	High lymphoblastic counts in the peripheral blood and lymphoid-like blasts disseminated in the KM but also in distant organs	Sabaawy et al., 2006
Primary immunodeficiencies				
Wiskott-Aldrich syndrome	<i>was</i> ; loss of function	TILLING	Impaired immune function and defective thrombus formation	Cvejic et al., 2008
ZAP70-related combined immunodeficiency	<i>zap70^{Y442}</i> ; loss of function	TALEN	Reduced number of thymic T cells, as well as a lack of mature T cells in the KM	Moore et al., 2016
Reticular dysgenesis	<i>ak2</i>	MO knockdown, mutant generated by ZFN	Aberrant leukocyte development and impaired HSPC development	Pannicke et al., 2009; Rissone et al., 2015
WHIM syndrome	Truncated zebrafish <i>cxcr4</i> ; gain of function	Transgenic expression of truncated gene	Neutropenia, with impaired neutrophil recruitment to wounds and tissue inflammation	Walters et al., 2010
Chronic granulomatous disease	<i>ncf1</i> , <i>cybb</i>	MO knockdown	Defects in NADPH oxidase lead to disturbed ROS-mediated killing of phagocytosed pathogens	Brothers et al., 2011; Yang et al., 2012
Leukocyte adhesion deficiency	<i>rac2</i>	MO knockdown, transgenic expression, TALEN	Defect in host defense due to aberrant neutrophil or macrophage motility	Deng et al., 2011; Rosowski et al., 2016
Inherited bone marrow failure				
Diamond Blackfan anemia	<i>rps19</i>	MO knockdown	Defective erythropoiesis and developmental abnormalities	Danilova et al., 2008; Jia et al., 2013; Uechi et al., 2008
	<i>rps14</i>	MO knockdown, CRISPR/Cas9	Anemia due to a late-stage erythropoietic defect	Ear et al., 2016; Narla et al., 2014; Payne et al., 2012
	<i>rpl11</i>	MO knockdown	Defective hematopoiesis and hemoglobin biosynthesis due to iron-metabolism dysregulation; hematopoietic defects are also linked to impaired HSC formation, differentiation and proliferation	Chakraborty et al., 2018; Danilova et al., 2011; Zhang et al., 2014b; Zhang et al., 2013
	<i>rps29</i>	Transgenic line with insertion in the first exon	Significant defects in red blood cell development, shown by reduced hemoglobin levels	Mirabello et al., 2014; Taylor et al., 2012
	<i>rpl5</i>	MO knockdown	Hematopoietic and developmental abnormalities, including a ventrally bent tail, smaller head and reduction in circulating blood cells	Wan et al., 2016
	<i>rps24</i>	MO knockdown	Tail deformities and hematopoietic defects	Song et al., 2014
	<i>rpl35a</i>	MO knockdown	Anemic phenotype and developmental defects such as smaller head and eyes, a defective heart and reduced pigmentation	Yadav et al., 2014

Continued

Table 1. Continued

Disease	Mutant	Method	Mutant phenotype	References
Dyskeratosis congenita	<i>rps7</i>	Mutant line generated by viral insertions	Impaired hematopoiesis and development, including smaller head and eyes, and inflated hindbrain, but also display an increased number of apoptotic cells	Antunes et al., 2015
	<i>rps27/rpl27</i> ; double morphant	MO knockdown	Impairments of erythrocyte production and tail/brain development	Wang et al., 2015
	<i>nop10</i>	Mutant line generated in an insertional mutagenesis screen	Developmental defects such as smaller head and eyes and underdeveloped liver and gut; also fail to produce hematopoietic stem cells	Pereboom et al., 2011
	<i>dkc1</i>	MO knockdown	Defects in ribosomal biogenesis and hematopoiesis	Zhang et al., 2012
	<i>nola1</i>	Retroviral insertional mutation	Developmental defects, decreased hemoglobin levels and decreased numbers of definitive HSCs	Zhang et al., 2012
Fanconi anemia	<i>tert</i> ; knockdown	TILLING	Embryonic hematopoietic defects, impaired differentiation of blood cells and their eventual apoptosis	Anchelin et al., 2013; Henriques et al., 2017
	<i>fancd2</i>	MO knockdown	Shortened body length, microcephaly and microphthalmia	Liu et al., 2003
Schwachman-Diamond syndrome	<i>rad51</i> ; loss of function	CRISPR/Cas9	Hypocellular KM, shortened body length and chromosomal instability	Botthof et al., 2017
	<i>sbds</i>	MO knockdown	Morphogenic defects in the exocrine pancreas and abnormal myeloid development	Provost et al., 2012; Venkatasubramani and Mayer, 2008
Severe congenital neutropenia	<i>srp54</i>	MO knockdown	Neutropenia and exocrine pancreas defects	Carapito et al., 2017
	<i>cfs3</i> (<i>cfs3</i> ligands and <i>cfs3r</i>) <i>csfr3</i>	MO knockdown CRISPR/Cas9	Transient neutrophil depletion Stable mutants for <i>csfr3</i> have a persistent impairment in granulopoiesis during adulthood marked by decreased neutrophil numbers in the KM and peripheral tissues	Liongue et al., 2009; Stachura et al., 2013 Pazhakh et al., 2017
Thrombocytopenia	<i>mpl</i>	TALEN	Severe reduction in thrombocytes, a high bleeding tendency and defects in adult HSPCs	Lin et al., 2017
	<i>ptprj</i>	CRISPR/Cas9	Reduced numbers of CD41+ thrombocytes	Marconi et al., 2019
Anemia				
Hereditary elliptocytosis	<i>merlot</i> and <i>chablis</i>	Mutant line generated in a large-scale forward genetic screen	Defective protein 4.1 (P4.1) leads to elliptical erythroid cell morphology, reduced deformability and disrupted skeletal network	Shafizadeh et al., 2002
Hereditary spherocytosis	<i>riesling</i> ; mutated erythroid <i>beta-spectrin</i> (<i>sptb</i>)	Mutant line generated in a large-scale forward genetic screen	Spherical erythroid cell morphology due to disrupted membrane protein network	Liao et al., 2000
Dyserythropoietic anemia type II	<i>retsina</i> ; mutation in the gene <i>slc4a1</i> , encoding for the anion exchanger 1 (AE1)	Mutant line generated in a large-scale forward genetic screen	Erythroid binocularity and apoptosis due to incomplete chromosome segregation	Paw et al., 2003
Hypochromic microcytic anemia	<i>zinfandel</i>	Mutant line generated in a large-scale forward genetic screen	Defects in embryonic globin production; rescue during adulthood	Brownlie et al., 2003

Table 1. Continued

Disease	Mutant	Method	Mutant phenotype	References
Hypochromic anemia (congenital sideroblastic anemia)	<i>sauternes</i>	Mutant line generated in a large-scale forward genetic screen	Disrupted heme biosynthesis	Brownlie et al., 1998
Hypochromic anemia (hemochromatosis)	<i>weissherbst</i> ; mutations in <i>ferroportin 1</i> , an iron transporter conserved in humans	Mutant line generated in a large-scale forward genetic screen	Low iron levels in circulation leading to insufficient hemoglobinization	Donovan et al., 2000; Fraenkel et al., 2005
	<i>chianti</i> ; mutations in <i>transferrin receptor 1</i>	Mutant line generated in a large-scale forward genetic screen	Defective iron acquisition in erythrocytes	Wingert et al., 2004
	<i>chardonnay</i> ; mutated iron transporter <i>dmt1</i>	Mutant line generated in a large-scale forward genetic screen	Disrupted iron homeostasis	Donovan et al., 2002
Erythropoietic protoporphyria	<i>dracula</i>	Mutant line generated in a large-scale forward genetic screen	Highly light sensitive erythrocytes; <i>dracula</i> gene shown to encode for ferrochelatase, the terminal enzyme in the pathway of heme biosynthesis	Childs et al., 2000

James et al., 2005; Kralovics et al., 2005; Vainchenker and Kralovics, 2017). To model this disease in zebrafish, an ortholog of human *JAK2^{V617F}* was created by site-directed mutagenesis (see poster: Myeloproliferative neoplasia). The mutant had a high degree of similarity to human PV, mainly characterized by erythroid expansion (Ma et al., 2009). Another gene commonly mutated in MPN patients without *JAK2^{V617F}* is *CALR*, which encodes the endoplasmic reticulum chaperone calreticulin. Expression of mutated human *CALR* in zebrafish embryos by mRNA injection caused an increase in thrombopoiesis via Jak/Stat signaling upregulation, resembling the phenotype observed in ET patients (see poster: Myeloproliferative neoplasia) (Lim et al., 2016). Both lines provide robust models for screening for therapeutic agents targeting Jak/Stat signaling. An accurate zebrafish model for primary myelofibrosis has not yet been developed.

Myelodysplastic syndromes

Owing to their heterogeneity, MDS are particularly challenging to accurately model in animals. Mutations in genes associated with myeloid malignancies or pre-malignancy [clonal hematopoiesis of indeterminate potential (CHIP)] (Heuser et al., 2016) and especially mutations of epigenetic or splicing factors are commonly detected in MDS, either alone or in various combinations. One of the genes most commonly associated with CHIP and myeloid malignancies is *TET2*, an epigenetic factor regulating DNA methylation. Somatic loss-of-function *tet2^{m/m}* zebrafish mutants engineered by zinc-finger nuclease (ZFN) genome editing develop normally during embryogenesis, but show progression to clonal myelodysplasia as they age and eventually develop MDS-like features at 24 months post-fertilization (Gjini et al., 2015). Subsequently, the same group generated an *asx11* mutant (see poster: Myeloid neoplasms). Somatic loss-of-function mutations of this gene are common genetic abnormalities in human myeloid malignancies and induce clonal expansion of mutated HSPCs. The authors showed that half of the heterozygous fish developed MPN by 5 months of age. Interestingly, the combination of heterozygous loss of *asx11* with heterozygous loss of their previously generated *tet2* mutant led to a more penetrant phenotype, while *asx11^{+/-}* together with complete loss of *tet2* even caused AML (Gjini et al., 2019).

In another recent model, a loss-of-function mutation of *sf3b1* in zebrafish leads to spliceosomal defects and thus MDS-like phenotypes (De La Garza et al., 2016). Furthermore, the *cephaloponus* mutant,

which was isolated from a forward genetic screen followed by a positional cloning scan, showed that its driver mutation was affecting the splicing factor gene *prpf8* (Keightley et al., 2013). Another mutant identified in a forward genetic screen is *crimsonless*, which represents one of the very first zebrafish MDS models and was shown to carry a mutation in a gene encoding a ubiquitously expressed matrix chaperone, *hsps9b* (Craven et al., 2005). Next to these approaches, targeting induced local lesions in genomes (TILLING) is a reverse genetic method that enabled the association of *spi1* loss of function with MDS development (Sun et al., 2013). Furthermore, a rather unusual but promising zebrafish model for MDS is the *c-myb^{hyper}* strain, initially developed as a *Tg(c-myb:GFP)* reporter line (North et al., 2007). Liu and colleagues, however, discovered that the transgene causes hyperactivation of *c-myb* by expressing an alternative transcript lacking the negative regulatory domain; this *c-myb* hyperactivation eventually led to MDS that progresses to transplantable AML and acute lymphoblastic leukemia (ALL) (Liu et al., 2017), and thus provides a promising model for future drug screenings.

5q- syndrome and CML-like disease

5q- syndrome is a distinct form of MDS caused by a deletion on chromosome 5. Patients with this syndrome suffer from macrocytic anemia with other hematological phenotypes (i.e. thrombocytosis and megakaryocyte hyperplasia). Ear and colleagues used clustered regularly interspaced short palindromic repeats (CRISPR)/Cas9 to target *rps14* by introducing an early stop codon via non-homologous end joining (Ear et al., 2016). This technology has revolutionized genome editing and massively facilitated the engineering of animal models of disease (Boel et al., 2018; Prykhodzhiy et al., 2017). Targeted mutation of *rps14* indeed led to anemic defects resembling those seen in 5q- syndrome (Ear et al., 2016), which was already modeled by morpholino oligonucleotide (MO) knockdown in a previous study (Payne et al., 2012). Besides, researchers also used transcription activator-like effector nucleases (TALENs) to generate mutations in the *irf8* gene in zebrafish, which – as in mice – causes a type of MPN known as chronic myeloid leukemia (CML)-like disease (Holtshcke et al., 1996; Zhao et al., 2018).

Acute myeloid leukemia

AML is defined as acute malignant disease characterized by uncontrolled proliferation and accumulation of leukemic blasts in

Box 3. Gene/protein symbols and names

ADP: adenosine diphosphate
AE1: anion exchanger 1
AK2: adenylate kinase 2
AKT: protein kinase B
AML1: acute myeloid leukemia 1 gene; also known as *RUNX1*
AMP: adenosine monophosphate
asx11: additional sex combs like
ATG5: autophagy protein 5
ATP: adenosine triphosphate
BCL2: B-cell lymphoma 2
BIM: Bcl2-interacting protein
CALR: calreticulin
Cas9: caspase 9
c-myb: myb proto-oncogene
COX: cyclooxygenase
Cre: cAMP response element
CSF3R: colony-stimulating factor 3 receptor, granulocyte
CXCR4: CXC chemokine receptor 4
DKC1: dyskerin
DMT1: FTD3 frontotemporal dementia, chromosome 3-linked
ER: estrogen receptor
ETO: RUNX1 translocation partner 1
ETV5: ETS variant gene 5
EZH2: enhancer of zeste, Drosophila, homolog 2
fancd2: Fanconi anemia, complementation group D2
FLT3: Fms-related tyrosine kinase 3
Gal4: Gal4 transcription factor
gar1: H/ACA ribonucleoprotein complex subunit 1
GCSF(R): granulocyte colony stimulating factor (receptor)
GFP: green fluorescent protein
HOX: homeobox transcription factor
HRAS: V-HA-RAS Harvey rat sarcoma viral oncogene homolog
hspa9b: heat-shock 70-kD protein 9 variant b
irf8: interferon regulatory factor 8
JAK2: Janus kinase 2
KRAS: V-KI-RAS2 Kirsten rat sarcoma viral oncogene homolog
lck: lymphocyte-specific protein-tyrosine kinase
LEF1: lymphoid enhancer-binding factor 1
lmo2: LIM domain only protein 2; encodes Rhotbin-like 1
MPL: myeloproliferative leukemia virus oncogene
MYST3: histone acetyltransferase KAT6A
mTOR: mechanistic target of rapamycin
NADPH: nicotinamide adenine dinucleotide phosphate
NCOA2: nuclear receptor co-activator 2
n-Myc: v-Myc avian myelocytomatosis viral-related oncogene, neuroblastoma-derived
nola1: nucleolar protein family A, member 1
nop10: H/ACA ribonucleoprotein complex subunit 3
NUP98: nucleoporin 98
prpf8: precursor mRNA-processing factor
PTEN: phosphatase and tensin homolog
PTPRJ: receptor-type tyrosine-protein phosphatase eta
RAC2: Ras-related C3 botulinum toxin substrate 2
rad51: DNA repair protein RAD51 homolog 2
rag2: recombination-activating gene 2
RPL: ribosomal protein L
RPS: ribosomal protein
RUNX1: Runt-related transcription factor 1
scl: stem cell leukemic protein
sf3b1: splicing factor 3B, subunit 1
slc4a1: solute carrier family 4 (anion exchanger), member 1
spi1: spleen focus forming virus proviral integration oncogene
sptb: erythroid beta-spectrin
SRP54: signal recognition particle 54
stat5.1: signal transducer and activator of transcription 1
syk: spleen tyrosine kinase
TCR: T-cell receptor
TEL: TEL1 oncogene
TERT: telomerase reverse transcriptase

TET2: Tet methylcytosine dioxygenase 2

TOX: thymocyte selection-associated high mobility group box protein

tp53: cellular tumor antigen p53

ZAP70: zeta chain of T cell receptor associated protein kinase 70

the bone marrow (BM), peripheral blood (PB) and other organs (Ferrara and Schiffer, 2013; Greim et al., 2014). It is the most common type of acute leukemia in adults and can occur at all ages, but more frequently affects elderly people, where it mainly progresses with an aggressive clinical course (Herrmann et al., 2012; Juliusson et al., 2009; Mrózek et al., 2012). Although the outlook for AML patients has improved over recent decades, more than half of young-adult and about 90% of elderly patients die from the disease (Mrózek et al., 2012). The main obstacles to cure are refractoriness to initial induction treatment and, more frequently, relapse after apparent remission.

One of the first AML models in zebrafish involved the transient expression of the human fusion oncogene *AML1 (RUNX1)-ETO* in zebrafish embryos. This disrupted normal hematopoiesis, with accumulation of immature hematopoietic blast cells in the intermediate cell mass (ICM), and circulating erythroid cells with dysplastic features (Kalev-Zylinska et al., 2002). Following this model, several others were developed, predominantly through the (over)expression of fusion oncogenes (Tan et al., 2018), and furthermore demonstrated potential for drug screenings. However, although these models enabled extensive studies on embryonic phenotypes, they associated with early embryonic lethality and were thus not suitable for studies in adult animals. The first successful zebrafish model of stable and embryonic non-lethal AML was established by Zhuravleva et al. (2008). It featured transient expression of a fusion of the human histone acetyl-transferase *MYST3* with *NCOA2* under the control of the myeloid-specific *spi1* promoter. A small number of transgenic embryos expressing the fusion transgene presented 14–26 months later with myeloid blast expansion in the kidney marrow (KM), as is commonly observed in human AML. Owing to its specificity to early myeloid lineages, *spi1*-driven oncogene expression was used in several additional myeloid malignancy models, e.g. involving the oncogenic fusion proteins *FLT3-ITD* [internal tandem duplication (ITD) of *FLT3*; He et al., 2014; Lu et al., 2016], *tel-jak2a* (CML) (Onnebo et al., 2005, 2012) and *NUP98-HOXA9* (see poster: Myeloid neoplasms) (Deveau et al., 2015; Forrester et al., 2011). Interestingly, the latter led to the identification of specific epigenetic therapies that restore healthy hematopoiesis in *NUP98-HOXA9* fish and of synergistic effects between DNA methyltransferase and cyclooxygenase inhibitors (Deveau et al., 2015).

An alternative way to overcome embryonic lethality upon human oncogene expression in zebrafish is to make use of temporal and spatial promoter activity by heat-shock treatment combined with Cre-mediated induction. Yeh et al. developed a heat-shock-inducible *AML1-ETO* model (see poster: Myeloid neoplasms), which, upon induction, resulted in morphological and transcriptional characteristics of human AML without causing vascular defects and early death during embryogenesis (Yeh et al., 2008). Interestingly, expression profiles of these fish resemble those seen in human AML, and the authors found *scl* to be an essential modifier of the ability of *AML1-ETO* to reprogram hematopoietic cell fate decisions (Yeh et al., 2008). A subsequent modifier screen surprisingly exposed roles of COX2- and β -catenin-dependent pathways in *AML1-ETO* function (Yeh et al., 2009). In another heat-shock-inducible system, Shen et al. timed expression of the murine *n-Myc* and thereby succeeded in inducing myeloid defects while avoiding early embryonic death. Specifically,

n-Myc promoted cell cycle progression and increased the ratios of myeloid cells and their precursors (Shen et al., 2013). Following the same principle of timed heat-shock induction, Le and colleagues showed KRAS^{G12D}-associated myeloid cell expansion in the KM (Le et al., 2007). A different approach of selective oncogene expression was exemplified by Alghisi and colleagues, who used the Gal4-UAS (upstream activated sequence) binary system (Scheer and Campos-Ortega, 1999) to express HRAS^{V12G} specifically in endothelial cells, which induced hyperproliferation of hematopoietic cells in the caudal hematopoietic tissue (CHT) (Alghisi et al., 2013). Remarkably, the authors showed that the abnormal phenotype in their model was associated with downregulation of the Notch pathway, which could be rescued by Notch overexpression in endothelial cells. Other models involve constitutive activation of *stat5.1* (Lewis et al., 2006) or expression of known mutations involved in myeloid neoplasms (Barbieri et al., 2016; Bolli et al., 2010; Shi et al., 2015; Zhao et al., 2018). Although these models provide opportunities for further research, most of them do not fully recapitulate the features of human AML. In fact, some of these models might represent pre-leukemic stages, probably because they are based on a single genetic manipulation, while human leukemogenesis requires several genetic alterations. Owing to recent technological advances in genome editing, and especially to the generation of efficient inducible promoters that circumvent early embryonic lethality, it may soon be possible to simultaneously manipulate multiple genes within the same cell lineage and to thereby obtain more robust leukemia models.

Lymphoid neoplasms

ALL is a malignant disorder of lymphoid progenitor cells affecting both children and adults. It can be separated into T-cell acute lymphoblastic leukemia (T-ALL) and B-cell acute lymphoblastic leukemia (B-ALL). Multi-agent combination chemotherapy regimens exist and result in cure rates of >90% for children and 40% for adults (Dinner and Liedtke, 2018).

T-cell acute lymphoblastic leukemia

T-ALL is characterized by immature T-cell-progenitor infiltration in the BM and accounts for 15% of ALL cases in pediatric patients and 25% of ALL in adults (Dinner and Liedtke, 2018). Mutations and rearrangements in several genes have been implicated in T-ALL, such as in HOX genes, genes regulating RAS signaling (e.g. *FLT3*), histone-modifying genes (e.g. *EZH2*), transcription-factor tumor suppressors (e.g. *AML1*, *ETV5* or *LEF1*), mutations affecting the *NOTCH1* pathway, and many more. In many T-ALL cases, either *MYC* or *MYC-n* are upregulated, suggesting the *MYC* pathway as a central regulator of T-ALL in humans. The majority of the reported ALL zebrafish models show a T-ALL phenotype, and transgenic *rag2-mMyc* zebrafish were the first cancer models described in zebrafish (Langenau et al., 2003). This is mainly due to the use of the lymphoid cell promoter *rag2* to drive specific oncogenic expression. Although involved in both T-ALL and B-ALL development in zebrafish (Borga et al., 2019; Garcia et al., 2018), all early *rag2*-driven ALL models developed in the 2000s exclusively induced T-cell neoplasia. Leukemias convincingly presented with hyperproliferation of lymphoid cells with accumulation and infiltration of immature T-cell blasts in various tissues and organs. The commonly used oncogene in these models is *c-Myc*. Various different *rag2:Myc* models have been described, mainly differing in the way the oncogene is expressed. The initial T-ALL model described in 2003 was exclusively propagated by *in vitro* fertilization due to premature lethality (Langenau et al., 2003). Later on, the use of inducible promoters overcame early lethality. Langenau et al. used a Cre-

inducible model (Langenau et al., 2005a) and Gutierrez et al. established conditional tamoxifen-inducible *rag2:Myc-ER* fish, which allowed improved analyses and assessed direct causality between *Myc* oncogene expression and T-ALL (Gutierrez et al., 2011). Interestingly, all *Myc*-induced T-ALL models follow a similar disease progression pattern, starting with localized T-lymphoblastic lymphoma with minor outgrowth before disseminating into the circulation and infiltrating other tissues with T-ALL-like cells (see poster; Acute lymphoblastic leukemia) (Feng et al., 2007; Langenau et al., 2005b, 2008; Rudner et al., 2011). The similarities between zebrafish and mammalian *Myc*-induced T-ALL enabled detailed analyses of the mechanisms underlying leukemic transformation (Blackburn et al., 2014; Feng et al., 2010; Reynolds et al., 2014). As such, and in line with the expression patterns observed in subtypes of human T-ALL (Langenau et al., 2005a), the effect of p53 inactivation during *Myc*-induced T-ALL onset could be determined by zebrafish studies (Feng et al., 2007, 2010; Gutierrez et al., 2014a). Additionally, researchers dissected the MYC-PTEN-AKT-BIM pathway in zebrafish, which demonstrated that PTEN-inactivating mutations promote loss of *MYC* oncogene dependence, and upregulation of the oncogenes *scl* and *lmo2* was found in *Myc*-induced cells in zebrafish (Gutierrez et al., 2011, 2014a; Reynolds et al., 2014). Notably, these lines were used to identify novel players and compounds for T-ALL treatment. In an attempt to identify compounds with selective toxicity against ALL, Ridges and colleagues used transgenic *Tg(lck:eGFP)* fish for a small-molecule screen and then confirmed hits in tamoxifen-inducible *rag2:Myc-ER* animals. They identified Lenalidomide, which is an active compound against immature normal and MYC-transformed leukemic T cells in adult zebrafish (Ridges et al., 2012). In another screen, phenothiazines were identified as compounds with NOTCH-independent anti-T-ALL activity (Gutierrez et al., 2014b). Additionally, researchers found TOX in a transgenic screen, which regulates growth, DNA repair, and genomic instability in T-ALL (Lobbardi et al., 2017).

Another central oncogene associated with T-ALL is *NOTCH1*. *rag2*-driven expression of the Notch1 intracellular domain (ICN1) causes constitutive activation of Notch signaling in T cells, eventually leading to the development of T-ALL in zebrafish (Blackburn et al., 2012; Chen et al., 2007). The combination of constitutive Notch activation with expression of the anti-apoptotic molecule *bcl2* further increased T-ALL incidence and accelerated manifestation with an earlier disease onset than with Notch activation alone (Chen et al., 2007). Later studies showed that Notch, which was thought to mainly exert its oncogenic function through transcriptional activation of *Myc*, also acts via *Myc*-independent mechanisms. However, Notch activation alone only leads to the expansion of a pre-malignant thymocyte pool without affecting the overall number of leukemia propagating cells (Blackburn et al., 2014).

B-cell acute lymphoblastic leukemia

B-ALL is a hematologic malignancy derived from immature B-cell precursors. It is the most prevalent childhood leukemia and the leading cause of childhood cancer-related deaths. B-ALL can be divided into several subtypes, including pro-B, pre-B, common and mature B-ALL. Although 75% of human ALL cases are B-ALL, modelling this disease in zebrafish is difficult due to the T-cell bias of the *rag2* promoter. Until recently, only one model of pre-B-ALL induction through global expression of the fusion oncogene *TEL-AML1* has been described (see poster; Acute lymphoblastic leukemia) (Sabaawy et al., 2006). However, the low incidence and the long latency of leukemia development in this model suggests that acquisition of additional mutations is most likely necessary to induce leukemic transformation.

A recent promising and surprising discovery was the development of coincident B-ALL in *rag2*-driven *Myc* models, which were before considered to be T-ALL specific. Borga et al. used a tissue-specific reporter line (*Tg(lck:eGFP)*), which differentially labels B and T cells, and observed clustering of *rag2*-induced *hMYC* ALL models according to the overall GFP intensity. Intensive investigation of the different clusters revealed the expression of B-cell-specific genes – predominantly in low-GFP-expressing ALL cells – and the development of pre-B-ALL (Borga et al., 2019). At the same time, another group discovered B-ALL features in a subset of *Tg(rag2:mMyc)* zebrafish by propagating ALL via single-cell allotransplantation followed by single-cell transcript expression (Garcia et al., 2018). These novel findings may represent an alternative way of using the *rag2* promoter to establish B-ALL zebrafish models.

Primary immunodeficiencies

Primary immunodeficiencies (PIDs) comprise all disorders that feature impaired immunity, which often leads to increased susceptibility to infections (Raje and Dinakar, 2015). The most dangerous forms of PID are severe combined immunodeficiencies (SCID). This subgroup is characterized by a block in T-cell differentiation associated with an additional defect in any other immune cell lineage (Fischer, 2000).

Wiskott-Aldrich syndrome

Wiskott-Aldrich syndrome (WAS) is caused by mutations in the X-linked *WAS* gene, which encodes the WAS protein (WASp). WASp is only produced in hematopoietic cells and plays a central role in transmitting cell-surface signals to the actin cytoskeleton. Several different inactivating mutations of *WAS* manifest in eczema, microthrombocytopenia and recurrent infections, and the severity of symptoms correlates with the degree of WASp loss (Massaad et al., 2013). Cvejic et al. performed detailed live-imaging experiments on zebrafish *was* morphants and loss-of-function mutants that they generated by TILLING. They observed impaired innate immune function associated with defective thrombus formation (Cvejic et al., 2008). Later, the same lab used the Gal4/UAS system to dissect the function of different human *WAS* mutant alleles by targeting their expression specifically to neutrophils and macrophages in WASp-null zebrafish (see poster: Primary immunodeficiencies) (Jones et al., 2013).

ZAP70-related combined immunodeficiency

ZAP70-related combined immunodeficiency (CID) is the rarest form of SCID, with around 50 known affected individuals. A mutation in *ZAP70* leads to abnormal TCR signaling, resulting in the absence of peripheral CD8⁺ and non-functional CD4⁺ T cells. Furthermore, the absence of T cells facilitates impaired immunoglobulin production in B cells (Arpaia et al., 1994; Elder, 1996; Elder et al., 1994, 1995). Zebrafish models have been extensively used to study ZAP70 deficiency and a possible compensatory mechanism by *syk*. Whilst research on the first knockdown models mainly focused on vascular development (Christie et al., 2010), a mutant developed by TALENs successfully recapitulated the immune defects seen in humans (see poster; Primary immunodeficiencies) (Moore et al., 2016).

Reticular dysgenesis

Patients suffering from reticular dysgenesis (RD) commonly present with SCID in combination with agranulocytosis and sensorineural deafness. The underlying genetic cause of RD is mutations in the *AK2* gene, encoding for adenylate kinase 2, which catalyzes the phosphotransfer from ATP to AMP, resulting in ADP production

(Dzeja et al., 1998). Currently, HSC transplantation is the only option to treat RD patients (Hoenig et al., 2017). Morpholino knockdown was performed to mimic RD in zebrafish (Pannicke et al., 2009) and data from this study were recently confirmed by Rissone and colleagues, who aimed to generate a variety of different *ak2* mutations, as seen in humans, and thus analyzed a loss-of-function *ak2* mutant from a DNA library of N-ethyl-N-nitrosourea (ENU)-induced mutations (Sood et al., 2006) and furthermore generated a knockout (KO) model for *ak2* by using ZFNs to introduce targeted frameshift mutations in the first exon (Rissone et al., 2015).

WHIM syndrome

Myelokathexis is a rare disorder with recurrent bacterial infections caused by a reduced number and function of neutrophils. WHIM syndrome refers to the association of features from which its name derives, including warts, hypogammaglobulinemia and infections with myelokathexis. In most patients, WHIM arises from gain-of-function mutations in *CXCR4* (Kawai and Malech, 2009). To model the disease in zebrafish, a truncated version of *CXCR4* was stably expressed in neutrophils. Whole-mount *in situ* hybridization and live imaging of these fish revealed a high degree of similarity to WHIM phenotypes observed in patients (Walters et al., 2010).

Chronic granulomatous disease

CGD is an inherited PID characterized by dysregulated inflammation, autoimmunity and severe infections caused by defects of the NADPH oxidase complex in neutrophilic granulocytes and monocytes (Arnold and Heimall, 2017). In zebrafish, different morphants demonstrated the necessity of a functional NADPH oxidase complex for reactive oxygen species (ROS)-mediated killing of phagocytosed pathogens (Brothers et al., 2011; Harvie and Huttenlocher, 2015; Yang et al., 2012). However, no stable zebrafish model for CGD has been established yet.

Leukocyte adhesion deficiency

Leukocyte adhesion deficiency (LAD) syndromes are rare PIDs characterized by adhesion-dependent malfunctions of leukocytes. Until now, three different subtypes of LAD have been described (LAD I-III). LAD-I is characterized by absent or reduced expression of $\beta 2$ integrins, LAD-II is hallmarked by defects in fucosylation of selectin ligands and LAD-III patients suffer from defects in integrin signaling (Harris et al., 2013). Owing to the aberrant adhesion properties, all LAD patients have increased numbers of circulating neutrophils. Huttenlocher and co-workers established a zebrafish model mimicking phenotypes observed in LAD patients by mutating *rac2*, a Rho GTPase largely restricted to hematopoietic cells. *rac2* morphants, zebrafish expressing mutated *rac2* in neutrophils, or *rac2* TALEN knockouts all present with defects in host defense due to aberrant neutrophil or macrophage motility (Deng et al., 2011; Rosowski et al., 2016). However, several phenotypes observed upon human *RAC2* deficiency, such as altered polarity and mobilization from the CHT, were missing in the zebrafish KO models, indicating that alternative *rac2* isoforms may contribute to the phenotypic manifestation.

Inherited bone marrow failure syndromes

Inherited BM failure syndromes (IBMFS) are a heterogeneous group of rare disorders characterized by BM failure resulting in cytopenias and increased risk of leukemia development (Dokal and Vulliamy, 2010). Many IBMFS have been successfully reconstituted in zebrafish (Oyarbide et al., 2019).

Diamond-Blackfan anemia

Diamond-Blackfan anemia (DBA) is a genetically very heterogeneous sporadic disorder. Although its main characteristic is erythrocyte aplasia that normally presents before 1 year of age, it is accompanied by a wide variety of phenotypic anomalies, such as skeletal deformations and short stature (Diamond et al., 1961; Engidaye et al., 2019; Ito et al., 2010). More than 50% of DBA patients carry mutations in genes encoding ribosomal proteins (Taylor and Zon, 2011; Vlachos and Muir, 2010). The first zebrafish models of DBA were established in 2008 by two different laboratories, both using MO injection to knock down *rps19*. The knockdown led to DBA-like phenotypes hallmarked by defective erythropoiesis and developmental abnormalities (Danilova et al., 2008; Jia et al., 2013; Uechi et al., 2008). These findings rapidly triggered the establishment of numerous novel ribosomal-protein-driven DBA models, such as *rps14* (Narla et al., 2014), *rpl11* (Chakraborty et al., 2018; Danilova et al., 2011; Zhang et al., 2013, 2014b), *rps29* (Mirabello et al., 2014; Taylor et al., 2012) (see poster: Bone marrow failure syndromes), *rpl5* (Wan et al., 2016), *rps24* (Song et al., 2014), *rpl35a* (Yadav et al., 2014), *rps7* (Antunes et al., 2015), *rps27/rpl27* (Wang et al., 2015) and *rps11* (Zhang et al., 2014a). Most of these were first developed using MO knockdown and later established as stable transgenic zebrafish lines, predominantly by using TALENs. A common finding in all models was the upregulation of the p53 pathway upon ribosomal protein deficiency. However, simultaneous knockdown of *tp53* was not able to completely rescue BM defects, indicating the involvement of p53-independent mechanisms (Antunes et al., 2015; Chakraborty et al., 2018; Danilova et al., 2008; 2011; Torihara et al., 2011; Wan et al., 2016; Yadav et al., 2014; Zhang et al., 2013, 2014a). Interestingly, treatment of DBA embryos with an exogenous supply of nucleosides resulted in downregulation of *tp53*, reduced apoptosis and rescue of hematopoiesis (Danilova et al., 2014). Furthermore, it has recently been suggested that the immune system might be involved in the pathophysiology of DBA. Using two models (*rpl11* mutants and *rps19* morphants), Danilova and colleagues showed upregulation of interferons, inflammatory pathways and the complement system in DBA zebrafish models (Danilova et al., 2018). Remarkably, Payne and others could show that the amino acids L-leucine (Narla et al., 2014; Payne et al., 2012; Yadav et al., 2014) and L-arginine improve DBA symptoms via the mTOR pathway. This has led to a first clinical pilot phase I/II study of leucine in the treatment of DBA patients (<https://clinicaltrials.gov/ct2/show/NCT01362595>). Moreover, SMER28 (6-bromo-N-2-propenyl-4-quinazolinamine), a small-molecule inducer of ATG5-dependent autophagy, has been identified in a screen using DBA induced pluripotent stem cells and was confirmed in zebrafish models (Doulatov et al., 2017), highlighting the fact that zebrafish are a valuable model for drug identification and screening.

Dyskeratosis congenita

Dyskeratosis congenita (DC) is a rare inherited disorder phenotypically characterized by BM failure, mucocutaneous abnormalities and premature aging. Genetically, DC patients almost exclusively present with mutations linked to the H/ACA ribonucleoprotein complex or telomere maintenance, thus often carrying shortened telomeres (Nelson and Bertuch, 2012). In 2011, Pereboom and colleagues described a zebrafish mutant that developed a DC-like phenotype (Pereboom et al., 2011). The mutant was generated in a large-scale insertional mutagenesis screen and featured viral insertion in the *nop10* gene, resulting in decreased transcript levels (Amsterdam et al., 1999). Nop10 is a dual-function protein involved in 18S ribosomal RNA (rRNA) processing and in the

telomerase complex. Its knockdown in zebrafish resulted in ribosome biogenesis defects eventually leading to cytopenia. The most common and most severe form of DC is the X-linked form caused by mutations in *DKC1*, encoding the protein dyskerin. Dyskerin is a subunit of the H/ACA ribonucleoprotein complex and zebrafish *dkc1* mutants showed defects in ribosomal biogenesis and hematopoiesis. In the same study, a retrovirally mutated *nolal* zebrafish strain, which encodes for *gar1* and plays crucial roles in rRNA maturation and telomerase activity, developed similar phenotypes to *dkc1* mutants. Surprisingly, none of these models developed telomere defects (Zhang et al., 2012). Another gene commonly mutated in DC patients is *TERT*, which encodes the reverse transcriptase subunit of the telomerase complex. Three different studies described a zebrafish *tert*^{-/-} mutant with disrupted tissue homeostasis and premature aging, thus representing a model for telomere shortening and disease anticipation in DC; however, it lacked classical symptoms such as BM failure and mucocutaneous abnormalities (Anchelin et al., 2013; Carneiro et al., 2016; Henriques et al., 2017).

Fanconi anemia

Fanconi anemia (FA) is an autosomal recessive disorder manifesting with BM failure associated with other syndromic malformations such as skeletal defects and an increased risk of malignant transformation (Oyarbide et al., 2019; Tischkowitz and Hodgson, 2003). The genetic background of FA includes known mutations in different FA pathway genes, which are required for efficient DNA repair (Bagby, 2018). Two different zebrafish models for FA have been published so far. The first is a *fancd2* morphant whose phenotype resembles that observed in children suffering from FA, hallmarked by shortened body length, microcephaly, and microphthalmia due to an increase in spontaneous chromosomal breakage (Liu et al., 2003). The second model is a loss-of-function mutant of the DNA recombination gene *rad51*. Similar to the *fancd2* morphant, *rad51* loss of function leads to the development of an FA-like phenotype including hypocellular KM, shortened body length and chromosomal instability (Botthof et al., 2017).

Shwachman-Diamond syndrome

Shwachman-Diamond syndrome (SDS) is a rare multisystem disorder that belongs to the severe congenital neutropenia (CN) group of disorders. It is characterized by exocrine pancreatic insufficiency, skeletal abnormalities and hematopoietic defects, with most patients suffering from neutropenia and increased risk of leukemic transformation. In total, 90% of SDS patients carry mutations in the Shwachman-Bodian-Diamond syndrome (*SBDS*) gene, which encodes a protein essential for ribosome biogenesis (Burroughs et al., 2009). The zebrafish *sbds* gene has been successfully knocked down by MO injection. Morphant fish developed a phenotype highly similar to that of SDS patients, with morphogenic defects in the exocrine pancreas and abnormal myeloid development (Provost et al., 2012; Venkatasubramani and Mayer, 2008). Recently, mutations in *SRP54* were described as being associated with SDS-like phenotypes or CN in patients (Bellanné-Chantelot et al., 2018; Carapito et al., 2017). An *srp54*-knockdown zebrafish model was established by Carapito and Konantz and colleagues that revealed that suppression of *srp54* induces neutropenia and exocrine pancreas defects in zebrafish embryos (see poster: Bone marrow failure syndromes) (Carapito et al., 2017).

Severe congenital neutropenia

CN describes a heterogeneous group of hematological disorders that share the common feature of an absolute neutrophil count below

$0.5 \times 10^9/L$ and increased incidence of infections in most patients. Around 60-80% of CN patients carry mutations in the neutrophil elastase gene (*ELA2/ELANE*) (Skokowa et al., 2017; Welte and Zeidler, 2009). *csf3* ligands and *csf3r* [zebrafish homologs of granulocyte colony stimulating factor and its receptor (*GCSF/R*)] are known to regulate and maintain neutrophil numbers during primitive and definitive hematopoiesis as shown by MO-mediated knockdown experiments (Liongue et al., 2009; Stachura et al., 2013). Various groups furthermore demonstrated that mutations in CSF3R lead to severe CN (e.g. Klimiankou et al., 2015; Triot et al., 2014). Pazhakh and colleagues therefore used CRISPR/Cas9 targeting to develop stable transgenic lines in zebrafish that maintained neutropenia in adulthood (Pazhakh et al., 2017), serving as a new animal model of human CSF3R-dependent CN.

Thrombocytopenia

Like CNs, thrombocytopenias describe a variety of heterogeneous disorders. In humans, thrombocytopenia is defined by a platelet count of less than $150 \times 10^3/\mu l$ (Gauer and Braun, 2012). A zebrafish model for congenital amegakaryocytic thrombocytopenia was developed by mutating the *mpl* gene with TALENs (Lin et al., 2017). Recently, Marconi and colleagues identified loss-of-function variants of *PTPRJ* in inherited thrombocytopenia patients without a known genetic background. Ablation of zebrafish *ptprja* by CRISPR/Cas9 successfully recapitulated the patient phenotypes in zebrafish (see poster: Bone marrow failure syndromes) (Marconi et al., 2019).

Anemia

Several forms of anemia (a reduction of erythrocytes) have been modeled in zebrafish. Genetic anemia models were mainly identified in large-scale genetic screens in the 1990s and later cloned and characterized (Driever et al., 1996; Haffter et al., 1996; Ransom et al., 1996). Hereditary elliptocytosis (HE) and hereditary spherocytosis (HS), two forms of hemolytic anemia that are caused by abnormal membrane cytoskeleton, for example, were reconstituted in zebrafish from mutants originally generated in one of these large-scale screens. The *merlot* and *chablis* strains share common features of HE, which, as shown by Shafizadeh et al., is due to protein 4.1 (P4.1) deficiency. As in HE patients, P4.1 defects led to elliptical erythroid cell morphology, reduced cell deformability and disrupted skeletal network (Shafizadeh et al., 2002). Another mutant called *riesling* was identified as a model for HS, as it carries a mutation in *sptb*, which as in humans results in spherical erythroid cell morphology due to disrupted membrane protein network (Liao et al., 2000). The zebrafish mutant *retsina* represents a model for dyserythropoietic anemia type II. The driver mutation in *retsina* is in the *slc4a1* gene encoding for the anion exchanger AE1, eventually resulting in erythroid binocularity and apoptosis due to incomplete chromosome segregation (Paw et al., 2003).

Furthermore, various zebrafish models for hypochromic anemia exist. Hypochromic anemia is characterized by pale and small erythrocytes, normally caused by globin or iron deficiencies (Iolascon et al., 2009). Whilst the zebrafish mutant *zinfandel* presents with hypochromic microcytic anemia due to defects in embryonic globin production (Brownlie et al., 2003), hypochromic anemia in the form of congenital sideroblastic anemia in the mutant *sauternes* is caused by disrupted heme biosynthesis (Brownlie et al., 1998). Another disease hallmarked by hypochromic anemia is hemochromatosis. In this disease, erythrocytes are fully functional; however, iron levels in circulation are too low to provide sufficient hemoglobinization. Characterization and positional cloning of the zebrafish mutant *weissherbst* enabled the discovery of a conserved

vertebrate iron exporter, Ferroportin 1, whose mutation causes the hypochromic phenotype in this strain (Donovan et al., 2000; Fraenkel et al., 2005). A mutant that shows a very similar phenotype to the one observed in *weissherbst* is the *chianti* strain. Unlike *weissherbst*, the underlying cause is not a lack in circulatory iron, but rather defective iron acquisition due to mutations in the gene encoding Transferrin receptor 1 in differentiating erythrocytes (Wingert et al., 2004).

Finally, the *chardonnay* zebrafish mutant adds another important player to the understanding of iron metabolism, by revealing an essential role of the iron transporter DMT1 in iron homeostasis (Donovan et al., 2002). Moreover, because of its transparency during embryonic development, zebrafish is a very suitable and direct model for porphyrias, which are disorders caused by disrupted heme biosynthesis often accompanied by light sensitivity. The zebrafish *dracula* mutant, which was, like most anemic zebrafish strains, identified in a genetic screen, represents a very accurate model for erythropoietic protoporphyria. The *dracula* gene was shown to encode for Ferrochelatase, the terminal enzyme in the heme biosynthesis pathway, and its inactivation rendered erythrocytes highly light sensitive (Childs et al., 2000). Interestingly, Lenard et al. successfully modeled drug-induced hemolytic and chemotherapy-induced anemia (see poster: Blood toxicity), and used live imaging technologies to visualize *in vivo* hemolysis and regeneration (Lenard et al., 2015).

Discussion

The blood system is highly conserved between zebrafish and mammals. This high degree of conservation indicates that knowledge obtained from zebrafish is potentially transferrable to humans, and zebrafish models can be used for modeling human blood disorders. The high fecundity and *ex utero* embryogenesis, facilitating non-invasive *in vivo* analyses of zebrafish, enable the application of a wide variety of genetic and drug screening approaches (Box 4), and can make important contributions to our understanding of disease pathophysiology, genotype-phenotype correlations, and eventually enable the discovery of new therapeutic targets and modalities. Limitations that still need to be overcome involve the concurrent and selective expression of oncogenes in adult zebrafish tissues, enabling improved phenocopying of human disorders. In this regard, an interesting novel approach has been recently demonstrated, allowing injection of DNA constructs in adult fish at a certain time point and at

Box 4. Drug screening in zebrafish

Drug screening of a whole organism allows concurrent observation of drug toxicity and *in vivo* drug effects, and allows the drug to interact with any biological pathway and all respective niches. Owing to their small size and high fecundity, chemical screening in fish is easily feasible and can be performed in a high-throughput manner with different read-outs, such as morphology, behavior and cell state. Morphology screens are designed based on a chosen morphology change of interest. For example, Shafizadeh and colleagues used o-dianisidine staining to detect changes in hemoglobin synthesis after chemical treatment and identified compounds that reduced hemoglobin abundance and as such led to hemolytic anemia (Shafizadeh et al., 2004). Behavior-based screens have also been performed, e.g. by measuring photomotor responses (Kokel et al., 2010). One important chemical screen using whole-mount *in situ* hybridization as a read-out has identified prostaglandin E2 as a novel compound to regulate HSC homeostasis (North et al., 2007). This compound has made it into clinical trials, highlighting the importance of zebrafish in drug screenings (Cutler et al., 2013).

any specific location (Callahan et al., 2018). This system, called ‘transgene electroporation in adult zebrafish’ might become useful for hematopoietic diseases, e.g. through injection of DNA constructs with specific hematopoietic promoters into the KM of adult zebrafish. Another important limitation for a wider adoption of zebrafish models is the availability of analysis tools such as reliable antibodies for labeling cell-surface markers to dissect zebrafish hematopoiesis in depth. Such reagents exist for mammalian systems, and their development for zebrafish would facilitate cross-model discovery and translational advances. At the moment, flow-cytometry-based analyses solely rely on forward-sideward scattering (Traver et al., 2003) or on the use of fluorochromes in transgenic lines. Functional assays, however, such as the zebrafish HSC/KM cells methylcellulose colony assays, which allows *ex vivo* characterization of zebrafish hematopoietic precursors (Stachura et al., 2011; Svoboda et al., 2016), further improved the analysis of zebrafish hematopoiesis. However, our knowledge of the zebrafish hematopoietic niche is still sparse and, although more and more studies investigate the interaction between blood cells, their niche and their relevance for blood disorders (Espín-Palazón et al., 2014; Kapp et al., 2018; Konantz et al., 2016; Mahony et al., 2016, 2018; Tamplin et al., 2015), the community needs continued support of basic research. In sum, zebrafish offer unique advantages complementary to mammalian models and promise to greatly facilitate the discovery of new drugs and novel molecular processes involved in healthy hematopoiesis and blood disorders.

Acknowledgements

We would like to thank Marcelle Baer and the animal facility of the Department of Biomedicine for their help with the zebrafish facility.

Competing interests

The authors declare no competing or financial interests.

Funding

This work was supported by grants of the Swiss National Science Foundation (SNF, 310030_149735, 310030_179239) to C.L. and the Stay on Track Program of the University of Basel to M.K.

DMM at a glance

A high-resolution version of the poster is available for downloading at <http://dmm.biologists.org/lookup/doi/10.1242/dmm.040360.supplemental>

References

- Alghisi, E., Distel, M., Malagola, M., Anelli, V., Santoriello, C., Herwig, L., Krudewig, A., Henkel, C. V., Russo, D. and Mione, M. C. (2013). Targeting oncogene expression to endothelial cells induces proliferation of the myeloid-erythroid lineage by repressing the Notch pathway. *Leukemia* **27**, 2229–2241. doi:10.1038/leu.2013.132
- Amsterdam, A., Burgess, S., Golling, G., Chen, W., Sun, Z., Townsend, K., Farrington, S., Haldi, M. and Hopkins, N. (1999). A large-scale insertional mutagenesis screen in zebrafish. *Genes Dev.* **13**, 2713–2724. doi:10.1101/gad.13.20.2713
- Anchelin, M., Alcaraz-Pérez, F., Martínez, C. M., Bernabé-García, M., Mulero, V. and Cayuela, M. L. (2013). Premature aging in telomerase-deficient zebrafish. *Dis. Model Mech.* **6**, 1101–1112. doi:10.1242/dmm.011635
- Antunes, A. T., Goos, Y. J., Pereboom, T. C., Hermkens, D., Wlodarski, M. W., Da Costa, L. and MacInnes, A. W. (2015). Ribosomal Protein Mutations Result in Constitutive p53 Protein Degradation through Impairment of the AKT Pathway. *PLoS Genet.* **11**, e1005326. doi:10.1371/journal.pgen.1005326
- Arnold, D. E. and Heimall, J. R. (2017). A Review of Chronic Granulomatous Disease. *Adv. Ther.* **34**, 2543–2557. doi:10.1007/s12325-017-0636-2
- Arpaia, E., Shahar, M., Dadi, H., Cohen, A. and Roifman, C. M. (1994). Defective T cell receptor signaling and CD8+ thymic selection in humans lacking zap-70 kinase. *Cell* **76**, 947–958. doi:10.1016/0092-8674(94)90368-9
- Bagby, G. (2018). Recent advances in understanding hematopoiesis in Fanconi Anemia. *F1000Res.* **7**, 105. doi:10.12688/f1000research.13213.1
- Barbieri, E., Deflorian, G., Pezzimenti, F., Valli, D., Saia, M., Meani, N., Gruszka, A. M. and Alcalay, M. (2016). Nucleophosmin leukemogenic mutant activates Wnt signaling during zebrafish development. *Oncotarget* **7**, 55302–55312. doi:10.18632/oncotarget.10878
- Baxter, E. J., Scott, L. M., Campbell, P. J., East, C., Fourouclas, N., Swanton, S., Vassiliou, G. S., Bench, A. J., Boyd, E. M., Curtin, N. et al. (2005). Acquired mutation of the tyrosine kinase JAK2 in human myeloproliferative disorders. *Lancet* **365**, 1054–1061. doi:10.1016/S0140-6736(05)71142-9
- Bellanné-Chantelot, C., Schmaltz-Panneau, B., Marty, C., Fenneteau, O., Callebaut, I., Clauin, S., Docet, A., Damaj, G. L., Leblanc, T., Pellier, I. et al. (2018). Mutations in the SRP54 gene cause severe congenital neutropenia as well as Shwachman-Diamond-like syndrome. *Blood* **132**, 1318–1331. doi:10.1182/blood-2017-12-820308
- Bentley, V. L., Veinotte, C. J., Corkery, D. P., Pinder, J. B., LeBlanc, M. A., Bedard, K., Weng, A. P., Berman, J. N. and Dellaire, G. (2015). Focused chemical genomics using zebrafish xenotransplantation as a pre-clinical therapeutic platform for T-cell acute lymphoblastic leukemia. *Haematologica* **100**, 70–76. doi:10.3324/haematol.2014.110742
- Bertrand, J. Y. and Traver, D. (2009). Hematopoietic cell development in the zebrafish embryo. *Curr. Opin Hematol.* **16**, 243–248. doi:10.1097/MOH.0b013e32832c05e4
- Bertrand, J. Y., Kim, A. D., Violette, E. P., Stachura, D. L., Cisson, J. L. and Traver, D. (2007). Definitive hematopoiesis initiates through a committed erythromyeloid progenitor in the zebrafish embryo. *Development* **134**, 4147–4156. doi:10.1242/dev.012385
- Bertrand, J. Y., Chi, N. C., Santoso, B., Teng, S., Stainier, D. Y. and Traver, D. (2010a). Haematopoietic stem cells derive directly from aortic endothelium during development. *Nature* **464**, 108–111. doi:10.1038/nature08738
- Bertrand, J. Y., Cisson, J. L., Stachura, D. L. and Traver, D. (2010b). Notch signaling distinguishes 2 waves of definitive hematopoiesis in the zebrafish embryo. *Blood* **115**, 2777–2783. doi:10.1182/blood-2009-09-244590
- Blackburn, J. S., Liu, S., Raiser, D. M., Martinez, S. A., Feng, H., Meeker, N. D., Gentry, J., Neuberg, D., Look, A. T., Ramaswamy, S. et al. (2012). Notch signaling expands a pre-malignant pool of T-cell acute lymphoblastic leukemia clones without affecting leukemia-propagating cell frequency. *Leukemia* **26**, 2069–2078. doi:10.1038/leu.2012.116
- Blackburn, J. S., Liu, S., Wilder, J. L., Dobrinski, K. P., Lobbardi, R., Moore, F. E., Martinez, S. A., Chen, E. Y., Lee, C. and Langenau, D. M. (2014). Clonal evolution enhances leukemia-propagating cell frequency in T cell acute lymphoblastic leukemia through Akt/mTORC1 pathway activation. *Cancer Cell* **25**, 366–378. doi:10.1016/j.ccr.2014.01.032
- Blum, M., De Robertis, E. M., Wallingford, J. B. and Niehrs, C. (2015). Morpholinos: Antisense and Sensibility. *Dev. Cell* **35**, 145–149. doi:10.1016/j.devcel.2015.09.017
- Boel, A., De Saffel, H., Steyaert, W., Callewaert, B., De Paepe, A., Coucke, P. J. and Willaert, A. (2018). CRISPR/Cas9-mediated homology-directed repair by ssODNs in zebrafish induces complex mutational patterns resulting from genomic integration of repair-template fragments. *Dis. Model Mech.* **11**, dmm035352. doi:10.1242/dmm.035352
- Boisset, J. C., van Cappellen, W., Andrieu-Soler, C., Galjart, N., Dzierzak, E. and Robin, C. (2010). In vivo imaging of haematopoietic cells emerging from the mouse aortic endothelium. *Nature* **464**, 116–120. doi:10.1038/nature08764
- Bolli, N., Payne, E. M., Grabher, C., Lee, J. S., Johnston, A. B., Falini, B., Kanki, J. P. and Look, A. T. (2010). Expression of the cytoplasmic NPM1 mutant (NPMc+) causes the expansion of hematopoietic cells in zebrafish. *Blood* **115**, 3329–3340. doi:10.1182/blood-2009-02-207225
- Borga, C., Park, G., Foster, C., Burroughs-Garcia, J., Marchesin, M., Shah, R., Hasan, A., Ahmed, S. T., Bresolin, S., Batchelor, L. et al. (2019). Simultaneous B and T cell acute lymphoblastic leukemias in zebrafish driven by transgenic MYC: implications for oncogenesis and lymphopoiesis. *Leukemia* **33**, 333–347. doi:10.1038/s41375-018-0226-6
- Botthof, J. G., Bielczyk-Maczyńska, E., Ferreira, L. and Cvejic, A. (2017). Loss of the homologous recombination gene *rad51* leads to Fanconi anemia-like symptoms in zebrafish. *Proc. Natl. Acad. Sci. USA* **114**, E4452–E4461. doi:10.1073/pnas.1620631114
- Brothers, K. M., Newman, Z. R. and Wheeler, R. T. (2011). Live imaging of disseminated candidiasis in zebrafish reveals role of phagocyte oxidase in limiting filamentous growth. *Eukaryot. Cell* **10**, 932–944. doi:10.1128/EC.05005-11
- Brownlie, A., Donovan, A., Pratt, S. J., Paw, B. H., Oates, A. C., Brugnara, C., Witkowska, H. E., Sassa, S. and Zon, L. I. (1998). Positional cloning of the zebrafish *sauternes* gene: a model for congenital sideroblastic anaemia. *Nat. Genet.* **20**, 244–250. doi:10.1038/3049
- Brownlie, A., Hersey, C., Oates, A. C., Paw, B. H., Falick, A. M., Witkowska, H. E., Flint, J., Higgs, D., Jessen, J., Bahary, N. et al. (2003). Characterization of embryonic globin genes of the zebrafish. *Dev. Biol.* **255**, 48–61. doi:10.1016/S0012-1606(02)00041-6
- Burroughs, L., Woolfrey, A. and Shimamura, A. (2009). Shwachman-Diamond syndrome: a review of the clinical presentation, molecular pathogenesis, diagnosis, and treatment. *Hematol. Oncol. Clin. North Am.* **23**, 233–248. doi:10.1016/j.hoc.2009.01.007
- Callahan, S. J., Tepan, S., Zhang, Y. M., Lindsay, H., Burger, A., Campbell, N. R., Kim, I. S., Hollmann, T. J., Studer, L., Mosimann, C. et al. (2018). Cancer modeling by Transgene Electroporation in Adult Zebrafish (TEAZ). *Dis. Model Mech.* **11**, dmm034561. doi:10.1242/dmm.034561

- Carapito, R., Konantz, M., Paillard, C., Miao, Z., Pichot, A., Leduc, M. S., Yang, Y., Bergstrom, K. L., Mahoney, D. H., Shardy, D. L. et al. (2017). Mutations in signal recognition particle SRP54 cause syndromic neutropenia with Shwachman-Diamond-like features. *J. Clin. Invest.* **127**, 4090-4103. doi:10.1172/JCI92876
- Carneiro, M. C., de Castro, I. P. and Ferreira, M. G. (2016). Telomeres in aging and disease: lessons from zebrafish. *Dis. Model Mech.* **9**, 737-748. doi:10.1242/dmm.025130
- Chakraborty, A., Uechi, T., Nakajima, Y., Gazda, H. T., O'Donohue, M. F., Gleizes, P. E. and Kenmochi, N. (2018). Cross talk between TP53 and c-Myc in the pathophysiology of Diamond-Blackfan anemia: Evidence from RPL11-deficient in vivo and in vitro models. *Biochem. Biophys. Res. Commun.* **495**, 1839-1845. doi:10.1016/j.bbrc.2017.12.019
- Chen, A. T. and Zon, L. I. (2009). Zebrafish blood stem cells. *J. Cell. Biochem.* **108**, 35-42. doi:10.1002/jcb.22251
- Chen, J., Jette, C., Kanki, J. P., Aster, J. C., Look, A. T. and Griffin, J. D. (2007). NOTCH1-induced T-cell leukemia in transgenic zebrafish. *Leukemia* **21**, 462-471. doi:10.1038/sj.leu.2404546
- Childs, S., Weinstein, B. M., Mohideen, M. A., Donohue, S., Bonkovsky, H. and Fishman, M. C. (2000). Zebrafish dracula encodes ferrochelatase and its mutation provides a model for erythropoietic protoporphyria. *Curr. Biol.* **10**, 1001-1004. doi:10.1016/S0960-9822(00)00653-9
- Christie, T. L., Carter, A., Rollins, E. L. and Childs, S. J. (2010). Syk and Zap-70 function redundantly to promote angioblast migration. *Dev. Biol.* **340**, 22-29. doi:10.1016/j.ydbio.2010.01.011
- Craven, S. E., French, D., Ye, W., de Sauvage, F. and Rosenthal, A. (2005). Loss of Hspa9b in zebrafish recapitulates the ineffective hematopoiesis of the myelodysplastic syndrome. *Blood* **105**, 3528-3534. doi:10.1182/blood-2004-03-1089
- Cunningham, L., Finckbeiner, S., Hyde, R. K., Southall, N., Marugan, J., Yedavalli, V. R., Dehdashti, S. J., Reinhold, W. C., Alemu, L., Zhao, L. et al. (2012). Identification of benzodiazepine Ro5-3335 as an inhibitor of CBF leukemia through quantitative high throughput screen against RUNX1-CBFbeta interaction. *Proc. Natl. Acad. Sci. USA* **109**, 14592-14597. doi:10.1073/pnas.1200037109
- Cutler, C., Multani, P., Robbins, D., Kim, H. T., Le, T., Hoggatt, J., Pelus, L. M., Desponts, C., Chen, Y. B., Reznier, B. et al. (2013). Prostaglandin-modulated umbilical cord blood hematopoietic stem cell transplantation. *Blood* **122**, 3074-3081. doi:10.1182/blood-2013-05-503177
- Cvejic, A., Hall, C., Bak-Maier, M., Flores, M. V., Crosier, P., Redd, M. J. and Martin, P. (2008). Analysis of WASp function during the wound inflammatory response – live-imaging studies in zebrafish larvae. *J. Cell Sci.* **121**, 3196-3206. doi:10.1242/jcs.032235
- Danilova, N., Sakamoto, K. M. and Lin, S. (2008). Ribosomal protein S19 deficiency in zebrafish leads to developmental abnormalities and defective erythropoiesis through activation of p53 protein family. *Blood* **112**, 5228-5237. doi:10.1182/blood-2008-01-132290
- Danilova, N., Sakamoto, K. M. and Lin, S. (2011). Ribosomal protein L11 mutation in zebrafish leads to haematopoietic and metabolic defects: Effects of rpl11 Deficiency. *Br. J. Haematol.* **152**, 217-228. doi:10.1111/j.1365-2141.2010.08396.x
- Danilova, N., Bibikova, E., Covey, T. M., Nathanson, D., Dimitrova, E., Konto, Y., Lindgren, A., Glader, B., Radu, C. G., Sakamoto, K. M. et al. (2014). The role of the DNA damage response in zebrafish and cellular models of Diamond Blackfan anemia. *Dis. Model Mech.* **7**, 895-905. doi:10.1242/dmm.015495
- Danilova, N., Wilkes, M., Bibikova, E., Youn, M. Y., Sakamoto, K. M. and Lin, S. (2018). Innate immune system activation in zebrafish and cellular models of Diamond Blackfan Anemia. *Sci. Rep.* **8**, 5165. doi:10.1038/s41598-018-23561-6
- Davidson, A. J. and Zon, L. I. (2004). The 'definitive' (and 'primitive') guide to zebrafish hematopoiesis. *Oncogene* **23**, 7233-7246. doi:10.1038/sj.onc.1207943
- De La Garza, A., Cameron, R. C., Nik, S., Payne, S. G. and Bowman, T. V. (2016). Spliceosomal component Sf3b1 is essential for hematopoietic differentiation in zebrafish. *Exp. Hematol.* **44**, 826-837.e4. doi:10.1016/j.exphem.2016.05.012
- Deng, Q., Yoo, S. K., Cavnar, P. J., Green, J. M. and Huttenlocher, A. (2011). Dual roles for Rac2 in neutrophil motility and active retention in zebrafish hematopoietic tissue. *Dev. Cell* **21**, 735-745. doi:10.1016/j.devcel.2011.07.013
- Detrich, H. W., 3rd, Kieran, M. W., Chan, F. Y., Barone, L. M., Yee, K., Rundstadler, J. A., Pratt, S., Ransom, D. and Zon, L. I. (1995). Intraembryonic hematopoietic cell migration during vertebrate development. *Proc. Natl. Acad. Sci. USA* **92**, 10713-10717. doi:10.1073/pnas.92.23.10713
- Deveau, A. P., Forrester, A. M., Coombs, A. J., Wagner, G. S., Grabher, C., Chute, I. C., Léger, D., Mingay, M., Alexe, G., Rajan, V. et al. (2015). Epigenetic therapy restores normal hematopoiesis in a zebrafish model of NUP98-HOXA9-induced myeloid disease. *Leukemia* **29**, 2086-2097. doi:10.1038/leu.2015.126
- Diamond, L. K., Allen, D. M. and Magill, F. B. (1961). Congenital (erythroid) hypoplastic anemia. A 25-year study. *Am. J. Dis. Child.* **102**, 403-415. doi:10.1001/archpedi.1961.02080010405019
- Dinner, S. and Liedtke, M. (2018). Antibody-based therapies in patients with acute lymphoblastic leukemia. *Hematology Am. Soc. Hematol. Educ. Program.* **1**, 9-15. doi:10.1182/asheducation-2018.1.9
- Dokal, I. and Vulliamy, T. (2010). Inherited bone marrow failure syndromes. *Haematologica* **95**, 1236-1240. doi:10.3324/haematol.2010.025619
- Donovan, A., Brownlie, A., Zhou, Y., Shepard, J., Pratt, S. J., Moynihan, J., Paw, B. H., Drejer, A., Barut, B., Zapata, A. et al. (2000). Positional cloning of zebrafish ferroportin1 identifies a conserved vertebrate iron exporter. *Nature* **403**, 776-781. doi:10.1038/35001596
- Donovan, A., Brownlie, A., Dorschner, M. O., Zhou, Y., Pratt, S. J., Paw, B. H., Phillips, R. B., Thisse, C., Thisse, B. and Zon, L. I. (2002). The zebrafish mutant gene chardonnay (cdy) encodes divalent metal transporter 1 (DMT1). *Blood* **100**, 4655-4659. doi:10.1182/blood-2002-04-1169
- Doulatov, S., Vo, L. T., Macari, E. R., Wahlster, L., Kinney, M. A., Taylor, A. M., Barragan, J., Gupta, M., McGrath, K., Lee, H.-Y. et al. (2017). Drug discovery for Diamond-Blackfan anemia using reprogrammed hematopoietic progenitors. *Sci. Transl. Med.* (2017), **9**, eaah5645. doi:10.1126/scitranslmed.aah5645
- Driever, W., Solnica-Krezel, L., Schier, A. F., Neuhauss, S. C., Malicki, J., Stemple, D. L., Stainier, D. Y., Zwartkruis, F., Abdelilah, S., Rangini, Z. et al. (1996). A genetic screen for mutations affecting embryogenesis in zebrafish. *Development* **123**, 37-46.
- Dzeja, P. P., Zeleznikar, R. J. and Goldberg, N. D. (1998). Adenylate kinase: kinetic behavior in intact cells indicates it is integral to multiple cellular processes. *Mol. Cell. Biochem.* **184**, 169-182. doi:10.1023/A:1006859632730
- Ear, J., Hsueh, J., Nguyen, M., Zhang, Q., Sung, V., Chopra, R., Sakamoto, K. M. and Lin, S. (2016). A Zebrafish Model of 5q-Syndrome Using CRISPR/Cas9 Targeting RPS14 Reveals a p53-Independent and p53-Dependent Mechanism of Erythroid Failure. *J. Genet. Genomics* **43**, 307-318. doi:10.1016/j.jgg.2016.03.007
- Elder, M. E. (1996). Severe combined immunodeficiency due to a defect in the tyrosine kinase ZAP-70. *Pediatr. Res.* **39**, 743-748. doi:10.1203/00006450-199605000-00001
- Elder, M. E., Lin, D., Clever, J., Chan, A. C., Hope, T. J., Weiss, A. and Parslow, T. G. (1994). Human severe combined immunodeficiency due to a defect in ZAP-70, a T cell tyrosine kinase. *Science* **264**, 1596-1599. doi:10.1126/science.8202712
- Elder, M. E., Hope, T. J., Parslow, T. G., Umetsu, D. T., Wara, D. W. and Cowan, M. J. (1995). Severe combined immunodeficiency with absence of peripheral blood CD8+ T cells due to ZAP-70 deficiency. *Cell. Immunol.* **165**, 110-117. doi:10.1006/cimm.1995.1193
- Engidaye, G., Melku, M. and Enawgaw, B. (2019). Diamond Blackfan Anemia: Genetics, Pathogenesis, Diagnosis and Treatment. *EJIFCC* **30**, 67-81.
- Espín-Palazón, R., Stachura, D. L., Campbell, C. A., García-Moreno, D., Del Cid, N., Kim, A. D., Candel, S., Meseguer, J., Mulero, V. and Traver, D. (2014). Proinflammatory signaling regulates hematopoietic stem cell emergence. *Cell* **159**, 1070-1085. doi:10.1016/j.cell.2014.10.031
- Feng, H., Langenau, D. M., Madge, J. A., Quinkertz, A., Gutierrez, A., Neuberger, D. S., Kanki, J. P. and Thomas Look, A. T. (2007). Heat-shock induction of T-cell lymphoma/leukaemia in conditional Cre/lox-regulated transgenic zebrafish. *Br. J. Haematol.* **138**, 169-175. doi:10.1111/j.1365-2141.2007.06625.x
- Feng, H., Stachura, D. L., White, R. M., Gutierrez, A., Zhang, L., Sanda, T., Jette, C. A., Testa, J. R., Neuberger, D. S., Langenau, D. M. et al. (2010). T-lymphoblastic lymphoma cells express high levels of BCL2, S1P1, and ICAM1, leading to a blockade of tumor cell intravasation. *Cancer Cell* **18**, 353-366. doi:10.1016/j.ccr.2010.09.009
- Ferrara, F. and Schiffer, C. A. (2013). Acute myeloid leukaemia in adults. *Lancet* **381**, 484-495. doi:10.1016/S0140-6736(12)61727-9
- Fischer, A. (2000). Severe combined immunodeficiencies (SCID). *Clin. Exp. Immunol.* **122**, 143-149. doi:10.1046/j.1365-2249.2000.01359.x
- Forrester, A. M., Grabher, C., McBride, E. R., Boyd, E. R., Vigerstad, M. H., Edger, A., Kai, F. B., Da'as, S. I., Payne, E., Look, A. T. et al. (2011). NUP98-HOXA9-transgenic zebrafish develop a myeloproliferative neoplasm and provide new insight into mechanisms of myeloid leukaemogenesis. *Br. J. Haematol.* **155**, 167-181. doi:10.1111/j.1365-2141.2011.08810.x
- Fraenkel, P. G., Traver, D., Donovan, A., Zahrieh, D. and Zon, L. I. (2005). Ferroportin1 is required for normal iron cycling in zebrafish. *J. Clin. Invest.* **115**, 1532-1541. doi:10.1172/JCI23780
- Gacha-Garay, M. J., Niño-Joya, A. F., Bolaños, N. I., Abenoza, L., Quintero, G., Ibarra, H., Gonzalez, J. M., Akle, V. and Garavito-Aguilar, Z. V. (2019). Pilot Study of an Integrative New Tool for Studying Clinical Outcome Discrimination in Acute Leukemia. *Front. Oncol.* **9**, 245. doi:10.3389/fonc.2019.00245
- García, E. G., Iyer, S., García, S. P., Loontjens, S., Sadreyev, R. I., Speleman, F. and Langenau, D. M. (2018). Cell of origin dictates aggression and stem cell number in acute lymphoblastic leukemia. *Leukemia* **32**, 1860-1865. doi:10.1038/s41375-018-0130-0
- Gauer, R. L. and Braun, M. M. (2012). Thrombocytopenia. *Am. Fam. Physician* **85**, 612-622.
- Gjini, E., Mansour, M. R., Sander, J. D., Moritz, N., Nguyen, A. T., Kesarsing, M., Gans, E., He, S., Chen, S., Ko, M. et al. (2015). A zebrafish model of myelodysplastic syndrome produced through *tet2* genomic editing. *Mol. Cell. Biol.* **35**, 789-804. doi:10.1128/MCB.00971-14
- Gjini, E., Jing, C. B., Nguyen, A. T., Reyon, D., Gans, E., Kesarsing, M., Peterson, J., Pozdnyakova, O., Rodig, S. J., Mansour, M. R. et al. (2019). Disruption of *asx1* results in myeloproliferative neoplasms in zebrafish. *Dis. Model Mech.* **12**, dmm035790. doi:10.1242/dmm.035790
- Greim, H., Kaden, D. A., Larson, R. A., Palermo, C. M., Rice, J. M., Ross, D. and Snyder, R. (2014). The bone marrow niche, stem cells, and leukemia: impact of drugs, chemicals, and the environment: The bone marrow niche, stem cells, and leukemia. *Ann. N Y Acad. Sci.* **1310**, 7-31. doi:10.1111/nyas.12362

- Gutierrez, A., Grebliunaite, R., Feng, H., Kozakewich, E., Zhu, S., Guo, F., Payne, E., Mansour, M., Dahlberg, S. E., Neuberg, D. S. et al. (2011). Pten mediates Myc oncogene dependence in a conditional zebrafish model of T cell acute lymphoblastic leukemia. *J. Exp. Med.* **208**, 1595-1603. doi:10.1084/jem.20101691
- Gutierrez, A., Feng, H., Stevenson, K., Neuberg, D. S., Calzada, O., Zhou, Y., Langenau, D. M. and Look, A. T. (2014a). Loss of function *tp53* mutations do not accelerate the onset of myc-induced T-cell acute lymphoblastic leukaemia in the zebrafish. *Br. J. Haematol.* **166**, 84-90. doi:10.1111/bjh.12851
- Gutierrez, A., Pan, L., Groen, R. W. J., Baleydiere, F., Kentsis, A., Marineau, J., Grebliunaite, R., Kozakewich, E., Reed, C., Pflumio, F. et al. (2014b). Phenothiazines induce PP2A-mediated apoptosis in T cell acute lymphoblastic leukemia. *J. Clin. Invest.* (2014), **124**: 644-655. doi:10.1172/jci65093
- Haffter, P., Granato, M., Brand, M., Mullins, M. C., Hammerschmidt, M., Kane, D. A., Odenthal, J., van Eeden, F. J., Jiang, Y. J., Heisenberg, C. P. et al. (1996). The identification of genes with unique and essential functions in the development of the zebrafish, *Danio rerio*. *Development* **123**, 1-36.
- Harris, E. S., Weyrich, A. S. and Zimmerman, G. A. (2013). Lessons from rare maladies: leukocyte adhesion deficiency syndromes. *Curr. Opin. Hematol.* **20**, 16-25.
- Harvie, E. A. and Huttenlocher, A. (2015). Neutrophils in host defense: new insights from zebrafish. *J. Leukoc. Biol.* **98**, 523-537. doi:10.1189/jlb.4MR1114-524R
- He, B. L., Shi, X., Man, C. H., Ma, A. C., Ekker, S. C., Chow, H. C., So, C. W., Choi, W. W., Zhang, W., Zhang, Y. and et al. (2014). Functions of *flt3* in zebrafish hematopoiesis and its relevance to human acute myeloid leukemia. *Blood* **123**, 2518-2529. doi:10.1182/blood-2013-02-486688
- Henriques, C. M., Carneiro, M. C., Tenente, I. M., Jacinto, A. and Ferreira, M. G. (2017). Correction: Telomerase Is Required for Zebrafish Lifespan. *PLoS Genet.* **13**, e1006652. doi:10.1371/journal.pgen.1006652
- Herrmann, H., Blatt, K., Shi, J., Gleixner, K. V., Cerny-Reiterer, S., Müllauer, L., Vakoc, C. R., Sperr, W. R., Horny, H. P., Bradner, J. E. et al. (2012). Small-molecule inhibition of BRD4 as a new potent approach to eliminate leukemic stem- and progenitor cells in acute myeloid leukemia (AML). *Oncotarget* **3**, 1588-1599. doi:10.18632/oncotarget.733
- Heuser, M., Thol, F. and Ganser, A. (2016). Clonal Hematopoiesis of Indeterminate Potential. *Dtsch Arztebl Int* **113**, 317-322. doi:10.3238/arztebl.2016.0317
- Hoenig, M., Lagresle-Peyrou, C., Pannicke, U., Notarangelo, L. D., Porta, F., Gennery, A. R., Slatter, M., Cowan, M. J., Stepensky, P., Al-Mousa, H. et al. (2017). Reticular dysgenesis: international survey on clinical presentation, transplantation, and outcome. *Blood* **129**, 2928-2938. doi:10.1182/blood-2016-11-745638
- Holtschke, T., Löhler, J., Kanno, Y., Fehr, T., Giese, N., Rosenbauer, F., Lou, J., Knobloch, K. P., Gabriele, L., Waring, J. F. et al. (1996). Immunodeficiency and chronic myelogenous leukemia-like syndrome in mice with a targeted mutation of the ICSBP gene. *Cell* **87**, 307-317. doi:10.1016/S0092-8674(00)81348-3
- Howe, K., Clark, M. D., Torroja, C. F., Torrance, J., Berthelot, C., Muffato, M., Collins, J. E., Humphray, S., McLaren, K., Matthews, L., et al. (2013). The zebrafish reference genome sequence and its relationship to the human genome. *Nature* **496**, 498-503. doi:10.1038/nature12111
- Iolascon, A., De Falco, L. and Beaumont, C. (2009). Molecular basis of inherited microcytic anemia due to defects in iron acquisition or heme synthesis. *Haematologica* **94**, 395-408. doi:10.3324/haematol.13619
- Ito, E., Konno, Y., Toki, T. and Terui, K. (2010). Molecular pathogenesis in Diamond-Blackfan anemia. *Int. J. Hematol.* **92**, 413-418. doi:10.1007/s12185-010-0693-7
- James, C., Ugo, V., Le Couédic, J.-P., Staerk, J., Delhommeau, F., Lacout, C., Garçon, L., Raslova, H., Berger, R., Bennaceur-Griscelli, A. et al. (2005). A unique clonal JAK2 mutation leading to constitutive signalling causes polycythaemia vera. *Nature* **434**, 1144-1148. doi:10.1038/nature03546
- Jia, Q., Zhang, Q., Zhang, Z., Wang, Y., Zhang, W., Zhou, Y., Wan, Y., Cheng, T., Zhu, X., Fang, X. et al. (2013). Transcriptome analysis of the zebrafish model of Diamond-Blackfan anemia from RPS19 deficiency via p53-dependent and independent pathways. *PLoS One* **8**, e71782. doi:10.1371/journal.pone.0071782
- Jin, H., Xu, J. and Wen, Z. (2007). Migratory path of definitive hematopoietic stem/progenitor cells during zebrafish development. *Blood* **109**, 5208-5214. doi:10.1182/blood-2007-01-069005
- Jones, R. A., Feng, Y., Worth, A. J., Thrasher, A. J., Burns, S. O. and Martin, P. (2013). Modelling of human Wiskott-Aldrich syndrome protein mutants in zebrafish larvae using in vivo live imaging. *J. Cell Sci.* **126**, 4077-4084. doi:10.1242/jcs.128728
- Juliusson, G., Antunovic, P., Derolf, A., Lehmann, S., Mollgard, L., Stockelberg, D., Tidefelt, U., Wahlin, A. and Hoglund, M. (2009). Age and acute myeloid leukemia: real world data on decision to treat and outcomes from the Swedish Acute Leukemia Registry. *Blood* **113**, 4179-4187. doi:10.1182/blood-2008-07-172007
- Kalev-Zylinska, M. L., Horsfield, J. A., Flores, M. V., Postlethwait, J. H., Vitas, M. R., Baas, A. M., Crosier, P. S. and Crosier, K. E. (2002). Runx1 is required for zebrafish blood and vessel development and expression of a human RUNX1-CBF2T1 transgene advances a model for studies of leukemogenesis. *Development* **129**, 2015-2030. doi:10.1002/dvdy.10388
- Kapp, F. G., Perlin, J. R., Hagedorn, E. J., Gansner, J. M., Schwarz, D. E., O'Connell, L. A., Johnson, N. S., Amemiya, C., Fisher, D. E., Wöfle, U. et al. (2018). Protection from UV light is an evolutionarily conserved feature of the haematopoietic niche. *Nature* **558**, 445-448. doi:10.1038/s41586-018-0213-0
- Kawai, T. and Malech, H. L. (2009). WHIM syndrome: congenital immune deficiency disease. *Curr. Opin. Hematol.* **16**, 20-26. doi:10.1097/MOH.0b013e32831ac557
- Keightley, M. C., Crowhurst, M. O., Layton, J. E., Beilharz, T., Markmiller, S., Varma, S., Hogan, B. M., de Jong-Curtain, T. A., Heath, J. K. and Lieschke, G. J. (2013). In vivo mutation of pre-mRNA processing factor 8 (*Prpf8*) affects transcript splicing, cell survival and myeloid differentiation. *FEBS Lett.* **587**, 2150-2157. doi:10.1016/j.febslet.2013.05.030
- Kissa, K. and Herbomel, P. (2010). Blood stem cells emerge from aortic endothelium by a novel type of cell transition. *Nature* **464**, 112-115. doi:10.1038/nature08761
- Klimiankou, M., Klimenkova, O., Uenal, M., Zeidler, A., Mellor-Heineke, S., Kandabarau, S., Skokowa, J., Zeidler, C. and Welte, K. (2015). GM-CSF stimulates granulopoiesis in a congenital neutropenia patient with loss-of-function biallelic heterozygous CSF3R mutations. *Blood* **126**, 1865-1867. doi:10.1182/blood-2015-07-661264
- Kok, F. O., Shin, M., Ni, C. W., Gupta, A., Grosse, A. S., van Impel, A., Kirchmaier, B. C., Peterson-Maduro, J., Kourkoulis, G., Male, I. et al. (2015). Reverse genetic screening reveals poor correlation between morpholino-induced and mutant phenotypes in zebrafish. *Dev. Cell* **32**, 97-108. doi:10.1016/j.devcel.2014.11.018
- Kokel, D., Bryan, J., Laggner, C., White, R., Cheung, C. Y., Mateus, R., Healey, D., Kim, S., Werdich, A. A., Haggarty, S. J. et al. (2010). Rapid behavior-based identification of neuroactive small molecules in the zebrafish. *Nat. Chem. Biol.* **6**, 231-237. doi:10.1038/nchembio.307
- Konantz, M., Balci, T. B., Hartwig, U. F., Delleire, G., André, M. C., Berman, J. N. and Lengerke, C. (2012). Zebrafish xenografts as a tool for in vivo studies on human cancer: Human xenografts in zebrafish. *Ann. N Y Acad. Sci.* **1266**, 124-137. doi:10.1111/j.1749-6632.2012.06575.x
- Konantz, M., Alghisi, E., Müller, J. S., Lenard, A., Esain, V., Carroll, K. J., Kanz, L., North, T. E. and Lengerke, C. (2016). Evi1 regulates Notch activation to induce zebrafish hematopoietic stem cell emergence. *EMBO J.* **35**, 2315-2331. doi:10.15252/embj.201593454
- Kralovics, R., Passamonti, F., Buser, A. S., Teo, S. S., Tiedt, R., Passweg, J. R., Tichelli, A., Cazzola, M. and Skoda, R. C. (2005). A gain-of-function mutation of *JAK2* in myeloproliferative disorders. *N. Engl. J. Med.* **352**, 1779-1790. doi:10.1056/NEJMoa051113
- Krauss, J., Astrinides, P., Frohnhof, H. G., Walderich, B. and Nusslein-Volhard, C. (2013). transparent, a gene affecting stripe formation in Zebrafish, encodes the mitochondrial protein Mpv17 that is required for iridophore survival. *Biol. Open* **2**, 703-710. doi:10.1242/bio.20135132
- Langenau, D. M., Traver, D., Ferrando, A. A., Kutok, J. L., Aster, J. C., Kanki, J. P., Lin, S., Prochowik, E., Trede, N. S., Zon, L. I. and et al. (2003). Myc-induced T cell leukemia in transgenic zebrafish. *Science* **299**, 887-890. doi:10.1126/science.1080280
- Langenau, D. M., Feng, H., Berghmans, S., Kanki, J. P., Kutok, J. L. and Look, A. T. (2005a). Cre/lox-regulated transgenic zebrafish model with conditional myc-induced T cell acute lymphoblastic leukemia. *Proc. Natl. Acad. Sci. USA* **102**, 6068-6073. doi:10.1073/pnas.0408708102
- Langenau, D. M., Jette, C., Berghmans, S., Palomero, T., Kanki, J. P., Kutok, J. L. and Look, A. T. (2005b). Suppression of apoptosis by bcl-2 overexpression in lymphoid cells of transgenic zebrafish. *Blood* **105**, 3278-3285. doi:10.1182/blood-2004-08-3073
- Langenau, D. M., Keefe, M. D., Storer, N. Y., Jette, C. A., Smith, A. C., Ceol, C. J., Bourque, C., Look, A. T. and Zon, L. I. (2008). Co-injection strategies to modify radiation sensitivity and tumor initiation in transgenic Zebrafish. *Oncogene* **27**, 4242-4248. doi:10.1038/onc.2008.56
- Le, X., Langenau, D. M., Keefe, M. D., Kutok, J. L., Neuberg, D. S. and Zon, L. I. (2007). Heat shock-inducible Cre/Lox approaches to induce diverse types of tumors and hyperplasia in transgenic zebrafish. *Proc. Natl. Acad. Sci. USA* **104**, 9410-9415. doi:10.1073/pnas.0611302104
- Lenard, A., McGinnis, C. and Lengerke, C. (2015). Phenotypic assays using zebrafish hematopoiesis models for elucidation of hematopoietic toxicity. *Oncology Research and Treatment* **38**, 193-194.
- Lewis, R. S., Stephenson, S. E. and Ward, A. C. (2006). Constitutive activation of zebrafish Stat5 expands hematopoietic cell populations in vivo. *Exp. Hematol.* **34**, 179-187. doi:10.1016/j.exphem.2005.11.003
- Li, P., Lahvic, J. L., Binder, V., Pugach, E. K., Riley, E. B., Tamplin, O. J., Panigrahy, D., Bowman, T. V., Barrett, F. G., Heffner, G. C. et al. (2015). Epoxyeicosatrienoic acids enhance embryonic haematopoiesis and adult marrow engraftment. *Nature* **523**, 468-471. doi:10.1038/nature14569
- Liao, E. C., Paw, B. H., Peters, L. L., Zapata, A., Pratt, S. J., Do, C. P., Lieschke, G. and Zon, L. I. (2000). Hereditary spherocytosis in zebrafish riesling illustrates

- evolution of erythroid beta-spectrin structure, and function in red cell morphogenesis and membrane stability. *Development* **127**, 5123-5132.
- Lim, K. H., Chang, Y. C., Chiang, Y. H., Lin, H. C., Chang, C. Y., Lin, C. S., Huang, L., Wang, W. T., Gon-Shen Chen, C., Chou, W. C. and et al. (2016). Expression of CALR mutants causes mpl-dependent thrombocytosis in zebrafish. *Blood Cancer J* **6**, e481. doi:10.1038/bcj.2016.83
- Lin, Q., Zhang, Y., Zhou, R., Zheng, Y., Zhao, L., Huang, M., Zhang, X., Leung, A. Y. H. and Zhang, W. (2017). Establishment of a congenital amegakaryocytic thrombocytopenia model and a thrombocyte-specific reporter line in zebrafish. *Leukemia* **31**, 1206-1216. doi:10.1038/leu.2016.320
- Lindsley, R. C. (2017). Uncoding the genetic heterogeneity of myelodysplastic syndrome. *Hematol. Am. Soc. Hematol. Educ. Program* **2017**, 447-452. doi:10.1182/asheducation-2017.1.447
- Liongue, C., Hall, C. J., O'Connell, B. A., Crosier, P. and Ward, A. C. (2009). Zebrafish granulocyte colony-stimulating factor receptor signaling promotes myelopoiesis and myeloid cell migration. *Blood* **113**, 2535-2546. doi:10.1182/blood-2008-07-171967
- Lister, J. A., Robertson, C. P., Lepage, T., Johnson, S. L. and Raible, D. W. (1999). Nacre encodes a zebrafish microphthalmia-related protein that regulates neural-crest-derived pigment cell fate. *Development* **126**, 3757-3767.
- Liu, T. X., Howlett, N. G., Deng, M., Langenau, D. M., Hsu, K., Rhodes, J., Kanki, J. P., D'Andrea, A. D. and Look, A. T. (2003). Knockdown of zebrafish Fancd2 causes developmental abnormalities via p53-dependent apoptosis. *Dev. Cell* **5**, 903-914. doi:10.1016/S1534-5807(03)00339-3
- Liu, W., Wu, M., Huang, Z., Lian, J., Chen, J., Wang, T., Leung, A. Y., Liao, Y., Zhang, Z., Liu, Q. et al. (2017). c-myb hyperactivity leads to myeloid and lymphoid malignancies in zebrafish. *Leukemia* **31**, 222-233. doi:10.1038/leu.2016.170
- Lobbardi, R., Pinder, J., Martinez-Pastor, B., Theodorou, M., Blackburn, J. S., Abraham, B. J., Namiki, Y., Mansour, M., Abdelfattah, N. S., Molodtsov, A. et al. (2017). TOX Regulates Growth, DNA Repair, and Genomic Instability in T-cell Acute Lymphoblastic Leukemia. *Cancer Discov.* **7**, 1336-1353. doi:10.1158/2159-8290.CD-17-0267
- Lu, J. W., Hou, H. A., Hsieh, M. S., Tien, H. F. and Lin, L. I. (2016). Overexpression of FLT3-ITD driven by spi-1 results in expanded myelopoiesis with leukemic phenotype in zebrafish. *Leukemia* **30**, 2098-2101. doi:10.1038/leu.2016.132
- Ma, A. C., Fan, A., Ward, A. C., Liongue, C., Lewis, R. S., Cheng, S. H., Chan, P. K., Yip, S. F., Liang, R. and Leung, A. Y. (2009). A novel zebrafish jak2(V581F) model shared features of human JAK2(V617F) polycythemia vera. *Exp. Hematol.* **37**, 1379-1386.e4. doi:10.1016/j.exphem.2009.08.008
- Mahony, C. B., Fish, R. J., Pasche, C. and Bertrand, J. Y. (2016). tfec controls the hematopoietic stem cell vascular niche during zebrafish embryogenesis. *Blood* **128**, 1336-1345. doi:10.1182/blood-2016-04-710137
- Mahony, C. B., Pasche, C. and Bertrand, J. Y. (2018). Oncostatin M and Kit-Ligand Control Hematopoietic Stem Cell Fate during Zebrafish Embryogenesis. *Stem Cell Reports* **10**, 1920-1934. doi:10.1016/j.stemcr.2018.04.016
- Marconi, C., Di Buduo, C. A., LeVine, K., Barozzi, S., Faleschini, M., Bozzi, V., Palombo, F., McKinstry, S., Lassandro, G., Giordano, P. et al. (2019). A new form of inherited thrombocytopenia caused by loss-of-function mutations in. *Blood* **133**, 1346-1357. doi:10.1182/blood-2018-07-859496
- Massaad, M. J., Ramesh, N. and Geha, R. S. (2013). Wiskott-Aldrich syndrome: a comprehensive review. *Ann. N Y Acad. Sci.* **1285**, 26-43. doi:10.1111/nyas.12049
- Meyer, S. C. (2017). Mechanisms of Resistance to JAK2 Inhibitors in Myeloproliferative Neoplasms. *Hematol. Oncol. Clin. North Am.* **31**, 627-642. doi:10.1016/j.hoc.2017.04.003
- Mirabello, L., Macari, E. R., Jessop, L., Ellis, S. R., Myers, T., Giri, N., Taylor, A. M., McGrath, K. E., Humphries, J. M., Ballew, B. J. et al. (2014). Whole-exome sequencing and functional studies identify RPS29 as a novel gene mutated in multicausal Diamond-Blackfan anemia families. *Blood* **124**, 24-32. doi:10.1182/blood-2013-11-540278
- Moore, J. C., Mulligan, T. S., Torres Yordán, N., Castranova, D., Pham, V. N., Tang, Q., Lobbardi, R., Anselmo, A., Liwski, R. S., Berman, J. N. et al. (2016). T cell immune deficiency in zap70 mutant zebrafish. *Mol. Cell. Biol.* **36**, 2868-2876. doi:10.1128/MCB.00281-16
- Mrózek, K., Marcucci, G., Nicolet, D., Maharry, K. S., Becker, H., Whitman, S. P., Metzeler, K. H., Schwind, S., Wu, Y. Z., Kohlschmidt, J. et al. (2012). Prognostic significance of the European LeukemiaNet standardized system for reporting cytogenetic and molecular alterations in adults with acute myeloid leukemia. *J. Clin. Oncol.* **30**, 4515-4523. doi:10.1200/JCO.2012.43.4738
- Narla, A., Payne, E. M., Abayasekara, N., Hurst, S. N., Raiser, D. M., Look, A. T., Berliner, N., Ebert, B. L. and Khanna-Gupta, A. (2014). L-Leucine improves the anaemia in models of Diamond Blackfan anaemia and the 5q- syndrome in a TP53-independent way. *Br. J. Haematol.* **167**, 524-528. doi:10.1111/bjh.13069
- Nelson, N. D. and Bertuch, A. A. (2012). Dyskeratosis congenita as a disorder of telomere maintenance. *Mutat. Res./Fundamental and Molecular Mechanisms of Mutagenesis* **730**, 43-51. doi:10.1016/j.mrfmmm.2011.06.008
- North, T. E., Goessling, W., Walkley, C. R., Lengerke, C., Kopani, K. R., Lord, A. M., Weber, G. J., Bowman, T. V., Jang, I.-H., Grosser, T. et al. (2007). Prostaglandin E2 regulates vertebrate haematopoietic stem cell homeostasis. *Nature* **447**, 1007-1011. doi:10.1038/nature05883
- Onnebo, S. M., Condrón, M. M., McPhee, D. O., Lieschke, G. J. and Ward, A. C. (2005). Hematopoietic perturbation in zebrafish expressing a tel-jak2a fusion. *Exp. Hematol.* **33**, 182-188. doi:10.1016/j.exphem.2004.10.019
- Onnebo, S. M., Rasighaemi, P., Kumar, J., Liongue, C. and Ward, A. C. (2012). Alternative TEL-JAK2 fusions associated with T-cell acute lymphoblastic leukemia and atypical chronic myelogenous leukemia dissected in zebrafish. *Haematologica* **97**, 1895-1903. doi:10.3324/haematol.2012.064659
- Oyarbide, U., Topczewski, J. and Corey, S. J. (2019). Peering through zebrafish to understand inherited bone marrow failure syndromes. *Haematologica* **104**, 13-24. doi:10.3324/haematol.2018.196105
- Palis, J. and Yoder, M. C. (2001). Yolk-sac hematopoiesis: the first blood cells of mouse and man. *Exp. Hematol.* **29**, 927-936. doi:10.1016/S0301-472X(01)00669-5
- Pannicke, U., Höning, M., Hess, I., Friesen, C., Holzmann, K., Rump, E. M., Barth, T. F., Rojewski, M. T., Schulz, A., Boehm, T. et al. (2009). Reticular dysgenesis (aleukocytosis) is caused by mutations in the gene encoding mitochondrial adenylate kinase 2. *Nat. Genet.* **41**, 101-105. doi:10.1038/ng.265
- Parada-Kusz, M., Penaranda, C., Hagedorn, E. J., Clatworthy, A., Nair, A. V., Henninger, J. E., Ernst, C., Li, B., Riquelme, R., Jijon, H. et al. (2018). Generation of mouse-zebrafish hematopoietic tissue chimeric embryos for hematopoiesis and host-pathogen interaction studies. *Dis. Model Mech.* **11**, dmm034876. doi:10.1242/dmm.034876
- Paw, B. H., Davidson, A. J., Zhou, Y., Li, R., Pratt, S. J., Lee, C., Trede, N. S., Brownlie, A., Donovan, A., Liao, E. C. et al. (2003). Cell-specific mitotic defect and dyserythropoiesis associated with erythroid band 3 deficiency. *Nat. Genet.* **34**, 59-64. doi:10.1038/ng1137
- Payne, E. M., Virgilio, M., Narla, A., Sun, H., Levine, M., Paw, B. H., Berliner, N., Look, A. T., Ebert, B. L. and Khanna-Gupta, A. (2012). L-Leucine improves the anemia and developmental defects associated with Diamond-Blackfan anemia and del(5q) MDS by activating the mTOR pathway. *Blood* **120**, 2214-2224. doi:10.1182/blood-2011-10-382986
- Pazhakh, V., Clark, S., Keightley, M. C. and Lieschke, G. J. (2017). A GCSFR/CSF3R zebrafish mutant models the persistent basal neutrophil deficiency of severe congenital neutropenia. *Sci. Rep.* **7**, 44455. doi:10.1038/srep44455
- Pereboom, T. C., van Weele, L. J., Bondt, A. and MacInnes, A. W. (2011). A zebrafish model of dyskeratosis congenita reveals hematopoietic stem cell formation failure resulting from ribosomal protein-mediated p53 stabilization. *Blood* **118**, 5458-5465. doi:10.1182/blood-2011-04-351460
- Phillips, J. B. and Westerfield, M. (2014). Zebrafish models in translational research: tipping the scales toward advancements in human health. *Dis. Model Mech.* **7**, 739-743. doi:10.1242/dmm.015545
- Provost, E., Wehner, K. A., Zhong, X., Ashar, F., Nguyen, E., Green, R., Parsons, M. J. and Leach, S. D. (2012). Ribosomal biogenesis genes play an essential and p53-independent role in zebrafish pancreas development. *Development* **139**, 3232-3241. doi:10.1242/dev.077107
- Prykhodzhiy, S. V., Steele, S. L., Razaghi, B. and Berman, J. N. (2017). A rapid and effective method for screening, sequencing and reporter verification of engineered frameshift mutations in zebrafish. *Dis. Model Mech.* **10**, 811-822. doi:10.1242/dmm.026765
- Raje, N. and Dinakar, C. (2015). Overview of Immunodeficiency Disorders. *Immunol. Allergy Clin. North Am.* **35**, 599-623. doi:10.1016/j.iac.2015.07.001
- Ransom, D. G., Haffter, P., Odenthal, J., Brownlie, A., Vogelsang, E., Kelsch, R. N., Brand, M., van Eeden, F. J., Furutani-Seiki, M., Granato, M. et al. (1996). Characterization of zebrafish mutants with defects in embryonic hematopoiesis. *Development* **123**, 311-319. doi:10.1016/0736-5748(96)80313-3
- Reynolds, C., Roderick, J. E., LaBelle, J. L., Bird, G., Mathieu, R., Bodaar, K., Colon, D., Pyati, U., Stevenson, K. E., Qi, J. et al. (2014). Repression of BIM mediates survival signaling by MYC and AKT in high-risk T-cell acute lymphoblastic leukemia. *Leukemia* **28**, 1819-1827. doi:10.1038/leu.2014.78
- Ridges, S., Heaton, W. L., Joshi, D., Choi, H., Eiring, A., Batchelor, L., Choudhry, P., Manos, E. J., Soffa, H., Sanati, A. et al. (2012). Zebrafish screen identifies novel compound with selective toxicity against leukemia. *Blood* **119**, 5621-5631. doi:10.1182/blood-2011-12-398818
- Rissone, A., Weinacht, K. G., la Marca, G., Bishop, K., Giocaliere, E., Jagadeesh, J., Felgentreff, K., Dobbs, K., Al-Herz, W., Jones, M. et al. (2015). Reticular dysgenesis-associated AK2 protects hematopoietic stem and progenitor cell development from oxidative stress. *J. Exp. Med.* **212**, 1185-1202. doi:10.1084/jem.20141286
- Rosowski, E. E., Deng, Q., Keller, N. P. and Huttenlocher, A. (2016). Rac2 Functions in Both Neutrophils and Macrophages To Mediate Motility and Host Defense in Larval Zebrafish. *J. Immunol.* **197**, 4780-4790. doi:10.4049/jimmunol.1600928
- Rudner, L. A., Brown, K. H., Dobrinski, K. P., Bradley, D. F., Garcia, M. I., Smith, A. C., Downie, J. M., Meeker, N. D., Look, A. T., Downing, J. R. et al. (2011). Shared acquired genomic changes in zebrafish and human T-ALL. *Oncogene* **30**, 4289-4296. doi:10.1038/onc.2011.138
- Sabaawy, H. E., Azuma, M., Embree, L. J., Tsai, H. J., Starost, M. F. and Hickstein, D. D. (2006). TEL-AML1 transgenic zebrafish model of precursor B cell acute lymphoblastic leukemia. *Proc. Natl. Acad. Sci. USA* **103**, 15166-15171. doi:10.1073/pnas.0603349103

- Scheer, N. and Campos-Ortega, J. A.** (1999). Use of the Gal4-UAS technique for targeted gene expression in the zebrafish. *Mech. Dev.* **80**, 153-158. doi:10.1016/S0925-4773(98)00209-3
- Shafizadeh, E., Paw, B. H., Foott, H., Liao, E. C., Barut, B. A., Cope, J. J., Zon, L. I. and Lin, S.** (2002). Characterization of zebrafish merlot/chablis as non-mammalian vertebrate models for severe congenital anemia due to protein 4.1 deficiency. *Development* **129**, 4359-4370.
- Shafizadeh, E., Peterson, R. T. and Lin, S.** (2004). Induction of reversible hemolytic anemia in living zebrafish using a novel small molecule. *Comp. Biochem. Physiol. C Toxicol. Pharmacol.* **138**, 245-249. doi:10.1016/j.cca.2004.05.003
- Shen, L. J., Chen, F. Y., Zhang, Y., Cao, L. F., Kuang, Y., Zhong, M., Wang, T. and Zhong, H.** (2013). MYCN transgenic zebrafish model with the characterization of acute myeloid leukemia and altered hematopoiesis. *PLoS One* **8**, e59070. doi:10.1371/journal.pone.0059070
- Shi, X., He, B. L., Ma, A. C., Guo, Y., Chi, Y., Man, C. H., Zhang, W., Zhang, Y., Wen, Z., Cheng, T. and et al.** (2015). Functions of *idh1* and its mutation in the regulation of developmental hematopoiesis in zebrafish. *Blood* **125**, 2974-2984. doi:10.1182/blood-2014-09-601187
- Skokowa, J., Dale, D. C., Touw, I. P., Zeidler, C. and Welte, K.** (2017). Severe congenital neutropenias. *Nat. Rev. Dis. Primers* **3**, 17032. doi:10.1038/nrdp.2017.32
- Song, B., Zhang, Q., Zhang, Z., Wan, Y., Jia, Q., Wang, X., Zhu, X., Leung, A. Y., Cheng, T., Fang, X. et al.** (2014). Systematic transcriptome analysis of the zebrafish model of diamond-blackfan anemia induced by RPS24 deficiency. *BMC Genomics* **15**, 759. doi:10.1186/1471-2164-15-759
- Sood, R., English, M. A., Jones, M., Mullikin, J., Wang, D. M., Anderson, M., Wu, D., Chandrasekharappa, S. C., Yu, J., Zhang, J. and et al.** (2006). Methods for reverse genetic screening in zebrafish by resequencing and TILLING. *Methods* **39**, 220-227. doi:10.1016/j.ymeth.2006.04.012
- Stachura, D. L., Svoboda, O., Lau, R. P., Balla, K. M., Zon, L. I., Bartunek, P. and Traver, D.** (2011). Clonal analysis of hematopoietic progenitor cells in the zebrafish. *Blood* **118**, 1274-1282. doi:10.1182/blood-2011-01-331199
- Stachura, D. L., Svoboda, O., Campbell, C. A., Espín-Palazón, R., Lau, R. P., Zon, L. I., Bartunek, P. and Traver, D.** (2013). The zebrafish granulocyte colony-stimulating factors (*Gcsfs*): 2 paralogous cytokines and their roles in hematopoietic development and maintenance. *Blood* **122**, 3918-3928. doi:10.1182/blood-2012-12-475392
- Stainier, D. Y. R., Raz, E., Lawson, N. D., Ekker, S. C., Burdine, R. D., Eisen, J. S., Ingham, P. W., Schulte-Merker, S., Yelon, D., Weinstein, B. M. et al.** (2017). Guidelines for morpholino use in zebrafish. *PLoS Genet.* **13**, e1007000. doi:10.1371/journal.pgen.1007000
- Sun, J., Liu, W., Li, L., Chen, J., Wu, M., Zhang, Y., Leung, A. Y., Zhang, W., Wen, Z. and Liao, W.** (2013). Suppression of Pu.1 function results in expanded myelopoiesis in zebrafish. *Leukemia* **27**, 1913-1917. doi:10.1038/leu.2013.67
- Svoboda, O., Stachura, D. L., Machonova, O., Zon, L. I., Traver, D. and Bartunek, P.** (2016). Ex vivo tools for the clonal analysis of zebrafish hematopoiesis. *Nat. Protoc.* **11**, 1007-1020. doi:10.1038/nprot.2016.053
- Tamplin, O. J., Durand, E. M., Carr, L. A., Childs, S. J., Hagedorn, E. J., Li, P., Yzaguirre, A. D. and Speck, N. A.** (2015). Hematopoietic stem cell arrival triggers dynamic remodeling of the perivascular niche. *Cell* **160**, 241-252. doi:10.1016/j.cell.2014.12.032
- Tan, J., Zhao, L., Wang, G., Li, T., Li, D., Xu, Q., Chen, X., Shang, Z., Wang, J. and Zhou, J.** (2018). Human MLL-AF9 Overexpression Induces Aberrant Hematopoietic Expansion in Zebrafish. *Biomed. Res. Int.* **2018**, 6705842. doi:10.1155/2018/6705842
- Taylor, A. M. and Zon, L. I.** (2011). Modeling Diamond Blackfan anemia in the zebrafish. *Semin. Hematol.* **48**, 81-88. doi:10.1053/j.seminhematol.2011.02.002
- Taylor, A. M., Humphries, J. M., White, R. M., Murphey, R. D., Burns, C. E. and Zon, L. I.** (2012). Hematopoietic defects in *rps29* mutant zebrafish depend upon p53 activation. *Exp. Hematol.* **40**, 228-237.e5. doi:10.1016/j.exphem.2011.11.007
- Tischkowitz, M. D. and Hodgson, S. V.** (2003). Fanconi anaemia. *J. Med. Genet.* **40**, 1-10. doi:10.1136/jmg.40.1.1
- Torihara, H., Uechi, T., Chakraborty, A., Shinya, M., Sakai, N. and Kenmochi, N.** (2011). Erythropoiesis failure due to RPS19 deficiency is independent of an activated Tp53 response in a zebrafish model of Diamond-Blackfan anaemia: Erythropoiesis Failure in RPS19/Tp53-Deficient Zebrafish. *Br. J. Haematol.* **152**, 648-654. doi:10.1111/j.1365-2141.2010.08535.x
- Traver, D., Paw, B. H., Poss, K. D., Penberthy, W. T., Lin, S. and Zon, L. I.** (2003). Transplantation and in vivo imaging of multilineage engraftment in zebrafish bloodless mutants. *Nat. Immunol.* **4**, 1238-1246. doi:10.1038/ni1007
- Triot, A., Jarvinen, P. M., Arostegui, J. I., Murugan, D., Kohistani, N., Dapena Diaz, J. L., Racek, T., Puchalka, J., Gertz, E. M., Schaffer, A. A. et al.** (2014). Inherited biallelic CSF3R mutations in severe congenital neutropenia. *Blood* **123**, 3811-3817. doi:10.1182/blood-2013-11-535419
- Uechi, T., Nakajima, Y., Chakraborty, A., Torihara, H., Higa, S. and Kenmochi, N.** (2008). Deficiency of ribosomal protein S19 during early embryogenesis leads to reduction of erythrocytes in a zebrafish model of Diamond-Blackfan anemia. *Hum. Mol. Genet.* **17**, 3204-3211. doi:10.1093/hmg/ddn216
- Vainchenker, W. and Kralovics, R.** (2017). Genetic basis and molecular pathophysiology of classical myeloproliferative neoplasms. *Blood* **129**, 667-679. doi:10.1182/blood-2016-10-695940
- Veinotte, C. J., Dellaire, G. and Berman, J. N.** (2014). Hooking the big one: the potential of zebrafish xenotransplantation to reform cancer drug screening in the genomic era. *Dis. Model Mech.* **7**, 745-754. doi:10.1242/dmm.015784
- Venkatasubramani, N. and Mayer, A. N.** (2008). A zebrafish model for the Shwachman-Diamond syndrome (SDS). *Pediatr. Res.* **63**, 348-352. doi:10.1203/PDR.0b013e3181659736
- Vlachos, A. and Muir, E.** (2010). How I treat Diamond-Blackfan anemia. *Blood* **116**, 3715-3723. doi:10.1182/blood-2010-02-251090
- Walters, K. B., Green, J. M., Surfus, J. C., Yoo, S. K. and Huttenlocher, A.** (2010). Live imaging of neutrophil motility in a zebrafish model of WHIM syndrome. *Blood* **116**, 2803-2811. doi:10.1182/blood-2010-03-276972
- Wan, Y., Zhang, Q., Zhang, Z., Song, B., Wang, X., Zhang, Y., Jia, Q., Cheng, T., Zhu, X., Leung, A. Y. et al.** (2016). Transcriptome analysis reveals a ribosome constituents disorder involved in the RPL5 downregulated zebrafish model of Diamond-Blackfan anemia. *BMC Med. Genomics* **9**, 13. doi:10.1186/s12920-016-0174-9
- Wang, R., Yoshida, K., Toki, T., Sawada, T., Uechi, T., Okuno, Y., Sato-Otsubo, A., Kudo, K., Kamimaki, I., Kanazaki, R. et al.** (2015). Loss of function mutations in *RPL27* and *RPS27* identified by whole-exome sequencing in Diamond-Blackfan anaemia. *Br. J. Haematol.* **168**, 854-864. doi:10.1111/bjh.13229
- Welte, K. and Zeidler, C.** (2009). Severe congenital neutropenia. *Hematol. Oncol. Clin. North Am.* **23**, 307-320. doi:10.1016/j.hoc.2009.01.013
- White, R. M., Sessa, A., Burke, C., Bowman, T., LeBlanc, J., Ceol, C., Bourque, C., Dovey, M., Goessling, W., Burns, C. E. and et al.** (2008). Transparent adult zebrafish as a tool for in vivo transplantation analysis. *Cell Stem Cell* **2**, 183-189. doi:10.1016/j.stem.2007.11.002
- Wingert, R. A., Brownlie, A., Galloway, J. L., Dooley, K., Fraenkel, P., Axe, J. L., Davidson, A. J., Barut, B., Noriega, L., Sheng, X. et al.** (2004). The chianti zebrafish mutant provides a model for erythroid-specific disruption of transferrin receptor 1. *Development* **131**, 6225-6235. doi:10.1242/dev.01540
- Yadav, G. V., Chakraborty, A., Uechi, T. and Kenmochi, N.** (2014). Ribosomal protein deficiency causes Tp53-independent erythropoiesis failure in zebrafish. *Int. J. Biochem. Cell Biol.* **49**, 1-7. doi:10.1016/j.biocel.2014.01.006
- Yang, C. T., Cambier, C. J., Davis, J. M., Hall, C. J., Crosier, P. S. and Ramakrishnan, L.** (2012). Neutrophils exert protection in the early tuberculous granuloma by oxidative killing of mycobacteria phagocytosed from infected macrophages. *Cell Host Microbe* **12**, 301-312. doi:10.1016/j.chom.2012.07.009
- Yeh, J. R., Munson, K. M., Chao, Y. L., Peterson, Q. P., Macrae, C. A. and Peterson, R. T.** (2008). AML1-ETO reprograms hematopoietic cell fate by downregulating *scl* expression. *Development* **135**, 401-410. doi:10.1242/dev.008904
- Yeh, J. R., Munson, K. M., Elagib, K. E., Goldfarb, A. N., Sweetser, D. A. and Peterson, R. T.** (2009). Discovering chemical modifiers of oncogene-regulated hematopoietic differentiation. *Nat. Chem. Biol.* **5**, 236-243. doi:10.1038/nchembio.147
- Zhang, Y., Morimoto, K., Danilova, N., Zhang, B. and Lin, S.** (2012). Zebrafish models for dyskeratosis congenita reveal critical roles of p53 activation contributing to hematopoietic defects through RNA processing. *PLoS One* **7**, e30188. doi:10.1371/journal.pone.0030188
- Zhang, Z., Jia, H., Zhang, Q., Wan, Y., Zhou, Y., Jia, Q., Zhang, W., Yuan, W., Cheng, T., Zhu, X. and et al.** (2013). Assessment of hematopoietic failure due to Rpl11 deficiency in a zebrafish model of Diamond-Blackfan anemia by deep sequencing. *BMC Genomics* **14**, 896. doi:10.1186/1471-2164-14-896
- Zhang, Y., Ear, J., Yang, Z., Morimoto, K., Zhang, B. and Lin, S.** (2014a). Defects of protein production in erythroid cells revealed in a zebrafish Diamond-Blackfan anemia model for mutation in RPS19. *Cell Death Dis.* **5**, e1352. doi:10.1038/cddis.2014.318
- Zhang, Z., Jia, H., Zhang, Q., Wan, Y., Song, B., Jia, Q., Liu, H., Zhu, X. and Fang, X.** (2014b). Transcriptome analysis of Rpl11-deficient zebrafish model of Diamond-Blackfan Anemia. *Genom. Data* **2**, 173-175. doi:10.1016/j.gdata.2014.06.008
- Zhao, F., Shi, Y., Huang, Y., Zhan, Y., Zhou, L., Li, Y., Wan, Y., Li, H., Huang, H., Ruan, H. et al.** (2018). *Irf8* regulates the progression of myeloproliferative neoplasm-like syndrome via *Mertk* signaling in zebrafish. *Leukemia* **32**, 149-158. doi:10.1038/leu.2017.189
- Zhuravleva, J., Paggetti, J., Martin, L., Hammann, A., Solary, E., Bastie, J. N. and Delva, L.** (2008). MOZ/TIF2-induced acute myeloid leukaemia in transgenic fish. *Br. J. Haematol.* **143**, 378-382. doi:10.1111/j.1365-2141.2008.07362.x

1.5 Protein Export and Signal Recognition Particle

As mentioned above (section 1.3.4) this thesis is focusing on *SRP54*-driven SCN and SDS. Therefore, it is crucial to understand the molecular role of *SRP54*. Importantly, *SRP54* is one of the subunits of the signal recognition particle (SRP) – the cellular machinery coupling protein synthesis to protein secretion and membrane localization.²⁶⁸ In detail, the eukaryotic SRP consists of six proteins (*SRP9*, *SRP14*, *SRP19*, *SRP54*, *SRP68* and *SRP72*) and an approximately 300 nucleotide (nt) 7S RNA (**Figure 5**).²⁶⁹ While all subunits have their own functional tasks, the core function of the SRP is exerted by *SRP54* and the associated 7S RNA.²⁶⁹ One part of this core function is to recognize a hydrophobic signal sequence presented at the N-terminus of the nascent polypeptide chains emerging from the ribosome, which are destined to be delivered to the endoplasmic reticulum (ER).²⁷⁰ The signal sequence is thereby directly docking to the so-called M-domain of *SRP54*, which thus represents the SRP's linker to the ribosome nascent chain (RNC) complex (**Figure 5**).^{271,272} However, signal recognition is not the only function of *SRP54*. Once the SRP-RNC complex is shuttled to the ER, it binds to the signal receptor (SR) on the ER-membrane via the NG-domain of *SRP54* (**Figure 5**).²⁷² The *SRP54*-SR interaction is highly dependent on GTP and only takes place if both, *SRP54* as well as SR have bound nucleotides. After this interaction has been successfully established, the SRP-RNC complex undergoes substantial rearrangements, thereby allowing the RNC to bind to the translocation channel and initiate the release of the signal sequence and the insertion of the polypeptide chain.²⁷³ Ultimately, GTP hydrolysis takes place, leading to the dissociation of the SRP-SR complex.²⁷⁰

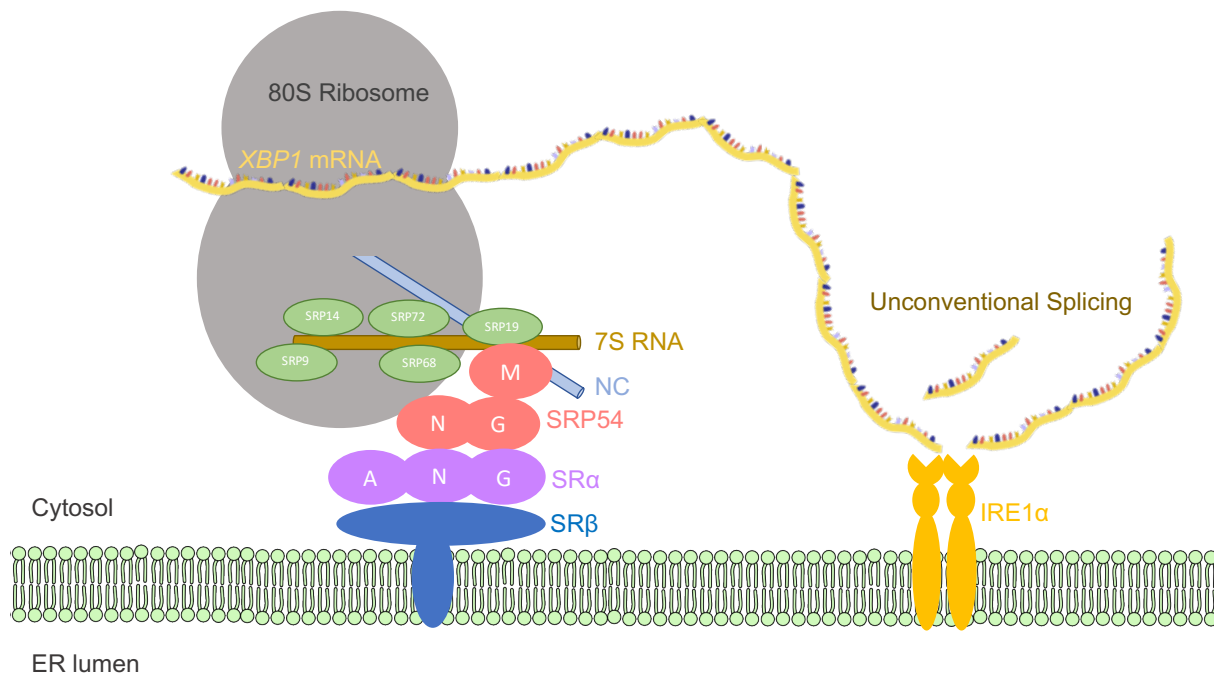


Figure 5: Binding of the RNC complex to the ER-membrane via SRP54 and unconventional splicing of *XBP1u* mRNA. The three domains of SRP54 are highlighted in red. Via its M domain, SRP54 binds the RNC complex; The N and G domains interact with the homologous domains (purple) of the SR α . The ER-membrane-resident endonuclease IRE1 α is depicted in yellow. Shown is the unconventional splicing of *XBP1u* mRNA, whilst it is still bound to the ribosome. Adapted and updated from Carapito et al.¹

1.5.1 *SRP54* Deficiencies

Particularly in higher eukaryotes, co-translational protein delivery to the ER-membrane, mediated by the SRP, is the predominant mode of protein export.²⁷⁰ Hence, impaired SRP function is often associated with severe consequences. Accordingly, also defective SRP54, which is responsible for the core functions of the SRP, is leading to harsh implications. On a molecular level, for example, it was demonstrated that point mutations in the G-Domain of *SRP54* are sufficient to completely abrogate protein translocation activity.²⁷⁴ Furthermore, gene disruption studies using the fission yeast *Schizosaccharomyces pombe* for the first time revealed that *SRP54* is essential for cellular viability.²⁷⁵

Clinically, *SRP54* lesions attracted attention for the first time 4 years ago, when the laboratory of Seiamak Bahram in collaboration with our research group for the first time described patients presenting with SCN or SDS due to point mutations in the *SRP54* gene.¹ Additionally, this study provides data suggesting that the three identified mutations (p.T115A, p.T117 Δ , p.G226E) are located within the NG-Domain of the protein and significantly impair GTPase activity. Importantly, zebrafish *srp54* morphants successfully recapitulated the disease, further supporting the idea of *SRP54* mutations as sole drivers of SDS and SCN.¹ Shortly

after this first report, a second publication identified 23 additional cases of *SRP54* mutations causing SCN or SDS.² Of note, 14 out of the 23 patients were carrying a deletion of Threonine117, which renders this mutation by far the most abundant *SRP54* defect. Mechanistically, the authors showed that granulocytic proliferation is significantly impaired upon *SRP54* knockdown and that patient cells were presenting with increased ER-stress levels as well as autophagy.²

Since these first two reports introduced *SRP54* mutations as novel, hitherto unknown drivers of SCN and SDS, research increasingly focused on understanding the molecular consequences of the different identified *SRP54* lesions and how these lesions are eventually causing neutropenia. Two recently published studies focused mainly on structural analyses of mutated *SRP54* variants.^{237,276} They demonstrate that the mutated proteins are critically destabilized and that the GTPase core is altered in a way that substantially reduces the GTP binding capacity. As a result of the reduced GTP binding, complex formation of the SRP with the SR on the ER-membrane is abolished, leading to severely hampered protein secretion by the SRP pathway.²⁷⁶

1.5.2 Endoplasmic Reticulum Stress and Unfolded Protein Response

As shown by Bellanné-Chantelot et al., patient cells carrying *SRP54* mutations are displaying elevated ER-stress levels.² The term “ER-stress” describes the perturbation or the imbalance of the ER – the first compartment of the secretory pathway, which is responsible for proper protein folding.²⁷⁷ Due to this imbalance, the ER’s capacity for protein folding cannot match the demand anymore, eventually leading to the accumulation of misfolded proteins in the ER lumen.²⁷⁸

Under normal conditions, proteins undergo several maturation steps in the ER before they adapt their final conformation. These maturation steps include the covalent addition of N-linked glycans, followed by folding through the action of chaperons, usually ending with the formation of disulfide bonds to stabilize the adapted conformation and to ensure proper protein function.²⁷⁹ Since protein folding in the ER is intrinsically error prone, the process needs to be tightly regulated and surveilled by a system called the ER quality control (ERQC). ERQC comprises both, protein-specific as well as general mechanisms, and involves several folding factors and chaperones, which ensure correct protein folding or in the case of decreased protein stability or incomplete folding, retain the proteins inside the ER instead of transporting them to the Golgi apparatus.²⁸⁰ Terminally misfolded proteins are eventually removed from the ER by a process called ER-associated degradation (ERAD). During ERAD,

misfolded proteins are recognized, re-translocated into the cytosol, ubiquitylated, and eventually degraded by the proteasome.^{280,281}

Despite the tight regulation of protein folding inside the ER and the considerable amount of energy and effort devoted by the cells to assure the removal of misfolded proteins, several mutations and conditions can easily imbalance this whole machinery and cause ER-stress.²⁸¹ Once the number of misfolded proteins in the ER reaches a certain threshold, the cell is able to activate a mechanism known as the unfolded protein response (UPR) to counteract the stress conditions.²⁸² Generally, the UPR is employing two different modes of action to alleviate ER-stress.^{277,282} The first one directly targets the ER by causing its physical expansion and by triggering the activation of additional chaperones and factors to increase the protein folding capacity. The second one on the other hand indirectly decreases the biosynthetic load of the ER by downregulating transcription and translation of secretory proteins. If these two modes of action are not able to overcome the stress conditions, apoptosis is initiated to eliminate the cell.^{277,282}

Molecularly, the UPR consists of three major signaling pathways, which are all mediated by different transmembrane proteins: IRE1 α , PERK, and ATF6 α (**Figure 6**).²⁸¹ In the absence of ER-stress, the luminal domains of these three proteins are all bound by the chaperone BiP, which keeps them in their inactive state. However, with the increasing number of unfolded proteins accumulating in the ER during stress conditions, BiP gets competitively titrated away from the UPR-mediators, since it also has a function in facilitating protein folding and thus shows high affinity for misfolded protein substrates.^{277,283} Once BiP is released from IRE1 α and PERK, they oligomerize and get activated (**Figure 6**). Upon BiP dissociation, ATF6 α on the other hand does not oligomerize, but rather translocates to the Golgi due to the activity of specific Golgi localization sequences and thereby exerts its function during UPR (**Figure 6**).²⁸⁴

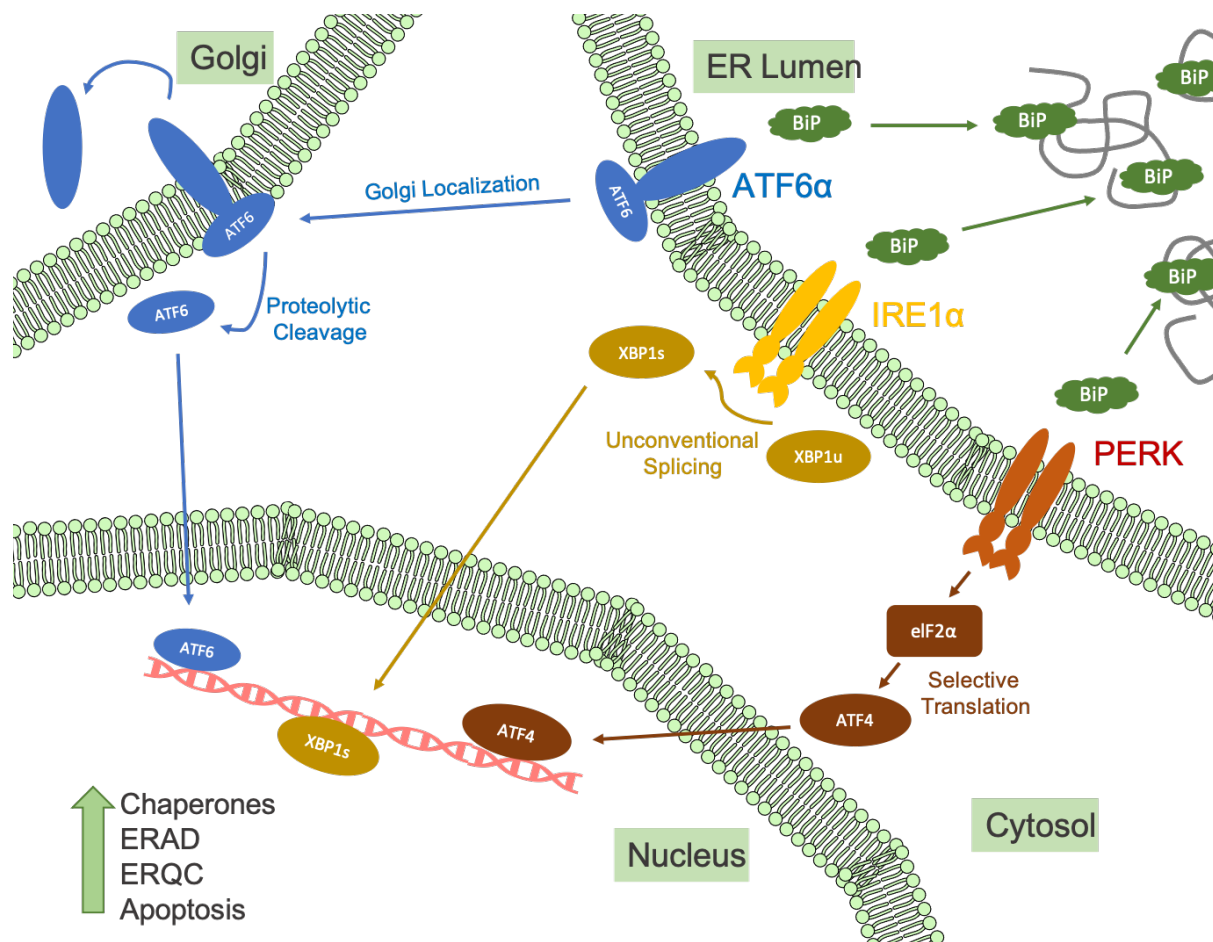


Figure 6: Overview of the three major branches of the UPR. Upon ER-stress, the chaperone BiP (green) gets titrated away from ATF6 (blue), IRE1 α (yellow) and PERK (brown), thereby causing their activation. ATF6 translocates to the Golgi, where it undergoes proteolytic cleavage. The truncated ATF6 fragment then enters the nucleus and acts as transcription factor. Upon BiP release, IRE1 α oligomerizes and cleaves the mRNA of *XBP1u* in a process termed unconventional splicing. The spliced XBP1 (XBP1s) functions as a transcription factor and enters the nucleus. Upon BiP release, PERK oligomerizes and phosphorylates eIF2 α , which in turn selectively stimulates the translation of the transcription factor ATF4. Truncated ATF6, XBP1s and ATF4 synergize and trigger the transcription of numerous genes either alleviating ER-Stress through the action of chaperones, ERAD or ERQC or initiate apoptosis.

In detail, upon oligomerization, the cytosolic domain of IRE1 α gains endoribonuclease activity and removes a 26-nucleotide sequence within the mRNA of *XBP1* in a process termed unconventional splicing (Figures 5 and 6). As a consequence, the reading-frame of the *XBP1* mRNA is altered, resulting in the translation of a longer variant of the XBP1 protein (spliced XBP1 or XBP1s). Whilst the role of unspliced XBP1 protein (XBP1u) remains largely unknown, XBP1s functions as an active transcription factor.²⁸⁵ Amongst the targets of XBP1s are several effectors of the UPR involving chaperones, components of ERAD and protein disulfide isomerases.^{281,286} In addition to the activation of XBP1, IRE1 α itself is also able to alleviate ER-stress by cleaving and destroying mRNAs of random proteins, thereby reducing the influx of secretory proteins into the ER.²⁸⁷

PERK - the second important mediator of the UPR – phosphorylates eIF2 α , a factor which inhibits the translation of capped mRNAs, thereby limiting the protein load in the ER (**Figure 6**). On the other hand, eIF2 α also initiates the translation of selected proteins, such as ATF4. ATF4 itself is a transcription factor regulating a variety of processes to alleviate ER-stress, but also binds the promoter of the gene *CHOP*, which is known to stimulate apoptosis.^{277,281,288}

As mentioned earlier, the third major mediator of the UPR, ATF6 α , gets activated by translocation to the Golgi apparatus followed by phosphorylation and protease-mediated cleavage.^{284,289} As a result of these proteolytic activities, a phosphorylated cytosolic fragment of ATF6 α is released, which functions as a transcription factor binding to UPR target genes supporting protein folding, ER expansion and ERAD (**Figure 6**).²⁹⁰

At first glance, the separation of the UPR according to the three transmembrane mediators IRE1 α , PERK and ATF6 α seems to be straight forward. However, numerous studies revealed that these three major UPR branches are highly intertwined and do not function as separate processes. Amongst the targets of the proteolytically cleaved ATF6 α transcription factor, for example, are *XBP1* and *BiP*, which are essential for the IRE1 α -branch and for the activation of the UPR in general, respectively.²⁹¹ Furthermore, ATF4, one of the downstream targets of PERK, was shown to induce the expression of IRE1 α , thereby increasing the splicing ratio of *XBP1* mRNA.²⁹²

1.6 Aim of this Thesis

Mutations in the *SRP54* gene have recently been identified as novel drivers of SCN and its syndromic form SDS.¹ Ever since then, several case reports and studies addressed the hitherto unknown function of mutated *SRP54* as a disease causing gene and unveiled its heterogeneous clinical implications.^{2,3,237,239,276} Despite these advances, no transgenic animal model recapitulating the phenotypes observed upon *SRP54* defect exists yet, and the molecular details about the mechanisms leading to the disease are still largely unknown. However, the unexpectedly high prevalence of *SRP54* mutations as well as the nowadays trending pursuit of targeted therapies evoke the need for a better understanding of this disease, including an improved clinical classification, the uncovering of molecular mechanisms as well as the establishment of genotype-phenotype correlations.

The goal of this thesis is to contribute to the understanding of *SRP54*-driven CN and SDS by addressing the previously mentioned points. A necessity to achieve this goal in my eyes is the generation of an animal model, which adequately phenocopies the features observed in patients. A first step towards such a model system was already established by our lab in collaboration with the research group of Seiamak Bahram, when we described the defects observed in zebrafish *srp54* morphants.¹ However, morphants are prone to present with non-specific manifestations and injection is quite laborious, making morphants not optimally suited to eventually model human diseases successfully. Hence, the work described in this thesis aimed to establish the first stable transgenic zebrafish *in vivo* model of *SRP54* deficiency with the intention to gain novel insights into the mechanisms leading to the development of this disease.

The results presented in this thesis do not only demonstrate the reliability and accuracy by which *SRP54*-driven manifestations can be translated from a transgenic zebrafish model to a human background, but also substantially increase the molecular understanding of *SRP54* deficiencies and promise to eventually open the gates for the establishment of genotype-phenotype relationships and for the development of novel therapeutic approaches.

2 Results

2.1 *SRP54* mutations induce Congenital Neutropenia via dominant-negative effects on *XBP1* splicing

***SRP54* mutations induce Congenital Neutropenia via dominant-negative effects on *XBP1* splicing.** Christoph Schürch, Thorsten Schaefer, Joëlle Seraina Müller, Pauline Hanns, Marlon Arnone, Alain Dumlin, Jonas Schärer, Irmgard Sinning, Klemens Wild, Julia Skokowa, Karl Welte, Raphael Carapito, Seiamak Bahram, Martina Konantz, Claudia Lengerke; *SRP54* mutations induce Congenital Neutropenia via dominant-negative effects on *XBP1* splicing. *Blood* 2020; blood.2020008115. doi: <https://doi.org/10.1182/blood.202000811>



American Society of Hematology
2021 L Street NW, Suite 900,
Washington, DC 20036
Phone: 202-776-0544 | Fax 202-776-0545
editorial@hematology.org

SRP54 mutations induce Congenital Neutropenia via dominant-negative effects on *XBPI* splicing

Tracking no: BLD-2020-008115R1

Christoph Schürch (University Hospital Basel and University of Basel, Switzerland) Thorsten Schaefer (University Hospital Basel and University of Basel, Switzerland) Joëlle Müller (University Hospital Basel and University of Basel, Switzerland) Pauline Hanns (University Hospital Basel and University of Basel, Switzerland) Marlon Arnone (University Hospital Basel and University of Basel, Switzerland) Alain Dumlin (University Hospital Basel and University of Basel, Switzerland) Jonas Schärer (University Hospital Basel and University of Basel, Switzerland) Irmgard Sinning (Heidelberg University, Germany) Klemens Wild (Heidelberg University, Germany) Julia Skokowa (University Hospital Tuebingen, Germany) Karl Welte (Klinikum University Tuebingen, Germany) Raphael Carapito (University of Strasbourg, France) Seiamak Bahram (Faculté de Medecine, France) Martina Konantz (University Hospital Basel and University of Basel, Switzerland) Claudia Lengerke (University Hospital Tübingen, Germany)

Abstract:

Heterozygous *de novo* missense variants of *SRP54* were recently identified in patients with congenital neutropenia (CN), displaying symptoms overlapping with Shwachman-Diamond-Syndrome (SDS).¹ Here, we investigate *srp54* KO zebrafish as the first *in vivo* model of *SRP54* deficiency. *srp54*^{-/-} zebrafish are embryonically lethal and display, next to severe neutropenia, multi-systemic developmental defects. In contrast, *srp54*^{+/-} zebrafish are viable, fertile and only show mild neutropenia. Interestingly, injection of human *SRP54* mRNAs carrying mutations observed in patients (T115A, T117Δ and G226E) aggravated neutropenia and induced pancreatic defects in *srp54*^{+/-} fish, mimicking the corresponding human clinical phenotypes. These data suggest that the variable phenotypes observed in patients may be due to mutation-specific dominant negative effects on the functionality of the residual wildtype *SRP54* protein. Consistently, overexpression of mutated *SRP54* also induced neutropenia in wildtype fish and impaired granulocytic maturation of human promyelocytic HL-60 cells as well as of healthy cord-blood derived CD34⁺ HSPCs. Mechanistically, *srp54* mutant fish and human cells show impaired unconventional splicing of the transcription factor X-box binding protein 1 (*Xbp1*). Vice-versa, *xbp1* morphants recapitulate phenotypes observed in *srp54* deficiency and, importantly, injection of spliced, but not unspliced *xbp1* mRNA rescues neutropenia in *srp54*^{+/-} zebrafish. Together, these data indicate that *SRP54* is critical for the development of various tissues, with neutrophils reacting most sensitively to *SRP54* loss. The heterogenic phenotypes observed in patients, ranging from mild CN to SDS-like disease, may be due to different dominant negative effects of mutated *SRP54* proteins on downstream *XBPI* splicing, which represents a potential therapeutic target.

Conflict of interest: No COI declared

COI notes:

Preprint server: No;

Author contributions and disclosures: CS, MK and CL designed the study, analyzed the data, and wrote the manuscript. CS, MK, PH, JSM and JS (Basel) performed zebrafish experiments and interpreted data. CS and TS performed *in vitro* experiments and interpreted data. RC, SB, KW and JS (Tübingen) interpreted data. All authors contributed to the writing and approved the final version of the manuscript.

Non-author contributions and disclosures: No;

Agreement to Share Publication-Related Data and Data Sharing Statement: Data can be shared via email to the corresponding authors

Clinical trial registration information (if any):

Title: *SRP54* mutations induce Congenital Neutropenia via dominant-negative effects on *XBP1* splicing

Running Title: Mutant *SRP54* induces CN by impairing *XBP1* splicing

Christoph Schürch¹, Thorsten Schaefer¹, Joëlle S. Müller¹, Pauline Hanns¹, Marlon Arnone¹, Alain Dumlin¹, Jonas Schärer¹, Irmgard Sinning², Klemens Wild², Julia Skokowa³, Karl Welte³, Raphaël Carapito^{4,5,6}, Seiamak Bahram^{4,5,6}, Martina Konantz^{1,#}, Claudia Lengerke^{1,3,7, #}

¹Department of Biomedicine, University Hospital Basel, University of Basel, Basel, Switzerland

²Heidelberg University Biochemistry Center (BZH), Heidelberg, Germany

³Department of Internal Medicine, Hematology, Oncology, Clinical Immunology and Rheumatology, University Hospital Tuebingen, Tuebingen, Germany

⁴Laboratoire d'ImmunoRhumatologie Moléculaire, Plateforme GENOMAX, INSERM UMR_S 1109, Faculté de Médecine, Fédération Hospitalo-Universitaire OMICARE, Fédération de Médecine Translationnelle de Strasbourg (FMTS), Université de Strasbourg, Strasbourg, France

⁵LabEx TRANSPLANTEX, Faculté de Médecine, Université de Strasbourg, Strasbourg, France

⁶Service d'Immunologie Biologique, Plateau Technique de Biologie, Pôle de Biologie, Nouvel Hôpital Civil, Strasbourg, France

⁷Division of Hematology, University Hospital Basel, University of Basel, Basel, Switzerland

#equal contribution

Corresponding authors

Martina Konantz (martina.konantz@unibas.ch)

&

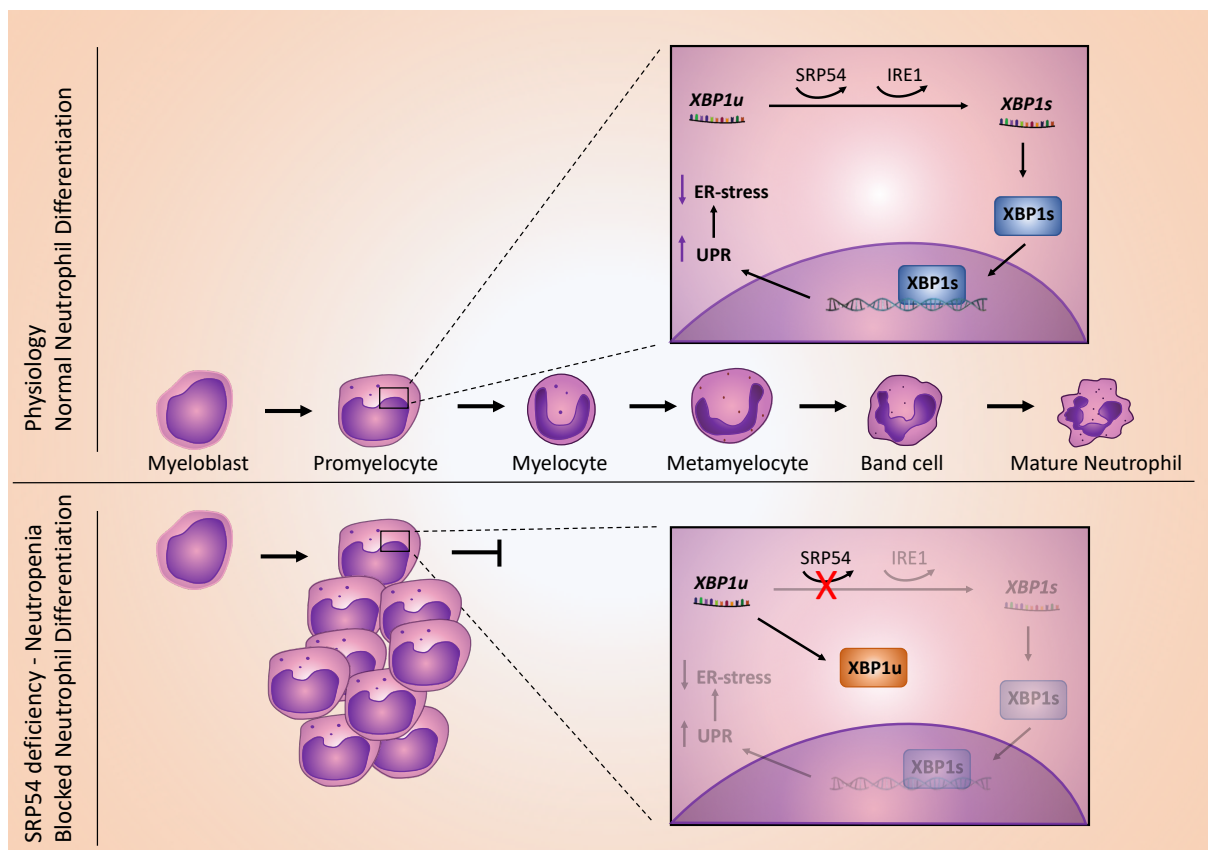
Claudia Lengerke (claudia.lengerke@med.uni-tuebingen.de)

Department of Biomedicine
University Hospital Basel, University of Basel, Basel, Switzerland
Hebelstr. 20
4031 Basel
Switzerland

Scientific category: Granulopoiesis

Key Points

- *SRP54* mutations induce Congenital Neutropenia and its syndromic form Shwachman-Diamond-Syndrome
- Impaired unconventional splicing of *XBP1* is a key player in *SRP54* mediated disease



Abstract

Heterozygous *de novo* missense variants of *SRP54* were recently identified in patients with congenital neutropenia (CN), displaying symptoms overlapping with Shwachman-Diamond-Syndrome (SDS).¹ Here, we investigate *srp54* KO zebrafish as the first *in vivo* model of *SRP54* deficiency. *srp54*^{-/-} zebrafish are embryonically lethal and display, next to severe neutropenia, multi-systemic developmental defects. In contrast, *srp54*^{+/-} zebrafish are viable, fertile and only show mild neutropenia. Interestingly, injection of human *SRP54* mRNAs carrying mutations observed in patients (T115A, T117Δ and G226E) aggravated neutropenia and induced pancreatic defects in *srp54*^{+/-} fish, mimicking the corresponding human clinical phenotypes. These data suggest that the variable phenotypes observed in patients may be due to mutation-specific dominant negative effects on the functionality of the residual wildtype SRP54 protein. Consistently, overexpression of mutated *SRP54* also induced neutropenia in wildtype fish and impaired granulocytic maturation of human promyelocytic HL-60 cells as well as of healthy cord-blood derived CD34⁺ HSPCs. Mechanistically, *srp54* mutant fish and human cells show impaired unconventional splicing of the transcription factor X-box binding protein 1 (Xbp1). Vice-versa, *xbp1* morphants recapitulate phenotypes observed in *srp54* deficiency and, importantly, injection of spliced, but not unspliced *xbp1* mRNA rescues neutropenia in *srp54*^{+/-} zebrafish.

Together, these data indicate that SRP54 is critical for the development of various tissues, with neutrophils reacting most sensitively to SRP54 loss. The heterogenic phenotypes observed in patients, ranging from mild CN to SDS-like disease, may be due to different dominant negative effects of mutated SRP54 proteins on downstream *XBP1* splicing, which represents a potential therapeutic target.

Introduction

Congenital Neutropenias (CN) encompass a group of heterogeneous inherited disorders characterized by recurrent infections and an elevated risk for the development of myeloid malignancies, next to the name giving reduction of neutrophil counts. Depending on the underlying genetic cause, additional defects may occur, such as exocrine pancreatic insufficiency in patients with Shwachman-Diamond Syndrome (SDS)²⁻⁵ or cardiac and urogenital malformations in patients harboring *G6PC3* mutations.^{4,6-8}

Mutations in the genes *ELANE* and *SBDS* range amongst the most common genetic aberrations in CN and its syndromic form SDS, respectively.^{4,9} In the past years, research increasingly focused on identifying other, hitherto unknown mutations in CN patients without established genetic background, eventually leading to the discovery of more than 20 genetic lesions associated with CN.^{4,10,11} By performing classical exome sequencing on *SBDS*-negative SDS-like patients we recently identified mutations in the gene encoding Signal Recognition Particle 54 (*SRP54*) as a novel cause of the disease.¹ *SRP54* is a part of the Signal Recognition Particle (SRP) ribonucleoprotein complex that mediates the co-translational targeting of nascent proteins to the endoplasmic reticulum (ER).^{1,12} Interestingly, heterozygous *SRP54* mutations associate with a wide phenotypic disease range, from mild CN to severe SDS. In our initial study, two of the three identified novel mutations were found in patients with SDS-like features (p.T115A, p.G226E), whilst the third one was found in a patient suffering from isolated CN (p.T117Δ). In accordance with our results, another study identified the p.T117Δ mutation to commonly occur in CN.^{13,14}

Here, we show that the heterogenic clinical phenotypes observed with different *SRP54* lesions can be explained by variable, mutation-specific dominant effects of the mutated on the residual wild-type *SRP54* protein. Furthermore, we provide in depth characterization of an *srp54* zebrafish knock-out (KO) mutant and demonstrate that *SRP54* mutations impair granulocytic maturation by hampering the unconventional splicing of the transcription factor *XBP1* which ultimately leads to unresolved ER stress and blockade of terminal neutrophil differentiation.

Methods

Zebrafish husbandry and genetic strains.

Zebrafish were bred and maintained at 28°C as described.¹⁵ Staging was performed in hours post fertilization (hpf) and according to Federation of European Laboratory Animal Science Associations (FELASA) and Swiss federal law guidelines.¹⁶ The following lines were used in this study: WT Tübingen strains, *Tg(mpo:eGFP)* and *srp54^{sa11820}*.^{17,18} Kaplan-Meier survival analysis was performed on *srp54^{+/-}*, *srp54^{-/-}* and WT siblings. Genotyping was performed on whole embryos, tail clips or dissociated cells according to standard protocols.¹⁹ PCR was performed using primers spanning the *sa11820* mutation (fwd: 5'-TTTGCAGATGCAGATGCACTTCTTAAAAT-3'; rev: 5'-CCATGCAATGACGTTTTGTT-3'). Sanger sequencing was performed using the before-mentioned reverse primer and data was analyzed using Lasergene SeqMan Pro software (DNASTAR inc. Madison, Wisconsin, USA).

mRNA injections

Capped mRNA of human *SRP54* mutants was produced as described previously.¹ For the generation of capped mRNA of zebrafish *xbp1s* and *xbp1u*, total RNA was extracted from approximately 50 pooled WT embryos according to Peterson & Freeman.²⁰ Reverse Transcription (RT) was performed using Multiscribe Reverse Transcriptase (Thermo Scientific™, Waltham, Massachusetts, USA). PCR using Phusion Polymerase (Thermo Scientific™) was performed on cDNA (*xbp1u*-fwd: 5'-CCA TCG ATT CGA ATT ATG GTC GTA GTT ACA GCA GGG AC-3', *xbp1u*-rev: 5'-GAG AGG CCT TGA ATT TCA GTT CAT TAA GGG CTT CCA GCT-3', *xbp1s*-fwd: 5'-CCA TCG ATT CGA ATT ATG GTC GTA GTT ACA GCA GGG AC-3', *xbp1s*-rev: 5'-GAG AGG CCT TGA ATT TCA GAC GCT AAT CAG TTG GGG G-3') and cloned into the PCS2+ vector by InFusion cloning (Takara Bio Europe, Saint-Germain-en-Laye, France). Capped mRNA was generated with the AmpliCap SP6 High Yield Message Maker Kit (CELLSCRIPT, Madison, WI, USA) and purified with ammonium acetate according to standard protocols.

Embryos were injected at the single-cell stage using mRNA concentrations of 50 ng/μl. Phenol red (0.05%) (Sigma-Aldrich®, St. Louis, MI, USA) was added as an injection tracer. Embryos were raised to appropriate stages and fixed in 4% paraformaldehyde (PFA) in PBS for further analyses. For rescue experiments, human WT and mutated *SRP54* mRNAs were generated as described¹.

Injection of Morpholino Oligonucleotides (MO)

An *xbp1* splice MO skipping Exon 2 to prevent pre-mRNA splicing was synthesized by Gene Tools (Gene Tools, LLC, Philomath, OR, USA): ACAATGGTCAAAGTACCTCCAGCTC. The morpholino was validated by RT-PCR. The primers were designed in the exons before and after Exon 2 respectively (fwd: CCTCTGGACCACCACTGAGA; rev: CCAGTCTCTGTCTCAGCTCC). Embryos were injected at the single-cell stage. Phenol red (0.05%) (Sigma-Aldrich) was added as an injection

tracer. Embryos were raised to appropriate stages and fixed in 4% paraformaldehyde (PFA) in PBS for further analyses.

WISH and flow cytometry

WISH was performed as described previously.^{1,21} Positive cells from WISH were semi-automatically counted using Fiji software,²² which was also used to measure changes in the pancreas size. For histopathological analyses, fish were fixed according to standard procedures. Fixed embryos were then automatically prepared and subsequently paraffin embedded using the Tissue Processor TPC15 and the TBS88 Parafin Embedding System (Meditate GmbH, Burgdorf, Germany) and cut into 5 μm thick slices with the help of the Microtom HM430 (Thermo ScientificTM). Pictures were taken with a Leica DM 2000 LED microscope.

For flow cytometry, single dechorionated transgenic embryos were dissociated into single cells as previously described¹ in a 96-well plate. The number of fluorescence-labeled cells was then determined on a Beckman Coulter CytoFlex flow cytometer and data analyzed using FlowJo software (FlowJo LCC, Ashland, OR, USA). Remaining cells were used for genotyping as described above.

Neutrophil Migration Assay

Tg(srp54^{+/-}, mpo:GFP) zebrafish were crossed to *Tg(srp54^{+/-})* and their progeny was raised to 48 hpf. At 48 hpf, tail fin wounding was performed as described previously.¹ *mpo*-positive cells were counted automatically using FIJI software.²² Imaging was performed with a Leica SP5-II-MATRIX microscope.

Isolation of Whole Kidney Marrow (WKM) and flow cytometric analysis

2-year-old *Tg(mpo:GFP)* and *Tg(srp54^{+/-}; mpo:GFP)* zebrafish were euthanized and WKM was isolated according to LeBlanc et al.²³ Flow cytometric analysis was performed following previously described gating strategies.²⁴

Neutrophil Differentiation Assay

cDNA encoding for human *SRP54* (wt) or its derived mutant forms p.T115A, p.T117 Δ , and p.G226 were PCR amplified from pCS2 source vectors¹ (primer fwd: 5'-GCG AGA TCG ATC ACC ATG GTT CTA GCA GAC CTT GG-3'; rev: 5'-CTG ACA TCG ATT TAC ATA TTA TTG AAT CCC A-3') and sub-cloned into an SFFV overexpression (OE) vector using the ClaI site. Sequence verified plasmids were lentivirally integrated into promyeloid HL-60 cells (ATCC CCL-240) according to standard procedures and selected for co-transduced IRES/GFP by FACS (2x). Resultant *SRP54* OE cells were propagated in RPMI medium supplemented with 10% FCS and antibiotics, and granulocytic cell differentiation induced with 1 μM ATRA (Sigma-Aldrich®), as described.^{25,26} On day 6, nuclear lobulation was quantified as an indicator of neutrophilic differentiation²⁷ in Hematoxylin and Eosin (H&E) stained cytopspins (microscope: Leica DM 2000 LED, 40x objective, LAS EZ software), and granulocytic differentiation further assessed by respective surface staining (APC/Cy7 anti-human CD11b,

BioLegend, San Diego, CA, USA; APC Mouse anti-human CD15, BD Biosciences, San Jose, CA, USA; PE-Cy5 Mouse anti-human CD16, BD Biosciences) and flow cytometry (Fortessa, BD, Franklin Lakes, NJ, USA)

Isolation and differentiation of CD34⁺ HSPCs

Human cord blood samples of healthy newborn babies of both sexes were collected at the University Hospital Basel upon availability. Mononuclear cells were enriched by a ficoll gradient (Biocoll, Merck Millipore, Darmstadt, Germany) and CD34⁺ progenitors were purified by MACS. Purified cells were cultured in IMDM medium supplemented with IL-3 and SCF as described by Gupta et al.²⁸ After one day, the cells were lentivirally transduced with the beforehand described plasmids overexpressing either WT or p.G226E *SRP54* according to standard protocols. Subsequently, differentiation of transduced cells was carried out as described by Gupta et al.²⁸ Maturation was assessed by flow cytometric analyses of CD11b surface expression on cells that are double-positive for CD15 and CD16 (PE anti-human CD11b, BioLegend; APC Mouse anti-human CD15, BD Biosciences; PE-Cy5 Mouse anti-human CD16, BD Biosciences).

Tunicamycin treatment

Zebrafish: *Tg(srp54^{+/+}, mpo:GFP)* zebrafish were crossed with *Tg(srp54^{+/+})* fish and their progeny was raised to 24 hpf. At 24 hpf, embryos were treated with 2 µg/ml Tunicamycin (Tm, Sigma-Aldrich®) and incubated for 24 hours.²⁹ At 48 hpf, zebrafish embryos were dissociated into single cells as previously described.¹ 10% of the whole cell suspension was used for genotyping of the fish, whilst the remaining 90% were either used as input for qRT-PCR or for flow cytometric analysis of neutrophil counts.

HL-60 cell line: Transduced cells were treated with 5 µg/ml Tm for 5 hours, washed once with PBS and then analyzed by qRT-PCR.

qRT-PCR

Total RNA was extracted from cell suspensions of dissociated single embryos and transduced HL-60 cells using the PicoPure RNA isolation Kit (Thermo Scientific™). cDNA was generated by RT using Multiscribe Reverse Transcriptase (Thermo Scientific™) and later diluted 1/10 and used as input for real-time PCR. Real-time PCR was performed on an Applied Biosystems™ 7500 Real-Time PCR System (Thermo Scientific™) using FastStart Universal SYBR Green Master (Rox) (Sigma-Aldrich®) (xbp1s-fwd: 5'-TGT TGC GAG ACA AGA -3', xbp1s-rev: 5'-CCT GCA CCT GCT GCG GAC T-3', for *aff4*, *bip*, *chop* see Vacaru et al.³⁰, for *XBP1s* and *GAPDH* see Yoon et al.³¹).

Immunoblotting

Transduced HL-60 cells were disrupted in 1x Lysis Buffer (#9803, Cell Signaling, Danvers, MA, USA) supplemented with Protease/Phosphatase Inhibitor Cocktail (#78442, Thermo Scientific™) and cleared by centrifugation (15 min, 21.000 rcf, 4 °C). Cleared protein lysates were denatured with 4x Laemmli buffer.

5-10 zebrafish embryos (48 hpf) were dechorionated, deyolked and homogenized with a microfuge pestle in SDS sample buffer according to Westerfield.³²

HL-60 cells or zebrafish cell lysates respectively were separated over 12% bis-acrylamide (#161-0148, BioRad, Hercules, CA, USA) gels by Disc-SDS-PAGE, and transferred onto PVDF membrane (#10600021, Amersham, GE Healthcare Life Sciences, Chalfont St. Giles, UK) in a semi-dry blotting apparatus (Trans-Blot Turbo, BioRad). Membranes were blocked with 10% w/v nonfat dry milk (#9999S, Cell Signaling Technology (CST), Danvers, MA, US) diluted in TBS 0.1% Tween-20 (p1379, Sigma Aldrich®) and proteins stained with the following primary antibodies: anti-SRP54 (GTX115041, GeneTex Inc, Irvine, CA, USA) and anti-GAPDH (#5174, Cell Signaling Technologies, CST, used for human samples; #60004-1-Ig, Proteintech group, Rosemont, IL, USA, used for zebrafish samples). Proteins were detected by ECL reaction involving the HRP-linked anti-rabbit (#7074) or HRP-linked anti-mouse (#7076S) secondary reagent (CST).

Results

Loss of *srp54* induces neutropenia in zebrafish

To understand the phenotype-genotype relationship in *SRP54* deficiency, we characterized a novel zebrafish *srp54* mutant (*srp54*^{sa11820}), which carries a 3' proximal Adenosine to Thymidine transversion causing a premature stop codon in the N-Domain of *srp54*, effectively knocking out the gene function (**Figure 1A; Figure S1A**).¹⁸ Phenotypic analysis revealed that *srp54*^{sa11820/sa11820} (referred to as *srp54*^{-/-}) embryos are developmentally impaired showing broad systemic defects such as the absence of blood flow, heart edema, reduced body size, pronounced body curvature and other skeletal abnormalities (**Figure 1B; Figure S1B**). As a result of these developmental defects, *srp54*^{-/-} zebrafish are embryonically lethal, with first deaths being observed already before 60 hours post-fertilization (hpf) and no embryo surviving after 72 hpf (**Figure 1C**). *srp54*^{+/sa11820} (referred to as *srp54*^{+/-}) zebrafish on the other hand are viable and fertile and do not show any profound developmental defects (**Figure 1B - C**), indicating that the residual wildtype (from here on referred to as WT) *srp54* allele is sufficient to sustain tissue development. Of note, *srp54*^{-/-} fish are incapable to break the chorion, which is in line with the assumption that protein secretion is impaired upon *srp54* deficiency and might play a central role in the phenotypic manifestation (**Figure 1D**).

However, whole mount *in situ* hybridization (WISH) of 48 hpf old embryos using neutrophil specific probes against *myeloperoxidase* (*mpo*) and *lysozyme C* (*lyz*) indicated reduced neutrophil numbers in both *srp54*^{-/-} as well as *srp54*^{+/-} embryos compared to WT, with the effect being less severe in *srp54*^{+/-} (**Figure 1E - F**). These findings were confirmed by flow cytometric analyses using neutrophil specific transgenic lines (**Figure S1C**).

Interestingly, flow cytometric analyses of whole kidney marrow (WKM) (**Figure S1D - E**) in 2-year-old adult fish did not show differences in neutrophil counts between *srp54*^{+/-} and WT fish, temporarily restricting the neutropenia of *srp54*^{+/-} fish to early embryogenesis. This is in line with data from patients with neutropenia indicating that neutrophil counts can improve with age.³³

Assessment of the size of the exocrine pancreas as a second hallmark of SDS by WISH using trypsin (*try*) specific probes showed no differences between WT and *srp54*^{+/-} fish (**Figure 1G**). Analyzing the exocrine pancreas of *srp54*^{-/-} embryos was not feasible, as these fish die earlier than 72 hpf, when the first assessment of pancreas development can be performed in zebrafish embryos.

Of note, injection of human WT *SRP54* mRNA was able to transiently rescue embryonic lethality and neutropenia in *srp54*^{-/-} fish (**Figure S1F - G**).

To investigate whether blood cell lineages other than granulocytes are affected by *srp54* KO, we performed WISH of WT, *srp54*^{+/-} and *srp54*^{-/-} zebrafish embryos using *globin*, *runx1/c-myb* or *rag1* probes, specific for erythrocytes, hematopoietic stem and progenitor cells (HSPCs) and lymphocytes respectively (**Figure S2**). WISH using *globin* specific probes revealed no differences between WT and *srp54*^{+/-} embryos. In *srp54*^{-/-} fish, on the other hand, no *globin* signal was detectable in the periphery, indicating the absence of blood circulation due to heart edema. In agreement with that, *globin* signals were accumulating in the zebrafish heart (**Figure S2**).

runx1/c-myb as well as *rag1* specific probes showed no significant differences between the assessed genotypes (**Figure S2**). Of note, *rag1* expression could not be assessed in *srp54*^{-/-} embryos, since T-cells are not detectable yet in the thymus before *srp54*^{-/-} fish start to die.

Overexpression of mutated *SRP54* induces an SDS-like phenotype in zebrafish embryos

As all *SRP54* mutations in patients are heterozygous, we aimed to elucidate whether the defects are dominant negative or functional nulls. We injected capped, human mRNA of healthy and mutated *SRP54* into *srp54*^{+/-} zygotes. After 2 dpf and 3 dpf, respectively, we performed WISH using *mpo* and *trypsin* specific probes. Interestingly, injection of T115A, T117Δ and G226E *SRP54* mutants reduced the number of neutrophils and the size of the exocrine pancreas, suggesting potential dominant negative effects. Of note, T117Δ had less severe impacts compared to T115A and G226E, matching the phenotypes observed in patients (**Figure 2A - D**).¹ To further investigate the beforehand mentioned dominant negative effects, we injected capped, human mRNA of either WT *SRP54* or mutated *SRP54* into WT zygotes and again performed WISH using *mpo* and *trypsin* specific probes at 2 dpf and 3 dpf, respectively. Consistently, overexpression of mutated *SRP54* mRNA induced SDS phenotypes with T117Δ causing the least severe defects (**Figure S3A - B**), while injection of WT *SRP54* mRNA as control showed no effects. To assess the effects of mutated *SRP54* in a genetic null background with no healthy *srp54* alleles, we injected the three different mutated human mRNAs into *srp54*^{-/-} fish (**Figure S4**). Whilst T115A and G226E did not rescue the neutrophil counts, a partial rescue was observed upon T117Δ injection, indicating residual functionality of this particular mutated protein version. However, ectopically applied T117Δ *srp54* exerts detrimental effects on the healthy Srp54 protein (**Figure 2 and Figure S3**), indicating that this mutant variant also acts in a dominant-negative way (**Figure S4**).

To investigate, whether neutrophils were also qualitatively impaired by *SRP54* mutations, we performed neutrophil migration assays in *srp54*^{+/-} zebrafish. After inducing a tail wound in 2 dpf zebrafish embryos followed by incubation for 8 hours, the total number of neutrophils as well as the number of neutrophils at the injury site were measured (**Figure 2E - H**). Total numbers of neutrophils showed the same trends as already observed in non-injured embryos: *srp54*^{+/-} displayed less neutrophils compared to WT embryos, and injection of G226E human mRNA further reduced the neutrophil counts in a dominant negative manner (**Figure 2F**). Indicating persistent functional integrity of residual neutrophils though, the number of neutrophils at the injury site was not significantly altered between the different *srp54* genotypes and also not upon G226E injection (**Figure 2G**). Given the differences in total neutrophil counts and yet the constant number of neutrophils at the injury site, the relative proportion of cells at the injury site was even increased in *srp54*^{+/-} or upon G226E mRNA injection. In sum, these data suggest that neutrophil migration to an injury site is neither impaired in *srp54*^{+/-} embryos alone nor in *srp54*^{+/-} embryos injected with G226E mRNA, and that the residual functional Srp54 protein in these fish is sufficient to sustain the migratory ability of neutrophils (**Figure 2H**).

Dominant negative effects of *SRP54* mutations are conserved in human cells

To explore the conservation of the dominant negative effects of mutated *SRP54* in human cells, we first lentivirally transduced the promyelocytic HL-60 cell line known to differentiate upon all-trans retinoic acid (ATRA) treatment, with the three identified *SRP54* mutations (T115A, T117Δ and G226E, **Figure 3A**). Successful integration and expression of proteins was assessed by Western Blotting (**Figure 3B**). After treatment with ATRA for six days, the majority of cells showed neutrophil characteristics and expressed CD15 and CD16 (**Figure S5A and B**).³⁴ To visualize potential impairment by the expression of mutant *SRP54*, we assessed nuclear lobulation as a feature of granulocytic differentiation using H&E stained cytoplots (**Figure 3A and C**). Compared to WT transduced and empty control cells, the cells expressing mutated *SRP54* alleles showed markedly reduced lobulation of neutrophilic nuclei (**Figure 3D**). Additionally, the levels of CD11b, a surface marker of mature granulocytes, were significantly decreased upon T115A and G226E expression (**Figure 3E and F**). Of note, T117Δ affected granulocytic differentiation to a lower degree compared to T115A and G226E, again revealing the overall milder dominant negative effects of T117Δ which is consistent with its expression in CN rather than in SDS-like disease.

***SRP54* mutant alleles impair granulocytic differentiation of CD34⁺ cord blood cells**

Importantly, similar results were observed with transduced healthy hematopoietic cord blood derived CD34⁺ cells, where flow cytometric analyses of CD11b surface levels of CD15 and CD16 double positive cells revealed that exogenous expression of p.G226E significantly impaired *in vitro* differentiation towards neutrophil fate compared to WT *SRP54* transduced cells (**Figure 4A - D; Figure S6A - B**). Of note, exclusively the exogenous expression of p.G226E *SRP54*, but not p.T115A and p.T117Δ was investigated in CD34⁺ HSPCs, as the most profound phenotypes were expected with this mutation according to previous findings and patient data.

Insufficient *xbp1* splicing drives the SDS-like phenotype in *srp54* defective zebrafish embryos

XBP1 is one of the key transcription factors involved in the unfolded protein response (UPR).³⁵⁻³⁷ However, it only functions as an active transcription factor, if its mRNA is cleaved by the transmembrane endoribonuclease IRE1 in a process termed unconventional splicing. In conditions of ER-stress, unconventional splicing of *XBP1* predominantly takes place at the ER-membrane.^{38,39} The unspliced mRNA of *XBP1* (*XBP1u*) is thereby transported to the ER-membrane in a complex together with the ribosome and its own nascent polypeptide chain in an SRP-dependent manner (**Figure 5A**).⁴⁰ This dependence on a functional SRP and its previously established importance for neutrophil differentiation⁴¹ made us hypothesize that the splicing of *XBP1* mRNA might be a key factor contributing to the phenotypic manifestation of *SRP54* mutations in patients.

To verify our hypothesis, we knocked down *xbp1* in zebrafish embryos by MO injection (**Figure S7A and B**). Notably, alike *srp54*^{-/-} embryos, *xbp1* morphants were incapable to break the chorion (**Figure 5B** and Bennet et al.).⁴² Furthermore, WISH using *lyz* and *trypsin* specific probes revealed a significant reduction of the number of neutrophils and of the size of the exocrine pancreas (**Figure 5B**

- D), whereas WISH using *globin*, *runx1/c-myb* or *rag1* specific probes did not show any additional hematopoietic impairment (**Figure S7C and D**).

In a next step, we analyzed the levels of spliced *xbp1* (*xbp1s*) in uninjected WT, *srp54*^{-/-} and *srp54*^{+/-} zebrafish embryos and upon injection of G226E mutated human *SRP54* mRNA into *srp54*^{+/-} embryos (**Figure 5E**). qRT-PCR of total body cells revealed that *srp54*^{-/-} embryos showed increased *xbp1* splicing, indicating that the splicing of *xbp1* is not completely abolished upon homozygous *srp54* KO (**Figure 5F**). In order to determine if *xbp1* splicing is impaired in *srp54* defective zebrafish, we experimentally induced ER-stress in all genotypes by treating the embryos with Tunicamycin (Tm) (**Figure 5E**). Interestingly, after Tm treatment, *srp54*^{-/-} and *srp54*^{+/-} injected with G226E mRNA showed reduced levels of *xbp1s* compared to WT and *srp54*^{+/-} zebrafish (**Figure 5G - H**). These effects were specific for *xbp1s*, as the expression of other UPR players such as *atf4*, *bip* and *chop* was unaffected by *srp54* KO (**Figure S7E**).

To analyze if the impaired splicing capability of *srp54*^{-/-} and G226E injected *srp54*^{+/-} fish induced neutropenia, we evaluated the number of neutrophils by flow cytometry of DMSO and Tm treated embryos. Strikingly, Tm treatment significantly lowered the number of Mpo⁺ cells in *srp54*^{-/-} and G226E injected *srp54*^{+/-} fish (**Figure 5I**), as compared to DMSO treatment.

Finally, to functionally explore the relevance of impaired *xbp1* splicing for the phenotypes associated with *srp54* deficiency, we injected zebrafish mRNA of *xbp1s* and *xbp1u* into *srp54*^{+/-} embryos. Indeed, only *xbp1s* mRNA, but not *xbp1u* mRNA, was able to significantly rescue the neutrophil numbers in *srp54* deficient embryos (**Figure 5J - K**).

Impaired *XBP1* splicing is conserved in human *SRP54* mutant cells

To uncover potential conservation of the impairment of *XBP1* splicing in human cells, we treated transduced human HL-60 cells expressing either WT or G226E SRP54 with Tunicamycin and measured the levels of *XBP1s*. Importantly, G226E SRP54 expressing cells showed significantly lower levels of *XBP1s* after Tm treatment compared to WT transduced cells and presented with a more than 5-fold decreased capability to splice *XBP1u* under ER-stress conditions, thereby matching our findings in zebrafish *srp54* mutants (**Figure 6A - C**).

Discussion

Our data in homozygous *srp54* KO zebrafish embryos indicate that the Srp54 protein is critically required for the development of multiple tissues with neutrophils as cells with the highest dependency on proper SRP54 levels. The fact that complete loss of *srp54* is embryonically lethal might be the reason why no homozygous *SRP54* defects were identified in patients yet.^{1,14} Interestingly, *srp54*^{+/-} zebrafish are viable, healthy, fertile and only suffer from a mild form of neutropenia. Since all known patients with *SRP54*-associated neutropenia carry heterozygous defects, but still show variable but also more severe clinical phenotypes, we hypothesized that the underlying mutations must have dominant negative effects that compete with, and may effectively override the endogenous SRP54 functions derived from the persisting WT allele. Exogenous expression of mutated human *SRP54* in (*srp54*^{+/-} or wildtype) zebrafish embryos as well as in human HL-60 cells or CD34⁺ HSPCs confirmed

these dominant negative effects. In detail, HL-60 cells and healthy cord blood derived CD34⁺ HSPCs showed impaired granulocytic differentiation upon transduction with mutated human *SRP54*, but not upon transduction with WT human *SRP54*, indicating that *SRP54* overexpression is not per se disease-inducing but that observed phenotypes are specifically mediated by pathologic effects of mutated *SRP54*.

Importantly, the granulocytic differentiation defects observed in HL-60 cells and CD34⁺ HSPCs represent a novel cellular process, which in addition to elsewhere described proliferative defects, ER-stress, apoptosis and autophagy contributes to the neutropenic phenotype associated with *SRP54* deficiency.¹⁴

Of note, the migratory function of neutrophils in zebrafish embryos was not altered upon heterozygous *srp54* KO and G226E expression. The absolute number of neutrophils at the injury site was constant amongst the different conditions, indicating that the residual functional Srp54 protein in the investigated embryos was sufficient to sustain the migration capacity of mutant neutrophils. This finding adds a novel perspective to previous results shown by Carapito et al.,¹ where MO driven knock down of *srp54* led to neutrophil migratory defects. Considering that *srp54* morphants had lower levels of functional Srp54 protein compared to the herein analyzed *srp54*^{+/-} or G226E injected fish (**Figure S1A**; also noticeable by the severe form of neutropenia and strong exocrine pancreatic defects compared to the only mild form of neutropenia and absent, or weak exocrine pancreatic defects, respectively), we can conclude that a certain level of WT Srp54 protein needs to be present to sustain the neutrophil migratory function.

Furthermore, the unaffected migratory ability of the neutrophils in the herein investigated zebrafish model indicates that increased infection rates observed in patients are probably rather due to the overall reduced numbers of neutrophils or other potentially affected functions such as the formation of neutrophil extracellular traps (NETs) or the release of enzymes.

To investigate why and how *srp54* defects specifically impair neutrophil differentiation, we aimed to understand the underlying mechanistic details. As shown before,¹⁴ *SRP54* mutations lead to ER-stress. The ER-stress conditions might be the reason why neutrophils, but no other blood cells are affected, since Tanimura et al. revealed that ER-stress needs to be absent and UPR active in order to allow neutrophil, but not macrophage differentiation.⁴¹ However, in the case of *SRP54* mediated CN, it has been unclear yet how elevated ER-stress develops. We hypothesized that the important UPR mediator XBP1 might be contributing to the disease manifestation, as its activation by unconventional splicing is dependent on the SRP, and *SRP54* knock down in HELA cells was associated with dampened *XBP1* splicing.⁴⁰ Of note, Bellanné-Chantelot et al. showed that the *XBP1s* is elevated in *SRP54* deficient patient cells compared to healthy control cells.¹⁴ However, assuming that ER stress was present in patient-derived cells, genes involved in UPR would naturally be upregulated. In order to allow a comparison regarding *xbp1* splicing, we thus sought to induce ER-stress also in control cells. Consequently, we treated zebrafish embryos as well as human HL-60 cells with Tunicamycin (Tm), a natural ER stress inducer. We here show that insufficient splicing of *XBP1* contributes to

elevated ER-stress levels in *SRP54* defective human cells and zebrafish and that knockdown of *xbp1* in zebrafish embryos phenocopies several characteristics of *srp54^{-/-}* mutants. Furthermore, exogenous expression of *xbp1s* in *srp54^{+/-}* zebrafish was able to rescue the neutropenic phenotype, directly linking impaired *xbp1* splicing to disease manifestation and advocating the IRE1-XBP1 axis as a potential therapeutic target of *SRP54* deficiencies.

In **Figure 7** we summarize our findings and provide a hypothetical model explaining how *SRP54* mutations may impair *XBP1* splicing. In this model, the binding of the SRP to the Signal Receptor (SR) is destabilized by mutations in *SRP54*. Consequently, *XBP1u* mRNA does not get in proximity to the ER membrane resident endonuclease IRE1 and cannot be spliced anymore, leading to the absence of the UPR mediator XBP1s, which eventually leads to unresolved ER-stress. The dominant negative effects of *SRP54* mutations are thus a result of the functionally impaired mutant *SRP54* protein competing with endogenous WT *SRP54* for signal peptides of proteins that need to be secreted. Thereby, the nascent chain/ribosome complexes of these proteins are not available anymore for the functional WT *SRP54* and cannot be transported to the ER membrane.

The herein proposed model is in agreement with the findings of Goldberg et al.⁴³, in which the deletion of threonine115 in *SRP54* leads to the destabilization of the SRP-SR complex.

Taken together, we here provide a stable *in vivo* model for studies on *SRP54* which reveals novel mechanistic insights into the function of *SRP54* and associated mutations in the regulation of ER stress response and neutrophil development. Given the ubiquitous expression of *SRP54* and its fundamental requirement for various developmental processes, dose-dependent *SRP54* effects likely play important roles in the pathophysiology of other tissues as well.

Acknowledgements

This work was supported by grants from the Swiss National Science Foundation (SNF) (149735, to CL); the INTERREG V European regional development fund (European Union) program (project 3.2 TRIDIAG, to RC, SB, and CL). SB's laboratory is funded by grants from the Agence Nationale de la Recherche (ANR) - ANR-11-LABX-0070_TRANSPLANTEX and MSD-Avenir grant AUTOGEN. We thank the members of the Imaging Core Facility of the Biozentrum, University of Basel, Switzerland and the DBM Microscopy Facility, Basel, Switzerland for assistance with imaging and the members of the DBM Flowcytometry Facility, Basel, Switzerland for assistance with flow cytometry.

Authorship Contributions

CS, MK and CL designed the study, analyzed the data, and wrote the manuscript. CS, MK, PH, JSM and JS (Basel) performed zebrafish experiments and interpreted data. CS, AD, MA and TS performed *in vitro* experiments and interpreted data. IS and KW (Heidelberg) performed *in silico* structure function mapping. RC, SB, KW (Tübingen) and JS (Tübingen) interpreted data. All authors contributed to the writing and approved the final version of the manuscript.

Disclosure of Conflicts of Interest

The authors have declared that no conflict of interest exists.

Data sharing

For original data, please email the corresponding author.

References

1. Carapito R, Konantz M, Paillard C, et al. Mutations in signal recognition particle SRP54 cause syndromic neutropenia with Shwachman-Diamond-like features. *J Clin Invest*. 2017;127(11):4090-4103.
2. Burroughs L, Woolfrey A, Shimamura A. Shwachman-Diamond syndrome: a review of the clinical presentation, molecular pathogenesis, diagnosis, and treatment. *Hematol Oncol Clin North Am*. 2009;23(2):233-248.
3. Babushok DV, Bessler M, Olson TS. Genetic predisposition to myelodysplastic syndrome and acute myeloid leukemia in children and young adults. *Leuk Lymphoma*. 2016;57(3):520-536.
4. Skokowa J, Dale DC, Touw IP, Zeidler C, Welte K. Severe congenital neutropenias. *Nat Rev Dis Primers*. 2017;3:17032.
5. Shwachman H, Diamond LK, Oski FA, Khaw KT. The Syndrome of Pancreatic Insufficiency and Bone Marrow Dysfunction. *J Pediatr*. 1964;65:645-663.
6. Boztug K, Appaswamy G, Ashikov A, et al. A syndrome with congenital neutropenia and mutations in G6PC3. *N Engl J Med*. 2009;360(1):32-43.
7. McDermott DH, De Ravin SS, Jun HS, et al. Severe congenital neutropenia resulting from G6PC3 deficiency with increased neutrophil CXCR4 expression and myelokathexis. *Blood*. 2010;116(15):2793-2802.
8. Notarangelo LD, Savoldi G, Cavagnini S, et al. Severe congenital neutropenia due to G6PC3 deficiency: early and delayed phenotype in two patients with two novel mutations. *Ital J Pediatr*. 2014;40:80.
9. Myers KC, Davies SM, Shimamura A. Clinical and molecular pathophysiology of Shwachman-Diamond syndrome: an update. *Hematol Oncol Clin North Am*. 2013;27(1):117-128, ix.
10. Zhang J, Barbaro P, Guo Y, et al. Utility of next-generation sequencing technologies for the efficient genetic resolution of haematological disorders. *Clin Genet*. 2016;89(2):163-172.
11. Stepensky P, Chacón-Flores M, Kim KH, et al. Mutations in EFL1, an SBDS partner, are associated with infantile pancytopenia, exocrine pancreatic insufficiency and skeletal anomalies in a Shwachman-Diamond like syndrome. *J Med Genet*. 2017;54(8):558-566.
12. Walter P, Blobel G. Purification of a membrane-associated protein complex required for protein translocation across the endoplasmic reticulum. *Proc Natl Acad Sci U S A*. 1980;77(12):7112-7116.
13. Carden MA, Connelly JA, Weinzierl EP, Kobrynski LJ, Chandrakasan S. Severe Congenital Neutropenia associated with SRP54 mutation in 22q11.2 Deletion Syndrome: Hematopoietic Stem Cell Transplantation Results in Correction of Neutropenia with Adequate Immune Reconstitution. *J Clin Immunol*. 2018;38(5):546-549.
14. Bellanné-Chantelot C, Schmaltz-Panneau B, Marty C, et al. Mutations in the SRP54 gene cause severe congenitally neutropenia as well as Shwachman-Diamond-like syndrome. *Blood*. 2018.
15. Dahm R, Nüsslein-Volhard C. Zebrafish: A Practical Approach. In: eds., ed. Oxford, England: Oxford University Press; 2002.
16. Warga RM, Kimmel CB. Cell movements during epiboly and gastrulation in zebrafish. *Development*. 1990;108(4):569-580.
17. Renshaw SA, Loynes CA, Trushell DM, Elworthy S, Ingham PW, Whyte MK. A transgenic zebrafish model of neutrophilic inflammation. *Blood*. 2006;108(13):3976-3978.

18. Kettleborough RN, Busch-Nentwich EM, Harvey SA, et al. A systematic genome-wide analysis of zebrafish protein-coding gene function. *Nature*. 2013;496(7446):494-497.
19. Wilkinson RN, Elworthy S, Ingham PW, van Eeden FJ. A method for high-throughput PCR-based genotyping of larval zebrafish tail biopsies. *Biotechniques*. 2013;55(6):314-316.
20. Peterson SM, Freeman JL. RNA isolation from embryonic zebrafish and cDNA synthesis for gene expression analysis. *J Vis Exp*. 2009(30).
21. Konantz M, Alghisi E, Müller JS, et al. Evi1 regulates Notch activation to induce zebrafish hematopoietic stem cell emergence. *EMBO J*. 2016.
22. Schindelin J, Arganda-Carreras I, Frise E, et al. Fiji: an open-source platform for biological-image analysis. *Nat Methods*. 2012;9(7):676-682.
23. LeBlanc J, Bowman TV, Zon L. Transplantation of whole kidney marrow in adult zebrafish. *J Vis Exp*. 2007(2):159.
24. Traver D, Paw BH, Poss KD, Penberthy WT, Lin S, Zon LI. Transplantation and in vivo imaging of multilineage engraftment in zebrafish bloodless mutants. *Nat Immunol*. 2003;4(12):1238-1246.
25. Tasseff R, Jensen HA, Congleton J, et al. An Effective Model of the Retinoic Acid Induced HL-60 Differentiation Program. *Sci Rep*. 2017;7(1):14327.
26. Breitman TR, Selonick SE, Collins SJ. Induction of differentiation of the human promyelocytic leukemia cell line (HL-60) by retinoic acid. *Proc Natl Acad Sci U S A*. 1980;77(5):2936-2940.
27. Olins AL, Olins DE. Cytoskeletal influences on nuclear shape in granulocytic HL-60 cells. *BMC Cell Biol*. 2004;5:30.
28. Gupta D, Shah HP, Malu K, Berliner N, Gaines P. Differentiation and characterization of myeloid cells. *Curr Protoc Immunol*. 2014;104:22F.25.21-22F.25.28.
29. Li J, Chen Z, Gao LY, et al. A transgenic zebrafish model for monitoring xbp1 splicing and endoplasmic reticulum stress in vivo. *Mech Dev*. 2015;137:33-44.
30. Vacaru AM, Di Narzo AF, Howarth DL, et al. Molecularly defined unfolded protein response subclasses have distinct correlations with fatty liver disease in zebrafish. *Dis Model Mech*. 2014;7(7):823-835.
31. Yoon SB, Park YH, Choi SA, et al. Real-time PCR quantification of spliced X-box binding protein 1 (XBP1) using a universal primer method. *PLoS One*. 2019;14(7):e0219978.
32. Westerfield M. The Zebrafish Book. Vol. 5. Eugene, USA: University of Oregon Press; 2007.
33. Dale DC. How I manage children with neutropenia. *Br J Haematol*. 2017;178(3):351-363.
34. Gustafson MP, Lin Y, Maas ML, et al. A method for identification and analysis of non-overlapping myeloid immunophenotypes in humans. *PLoS One*. 2015;10(3):e0121546.
35. Shen X, Ellis RE, Lee K, et al. Complementary signaling pathways regulate the unfolded protein response and are required for *C. elegans* development. *Cell*. 2001;107(7):893-903.
36. Yoshida H, Matsui T, Yamamoto A, Okada T, Mori K. XBP1 mRNA is induced by ATF6 and spliced by IRE1 in response to ER stress to produce a highly active transcription factor. *Cell*. 2001;107(7):881-891.
37. Calton M, Zeng H, Urano F, et al. IRE1 couples endoplasmic reticulum load to secretory capacity by processing the XBP-1 mRNA. *Nature*. 2002;415(6867):92-96.

38. Uemura A, Oku M, Mori K, Yoshida H. Unconventional splicing of XBP1 mRNA occurs in the cytoplasm during the mammalian unfolded protein response. *J Cell Sci.* 2009;122(Pt 16):2877-2886.
39. Wang Y, Xing P, Cui W, et al. Acute Endoplasmic Reticulum Stress-Independent Unconventional Splicing of XBP1 mRNA in the Nucleus of Mammalian Cells. *Int J Mol Sci.* 2015;16(6):13302-13321.
40. Kanda S, Yanagitani K, Yokota Y, Esaki Y, Kohno K. Autonomous translational pausing is required for XBP1u mRNA recruitment to the ER via the SRP pathway. *Proc Natl Acad Sci U S A.* 2016;113(40):E5886-E5895.
41. Tanimura A, Miyoshi K, Horiguchi T, Hagita H, Fujisawa K, Noma T. Mitochondrial Activity and Unfolded Protein Response are Required for Neutrophil Differentiation. *Cell Physiol Biochem.* 2018;47(5):1936-1950.
42. Bennett JT, Joubin K, Cheng S, et al. Nodal signaling activates differentiation genes during zebrafish gastrulation. *Dev Biol.* 2007;304(2):525-540.
43. Goldberg L, Simon AJ, Rechavi G, et al. Congenital neutropenia with variable clinical presentation in novel mutation of the SRP54 gene. *Pediatr Blood Cancer.* 2020;67(6):e28237.

Figure 1: *srp54*^{+/-} and *srp54*^{-/-} fish display neutropenia, but no overt pancreatic defects

(A) Structure of the human SRP54 NG domain. The cartoon shows the domain organization of SRP54, the sites of CN relevant single acid mutations (T115A, T117Δ, G226E; encircled) and the truncation product of the *srp54*^{sa11820} variant in our zebrafish mutant (N-terminal 14 residues, blue). A non-hydrolyzable GTP-analogue (GNP) taken from the SRP54/SRα structure is shown superposed (sticks) in the active site of the SRP54 G domain. (B) Representative pictures of *srp54*^{+/-}, *srp54*^{-/-} and WT siblings. Fish were mounted in methylcellulose and pictures taken with a Zeiss SteREO Discovery.V20 microscope. (C) Kaplan-Meier survival analysis of genotyped fish (at least n=45 embryos per condition from n=3 biological replicates). (D) Representative images of WT (top) and *srp54*^{-/-} embryos after 54 hpf. Note that *srp54*^{-/-} embryos are still inside the chorion. (E - F) Assessment of neutrophil counts in genotyped *srp54*^{+/-}, *srp54*^{-/-} and WT siblings using WISH for *mpo* (E) or *lyz* (F), respectively. Representative pictures are shown. Numbers below the representative pictures indicate the sum of embryos with the respective phenotype per total number of embryos analyzed in all replication experiments for the respective condition. Arrows indicate downregulation (↓). Shown are data from n=3 biological replicates with at least n=3-10 larvae per replicate. An ordinary Student's *t*-test was applied for statistical analysis: *P < 0.05; **P < 0.01; ***P < 0.005; ****P < 0.0001. (G) Representative pictures after WISH for *trypsin* in *srp54*^{+/-} and WT siblings at 96 hpf (left) and corresponding tissue slices (right).

Figure 2: Injections of mutated mRNAs into *srp54*^{+/-} embryos induce an SDS-like phenotype, but the residual neutrophils are sufficient to be adequately recruited to injury sites

(A - D) Injection of T115A, T117Δ or G226E human mRNA (from top to bottom) into *srp54*^{+/-} embryos. Shown are representative pictures (A - B) with the corresponding quantifications (C - D) after WISH for *mpo* (A and C) and *trypsin* (B and D). (E) Fluorescent confocal microscopy images 8 hours post tail fin injury are shown. Left: Brightfield; Middle: Fluorescence; Right: Merge. Yellow rectangle indicates the analyzed tail region. (F - H) Quantification of neutrophil migration of WT siblings, WT siblings injected with human G226E mRNA, *srp54*^{+/-}, *srp54*^{+/-} injected with human G226E mRNA. (F) Total number of *mpo*⁺ cells. (G) *mpo*⁺ cells at wound. (H) Fraction of migrating cells towards the injury site. Images were acquired with a Point Scanning Confocal Leica SP5-II-MATRIX microscope (10X magnification). Neutrophils were automatically counted using ImageJ software. n=3 biological replicates with at least n=2-3 larvae were used per replicate. An ordinary Student's *t*-test was applied for statistical analysis: *P < 0.05; **P < 0.01; ***P < 0.005; ****P < 0.0001.

Figure 3: Dominant negative effects of SRP54 mutations are conserved in the human HL-60 cell line and lead to differentiation defects

(A) Schematic overview of the experimental set up. (B) Western blots document elevated SRP54 protein expression (top) in HL-60 cells upon transduction with mutant or wt SRP54 constructs (as indicated). Non-transduced control cells (-) are shown on the left. The following expression-fold changes were deduced from area counts relative to empty control as quantified by FIJI software: wt 2.8; T115A 2.9; T117Δ 1.9; G226E 3.5. GAPDH was used as loading control and for normalization.

(C) Representative pictures of cells during ATRA driven HL-60 cell differentiation (left: blast cell, day 0; middle: lobulated neutrophil, day 3; right: multilobulated neutrophil, day 6). Pictures were taken from H&E stained cytoplots. **(D)** Quantification of H&E stained cytoplots after 6 days of ATRA treatment. Plotted is the fraction (y-axis) of blasts (black), lobulated nuclei (light grey) and multilobed nuclei (dark grey) of the indicated *SRP54* mutant alleles. Criteria for classification: No lobules = blasts; 1-5 lobules = lobulated; >5 lobules = multilobed. Statistics: Empty vs. *SRP54* (wt): blasts, ns; lobulated, ns; multilobed, ns; Empty vs. T115A: blasts, ns; lobulated, *; multilobed, *; Empty vs. T117Δ: blasts, ns; lobulated, ns; multilobed, ns; Empty vs. G226E: blasts, ns; lobulated, ***, multilobed, ***. **(E)** Histograms indicating CD11b surface staining on empty control, *SRP54* (wt), (T115A), (T117Δ), and (G226E) transduced HL-60 cells (top to bottom) as analyzed by flow cytometry. Red curves represent mock cells; blue curves represent ATRA treated cells. **(F)** Corresponding quantification of CD11b expression on empty control, *SRP54* (wt), T115A, T117Δ, and G226E transduced cells. Plotted is the geometric mean fluorescence intensity shift in the CD11b channel upon ATRA-treatment (y-axis) per indicated cell lines (x-axis). Note slightly reduced CD11b surface induction in T117Δ cells, but a significant differentiation block in cells expressing T115A and G226E mutant forms of *SRP54*. A student's *t*-test was applied for statistical analysis: **P* < 0.05; ***P* < 0.01; ****P* < 0.005; *****P* < 0.0001.

Figure 4: *SRP54* mutant alleles impair granulocytic differentiation of CD34⁺ cord blood cells

(A) Schematic overview of the experimental set up for isolation, lentiviral transduction and *in vitro* cultivation of CD34⁺ cord blood cells followed by flow cytometric analyses. **(B)** Gating strategy to identify CD15 and CD16 double positive neutrophils. **(C)** Histograms of flow cytometric analyses of CD11b levels of *SRP54* (wt, light grey) or G226E (dark grey) transduced and differentiated CD34⁺ cells. **(D)** Flow cytometric quantification of CD11b expression of transduced and differentiated CD34⁺ cells. Plotted is the geometric mean fluorescence intensity of WT and G226E transduced cells. A ratio paired *t* test was applied for statistical analysis: **P* < 0.05; ***P* < 0.01; ****P* < 0.005; *****P* < 0.0001.

Figure 5: Insufficient *xbp1* splicing drives the SDS phenotype in *srp54* defective zebrafish embryos

(A) Graphical representation of the unconventional splicing of *XBP1*. Left: Cell without or with moderate ER-Stress. Right: Cell under ER-Stress conditions. **(B)** Representative pictures of WT embryos compared to *xbp1* morphants. Top row: Pictures showing the incapability of *xbp1* morphants to hatch and break the chorion at 72 hpf. Middle row: WISH using *lyz* specific probes. Bottom row: WISH using *trypsin* specific probes. **(C)** Quantification of neutrophils using *lyz* specific probes. Plotted is the number of *lyz*⁺ cells. **(D)** Measurement of the exocrine pancreas using *trypsin* specific probes. Plotted is the size of the exocrine pancreas, which was semi-automatically measured using ImageJ software. An ordinary Student's *t*-test was applied for statistical analysis: **P* < 0.05; ***P* < 0.01; ****P* < 0.005; *****P* < 0.0001. **(E)** Schematic overview of the experimental set up to assess *xbp1* levels in zebrafish embryos. **(F)** ΔC_T values of *xbp1s* of dissolved cells from DMSO treated WT, *srp54*^{+/-}, *srp54*^{+/-} injected with human G226E mRNA and *srp54*^{-/-} (from left to right) measured by qRT-PCR. **(G)** ΔC_T values of *xbp1s* of dissolved cells from Tm treated WT, *srp54*^{+/-}, *srp54*^{+/-} injected with human

G226E mRNA and *srp54*^{-/-} (from left to right) measured by qRT-PCR. **(H)** Fold change of *xbp1s* expression upon Tm treatment compared to DMSO treatment. From left to right: WT, *srp54*^{+/-}, *srp54*^{-/-} injected with human G226E mRNA and *srp54*^{-/-}. n=3 biological replicates with at least n=2 larvae per replicate were used. **(I)** Percentage of Mpo⁺ cells of Tm treated compared to DMSO treated embryos measured by flow cytometry. *Tg(srp54*^{+/-}, *mpo:eGFP*) zebrafish were incrossed and their progeny was genotyped and analyzed by flow cytometry. A minimum of n=5 embryos was pooled and dissociated per biological replicate. Each dot represents a biological replicate. From left to right: WT, *srp54*^{+/-}, *srp54*^{-/-} injected with human G226E mRNA and *srp54*^{-/-}. **(J)** Representative images of WISH using *lyz* specific probes performed on *srp54*^{+/-} embryos either uninjected (top), injected with *xbp1s* mRNA (middle) or injected with *xbp1u* mRNA (bottom). **(K)** Quantification of the number of *lyz*⁺ cells. n=4 biological replicates with at least n=3 larvae per replicate were used. An ordinary Student's *t*-test was applied for statistical analysis: *P < 0.05; **P < 0.01; ***P < 0.005; ****P < 0.0001.

Figure 6: XBP1 splicing defects are conserved in human HL-60 cells with mutant SRP54 expression

(A) ΔC_T values of *XBP1s* expression of DMSO treated *SRP54* (WT) transduced H-L60 cells compared to *SRP54* (G226E) transduced HL-60 cells measured by qRT-PCR. **(B)** ΔC_T values of *XBP1s* of Tm treated *SRP54* (WT) transduced compared to *SRP54* (G226E) transduced HL-60 cells measured by qRT-PCR. **(C)** Fold change of *XBP1s* expression upon Tm treatment compared to DMSO treatment for *SRP54* (WT) and *SRP54* (G226E) transduced HL-60 cells. n=3 biological replicates were used. An ordinary Student's *t*-test was applied for statistical analysis: *P < 0.05; **P < 0.01; ***P < 0.005; ****P < 0.0001.

Figure 7: Model of impaired XBP1 splicing upon SRP54 mutations

The binding of the SRP to the Signal Receptor (SR) is destabilized by mutations in SRP54. Consequently, *XBP1u* mRNA does not get spliced by IRE1, leading to the absence of the UPR mediator XBP1s, which eventually leads to unresolved ER-stress.

Figure 1

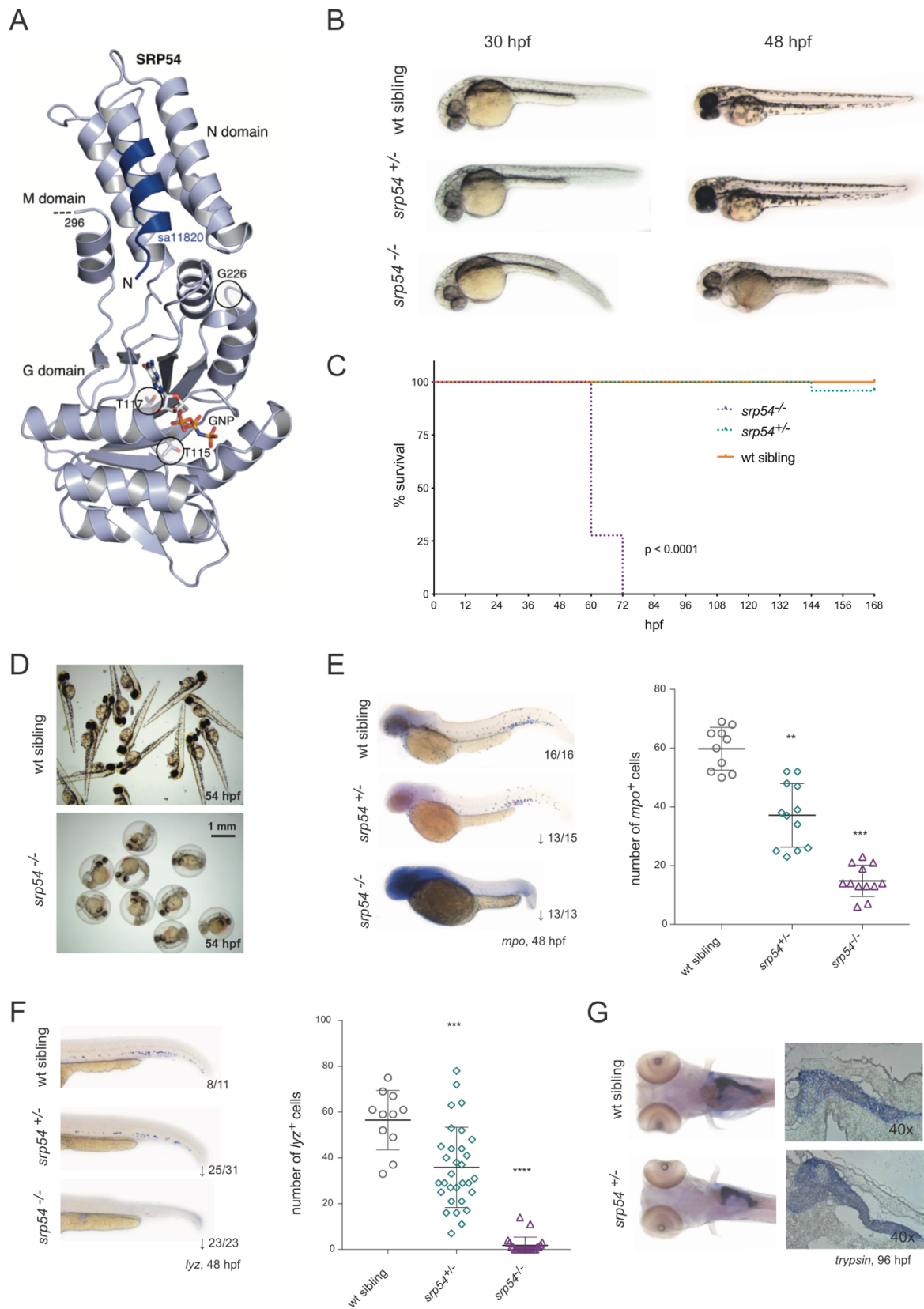


Figure 2

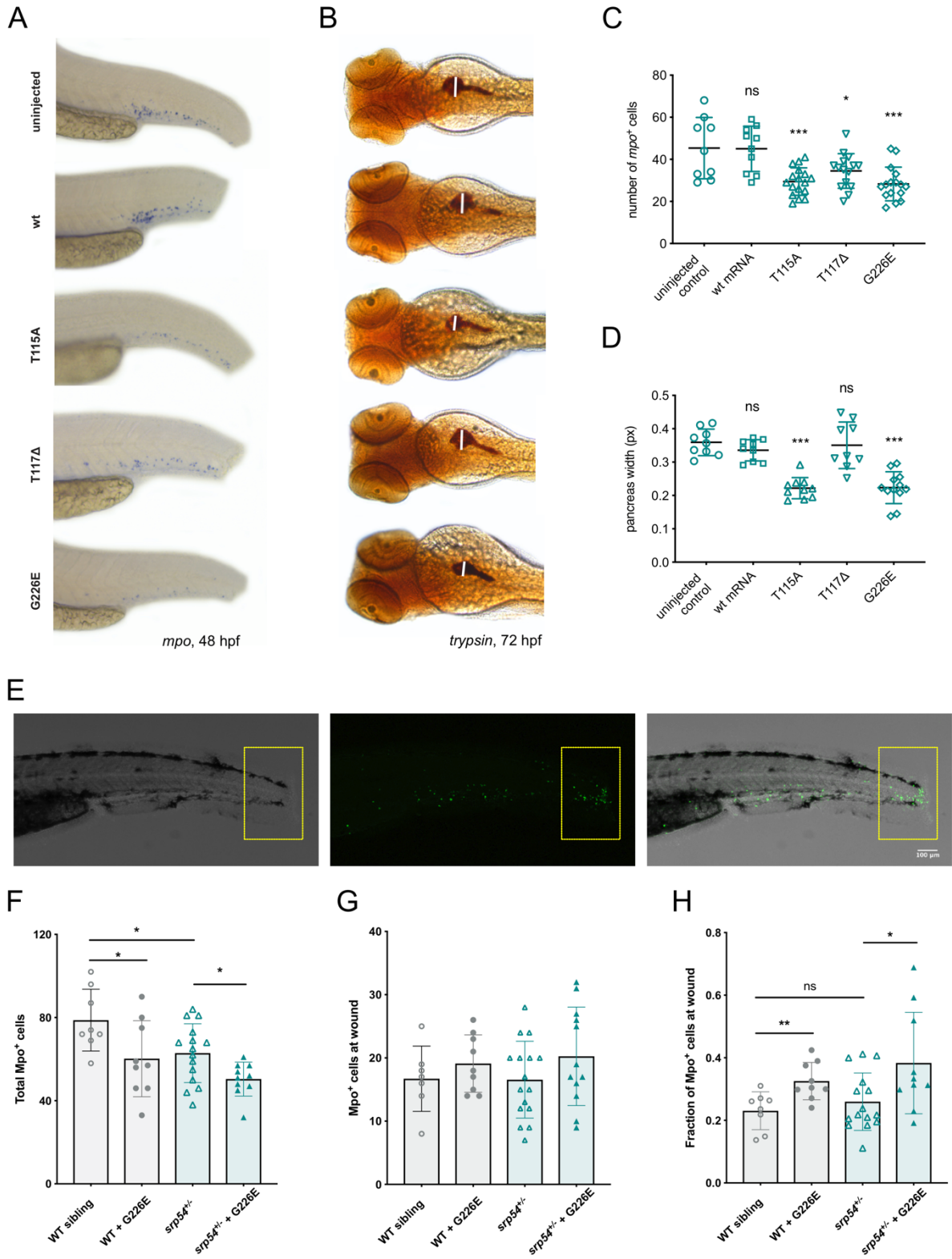


Figure 3

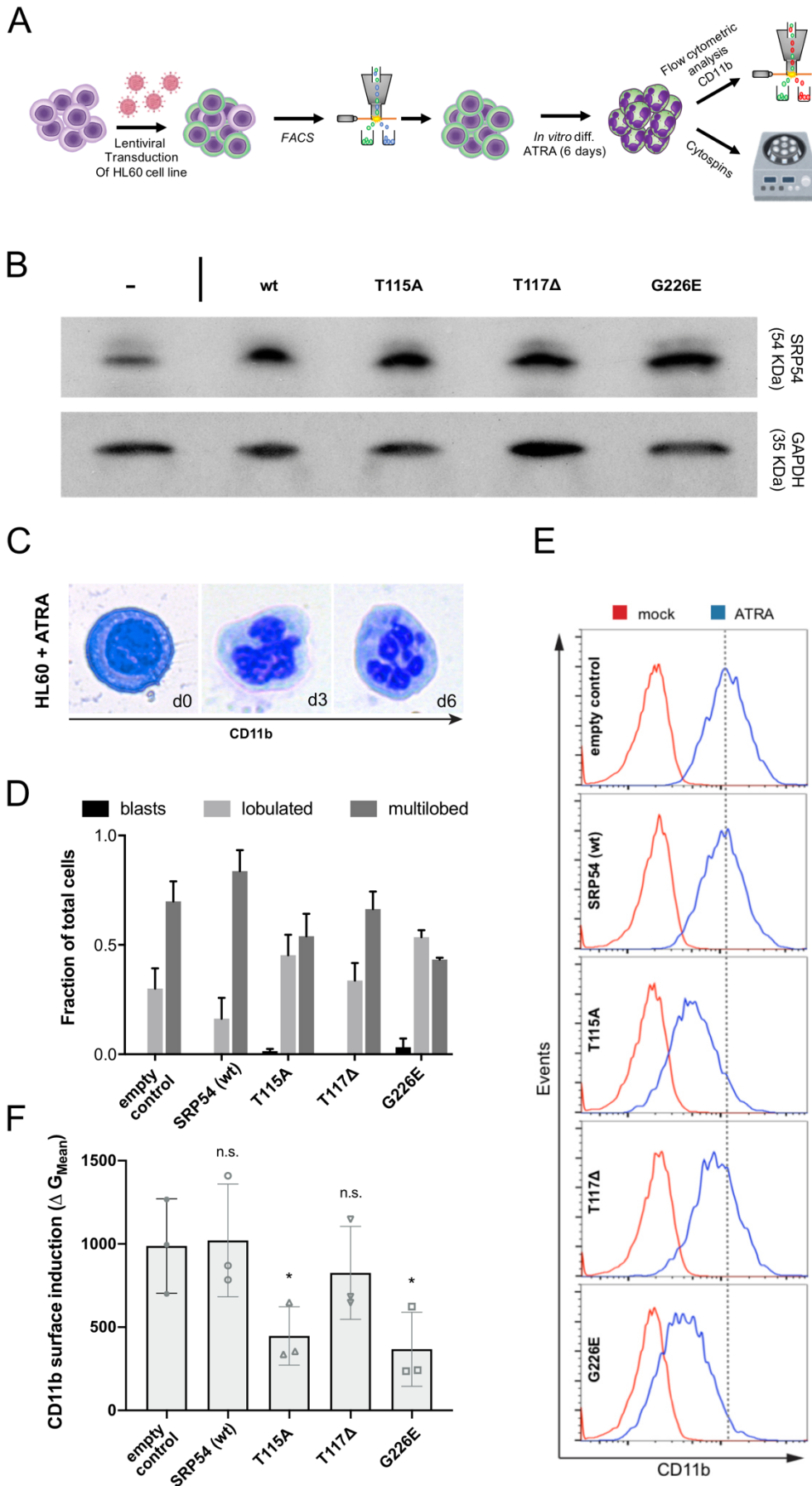
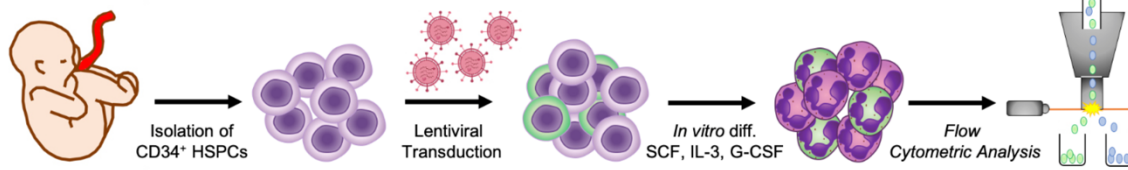
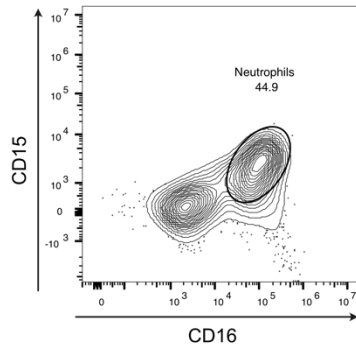


Figure 4

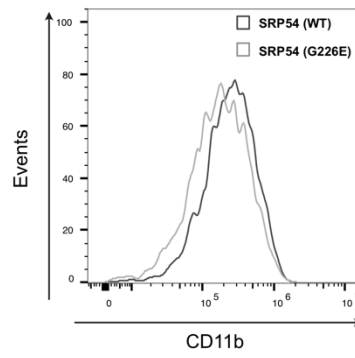
A



B



C



D

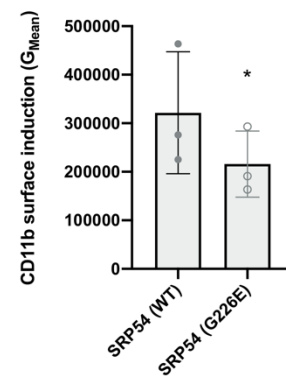
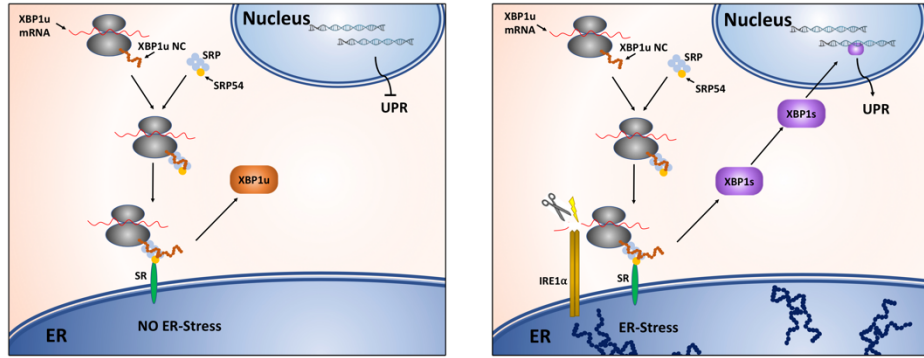
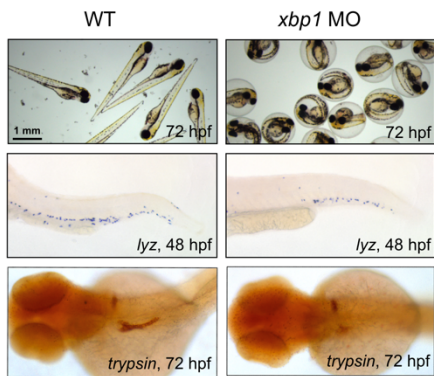


Figure 5

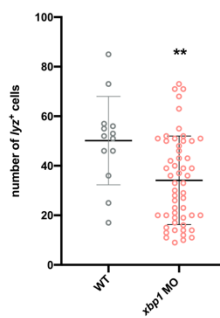
A



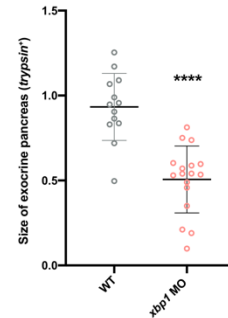
B



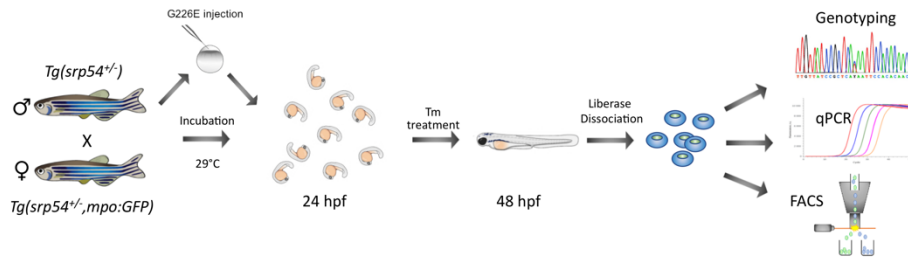
C



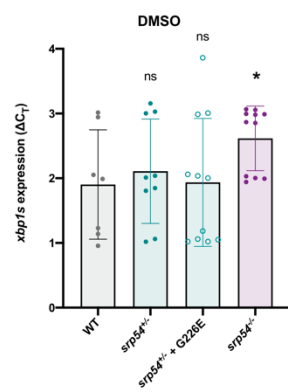
D



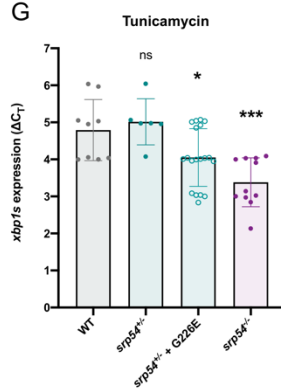
E



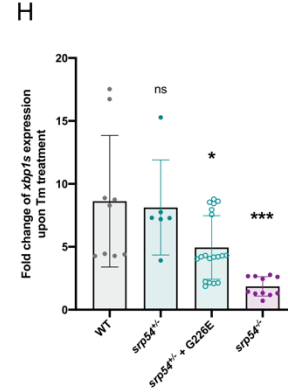
F



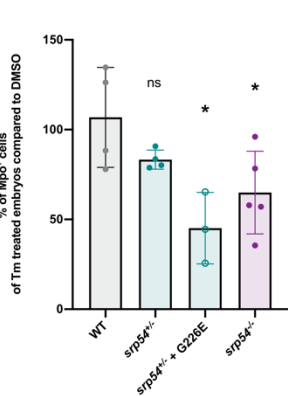
G



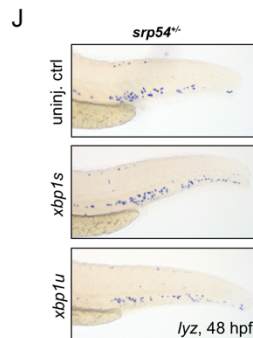
H



I



J



K

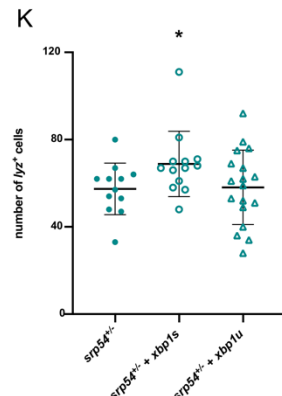


Figure 6

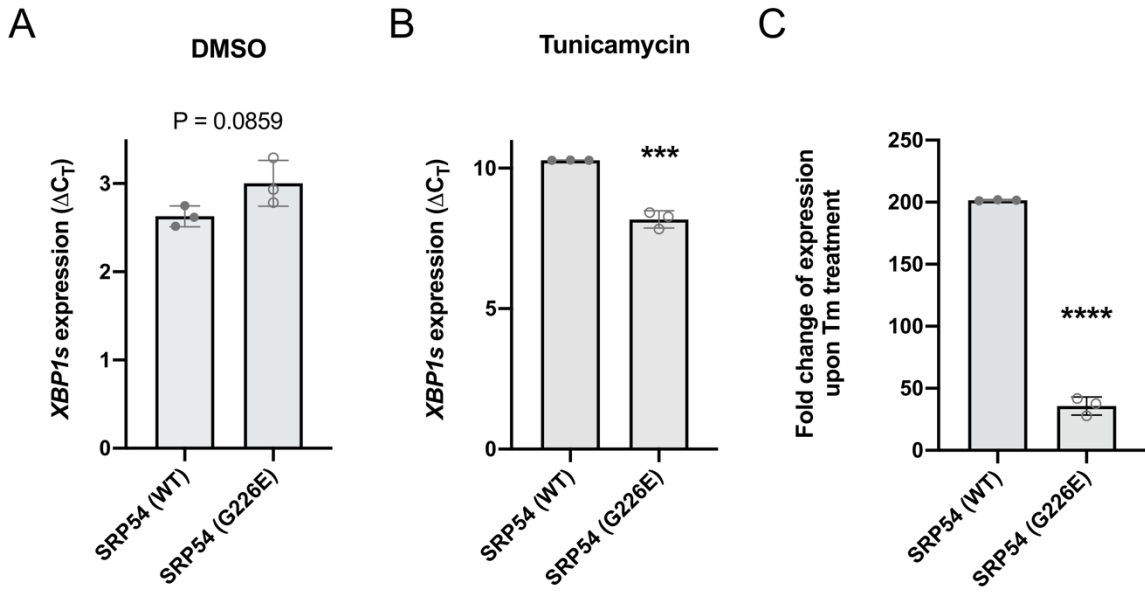
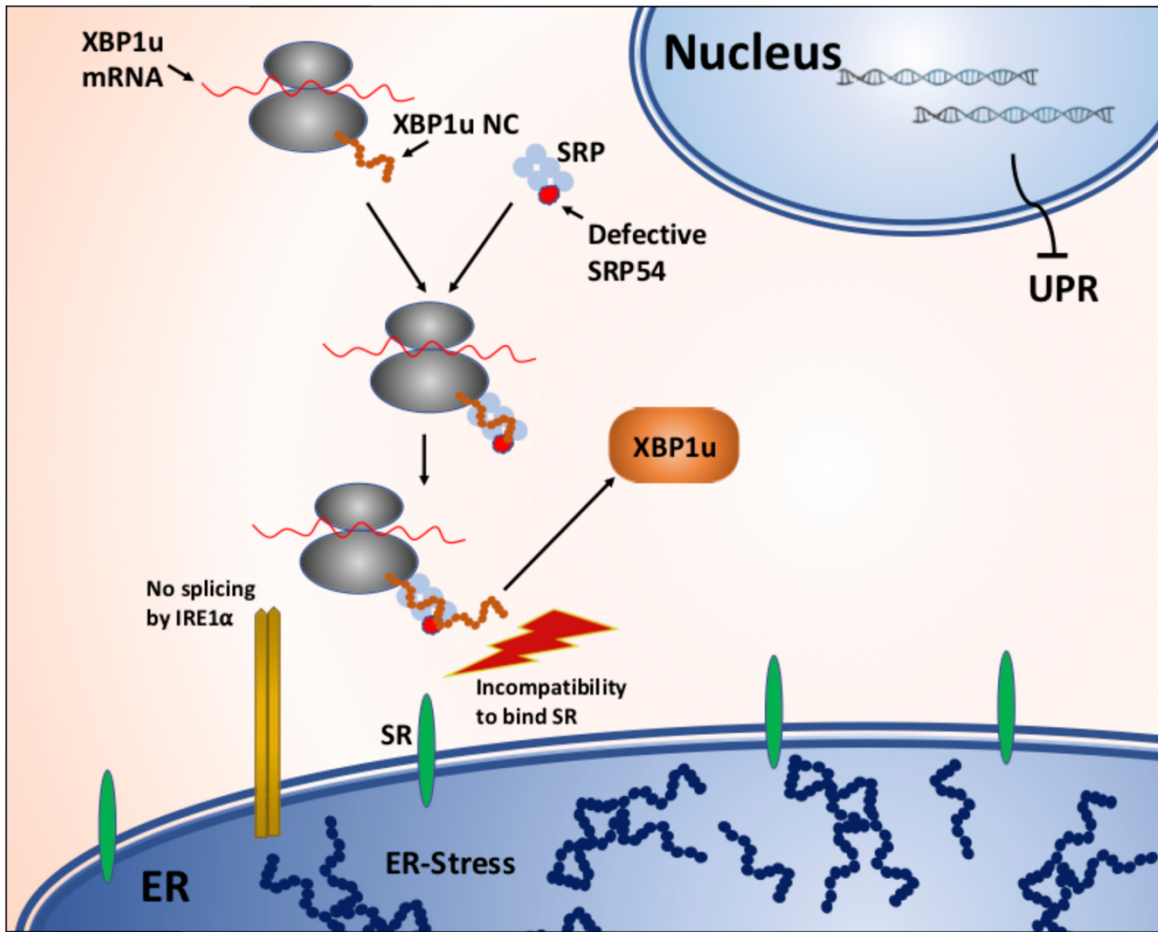


Figure 7



Supplementary Information

Title: *SRP54* mutations induce Congenital Neutropenia via dominant-negative effects on *XBP1* splicing

Running Title: Mutant *SRP54* induces CN by impairing *XBP1* splicing

Christoph Schürch¹, Thorsten Schaefer¹, Joëlle S. Müller¹, Pauline Hanns¹, Marlon Arnone¹, Alain Dumlin¹, Jonas Schärer¹, Irmgard Sinning², Klemens Wild², Julia Skokowa³, Karl Welte³, Raphaël Carapito^{4,5,6}, Seiamak Bahram^{4,5,6}, Martina Konantz^{1,#}, Claudia Lengerke^{1,3,7, #}

¹Department of Biomedicine, University Hospital Basel, University of Basel, Basel, Switzerland

²Heidelberg University Biochemistry Center (BZH), Heidelberg, Germany

³Department of Internal Medicine, Hematology, Oncology, Clinical Immunology and Rheumatology, University Hospital Tuebingen, Tuebingen, Germany

⁴Laboratoire d'ImmunoRhumatologie Moléculaire, Plateforme GENOMAX, INSERM UMR_S 1109, Faculté de Médecine, Fédération Hospitalo-Universitaire OMICARE, Fédération de Médecine Translationnelle de Strasbourg (FMTS), Université de Strasbourg, Strasbourg, France

⁵LabEx TRANSPLANTEX, Faculté de Médecine, Université de Strasbourg, Strasbourg, France

⁶Service d'Immunologie Biologique, Plateau Technique de Biologie, Pôle de Biologie, Nouvel Hôpital Civil, Strasbourg, France

⁷Division of Hematology, University Hospital Basel, University of Basel, Basel, Switzerland

#equal contribution

Corresponding authors

Martina Konantz (martina.konantz@unibas.ch)

&

Claudia Lengerke (claudia.lengerke@med.uni-tuebingen.de)

Department of Biomedicine
University Hospital Basel, University of Basel, Basel, Switzerland
Hebelstr. 20
4031 Basel
Switzerland

Contents:

Figure S1

Figure S2

Figure S3

Figure S4

Figure S5

Figure S6

Figure S7

Figure S1

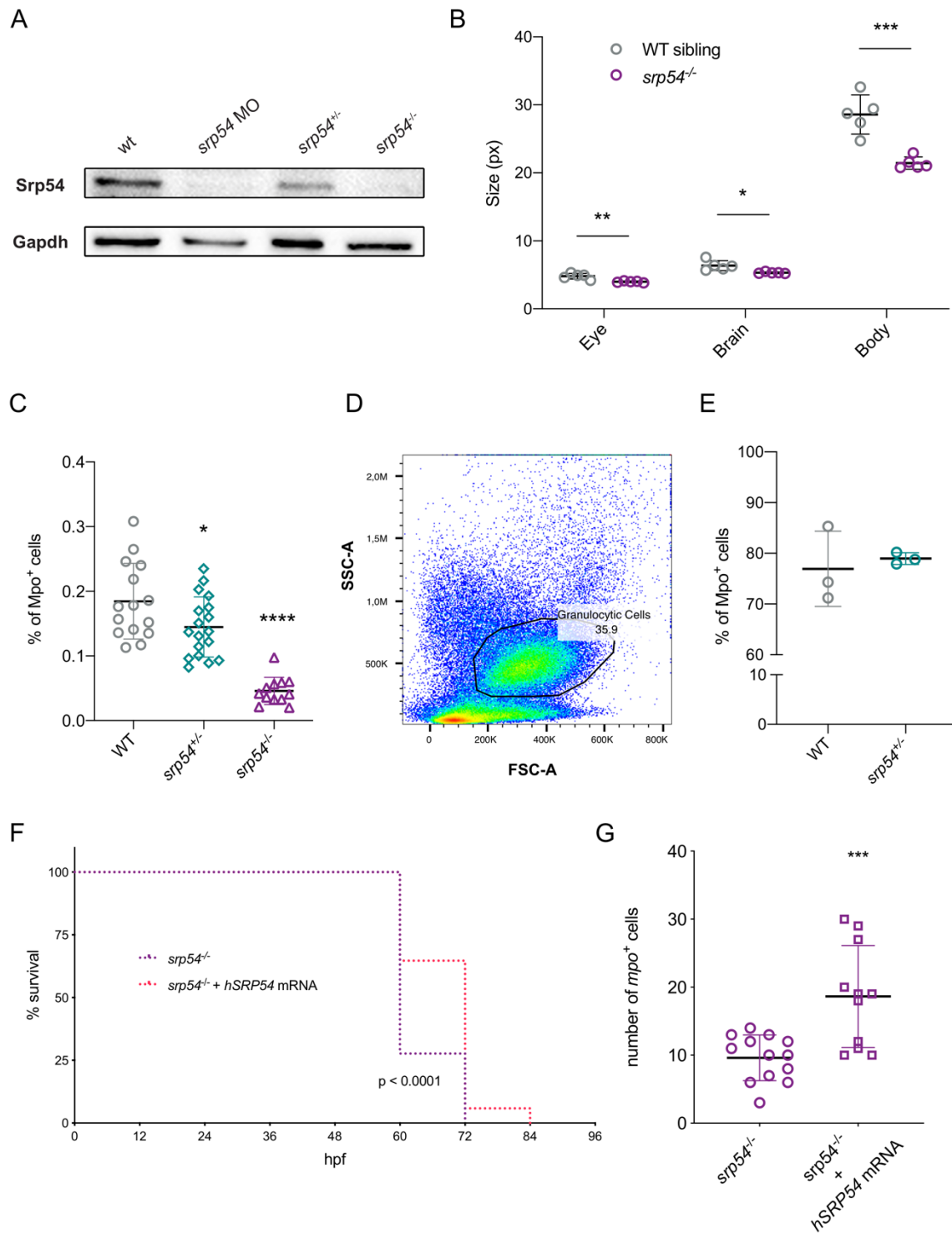


Figure S1: *srp54* KO causes severe developmental defects and neutropenia

(A) Western blot documenting zebrafish Srp54 levels of wt, *srp54* morphants, *srp54*^{+/-} and *srp54*^{-/-}. The following percentages of expression were deduced from area counts relative to wt as quantified by FIJI software: *srp54* MO: 2.5%; *srp54*^{+/-}: 53.6%; *srp54*^{-/-}: 2.2%. GAPDH was used as loading control and for normalization (B) Phenotypic quantification of *srp54*^{-/-} mutants compared to WT siblings. Shown are the pixel size of the eye, the brain and the body (from left to right) from n=2 biological replicates with at least n=2-4 larvae per replicate. (C) Flow cytometric analyses of neutrophil counts of *srp54* mutants compared to WT siblings. *Tg(srp54*^{+/-}, *mpo:eGFP*) zebrafish were incrossed and their progeny was genotyped and analyzed by flow cytometry. Plotted are the percentages of GFP⁺ cells from n=3 biological replicates with at least n=5 larvae per replicate. An ordinary Student's *t*-test was applied for statistical analysis: *P < 0.05; **P < 0.01; ***P < 0.005; ****P < 0.0001. (D) Forward- and side-scattering of dissolved WKM cells and gating strategy used to identify granulocytic cells. (E) Percentage of Mpo⁺ cells of granulocytic WKM cells from two-year-old WT and *srp54*^{+/-} zebrafish. (F) Kaplan-Meier survival analysis of *srp54*^{-/-} embryos compared to *srp54*^{-/-} embryos injected with human *SRP54* mRNA (at least n=45 embryos per condition from n=3 biological replicates). (G) Assessment of neutrophil counts by WISH using *mpo* specific probes in *srp54*^{-/-} embryos compared to *srp54*^{-/-} embryos injected with human *SRP54* mRNA. n=3 biological replicates with at least n=3 larvae were used per replicate. An ordinary Student's *t*-test was applied for statistical analysis: *P < 0.05; **P < 0.01; ***P < 0.005; ****P < 0.0001.

Figure S2

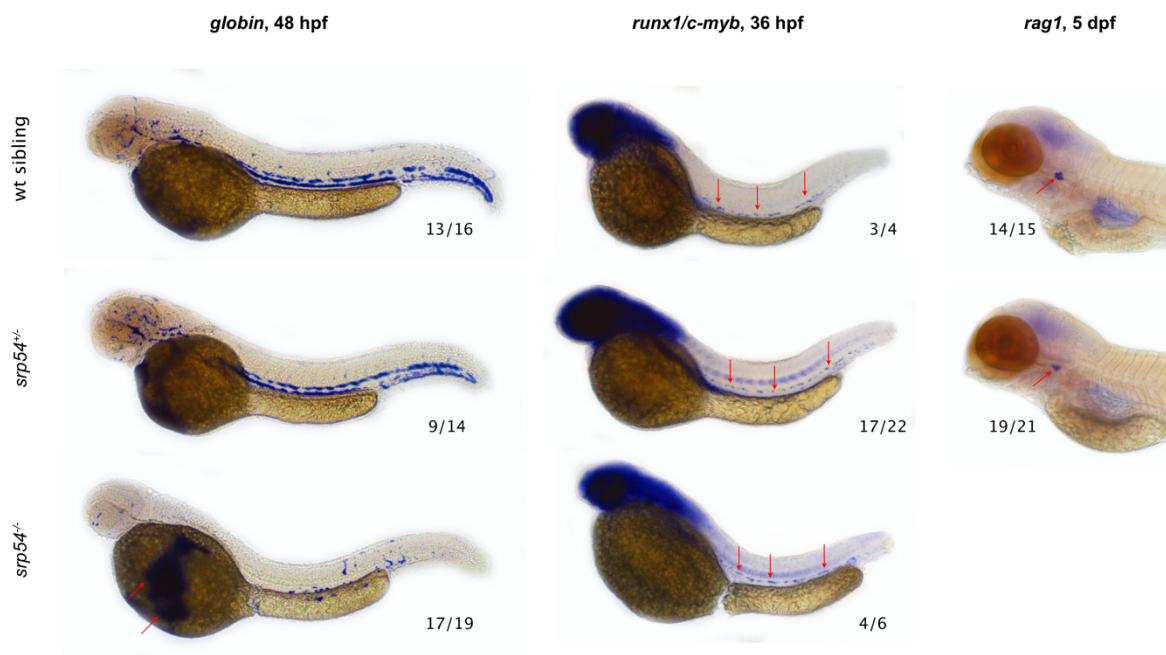


Figure S2: Other hematopoietic cell types are not affected by *srp54* deficiency

Representative pictures of WISH for *globin* at 48 hpf, *runx1/c-myb* at 36 hpf and *rag1* at 5 dpf (left to right). *runx1/c-myb* and *rag1* signals were not affected by *srp54* KO (red arrows). In *srp54*^{-/-} embryos, *globin* signal was significantly reduced in the peripheral blood and upregulated in the duct of Cuvier (red arrows). Numbers indicate the sum of embryos with the respective phenotype per total number of embryos analyzed in all replicate experiments for the respective condition. Black arrows indicate downregulation.

Figure S3

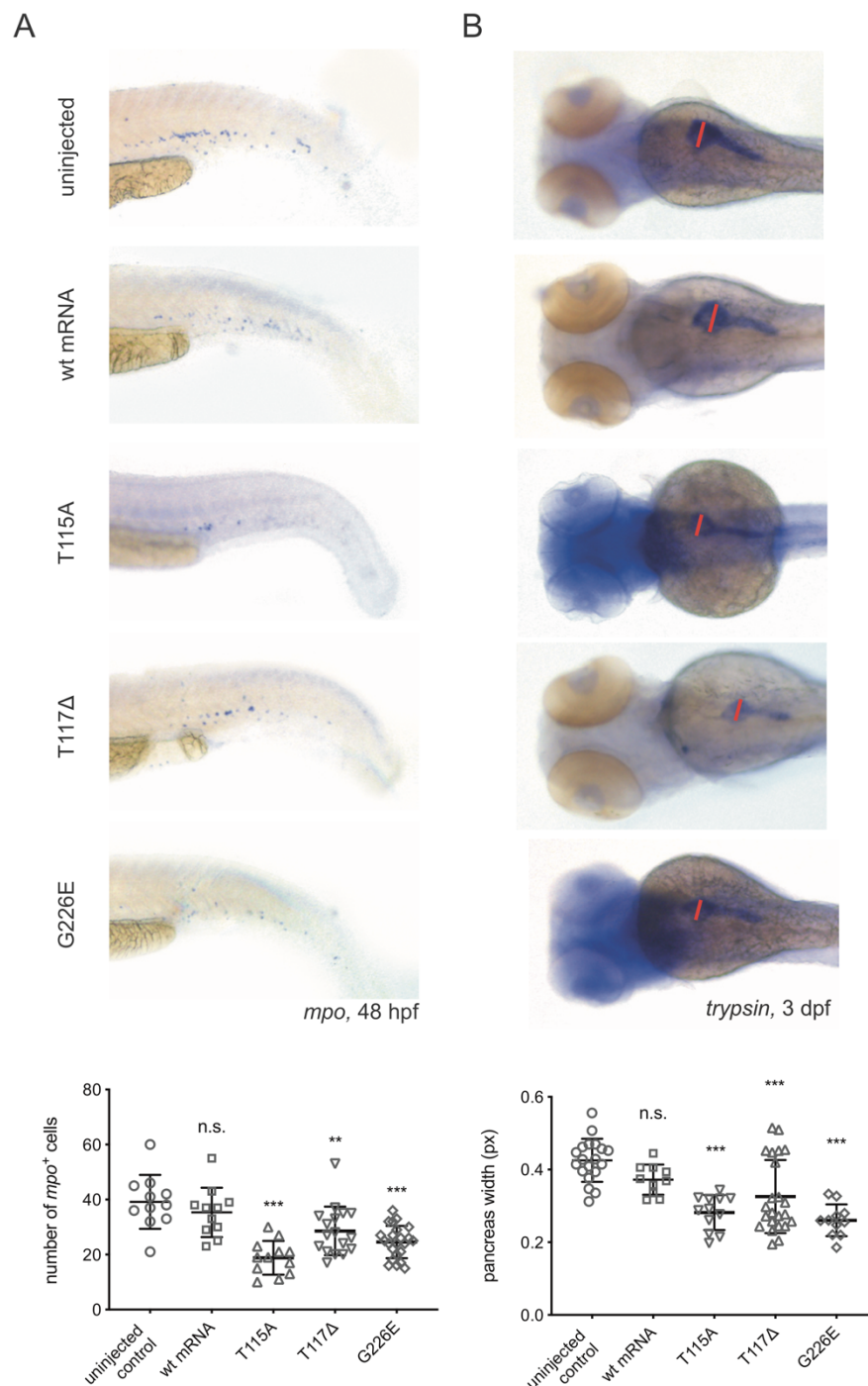


Figure S3: Injections of mutated mRNAs into WT embryos induce neutropenia and defects in the exocrine pancreas.

(A - B) Injection of wt mRNA, T115A, T117Δ or G226E mRNA (from top to bottom) into WT embryos. Shown are representative pictures (top) with the corresponding quantifications (bottom) after WISH for *mpo* **(A)** and *trypsin* **(B)**. n=3 biological replicates with at least n=3 larvae were used per replicate. An ordinary Student's *t*-test was applied for statistical analysis: *P < 0.05; **P < 0.01; ***P < 0.005; ****P < 0.0001.

Figure S4

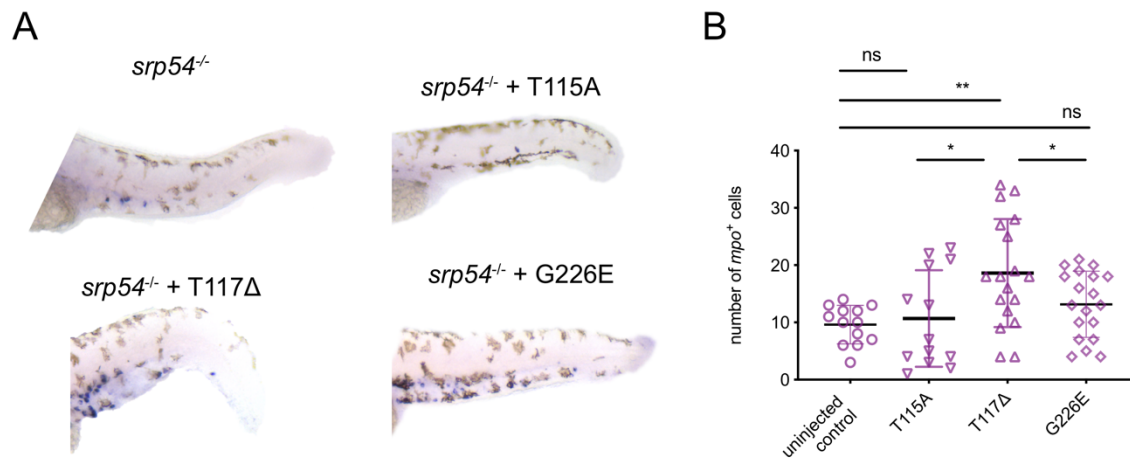


Figure S4: Injections of human T115A and G226E *SRP54* mRNA does not rescue neutropenia in *srp54*^{-/-} zebrafish, while neutropenia is partially rescued upon injections human T117Δ *SRP54* mRNA

(A) Representative images of WISH of *srp54*^{-/-}, *srp54*^{-/-} + T115A mRNA, *srp54*^{-/-} + T117Δ mRNA and *srp54*^{-/-} + G226E mRNA (top left to bottom right) using *mpo* specific probes. (B) Corresponding quantification of WISH. n=3 biological replicates with at least n=4 larvae were used per replicate. An ordinary Student's *t*-test was applied for statistical analysis: *P < 0.05; **P < 0.01; ***P < 0.005; ****P < 0.0001.

Figure S5

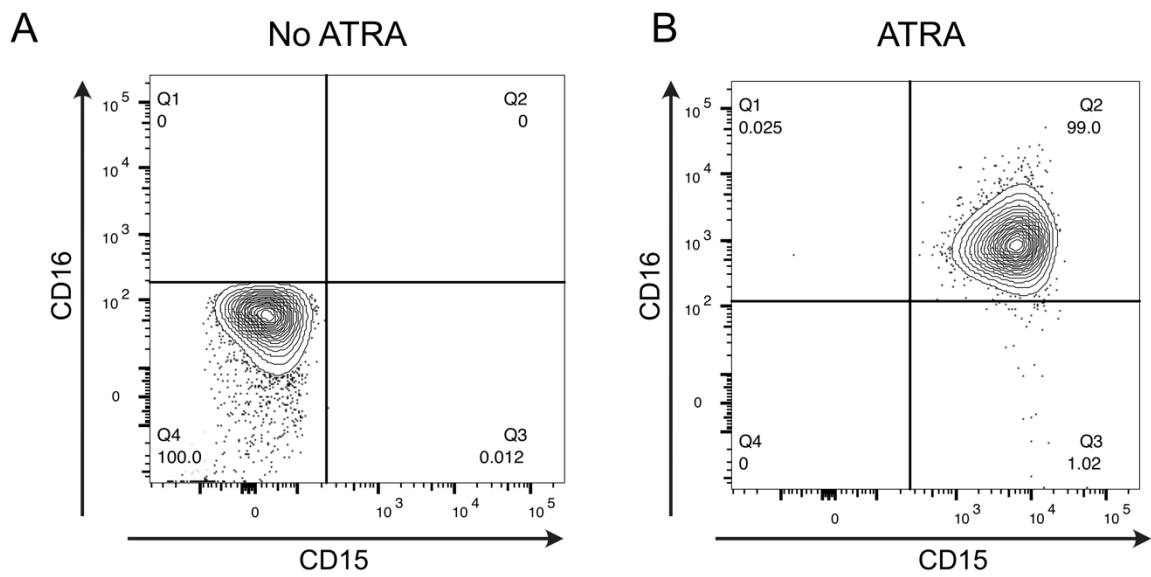


Figure S5: HL-60 cells express CD15 and CD16 after ATRA treatment

Flow cytometric analysis of CD15 and CD16 surface expression levels of HL-60 cells after DMSO (A) or ATRA (B) treatment for 6 days.

Figure S6

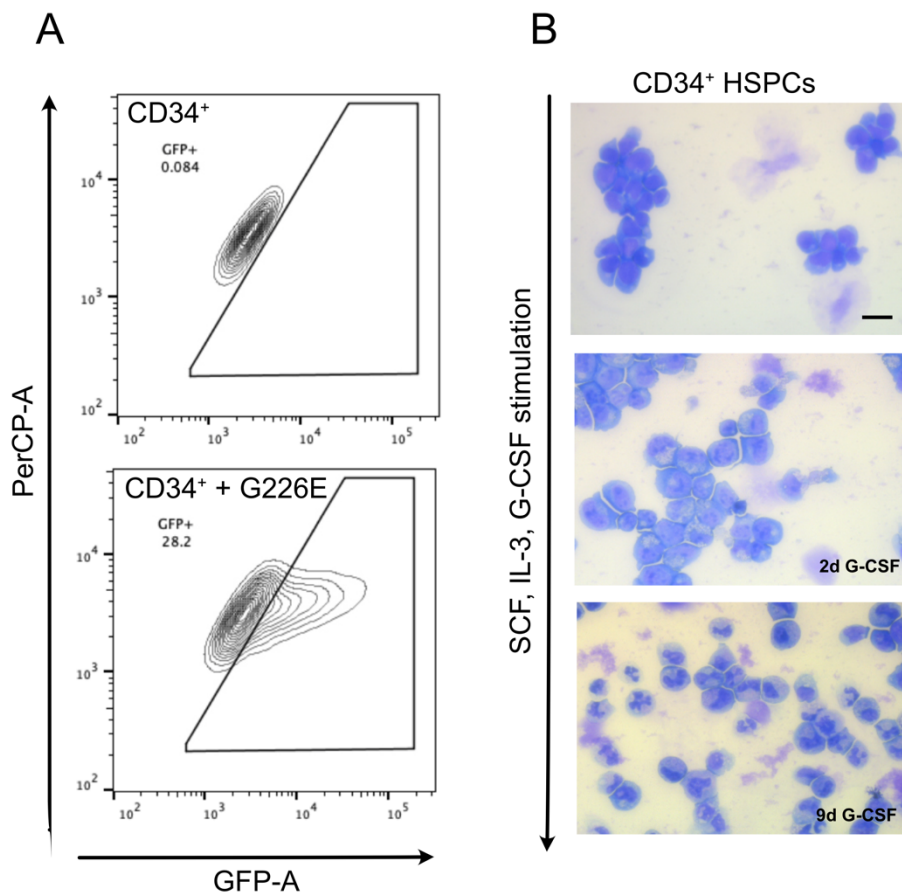
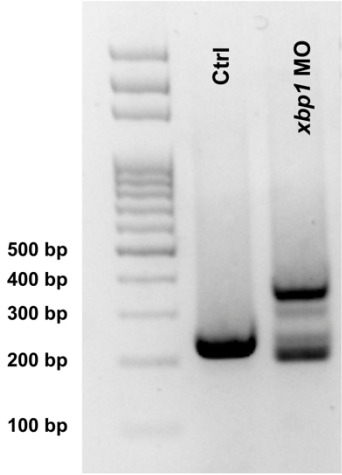


Figure S6: Transduction controls and differentiation of CD34⁺ progenitors

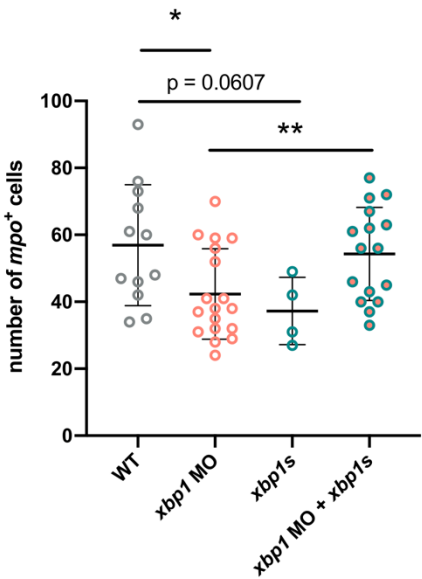
(A) Flow cytometric analysis of IRES:GFP expression after transduction of CD34⁺ cells with *SRP54* (G226E) compared to untransduced cells. GFP was plotted against PerCP to exclude autofluorescent cells. **(B)** Representative pictures of H&E stained cytoplots of CD34⁺ HSPCs directly before G-CSF administration (top), 2 days after G-CSF administration (middle) and 9 days after G-CSF administration. Scale bar = 25 μ m.

Figure S7

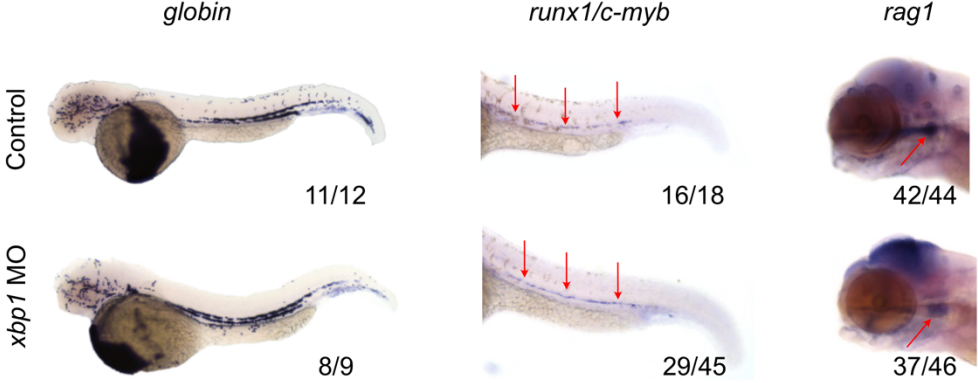
A



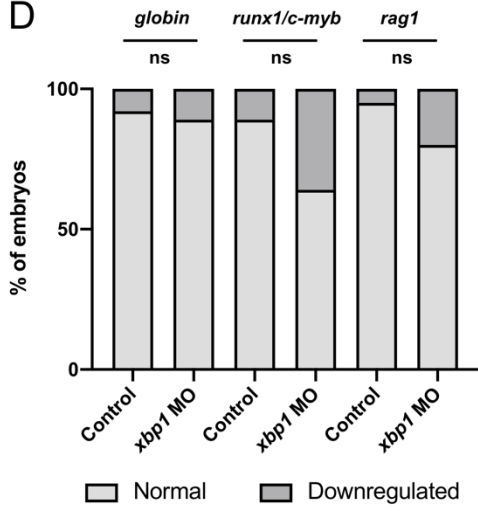
B



C



D



E

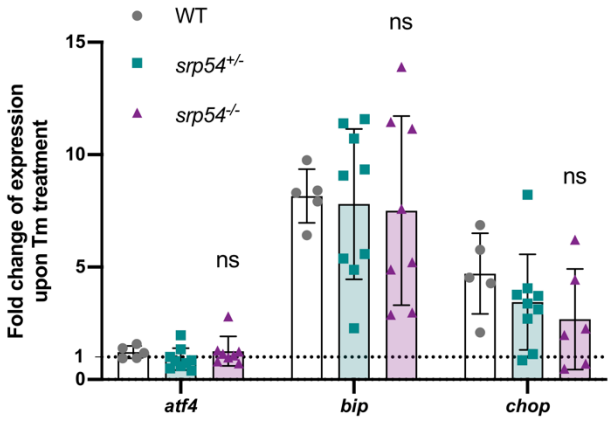


Figure S7: *xbp1* morphants can be rescued by *xbp1s* mRNA injection and show no further hematopoietic defects other than neutropenia – *xbp1s* is the only affected player of the UPR by *srp54* lesions

(A) *xbp1* morpholino validation by RT-PCR and subsequent analysis by gel electrophoresis. (B) Quantification of WISH of WT, *xbp1* MO injected, *xbp1s* mRNA injected and *xbp1* MO + *xbp1s* mRNA injected embryos using *mpo* specific probes. Of note, the reduction of neutrophils upon injection of *xbp1s* mRNA into WT embryos indicates that Xbp1s levels must be within a certain range for proper neutrophil differentiation. n=3 biological replicates with at least n=1 larva per replicate were used. An ordinary Student's *t*-test was applied for statistical analysis: *P < 0.05; **P < 0.01; ***P < 0.005; ****P < 0.0001. (C) Representative pictures of WISH for *globin* at 48 hpf, *runx1/c-myb* at 36 hpf and *rag1* at 5 dpf (left to right). Numbers indicate the sum of embryos with the respective phenotype per total number of embryos analyzed in all replicate experiments for the respective condition. Red arrows mark the signal of the respective probe. (D) Quantification of WISH for *globin*, *runx1/c-myb* and *rag1*. Plotted is the percentage of embryos presenting with a normal phenotype (light grey) and with downregulated signals for the respective probes (dark grey). (E) Fold change of expression upon Tm treatment of UPR players *atf4*, *bip* and *chop* (from left to right) for WT, *srp54*^{+/-} and *srp54*^{-/-} zebrafish embryos at 2 dpf measured by qRT-PCR. n=3 biological replicates with at least n=2 larvae were used per replicate. An ordinary Student's *t*-test was applied for statistical analysis: *P < 0.05; **P < 0.01; ***P < 0.005; ****P < 0.0001.

2.2 Additional Data: Single Cell RNA Sequencing of *srp54* Mutant Zebrafish

In our publication “*SRP54* mutations induce Congenital Neutropenia via dominant-negative effects on *XBP1* splicing”⁸² we identified impaired unconventional splicing of *XBP1* mRNA as a mechanism contributing to the development of CN upon *SRP54* deficiency. However, this finding only represents one part of the puzzle of mechanisms that collectively control the phenotypes seen in patients with *SRP54* defects. In order to unveil additional parts of this puzzle, we decided to sequence the transcriptome of *SRP54* defective cells. For this purpose we made use of the transgenic *srp54* zebrafish model we introduced and characterized in our previous publication.²⁹³

2.2.1 Experimental Setup

Based on the fact that CN is one of the major phenotypic manifestations of *SRP54* defective patients, we aimed to perform single cell RNA sequencing (scRNA-seq) of neutrophils from Tg(*srp54*^{-/-}; *mpo*:GFP), Tg(*srp54*^{+/-}; *mpo*:GFP), and Tg(*WT*; *mpo*:GFP) zebrafish embryos 2 days post fertilization (dpf). A major obstacle to overcome was the inability to differentiate *srp54*^{+/-} and *WT* embryos exclusively according to their phenotype (as described by Schürch et al.⁸², section 2.1), which evoked the need for genotyping. Since genotyping these embryos by fin clipping would have initiated a neutrophil flux towards the wound associated with a potential change in the transcriptome,²⁹⁴ we opted to dissolve the fish with the enzyme liberase and used one part of the cell suspension as input for genotyping, and the other part for Fluorescence Activated Cell Sorting (FACS), respectively (Figure 7). This approach, however, made it impossible to pool fish of the same genotype prior to FACS, because the respective genotypes were not known yet. Thus, single neutrophils of separately dissolved zebrafish embryos were sorted into 384-well plates containing lysis buffer (Figure 7). Eight wells were assigned for each embryo in a way that they could retrospectively be correlated to their respective genotype. Consequently, a total of 48 different embryos were used per 384-well plate. Once we received the results of the genotyping, we selected the well plate with the most balanced ratio of *srp54*^{-/-}, *srp54*^{+/-}, and *WT* wells as input for scRNA-seq (Figure 7).

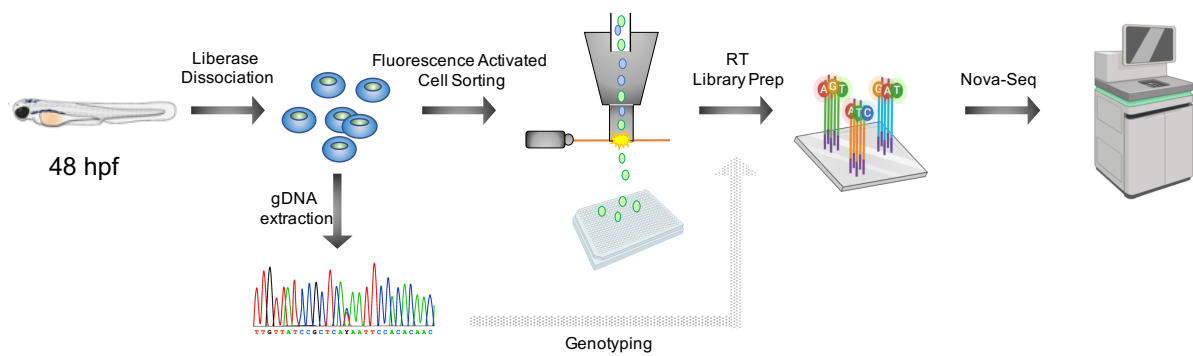


Figure 7: Experimental setup of the conducted scRNA-seq experiment. Transgenic 48 hpf old embryos were dissociated using the enzyme liberase. A part of the cell suspension was used for gDNA extraction and genotyping, whilst the rest served as input for FACS. Single GFP⁺ cells were directly sorted into a 384-well plate containing lysis buffer, followed by freezing of the plate. Once the genotypes of the dissolved fish were elucidated, the plate with the best ratio of different genotypes was selected for RT and library preparation. The prepared plate was then sequenced using a Nova-seq device.

2.2.2 Quality Control

Prior to sequencing, we performed several control experiments to verify that the applied setup indeed yields enough high-quality RNA per well of the 384-well plate. A major concern was the possibility that cells within the cell suspension might lyse before FACS and thus release their RNA content into the medium. This would lead to RNA contamination in every single well of the well plate and significantly reduce the quality and the reliability of the sequencing results. To prove that no RNA of lysed cells was sorted into the wells, we designed a 384-well plate setup, where we added beads to the cell suspension and alternately sorted GFP-positive cells and beads into the wells. Accordingly, only every second well of the plate should contain RNA and give rise to cDNA after RT. To prove if this was the case, the cDNA content was analyzed using a Bioanalyzer and the profiles of the different wells were compared to each other. Importantly, the cDNA profiles demonstrated that no RNA was present in the wells containing only beads, whilst the vast majority of the wells with single cells did contain substantial amounts of RNA (**Figure 8**).

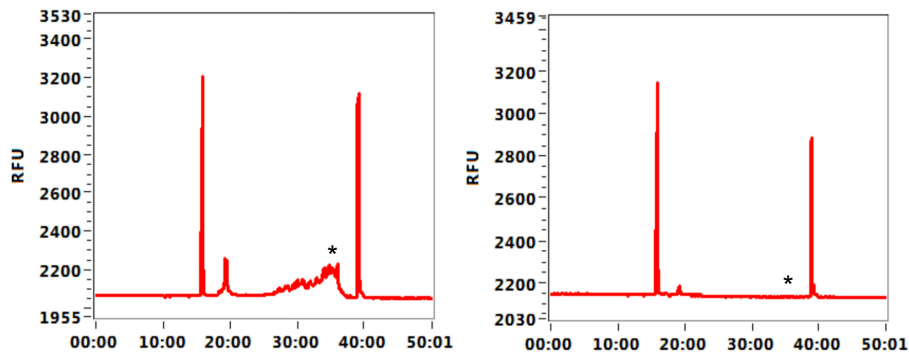


Figure 8: cDNA profiles of the 384-well trial plate. Left: cDNA profile of a well containing a sorted cell after RNA extraction and RT. Right: cDNA profile of a well containing a sorted bead after RNA extraction and RT. y-axis = Relative Fluorescence Units (RFU), x-axis = time in seconds. Note the cDNA signals (marked with *) of the well containing a cell (left) and the absence of such signals of the well containing a bead (right).

With the confirmation that high-quality RNA can be extracted from single zebrafish neutrophils sorted into a 384-well plate, we started the scRNA-seq of the selected plate.

The following analysis of the scRNA-seq data was performed in collaboration with Dr. Florian Geier of the Bioinformatics Core Facility of the Department of Biomedicine, University Hospital Basel. First mapping and quality control analyses revealed that the number of reads was very heterogenous amongst the different wells of the 384-well plate, with only few wells showing more than 6 million reads (**Figure 9**). Due to the mostly limited library size, we decided to repeat the scRNA-seq using the same 384-well plate as input, but this time with a larger flow cell. As a result of the resequencing, the library sizes increased substantially, with most wells showing more than 10 million reads (**Figure 9**).

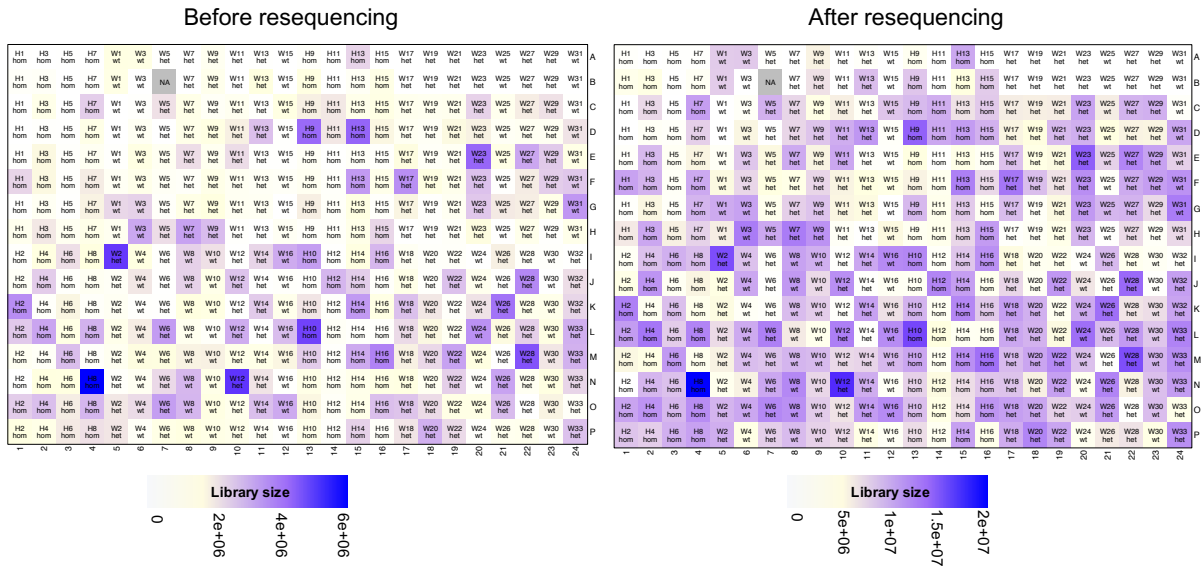


Figure 9: Library size of the 384-well plate selected for scRNA-seq. Left: Number of reads per well of the 384-well plate before resequencing. Right: Number of reads per well of the 384-well plate after resequencing using a larger flow cell. Note the different color-scales for the plate before and after resequencing.

2.2.3 Results – Additional Data

2.2.3.1 Sorted Cells are not Exclusively Neutrophils

For the analysis of the scRNA-seq data, wells with less than 1000 detected genes and a mitochondrial read ratio higher than 0.3 were filtered out, resulting in a total of 222 cells remaining in the analysis. Despite sorting only *mpo*:GFP⁺ cells, principal component analysis (PCA) of this filtered subset revealed a clear separation of the analyzed cells into two distinct clusters according to the zebrafish cellatlas²⁹⁵. One of them expressing neutrophil-specific and hematopoietic lineage genes, whereas the other one did not show any neutrophil characteristics at all (Figure 10). Associated with the non-neutrophilic cluster were cells originating from a wide variety of different tissues, such as bone, parachord, notochord or the fin region. This very diverse composition suggests that this cell cluster is of non-specific origin (Figure 10).

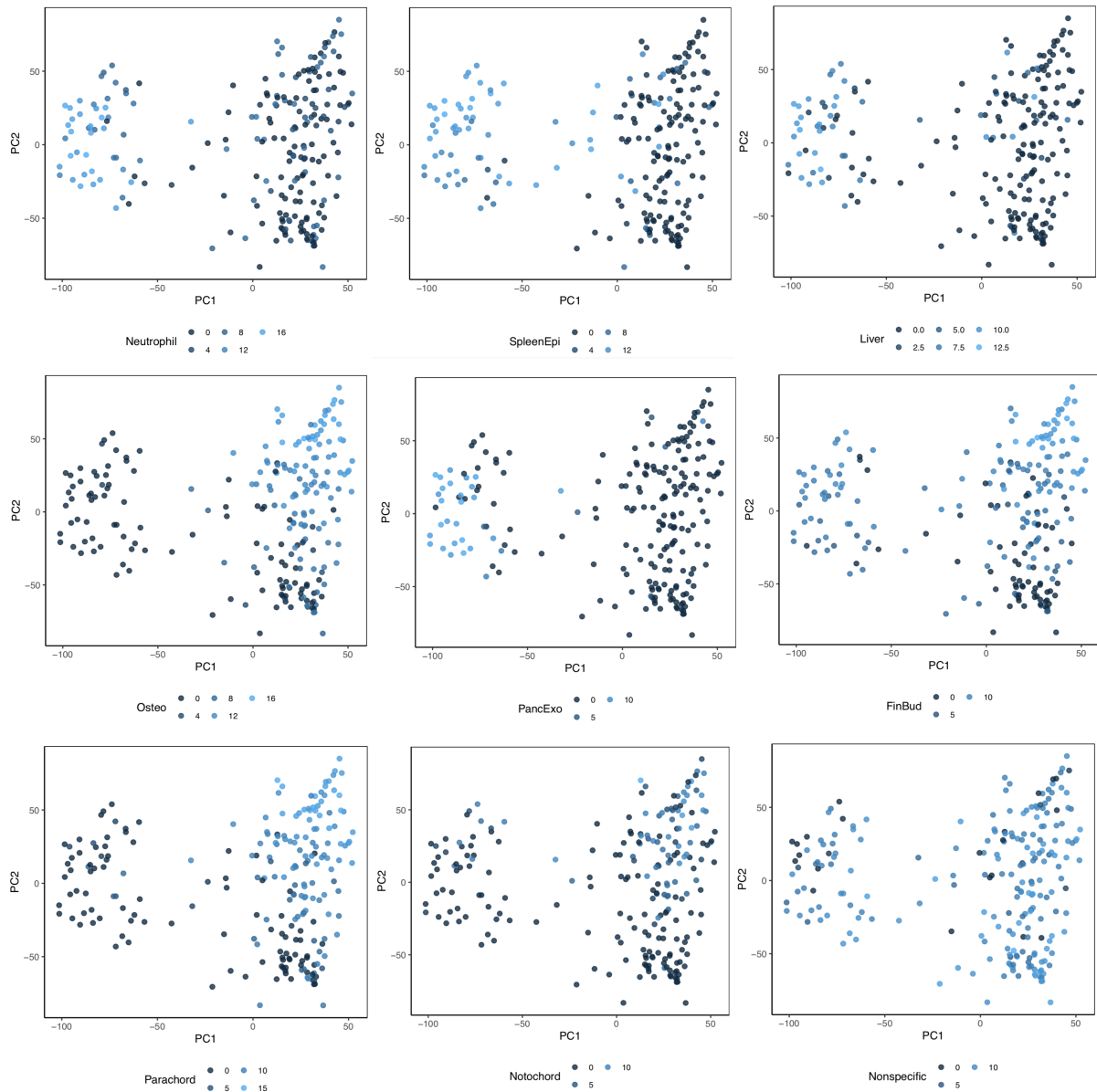


Figure 10: PCA of the filtered dataset and expression of gene-sets. Depicted is nine times the same PCA, each depiction showing the expression of a different gene-set according to the zebrafish cell atlas.²⁹⁵ Neutrophil = Genes associated with the neutrophil lineage; SpleenEpi = Genes associated with the spleen; Liver = Genes associated with the liver; Osteo = Genes associated with bone formation and homeostasis; PancExo = Genes associated with the exocrine pancreas; FinBud = Genes associated with fin budding; Parachord = Genes associated with the parachord; Notochord = Genes associated with the notochord; Nonspecific = Genes not associated with a specific gene cluster. PC1 = 10% of total variance, PC2 = 4% of total variance.

Interestingly, when assessing the distribution of the three different genotypes (*srp54^{-/-}*, *srp54^{+/-}*, *WT*) along principal component 1 (PC1, 10% of total variance) and principal component 2 (PC2, 4% of total variance), no clustering was observable (Figure 11). Each genotype showed a very heterogeneous distribution, with cells in both clusters, the neutrophilic and the non-specific one.

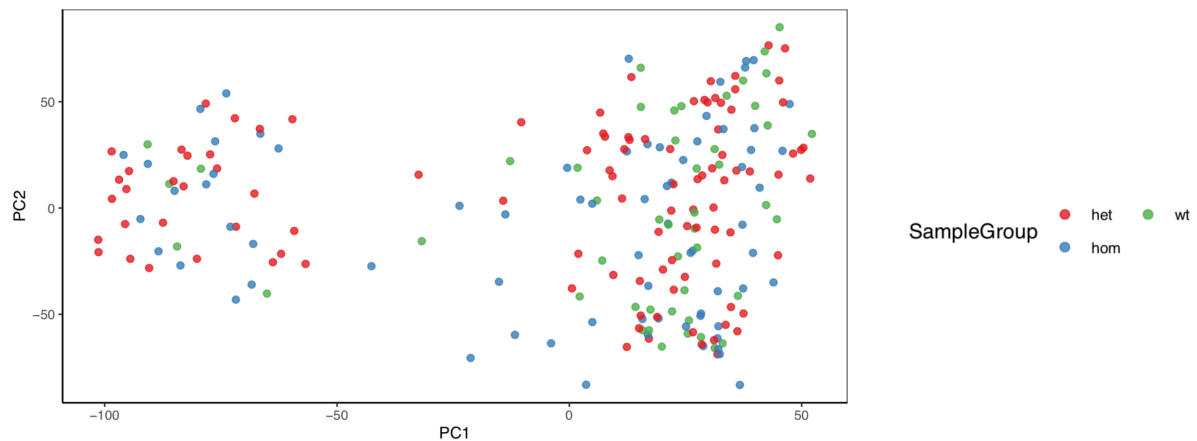


Figure 11: PCA of the filtered dataset showing the distribution of the different genotypes. Red = het, *srp54*^{+/-}; Green = wt, *srp54*^{+/+}; Blue = hom, *srp54*^{-/-}. PC1 = 10% of total variance, PC2 = 4% of total variance.

2.2.3.2 Several Genes are Found Differentially Expressed in *srp54* Mutant Cells

Despite the genotypes not clustering in the PCA, we aimed to identify differentially expressed (DE) genes. Since the RNA content per well of the 384-well plate was highly heterogeneous, the wells with low RNA levels were affected by high dropout rates. To minimize the dropout, we pooled the data of single cells from the same fish together, thereby increasing the amount of RNA. DE analysis of this novel dataset revealed several significant hits (**Figure 12**). Whilst some hits, such as *dnajc25* or *ntrk2a*, seemed to be affected by the limited sample size, as they were significantly lower expressed in *srp54*^{+/-} fish only and did not appear as DE genes between *srp54*^{-/-} and *WT* fish, others displayed more reliable expression profiles. Amongst these reliable candidates were *ppp1r26*, *si:ch211-191a24.4* (from now on referred to as *ch211*), *mgst1.1*, and *slc35e1* (**Figure 12**). However, functional interpretation of DE genes is difficult, since the dataset is composed of a highly heterogeneous group of cells and because the KO of *srp54* as a key player of protein secretion – an absolutely essential pathway- may lead to numerous unpredictable compensatory effects within a cell. Hence, as discussed later in section “3. Discussion”, the here presented hits do not allow the unraveling of cell -or lineage-specific mechanisms, but rather provide insights into general, non-specific processes contributing to the phenotypes observed in *srp54*-deficient cells.

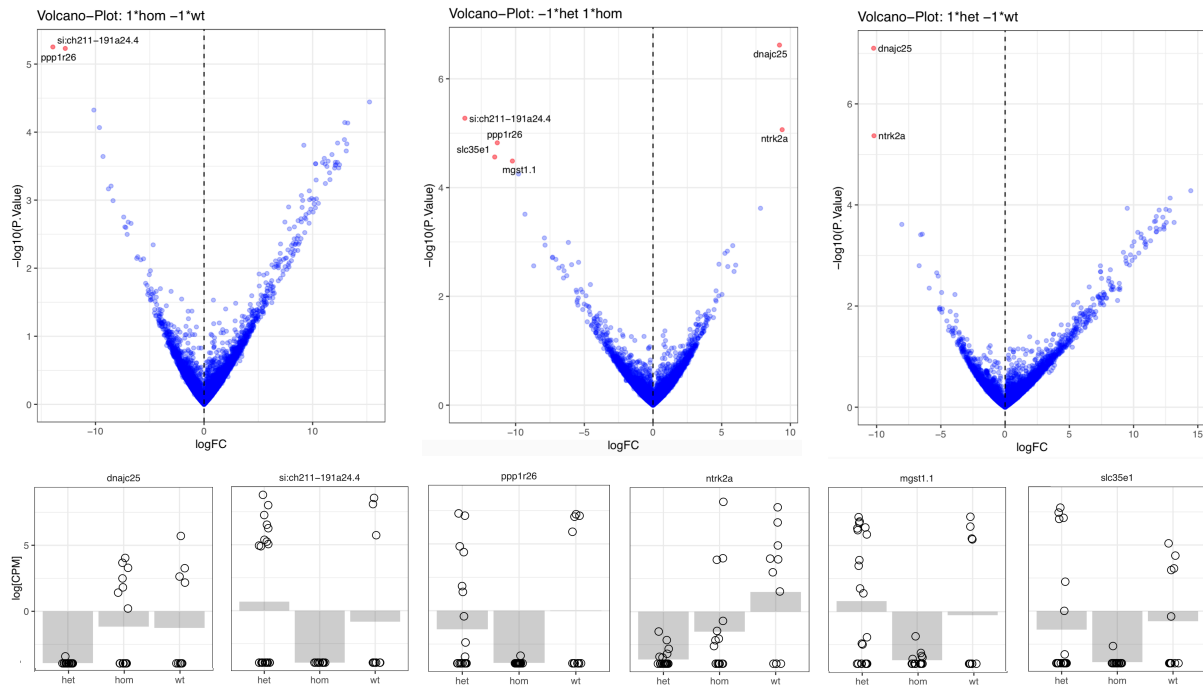


Figure 12: Differential gene expression analysis of pooled cells per fish. Top: Volcano plots showing the differential expression of genes comparing *srp54*^{-/-} and wt, *srp54*^{+/-} and *srp54*^{-/-} or *srp54*^{+/-} and wt (from left to right). Blue dots represent non-significantly DE genes; red dots represent significantly DE genes. Bottom: Genotype-specific log(CPM) of significantly DE genes. From left to right: *dnajc25*, *si:ch211-191a24.4*, *ppp1r26*, *ntrk2a*, *mgst1.1* and *slc35e1*.

2.2.3.3 qRT-PCR Confirms Hits of the scRNA-seq

To verify the obtained hits, we performed qRT-PCR analyses of the corresponding genes. Interestingly, *dnajc25*, *ch211*, *ntrk2a* and *scl35e1* showed significantly lower expression levels in *srp54*^{-/-} zebrafish compared to *srp54*^{+/-} and WT (Figure 13). For *ch211* and *slc35e1*, this finding matches the results observed in the scRNA-seq (Figure 12). For *dnajc25* and *ntrk2a* on the other hand, sequencing data suggested lower expression levels in *srp54*^{+/-} embryos compared to *srp54*^{-/-} and WT (Figure 12). This discrepancy might result from the still high dropout rates and the limited sample size of the scRNA-seq, which might have artificially altered the log(CPM) value of *srp54*^{-/-} and *srp54*^{+/-}, respectively. Consequently, we can conclude that qRT-PCR partially confirms the results of the scRNA-seq concerning *dnajc25* and *ntrk2a*, as it also demonstrates that fish carrying an *srp54* lesion (either homozygous or heterozygous) show reduced expression levels of these two candidate genes when compared to WT siblings. Of note, qRT-PCR data for *ppp1r26* and *mgst1.1* could not confirm the findings of the scRNA-seq (data not shown). Further experiments will be needed to definitely confirm or reject these two hits.

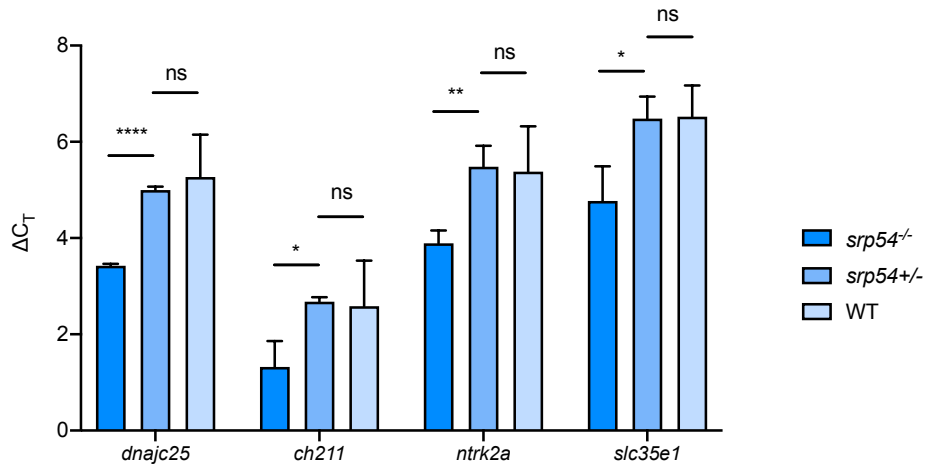


Figure 13: qRT-PCR of identified DE genes. Left to right: *dnajc25*, *ch211*, *ntrk2a* and *slc35e1*. For each gene, the ΔC_T value of the corresponding gene is plotted for *srp54*^{-/-}, *srp54*^{+/-} and WT zebrafish. n = 3 biological replicates were used per condition. *P < 0.05; **P < 0.01; ***P < 0.005; ****P < 0.0001.

2.2.3.4 DE Analysis of the Neutrophil Cluster Reveals Lineage-Specific Candidate Genes

Whilst the identification of the above presented DE genes provides us with novel information about the general mechanisms in *srp54* mutant cells, it does not unveil novel factors contributing to the defects we specifically observe in neutrophils. Consequently, for further analyses we focused on the neutrophil-specific cluster of the PCA. Similar to the whole dataset, PCA of this subset did not show any genotype specific clustering (data not shown). Moreover, the neutrophil-specific subset was substantially limited in the number of cells per genotype, with only 9 *srp54*^{-/-}, 17 *srp54*^{+/-} and 3 WT cells remaining in the analysis. Due to the limited cell numbers, we could not minimize the dropout rate by pooling the single neutrophils per fish, but rather had to analyze the transcriptome of each cell separately. Furthermore, with these very low cell numbers, especially for the WT condition, we were only able to identify one significantly differentially expressed gene: *nupr1b* (Figure 14). Interestingly, however, the human homologue of *nupr1b*, *NUPR1*, has recently been identified as a novel master regulator of the UPR.^{296,297} Additionally, several promising candidates associated with inflammation (*irf7*), neutrophil function and homeostasis (*snap23.1*), protein synthesis (*aars1*), ribosome biogenesis and regulation as well as ER-stress (*eif2s2*, *edf1*), transcription (*taf13*) or apoptosis (*psmd3*) showed trends towards differential expression (Figure 14). To eventually verify these highly promising candidates and to identify additional hits, which we missed due to the low sample size, a scRNA-seq experiment with higher cell numbers or adapted FACS strategy will be necessary.

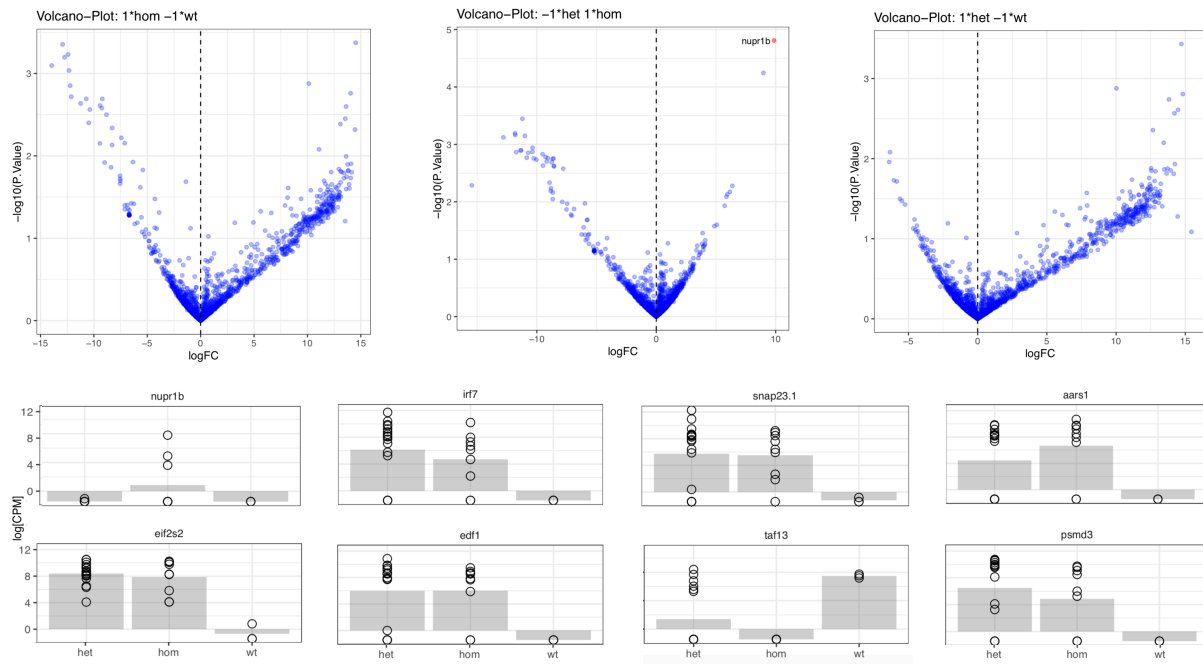


Figure 14: Differential gene expression analysis of single neutrophils. Top: Volcano plots showing the differential expression of genes comparing *srp54*^{-/-} and wt, *srp54*^{+/-} and *srp54*^{-/-} or *srp54*^{+/-} and wt (form left to right). Blue dots represent non-significantly DE genes; red dots represent significantly DE genes. Bottom: Genotype-specific log(CPM) of significantly DE genes. First row, left to right: *nupr1b*, *irf7*, *snap23.1*, *aars1*. Second row, left to right: *eif2s2*, *edf1*, *taf13*, *psmd3*.

2.2.4 Material and Methods – Additional Data

2.2.4.1 Zebrafish Husbandry and Genetic Strains.

Zebrafish were raised, bred and kept as described by Dahm and Nüsslein-Volhard.²⁹⁸ Staging was performed according to Federation of European Laboratory Animal Science Associations (FELASA) and Swiss federal law guidelines.²⁹⁹ For the experiments conducted in this study, the following transgenic zebrafish strains were used: WT Tübingen strains, *Tg(mpo:GFP)*³⁰⁰ and *srp54*^{sa11820}. Genotyping was performed on liberase dissociated single embryos according to standard protocols using the following primers for PCR: fwd: 5'-TTTGAGATGCAGATGCACTTCTTAAAT-3'; rev: 5'-CCATGCAATGACGTTTTGTT-3'. Sanger sequencing of the amplicon was performed using the reverse primer of the PCR. The analysis of the sanger sequencing data was performed with SeqMan Pro software (DNASTAR inc. Madison, Wisconsin, USA).

2.2.4.2 Single Cell Sorting

Single dechorionated zebrafish embryos were dissociated using liberase as described.¹ Subsequently, the cells were washed twice in PBS and filtered. 10% of the cell suspension were used for genotyping (as described before), whilst the remaining 90% were sorted using flow cytometry. Fluorescent activated cell sorting (FACS) was performed on a BD FACSAria™ III (BD Sciences, Franklin Lakes, New Jersey, USA). Single GFP⁺-cells were sorted into each well of a 384-well plate containing lysis buffer (1µl SUPERase In RNase Inhibitor (Thermo Fisher Scientific) in 19µl Triton-X 100 (0.2%, Sigma). After the sort, 384-well plates were frozen at -80°C.

2.2.4.3 Reverse Transcription and Library Preparation

RNA extraction, reverse transcription (RT) and library preparation were performed by the Quantitative Genomics Facility of the Department of Biosystems Science and Engineering (D-BSSE) of the ETH Zurich in Basel. The Smart-seq2 protocol was followed for RNA extraction, RT and library preparation.^{301,302} A mosquito LV nanolitre liquid handler (SPT Labtech Inc., Boston, MA, USA) was used for automated multichannel pipetting. The following primers were used: TSO primer (5'-AAG-CAG-TGG-TAT-CAA-CGC-AGA-GTA-CAT-rGrG+G-3'); Oligo-dT30VN (5'-AAG-CAG-TGG-TAT-CAA-CGC-AGG-AGT-AC(T30)VN-3'); ISPCR oligo (5'-AAG-CAG-TGG-TAT-CAA-CGC-AGA-GT-3'). scRNA-seq was performed on a Novaseq system (Illumina, Inc., San Diego, CA, USA) using a 50 bp paired-end run.

2.2.4.4 qRT-PCR

Tg(*srp54*^{+/-};*mpo:GFP*) zebrafish were crossed and their progeny raised to 48 hpf. After 48 hpf, embryos were dissociated using liberase as described elsewhere.¹ 10% of the resulting cell suspension were used for genotyping and the remaining 90% served as input for RNA extraction. Total RNA was extracted with the PicoPure RNA isolation Kit (Thermo Scientific™). cDNA was generated by RT using Multiscribe Reverse Transcriptase (Thermo Scientific™) and later diluted 1/7 and used as input for real-time PCR. Real-time PCR was performed on an Applied Biosystems™ 7500 Real-Time PCR System (Thermo Scientific™) using FastStart Universal SYBR Green Master (Rox) mix (Sigma-Aldrich®). *gapdh* was used as normalization control. The following primers were used: dnajc25-fwd: 5'-AGG-AGA-AGA-CTC-GCT-CCC-AA-3'; dnajc25-rev: 5'-GCT-CCA-CCA-GCT-GTA-ATA-CTG-AA-3'; ppp1r26-fwd: 5'-GAG-CAA-TGA-GGA-GAC-GAG-AGA-C-3'; ppp1r26rev: 5'-AAT-GAA-TAG-CCA-CAG-CCG-GA-3'; ntrk2a-fwd: 5'-ATT-ATG-ATG-CCA-CTA-CAG-ACG-A-3'; ntrk2a-rev: 5'-TTG-CTG-GAT-CAC-CGA-GGA-AGG-3'; mgst1.1-fwd: 5'-GGA-AAG-AGT-

GCG-ACG-ATG-CC-3'; mgst1.1-rev: 5'-ACA-GAA-GAC-CGA-TCA-CCA-CG-3'; slc35e-fwd: 5'-GGT-CAC-CGA-ACT-GTC-CTT-CG-3'; slc35e-rev: 5'-GTG-TCA-CGC-AAG-ACC-TTT-TTG-G-3'; si:ch211-191a24.4-fwd: 5'-TCG-CGT-ATT-GGG-TCG-TTC-AA-3'; si:ch211-191a24.4-rev: 5'-GTG-GCT-GGC-TCA-TTG-TTG-TTT-3'; For gapdh see Yoon et al.³⁰³.

3 Discussion

Note: The following discussion does not discuss the detailed results of our publication “SRP54 mutations induce Congenital Neutropenia via dominant-negative effects on XBP1 splicing”⁸², since such a paragraph is already integrated into said publication (section 2.1).⁸² Here, I rather emphasize the impact and the benefits of our publication and discuss the findings of the additional results, exclusively presented in this thesis.

SRP54 mutations are increasingly recognized as a novel cause of CN and SDS. According to the French CN Registry, they even represent the second most common mutation associated with CN.^{2,3} This hitherto unknown prevalence of SRP54 lesions evokes the need for a better understanding of how such lesions drive disease development in order to establish novel therapeutic approaches and to increase patient survival and health. In our publication “SRP54 mutations induce Congenital Neutropenia via dominant-negative effects on XBP1 splicing”⁸², published in *Blood*, we for the first time describe and establish a stable *in vivo* model of SRP54 deficiency and in addition propose impaired unconventional splicing of XBP1 as a disease-driving mechanism. The establishment of an *srp54* deficient zebrafish model not only substantially facilitates future research and opens the gate for the discovery of novel mechanisms and processes driving this disease, but also represents a tool we can exploit to perform chemical *in vivo* screenings for potential novel therapeutics. Moreover, the finding that the impairment of the unconventional splicing of XBP1 contributes to the development of CN in an SRP54 deficient background for the first time provides mechanistic insights into the pathogenesis of this disease and thus can be considered a breakthrough for the development of first targeted therapies for patients carrying SRP54 mutations.

In addition to the uncovering of potential therapeutic targets in SRP54 deficiencies, our data also shed light on the molecular resolution of the interplay between the UPR and neutrophil differentiation. Until today, the importance of the UPR, and specifically its mediator XBP1s, for neutrophil differentiation is highly controversial. While Bettigole et al. suggested that differentiation defects in XBP1-KO mice are restricted to the eosinophilic lineage, with neutrophil differentiation being unaffected, Tanimura and colleagues demonstrated the necessity of active XBP1 splicing for the differentiation of human neutrophilic cells.^{304,305} A potential explanation for this discrepancy might be that Bettigole et al. only focused on splenic and peripheral neutrophils, thereby completely neglecting BM neutrophils.³⁰⁴ Considering the low frequency of neutrophils in the spleen and the fact that only 1% of neutrophils is actively circulating in homeostatic mice, they thus only collected data from a

very small subset of most probably already specialized neutrophils.⁹⁵ Furthermore, Bettigole and colleagues quantify neutrophil differentiation by measuring the frequency of CD11b⁺Ly6G⁺ cells as adult neutrophils.³⁰⁴ However, both of these markers are expressed on all neutrophilic stages ranging from promyelocytes to mature neutrophils and thus are not well-suited for differentiation analyses and might lead to false interpretations.³⁰⁵ It might be beneficial in this case to numerically quantify CD11b expression, since it is gradually increasing during neutrophil differentiation.³⁰⁶ Contradictory to the results presented by Bettigole et al., Tanimura et al. demonstrated that the impairment of *IRE1α-XBP1* activation results in inhibited neutrophil differentiation of the human promyelocytic cell line HL-60.³⁰⁵ Our findings support the data presented by Tanimura et al. and, next to its hitherto known involvement in eosinophilic differentiation, highlight the importance of unconventional *XBP1* splicing for neutrophilic differentiation. However, it remains to be determined whether other hematopoietic lineages show similar dependencies on *XBP1s*.

In addition to demonstrating the involvement of *XBP1s* during neutrophil differentiation, our data also provide insights into the functional link between *SRP54* and effective *XBP1* splicing. We show that *SRP54* KO substantially reduces the splicing efficiency of *XBP1u* mRNA without, however, completely abolishing it. This finding is in agreement with Kanda et al., who postulate that *SRP54* knock down reduces the splicing activity of *XBP1u* mRNA by 29%.³⁰⁷ There might be multiple explanations for the non-complete abrogation of *XBP1* splicing upon *SRP54* KO. Kanda and colleagues hypothesize that ER-localized unconventional splicing of *XBP1* was limited by a certain threshold. They base their hypothesis on the fact that the ER-targeting efficiency of *XBP1u* mRNA was reduced by almost 60%, which is more than double the reduction of the splicing activity.³⁰⁷ These results, combined with our data generated with complete *srp54* KO zebrafish cells, suggest that even under ER-stress conditions, a substantial amount of *XBP1u* mRNA gets spliced inside the nucleus. This idea would significantly add to the understanding of unconventional splicing, which until now was thought to predominantly occur in the cytoplasm, with only basal splicing activity of *XBP1u* mRNA taking place in the nucleus.^{308,309}

Nonetheless, given that the majority of secreted proteins requires a functional SRP for their translocation into the ER and that *XBP1* splicing is only impaired but not completely abolished, we can conclude that the *IRE1α-XBP1* axis of the UPR is just one of the many players contributing to the development of the disease in *SRP54* deficient patients. Interestingly, despite the impaired potential of the *IRE1α-XBP1* axis to resolve ER-stress, it is surprising to see elevated ER-stress levels in *SRP54* mutated cells (as also shown by Bellanné-Chantelot et al.²), since one would rather expect lower ER-stress levels due to the

decreased number of proteins that are transported to the ER. A potential explanation for this observation might be that also the proteins involved in the UPR, such as chaperones or players of ERAD and ERQC, are not shuttled into the ER anymore, thereby synergizing with the effects of impaired *XBP1* activity and contributing to unresolved ER-stress. This hypothesis is supported by data presented by Kanda et al., who show that knock down of *SRP54* reduces the ER-targeting efficiency of the chaperone and UPR master regulator BiP by more than 80%.³⁰⁷

Since the disturbance of *SRP54* completely disrupts the balanced protein-homeostasis of a cell and leads to a highly complex cellular response, we decided to perform RNA sequencing on neutrophils of *srp54* defective zebrafish and aimed to get more insights into the pathogenesis of the disease. We focused on neutrophils, because we hoped to also identify novel lineage-specific effects contributing to blocked neutrophil differentiation. The decision to perform scRNA-seq was made due to expected differences between early neutrophil progenitors and mature polymorphonuclear cells, which were all expressing *GFP* under the control of the *mpo* promoter. As described in section 2.2.3.1 however, PCA divided the sorted cells into two distinct clusters, with only one of them expressing neutrophil-specific genes (**Figure 10**). The most probable explanations for this unwanted inclusion of non-neutrophilic cells are specificity problems during FACS. Although the Tg(*mpo:GFP*) zebrafish line effectively labels neutrophils, as shown by fluorescent microscopy,³⁰⁰ and although we used non-fluorescent zebrafish cells as negative gating controls during FACS, the inclusion of cells showing unexpected off-target expression of GFP at low levels cannot be excluded. Another potential explanation might be that the machine used for FACS (BD FACSAria™ III) was error-prone and did not only sort cells expressing GFP. Of note, the non-neutrophilic cell cluster was highly heterogeneous, comprising cells of the parachord, the notochord, cells involved in bone or fin formation, as well as nonspecific cells.

Due to the clustering of the sorted cells, we decided to conduct two different analyses: The first one covering the entire dataset, including all sorted cells, and the second one focusing only on the neutrophil cell cluster, thereby excluding non-specific cells. For both analyses, PCA did not reveal any clustering of the cells according to their genotype (**Figure 11**). Considering the very high heterogeneity of the cell populations for the analysis of the whole dataset, this finding is not surprising. For the analysis of the neutrophilic subset on the other hand, a clustering according to the different genotypes was more probable, however, also here the cellular heterogeneity, consisting of variable differentiation stages of the neutrophil lineage, caused more variance than the effects of the *srp54* defects in the respective genotypes. Furthermore, the small depth of the neutrophil-specific analysis with only very

few analyzed cells may also not have the power to represent actual genotype-specific clustering.

When performing DE analysis on the entire dataset, we were able to identify six differentially expressed genes: *ppp1r26*, *dnajc25*, *ch211*, *ntrk2a*, *mgst1.1*, and *slc35e1* (Figure 12). qRT-PCR confirmed the scRNA-seq results of *ch211* and *slc35e*, demonstrating that these two genes are significantly downregulated in *srp54*^{-/-} zebrafish when compared to *srp54*^{+/-} and WT (Figure 13). Of note, *ch211* is the zebrafish homologue of the human gene *MarvelD3*, which encodes a four-span transmembrane protein involved in the formation of tight junctions.³¹⁰ As the name implies, MarvelD3 is harboring a so called MARVEL domain. This recently discovered domain is found in a plethora of tight junction associated proteins and is hypothesized to mediate membrane apposition events occurring during biogenesis of transport vesicles or the formation of tight junctions.³¹¹ Interestingly, Occludin, another MARVEL-domain harboring protein sharing overlapping functions with MarvelD3,³¹² was shown to facilitate SNARE-dependent apical protein exocytosis as a means to protect secretory cells from ER-stress.³¹³ Assuming that MarvelD3 exerts similar functions as Occludin when it comes to alleviating ER-stress, its downregulation in *SRP54* mutated cells might contribute substantially to unresolved ER-stress. Nonetheless, it remains to be determined why *MarvelD3* is downregulated upon *SRP54* deficiency.

SLC35e is a member of the solute carrier family 35 (SLC35), which is a family consisting of nucleotide sugar transporters (NSTs).³¹⁴ Mechanistically, NSTs are essential for glycosylation, as they represent the link between the synthesis of activated sugars in the cytosol and their covalent attachment in the ER or the Golgi by glycosyltransferases.³¹⁵ Considering the pivotal role of glycosylation for the folding and function of proteins, its impairment by low expression levels of NSTs is likely to result in ER-stress. Furthermore, the activation of XBP1s, which we showed to be hampered due to defective *SRP54*, has recently been functionally linked to global N-glycan structure distribution patterns.³¹⁶ In detail, Wong et al. demonstrate that the alteration of global N-glycan patterns by activated XBP1s represents a novel way to translate intracellular stress signals to the extracellular milieu.³¹⁶ This novel functional relationship between *XBP1* and glycosylation may also affect the expression levels of *SLC35* family members, what might explain why *slc35e* appears differentially expressed in *srp54* mutant fish.

dnajc25 and *ntrk2a* were genes we also found to be downregulated in *srp54* mutant fish. However, while scRNA-seq showed significant downregulation in *srp54*^{+/-} embryos, qRT-PCR revealed that *srp54*^{-/-} siblings express the lowest mRNA levels of these genes. Considering this discrepancy, the identification of *dnajc25* and *ntrk2a* has to be further

validated to ensure reliable results. Nonetheless, especially the differential expression of *dnajc25* is highly interesting, as this gene is a member of the HSP40/DnaJ subfamily of heat shock proteins, and since *DNAJC25*, another member of this subfamily, is one of the few known mutated genes associated with SDS (Table 2).^{258,317} Generally, Hsp40 proteins act as chaperones and bind to Hsp70 proteins, thereby stimulating ATP hydrolysis and mediating protein folding.³¹⁷ Unsurprisingly, numerous members of the Hsp40/DnaJ chaperone family are involved in ER-stress and UPR.^{286,318,319} Hence, the identification of chaperones by scRNA-seq was expected. Why, however, only *dnajc25* was identified from all Hsp40 chaperones, and why it appears to be downregulated rather than upregulated, needs further investigation.

nrk2a on the other hand is a homologue of human *NTRK2*, a gene encoding TrkB, which is known to be the receptor of brain derived neurotrophic factor (BDNF). As the name of its ligand implies, TrkB is mainly present in neuronal tissues and found associated with brain disorders.³²⁰⁻³²² A recent publication, however, postulates that the BDNF-NTRK2 axis is also important in endometrial epithelial cells, where it improves cellular proliferation by protecting the cells from ER-stress.³²³

Taken together, despite being involved in completely different pathways and processes, *ch211*, *slc35e*, *dnajc25* as well as *nrk2a* are all somehow implicated in the development of ER-stress or the activation of the UPR. This very diverse group of players contributing to the phenotypic manifestations of *SRP54* deficiencies underlines the complexity of a cell's response to the disruption of an essential process such as protein secretion. In the case of *SRP54* deficiency, it remains to be investigated whether targeting one of the herein identified hits alone might alleviate the symptoms of the disease. Potentially, however, it is the interplay of numerous pathways and processes, all converging on the major axes of the UPR, which define the phenotype. Hence, further experiments are needed to approximate the therapeutic potential of *ch211*, *slc35e*, *dnajc25* and *nrk2a*, and whether targeting these genes might synergize with modulations of the promising *XPB1*-axis for example.

After focusing on the entire dataset of the scRNA-seq, we decided to analyze the neutrophil subset in more detail, with the aim to identify lineage-specific genetic alterations in *srp54* deficient zebrafish. Unfortunately, the analyzed subset was highly compromised in sample size with only 9 *srp54*^{-/-}, 17 *srp54*^{+/-} and 4 WT cells remaining in the analysis. As a consequence of these low cell numbers, the power of the analysis was substantially reduced and only one significantly differentially expressed gene, *nupr1b*, could be identified (Figure 14). The human homologue for *nupr1b* is *NUPR1*. *NUPR1* is a stress induced nuclear transcription regulator with a variety of different functions.³²⁴ Although not being known to

play crucial roles in neutrophil differentiation and homeostasis, recent data postulated an essential role for *NUPR1* during UPR.²⁹⁷ In detail, Santofimia-Castaño et al. showed that *NUPR1* inactivation antagonizes cell growth by impairing the ER-stress response and by initiating cell death via programmed necrosis. Interestingly, they also demonstrated that *NUPR1* directly controls *ATF6*, *IRE1a* and *PERK* at the transcriptional level.²⁹⁷ Thus, the significant upregulation of *nupr1b* in *srp54*^{-/-} neutrophils indicates a potential reaction of the cell to further enhance the UPR to alleviate ER-stress. In addition to the transcriptional involvement of *NUPR1* during UPR, novel data also describes a hitherto unknown role of *NUPR1* as physical orchestrator of protein translation during ER-stress.²⁹⁶ Intriguingly, co-immunoprecipitation revealed that *NUPR1* directly associates with eIF2 α , the major mediator of the *PERK*-axis of the UPR (Figure 6), thereby promoting the synthesis of proteins to allow the cell to recover from the ER-stress response.²⁹⁶ Taken together, these reports strongly support the hypothesis that *NUPR1*-governed UPR initiation, mainly through the controlled activation of the *PERK*-axis, might be one of the major pathways initiated by cells suffering from ER-stress as a result of defective *SRP54*. Importantly, in our scRNA-seq, several genes showed tendencies towards differential upregulation. Amongst these genes was *eif2s2*, whose human homologue, *EIF2S2*, is encoding eIF2 β , which, similar to eIF2 α , is a subunit of the eIF2 complex.^{325,326} The identification of this gene provides further evidence that *SRP54*-mutated cells try to compensate for the impairment of the *IRE1a-XBP1s* axis by initiating efficient *PERK* branch activity.

Although the identification of *NUPR1*-governed regulation of the *PERK*-axis significantly contributes to the understanding of the general programs and mechanisms initiated by a cell to alleviate *SRP54*-associated ER-stress, it cannot explain, why the neutrophil lineage is particularly affected by *SRP54* defects. Most of the genes showing tendencies towards significantly differential expression in the neutrophil-specific cluster of the scRNA-seq are somehow related to the distress caused by hampered protein secretion (Figure 14). *edf1* for example is known to coordinate cellular responses to ribosome collisions.³²⁷ Considering that most ribosomes, which carry proteins harboring a signal sequence might not reach the ER membrane in *srp54*-defective cells, it is likely that they are prone to stall and collide more frequently. Thus, the upregulation of *edf1* to coordinate the cell's response to this distress is plausible. Other genes showing tendencies towards differential expression are *aars1*, *taf3* and *psmd3*, which are involved in translation, transcriptional initiation and apoptosis, respectively.³²⁸⁻³³⁰ Hence, all of these genes might play important roles for the processes initiated during the UPR to alleviate ER-stress but do not explain the effects specifically observed in the neutrophil lineage either (Figure 14). Interestingly, however, a *PSMD3* variant

has recently been associated with neutropenia induced by interferon-based treatment of chronic hepatitis C.³³¹ Thus, *PSMD3* might harbor an unknown function during neutrophil differentiation.

The only two hits identified in the scRNA-seq, specifically associated with innate immunity, are *irf7* and *snap23.1*. *IRF7*, the human homologue of *irf7*, is known for its regulatory function of the innate immune response through the activation of type-1 interferons.³³² *SNAP23*, the human homologue of *snap23.1*, is a member of the SNARE family, which is essential for vesicular transport and in neutrophils particularly for degranulation and NETosis.³³³ Consequently, the upregulation of these two genes might represent the body's efforts to stimulate the innate immune response and to counteract the impaired immunity arising as a result of the low neutrophil counts in *SRP54*-deficient patients.

Taken together, we can conclude that most of the genes and pathways we found differentially expressed in the neutrophil as well as in the total dataset of the scRNA-seq are converging on the three main branches of the UPR. This observation suggests that *SRP54* mutant cells initiate pathways to compensate for the impaired *IRE1 α -XBP1* branch, with the focus lying on the controlled activation of the *PERK-eIF2 α* axis through *NUPR1*. To verify this hypothesis, especially with regards to the low cell numbers used in the scRNA-seq, however, additional experiments are needed. Nonetheless, the herein presented data provides novel evidence, highlighting the three major branches of the UPR as potential therapeutic targets of *SRP54* deficiencies.

4 Contribution to Publications

4.1 Regulation of Glioma Cell Invasion by 3q26 Gene Products PIK3CA, SOX2 and OPA1

Regulation of glioma cell invasion by 3q26 gene products PIK3CA, SOX2 and OPA1.

Schaefer, T., Ramadoss, A., Leu, S., Tintignac, L., Tostado, C., Bink, A., Schürch, C., Müller, J., Schärer, J., Moffa, G., Demougin, P., Moes, S., Stippich, C., Falbo, S., Neddersen, H., Bucher, H., Frank, S., Jenö, P., Lengerke, C., Ritz, M.-F., Mariani, L. and Boulay, J.-L. (2019). *Brain Pathol*, 29: 336-350. <https://doi.org/10.1111/bpa.12670>

4.1.1 Summary

Diffuse gliomas are the most common types of gliomas and rank amongst the most malignant human tumors. In contrast to the majority of solid tumors, diffuse gliomas do not metastasize into remote tissues and organs, but rather invade directly adjacent healthy brain regions. Consequently, the standard treatments for glioma patients, surgical resection and chemotherapy, almost inevitably lead to tumor recurrence. The limited prognostic effects of these state-of-the-art therapies evoke the need for a better understanding of the molecular mechanisms driving glioma cell invasion, potentially enabling the development of novel treatments and increasing patient survival.

Here, Thorsten Schaefer *et al.* investigated putative genetic imbalances of genes mapping to the chromosomal locus 3q26 – a locus known to be frequently imbalanced in gliomas. They analyzed a total of 129 glioma biopsies for copy number variations, thereby focusing on four genes, which are mapping within 15 megabases: *SOX2*, *PIK3CA*, *OPA1*, and *MFN1*. Out of these four genes, *SOX2* showed the highest relative amplification frequency, and *OPA1* the highest deletion frequency. Importantly, *SOX2* overexpression as well as *OPA1* knock down both resulted in increased invasion rates *in vitro* and *in vivo*.

Since *PIK3CA* was known to posttranslationally activate *SOX2* in breast cancer, Schaefer and colleagues investigated the functional connection between the *PI3K/AKT* signaling axis and *SOX2* in glioma cells. Interestingly, selective inactivation of *PI3K* and *AKT*, but not of downstream *mTORC1*, resulted in decreased *SOX2* expression, thus indicating that *SOX2* is a direct target of *AKT* and establishing a link between *PIK3CA* and *SOX2*.

Given that SOX2 is a transcriptional modulator itself, the authors performed chromatin immunoprecipitation (ChIP) and luciferase promoter activity assays to determine whether SOX2 binds to other 3q26 products. Whilst *MFN1* was not regulated by SOX2, *PIK3CA* and especially *OPA1* showed significantly upregulated promoter activity in response to SOX2.

In a last experiment, the authors performed neuroimaging of human glioma and found that SOX2 amplification as well as *OPA1* deletion are associated with substantially increased tumor necrosis volumes. Hence, we postulate a functional connectivity between glioma cell invasion and tumor necrosis.

4.1.2 Contribution

For this publication, I was involved in the *in vivo* studies conducted in zebrafish. To assess the effects of SOX2 amplification on tumor cell invasion, I received LN319 glioma cells overexpressing SOX2 (*TetON mCherry-SOX2*) and compared them to the corresponding *TetON* control cells. For the analysis of *OPA1* deletion, I received LN319 cells treated either with *OPA1* shRNA or control RNA. All four of these cell lines were treated with Doxycycline prior to handing them to me. After labeling with CellTracker™ CM-Dil (C7000, Life Technologies, Carlsbad, CA, USA), the cells were injected into 48 hours-old, anaesthetized WT zebrafish (Tu, Tuebingen) embryos. Approximately 100 glioma cells were injected directly into the vessel-free area of the yolk sac of the fish.³³⁴ After transplantation, the embryos were incubated at 35°C and successful and even injection of labeled cells was verified by fluorescent microscopy 2 hours post injection. 72 hours post injection, engraftment and tumor cell invasion were assessed by screening the injected embryos using a Zeiss Discovery V20 Stereo microscope and the behavior of the glioma cells was categorized according to one of the following three criteria: aggregate growth, invasive growth, dissemination to CHT. For more detailed analyses, fluorescent confocal microscopy was performed on a Zeiss LSM710 microscope and image analysis was conducted using FIJI software.³³⁵

Importantly, the obtained results were in agreement with *in vitro* observations: Both, SOX2 amplification as well as *OPA1* knock down led to increased invasion of the transplanted LN319 glioma cells compared to control cells (**Figure 15**). While most of the fish transplanted with control cells presented with stable cell masses in proximity to the injection site (aggregate growth), SOX2 overexpressing and *OPA1* knock down cells showed a significant tendency to disperse throughout the yolk sac (invasive growth, **Figure 15**).

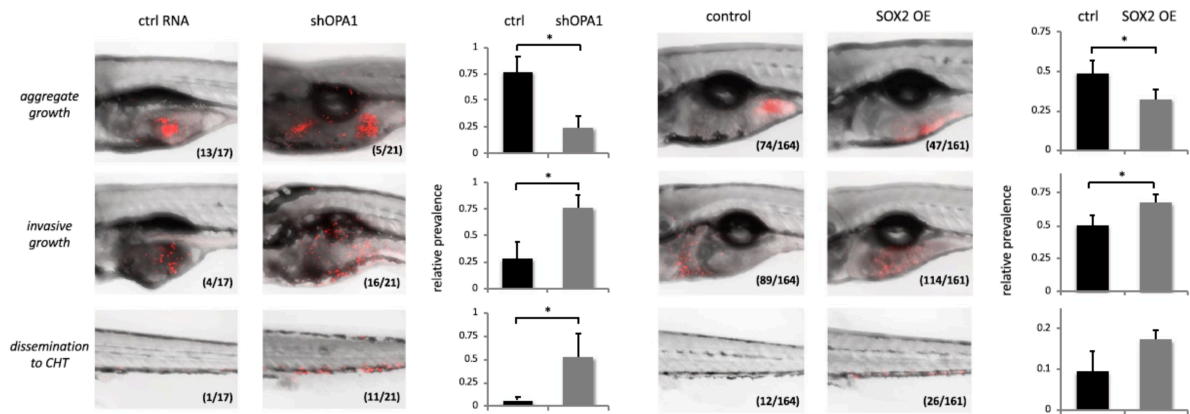


Figure 15: *OPA1* knock down and *SOX2* overexpression increase the invasiveness of LN319 cells *in vivo*.

Left: Confocal images of zebrafish xenotransplanted with control LN319 cells and sh*OPA1* LN319 cells as well as the corresponding relative quantification. Right: Confocal images of zebrafish xenotransplanted with control LN319 cells and *SOX2* overexpressing LN319 cells as well as the corresponding relative quantification. Top row: Aggregate growth; Middle row: Invasive growth; Bottom row: Dissemination to CHT. Transplanted LN319 cells are stained in red (CM-Dil). Inlays indicate absolute numbers of embryos showing the corresponding phenotype per condition. *P < 0.05.

4.2 Oncogenic KRAS^{G12D} Causes Myeloproliferation via NLRP3 Inflammasome Activation

Oncogenic Kras^{G12D} causes myeloproliferation via NLRP3 inflammasome activation.

Shaima'a Hamarsheh, Lena Osswald, Benedikt S. Saller, Susanne Unger, Donatella De Feo, Janaki Manoja Vinnakota, Martina Konantz, Franziska M. Uhl, Heiko Becker, Michael Lübbert, Khalid Shoumariyeh, Christoph Schürch, Geoffroy Andrieux, Nils Venhoff, Annette Schmitt-Graeff, Sandra Duquesne, Dietmar Pfeifer, Matthew A. Cooper, Claudia Lengerke, Melanie Boerries, Justus Duyster, Charlotte M. Niemeyer, Miriam Erlacher, Bruce R. Blazar, Burkard Becher, Olaf Groß, Tilman Brummer & Robert Zeiser.

Nat Commun **11**, 1659 (2020). <https://doi.org/10.1038/s41467-020-15497-1>

4.2.1 Summary

Oncogenic *RAS* mutations are recurrent events associated with various types of leukemia. In addition to the direct transforming effect via constant activation of the RAS/MEK/ERK signaling cascade, Hamarsheh et al. here propose an inflammation-related contribution of *RAS* mutations to the disease (Figure 16). By performing microarray-based studies they discovered that oncogenic KRAS^{G12D} leads to NLRP3 inflammasome activation in murine BM. In agreement with this finding, they also demonstrated increased caspase-1 and interleukin-1 β cleavage in KRAS^{G12D} BM dendritic cells, suggesting stronger inflammasome activation. To investigate the functional role of NLRP3 inflammasome in a Kras^{G12D} background, the authors generated a mouse model harboring an *NLRP3* KO and conditional *Kras* activation (Kras^{G12D};Nlrp3^{-/-}). Interestingly, NLRP3 deficiency reversed Kras^{G12D} cytopenia and myeloproliferation in the BM, the spleen and in the periphery. Moreover, *in vitro* cultivation of myeloid and BM dendritic cells derived from Kras^{G12D} mice showed increased proliferation rates compared to Kras^{G12D};Nlrp3^{-/-} derived cells, indicating a cell-autonomous connection between oncogenic Kras and NLRP3. However, WT-derived myeloid and BM dendritic cells showed even lower proliferation when compared to Kras^{G12D};Nlrp3^{-/-}, thus also adding a non-cell-autonomous component of the microenvironment to the Kras/NLRP3 connection. Of note, treatment of Kras^{G12D} mice with the IL-1 receptor type 1 antagonist Anakinra or the NLRP3 inhibitor MCC950 reversed myeloproliferation, thereby rendering the NLRP3/IL-1 β axis a potential therapeutic target to interfere with KRAS-driven diseases.

Furthermore, by performing gene expression analyses and inhibitor studies, Hamarsheh et al. identified RAC1 mediated reactive oxygen species (ROS) production as one of the major drivers of myeloproliferation in $Kras^{G12D}$ BM dendritic cells.

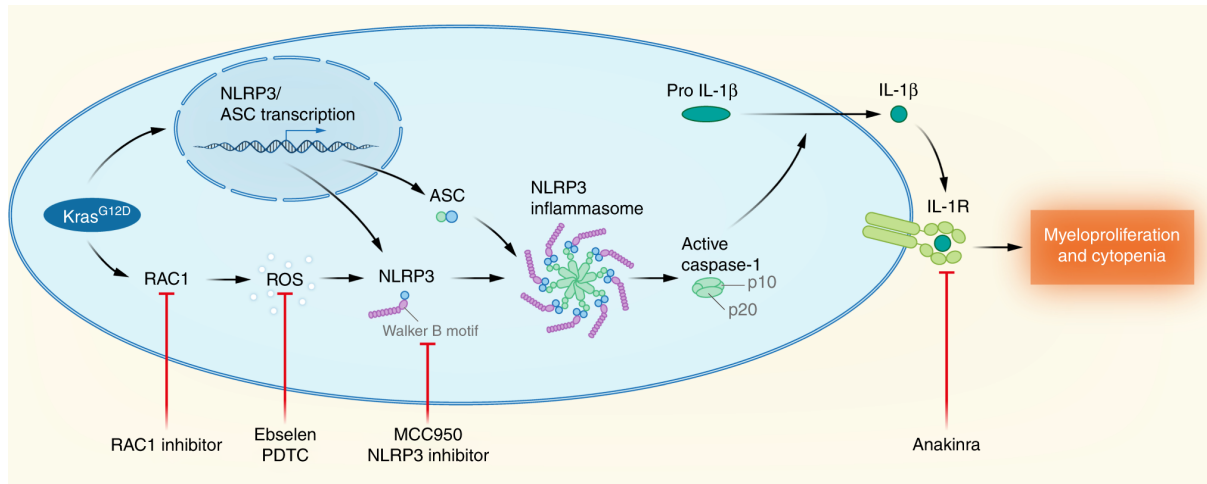


Figure 16: Schematic overview of $KRAS^{G12D}$ driven myeloproliferation and cytopenia via the activation of the NLRP3 inflammasome.

4.2.2 Contribution

For this publication, I performed zebrafish studies to investigate the non-cell-autologous effects of $KRAS^{G12V}$ on HSCs. In detail, we aimed to express $KRAS^{G12V}$ in endothelial cells and planned to quantify the activity of caspase-1 in HSCs.

In order to transiently overexpress $KRAS^{G12V}$ in endothelial cells, I PCR-amplified a sequence encoding β -crystallin:BFP and, by using In-Fusion cloning (Takara Bio USA, Inc.), inserted the amplicon into a destination vector harboring a UAS:eGFP- $KRAS^{G12V}$ cassette flanked by Tol2-sites. Subsequently, the plasmid (40 ng/ μ l) together with mRNA encoding Tol2-transposase (25 ng/ μ l) was co-injected into Tg((fli.1:Gal4FF^{ubs3}, UAS:RFP)^{rk8}; (c-myb:GFP)^{zf169}) embryos at the one-cell-stage of development. Successful expression of the microinjected construct was monitored by screening for the β -crystallin signal in the eye of the embryos 48 hpf.

To assess the effects of endothelial $KRAS^{G12V}$ on caspase-1 activity in HSCs, we dissociated the embryos at 48 hpf using liberase (Merck KGaA, Darmstadt, Germany) at 32°C for 40 min. To support liberase digestion, the embryos were mechanically disrupted after 20 min and 40 min of the digestion. Following dissociation, the cells were filtered through a 35 μ m filter and washed twice in PBS.

Caspase-1 activity was quantified using the FLICA 660 Caspase-1 Assay Kit (ImmunoChemistry Technologies) as described. Data acquisition was performed by flow

cytometry on either a Cytoflex using Cytexpert software (Beckman Coulter Life Sciences, Indianapolis, Indiana, USA) or an LSR II Fortessa (BD Biosciences). Additionally, SytoxBlue (ThermoFisher Scientific) was used to discriminate living and dead cells and the flow cytometry data was analyzed using FlowJo software (vX.0.7). According to the fluorophores used in the transgenic lines, HSCs were identified as eGFP⁺/RFP⁻, whilst endothelial cells were expressing both colors (eGFP⁺/RFP⁺).

Importantly, the percentage of HSCs showing caspase-1 activity was significantly lower in non-injected control fish compared to *KRAS*^{G12V} injected siblings (**Figure 17**). In agreement with the mouse and *in vitro* data presented in the publication, these results demonstrate increased *NLRP3* activation as a result of oncogenic *KRAS* expression.

Of note, my contribution for this publication was not included in the final publication but presented to the reviewers as a part of the rebuttal letter.

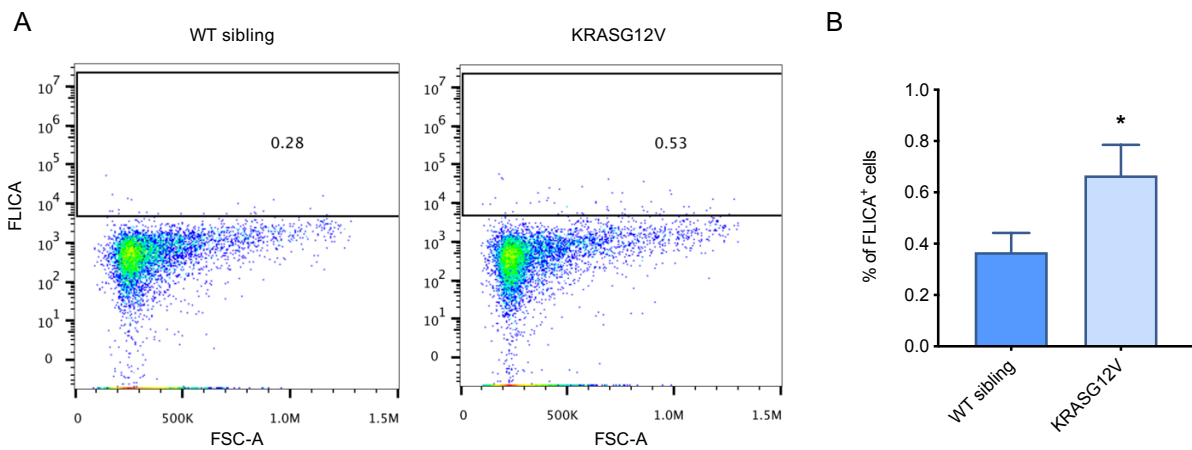


Figure 17: Mosaic expression of *KRAS*^{G12V} leads to increased caspase-1 activity in zebrafish.

(A) Flow cytometric analysis of FLICA⁺ HSCs from WT siblings (left) and *KRAS*^{G12V} expressing embryos (right). Inlays indicate FLICA⁺ HSCs as compared to unstained controls. **(B)** Quantification of flow cytometric analysis of FLICA⁺ HSCs from WT siblings (left) and *KRAS*^{G12V} expressing embryos (right). n = 3 biological replicates with at least 10 embryos per replicate were used. *P < 0.05.

4.4 Targeting Chronic NFAT Activation with Calcineurin Inhibitors in Diffuse Large B-Cell Lymphoma

Targeting Chronic NFAT Activation with Calcineurin Inhibitors in Diffuse Large B-Cell Lymphoma.

Philip Bucher, Tabea Erdmann, Paula Grondona, Wendan Xu, Anja Schmitt, Christoph Schürch, Myroslav Zapukhlyak, Caroline Schönfeld, Edgar Serfling, Daniela Kramer, Michael Grau, Pavel Klener, Claudia Lengerke, Klaus Schulze-Osthoff, Georg Lenz, Stephan Hailfinger; *Blood*2020; 135 (2): 121–132.doi: <https://doi.org/10.1182/blood.2019001866>

4.4.1 Summary

Diffuse large B-cell lymphoma (DLBCL) is the most common type of lymphoma in adults. According to gene expression profiles, DLBCLs can be divided into 2 major subtypes: Germinal center B-cell-like (GCB) and aggressive activated B-cell-like (ABC) DLBCLs. Whilst GCB DLBCLs are often associated with mutations in tumor suppressor genes and chronic activation of B-cell receptor signaling, ABC DLBCLs are hallmarked by dysregulation of immune receptor signaling eventually resulting in constitutive activation of NF- κ B. Another transcription factor family, which has been implicated in DLBCL pathogenesis is the NFAT family. In this publication, Bucher et al. investigated the role of NFAT in the development of ABC and GCB DLBCLs with the aim to identify novel therapeutic targets (**Figure 18**).

In detail, the authors initially discovered that inhibition of the phosphatase calcineurin induced cytotoxicity in ABC DLBCLs. Since calcineurin is known to dephosphorylate NFAT and thereby cause its nuclear localization and hence activation, Bucher et al. hypothesized that NFAT might be involved in the survival of the ABC subgroup of DLBCLs. To verify this hypothesis, they compared DLBCL cell lines with primary B-cells, Burkitt lymphoma cells or Jurkat T-cells. Interestingly, DLBCL cell lines showed increased intracellular calcium flux, higher permeability of calcium ion channels as well as enhanced dephosphorylation and nuclear localization of NFAT. All of these findings indicate chronic activation of the calcium-calcineurin-NFAT axis, not only in ABC but also in GCB DLBCLs (**Figure 18**). Importantly, none of the above-mentioned indications were arising from B-cell receptor (BCR) derived signals, as shown by inhibitor studies. However, Bucher et al. observed that inhibition of BCR derived signals in ABC DLBCLs lowered the protein levels of NFATc1, a member of the NFAT family. Since NF- κ B is known to be one of the major players in this subtype of lymphoma, the authors hypothesized that it might be involved in the expression of NFATc1. Indeed,

blocking NF- κ B activity significantly interfered with NFATc1 expression, which implies that although BCR-derived signals are not involved in NFAT activity, they still contribute to ABC DLBCL pathogenesis by controlling the expression levels of NFAT via NF- κ B.

To unravel the mechanism leading to cellular toxicity in ABC DLBCLs upon calcineurin inhibition, Bucher *et al.* analyzed the gene expression profiles of the ABC DLBCL cell line HBL-1 after treatment with the calcineurin inhibitors cyclosporin A (CsA) and FK506. Interestingly, gene set enrichment analysis revealed that many of the differentially expressed genes are target genes of NF- κ B, indicating that NFAT and NF- κ B regulate common gene sets in B-cells. Amongst the most interesting differentially expressed genes were *IL-6* and *IL-10*. The fact that the secretion of these two growth-promoting cytokines was dependent on NFAT activity suggests that the cytotoxicity observed in CsA and FK506 treated ABC DLBCLs might be a result of the downregulation of *IL-6* and *IL-10*. Interestingly, the expression of the transcription factor c-Jun, which mediates the interaction of tumor cells with the microenvironment but also regulates *IL-6* and *IL-10*, was also found impaired upon calcineurin inhibition. Importantly, both, overexpression of c-Jun as well as *IL-6/IL-10* supplementation, were able to partially compensate for the CsA/FK506 induced cytotoxicity in ABC DLBCLs.

In a last step, the authors investigated the therapeutic potential of calcineurin inhibitors *in vivo*. They found that calcineurin inhibitors significantly impair tumor formation in mouse and zebrafish ABC DLBCL xenograft models and that they synergize with BCL-2 and MCL-1 inhibitors.

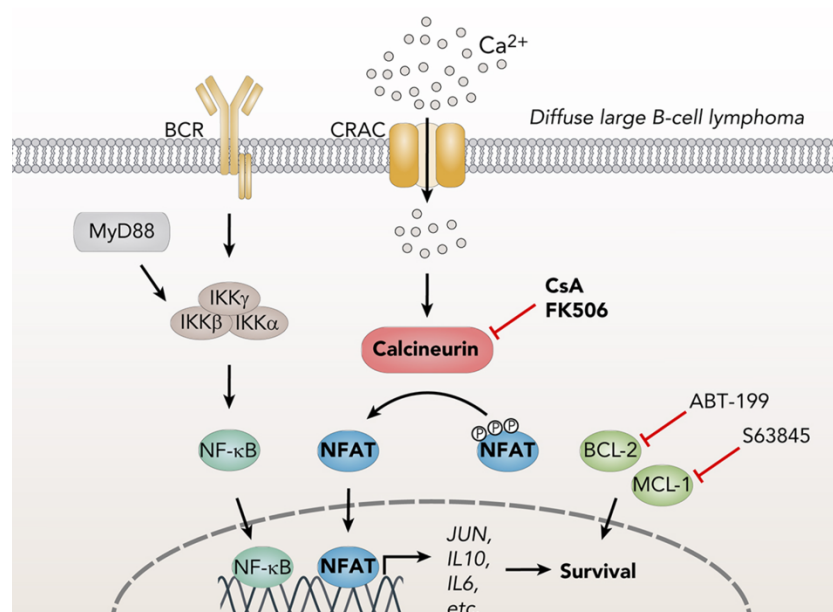


Figure 18: Schematic overview of the mechanisms mediating the survival of DLBCLs.

4.4.2 Contribution

For this publication, I performed the zebrafish xenotransplantation assays. In detail, we aimed to investigate the potential of the calcineurin inhibitors CsA and FK506 as well as of the BCL-2 inhibitor ABT-199 (Venetoclax) for the treatment of ABC DLBCLs *in vivo*. For this purpose, we stained the ABC DLBCL cell line TMD8 with CellTracker™ CM-Dil (C7000, Life Technologies, Carlsbad, CA, USA) and transplanted the labelled cells into the yolk sac of 48 hpf old zebrafish embryos (100 cells per embryo). One hour post transplantation, the embryos were transferred into medium containing either solvent (1 μ M DMSO), CsA (1 μ M), FK506 (1 μ M), ABT-199 (1 μ M) or CsA + ABT-199. After 3 days of incubation at 33°C, tumor formation was assessed by fluorescent microscopy and the ratio of zebrafish with tumors was calculated.

Interestingly, we found that CsA, FK506 as well as ABT-199 significantly reduced tumor formation, with the effect being most evident for FK506 (Figure 19). In addition, CsA and ABT-199 showed synergistic effects if applied together and reduced the ratio of zebrafish forming tumors by approximately 66% (Figure 19).

Taken together, these results demonstrate the therapeutic potential of calcineurin inhibitors for the treatment of ABC DLBCLs and further suggest combinatorial effects with BCL-2 inhibitors.

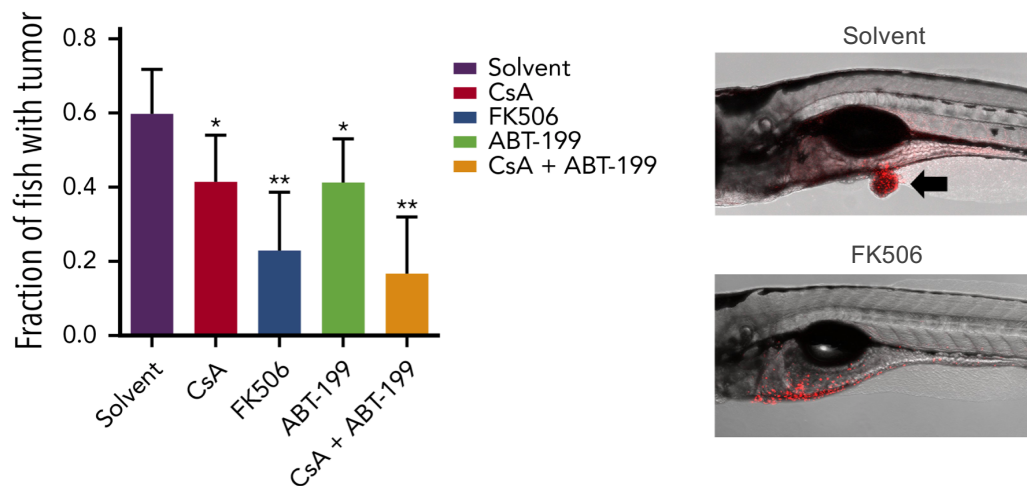


Figure 19: Calcineurin blockade synergizes with BCL-2 inhibitors.

Left: Quantification of tumor formation in zebrafish transplanted with TMD8 cells followed by treatment with either solvent (1 μ M DMSO), CsA (1 μ M), FK506 (1 μ M), ABT-199 (1 μ M) or CsA + ABT-199. Shown is the fraction of zebrafish with visible tumors. Right: Representative images of solvent (top) and FK506 (bottom) treated zebrafish 3 days after transplantation. Transplanted TMD8 cells are shown in red (CM-Dil). A minimum of $n = 20$ fish were analyzed per condition. * $P = 0.05$, ** $P = 0.01$.

References

1. Carapito R, Konantz M, Paillard C, et al. Mutations in signal recognition particle SRP54 cause syndromic neutropenia with Shwachman-Diamond-like features. *J Clin Invest*. 2017;127(11):4090-4103.
2. Bellanné-Chantelot C, Schmaltz-Panneau B, Marty C, et al. Mutations in the SRP54 gene cause severe congenital neutropenia as well as Shwachman-Diamond-like syndrome. *Blood*. 2018;132(12):1318-1331.
3. Oyarbide U, Corey SJ. SRP54 and a need for a new neutropenia nosology. *Blood*. 2018;132(12):1220-1222.
4. Doulatov S, Notta F, Laurenti E, Dick JE. Hematopoiesis: a human perspective. *Cell Stem Cell*. 2012;10(2):120-136.
5. Haynes A, Nigel R. Hematopoiesis - Growth Factors and Mechanisms of Regulation. In: J.L. J, ed. *Principles of Molecular Medicine*: Humana Press, Totowa, NJ; 1998:171 - 178.
6. Notta F, Zandi S, Takayama N, et al. Distinct routes of lineage development reshape the human blood hierarchy across ontogeny. *Science*. 2016;351(6269):aab2116.
7. Boisset JC, Robin C. On the origin of hematopoietic stem cells: progress and controversy. *Stem Cell Res*. 2012;8(1):1-13.
8. Neumann FEC. Über die Bedeutung des Knochenmarks für die Blutbildung, Ein Beitrag zur Entwicklungsgeschichte der Blutkörperchen. *Archiv für Heilkunde*. Vol. 10; 1868:68 - 102.
9. Neumann FEC. Hämatologische Studien. *Virchows Archiv für pathologische Anatomie und Physiologie und für klinische Medizin*. Vol. 207; 1912:379 - 412.
10. Maximov A. Der Lymphozyt als gemeinsame Stammzelle der verschiedenen Blutelemente in der embryonalen Entwicklung und im postfetalen Leben der Säugetiere. *Folia Haematologica*. Vol. 8; 1909:125 - 134.
11. THOMAS ED, LOCHTE HL, LU WC, FERREBEE JW. Intravenous infusion of bone marrow in patients receiving radiation and chemotherapy. *N Engl J Med*. 1957;257(11):491-496.
12. BECKER AJ, McCULLOCH EA, TILL JE. Cytological demonstration of the clonal nature of spleen colonies derived from transplanted mouse marrow cells. *Nature*. 1963;197:452-454.
13. MCCULLOCH EA, TILL JE. PROLIFERATION OF HEMOPOIETIC COLONY-FORMING CELLS TRANSPLANTED INTO IRRADIATED MICE. *Radiat Res*. 1964;22:383-397.
14. TILL JE, McCULLOCH EA. A direct measurement of the radiation sensitivity of normal mouse bone marrow cells. *Radiat Res*. 1961;14:213-222.
15. Jagannathan-Bogdan M, Zon LI. Hematopoiesis. *Development*. 2013;140(12):2463-2467.
16. Orkin SH, Zon LI. Hematopoiesis: an evolving paradigm for stem cell biology. *Cell*. 2008;132(4):631-644.
17. Lacaud G, Kouskoff V. Hemangioblast, hemogenic endothelium, and primitive versus definitive hematopoiesis. *Exp Hematol*. 2017;49:19-24.

18. Palis J. Primitive and definitive erythropoiesis in mammals. *Front Physiol.* 2014;5:3.
19. Palis J, Yoder MC. Yolk-sac hematopoiesis: the first blood cells of mouse and man. *Exp Hematol.* 2001;29(8):927-936.
20. Murray P. The development in vitro of the blood of the early chick embryo. *Proc R Soc Lond B.* 1932;111:497-520.
21. Choi K, Kennedy M, Kazarov A, Papadimitriou JC, Keller G. A common precursor for hematopoietic and endothelial cells. *Development.* 1998;125(4):725-732.
22. Huber TL, Kouskoff V, Fehling HJ, Palis J, Keller G. Haemangioblast commitment is initiated in the primitive streak of the mouse embryo. *Nature.* 2004;432(7017):625-630.
23. Vogeli KM, Jin SW, Martin GR, Stainier DY. A common progenitor for haematopoietic and endothelial lineages in the zebrafish gastrula. *Nature.* 2006;443(7109):337-339.
24. Mandal L, Banerjee U, Hartenstein V. Evidence for a fruit fly hemangioblast and similarities between lymph-gland hematopoiesis in fruit fly and mammal aorta-gonadal-mesonephros mesoderm. *Nat Genet.* 2004;36(9):1019-1023.
25. Kennedy M, D'Souza SL, Lynch-Kattman M, Schwantz S, Keller G. Development of the hemangioblast defines the onset of hematopoiesis in human ES cell differentiation cultures. *Blood.* 2007;109(7):2679-2687.
26. Tober J, Koniski A, McGrath KE, et al. The megakaryocyte lineage originates from hemangioblast precursors and is an integral component both of primitive and of definitive hematopoiesis. *Blood.* 2007;109(4):1433-1441.
27. Bertrand JY, Kim AD, Violette EP, Stachura DL, Cisson JL, Traver D. Definitive hematopoiesis initiates through a committed erythromyeloid progenitor in the zebrafish embryo. *Development.* 2007;134(23):4147-4156.
28. Frame JM, McGrath KE, Palis J. Erythro-myeloid progenitors: "definitive" hematopoiesis in the conceptus prior to the emergence of hematopoietic stem cells. *Blood Cells Mol Dis.* 2013;51(4):220-225.
29. McGrath KE, Frame JM, Fegan KH, et al. Distinct Sources of Hematopoietic Progenitors Emerge before HSCs and Provide Functional Blood Cells in the Mammalian Embryo. *Cell Rep.* 2015;11(12):1892-1904.
30. McGrath KE, Frame JM, Palis J. Early hematopoiesis and macrophage development. *Semin Immunol.* 2015;27(6):379-387.
31. McGrath KE, Frame JM, Fromm GJ, et al. A transient definitive erythroid lineage with unique regulation of the β -globin locus in the mammalian embryo. *Blood.* 2011;117(17):4600-4608.
32. Yokota T, Huang J, Tavian M, et al. Tracing the first waves of lymphopoiesis in mice. *Development.* 2006;133(10):2041-2051.
33. Yoshimoto M, Porayette P, Glossoon NL, et al. Autonomous murine T-cell progenitor production in the extra-embryonic yolk sac before HSC emergence. *Blood.* 2012;119(24):5706-5714.
34. Pietilä I, Vainio S. The embryonic aorta-gonad-mesonephros region as a generator of haematopoietic stem cells. *APMIS.* 2005;113(11-12):804-812.
35. Kissa K, Herbomel P. Blood stem cells emerge from aortic endothelium by a novel type of cell transition. *Nature.* 2010;464(7285):112-115.

36. Bertrand JY, Chi NC, Santoso B, Teng S, Stainier DY, Traver D. Haematopoietic stem cells derive directly from aortic endothelium during development. *Nature*. 2010;464(7285):108-111.
37. Morrison SJ, Kimble J. Asymmetric and symmetric stem-cell divisions in development and cancer. *Nature*. 2006;441(7097):1068-1074.
38. Ogawa M. Differentiation and proliferation of hematopoietic stem cells. *Blood*. 1993;81(11):2844-2853.
39. Morrison SJ, Weissman IL. The long-term repopulating subset of hematopoietic stem cells is deterministic and isolatable by phenotype. *Immunity*. 1994;1(8):661-673.
40. Morrison SJ, Uchida N, Weissman IL. The biology of hematopoietic stem cells. *Annu Rev Cell Dev Biol*. 1995;11:35-71.
41. Kondo M, Weissman IL, Akashi K. Identification of clonogenic common lymphoid progenitors in mouse bone marrow. *Cell*. 1997;91(5):661-672.
42. Akashi K, Traver D, Miyamoto T, Weissman IL. A clonogenic common myeloid progenitor that gives rise to all myeloid lineages. *Nature*. 2000;404(6774):193-197.
43. Kondo M. Lymphoid and myeloid lineage commitment in multipotent hematopoietic progenitors. *Immunol Rev*. 2010;238(1):37-46.
44. Weissman IL, Shizuru JA. The origins of the identification and isolation of hematopoietic stem cells, and their capability to induce donor-specific transplantation tolerance and treat autoimmune diseases. *Blood*. 2008;112(9):3543-3553.
45. Cheng H, Zheng Z, Cheng T. New paradigms on hematopoietic stem cell differentiation. *Protein Cell*. 2020;11(1):34-44.
46. Weissman I. How One Thing Led to Another. *Annu Rev Immunol*. 2016;34:1-30.
47. Velten L, Haas SF, Raffel S, et al. Human haematopoietic stem cell lineage commitment is a continuous process. *Nat Cell Biol*. 2017;19(4):271-281.
48. Karamitros D, Stoilova B, Aboukhalil Z, et al. Single-cell analysis reveals the continuum of human lympho-myeloid progenitor cells. *Nat Immunol*. 2018;19(1):85-97.
49. Paul F, Arkin Y, Giladi A, et al. Transcriptional Heterogeneity and Lineage Commitment in Myeloid Progenitors. *Cell*. 2015;163(7):1663-1677.
50. Buenrostro JD, Corces MR, Lareau CA, et al. Integrated Single-Cell Analysis Maps the Continuous Regulatory Landscape of Human Hematopoietic Differentiation. *Cell*. 2018;173(6):1535-1548.e1516.
51. Scala S, Aiuti A. In vivo dynamics of human hematopoietic stem cells: novel concepts and future directions. *Blood Adv*. 2019;3(12):1916-1924.
52. Psaila B, Barkas N, Iskander D, et al. Single-cell profiling of human megakaryocyte-erythroid progenitors identifies distinct megakaryocyte and erythroid differentiation pathways. *Genome Biol*. 2016;17:83.
53. Psaila B, Mead AJ. Single-cell approaches reveal novel cellular pathways for megakaryocyte and erythroid differentiation. *Blood*. 2019;133(13):1427-1435.
54. Hirschi KK, Nicoli S, Walsh K. Hematopoiesis Lineage Tree Uprooted: Every Cell Is a Rainbow. *Dev Cell*. 2017;41(1):7-9.
55. Haffter P, Granato M, Brand M, et al. The identification of genes with unique and essential functions in the development of the zebrafish, *Danio rerio*. *Development*. 1996;123:1-36.

56. Mullins MC, Hammerschmidt M, Haffter P, Nüsslein-Volhard C. Large-scale mutagenesis in the zebrafish: in search of genes controlling development in a vertebrate. *Curr Biol.* 1994;4(3):189-202.
57. Ransom DG, Haffter P, Odenthal J, et al. Characterization of zebrafish mutants with defects in embryonic hematopoiesis. *Development.* 1996;123:311-319.
58. Driever W, Solnica-Krezel L, Schier AF, et al. A genetic screen for mutations affecting embryogenesis in zebrafish. *Development.* 1996;123:37-46.
59. Orkin SH, Zon LI. Genetics of erythropoiesis: induced mutations in mice and zebrafish. *Annu Rev Genet.* 1997;31:33-60.
60. de Jong JL, Zon LI. Use of the zebrafish system to study primitive and definitive hematopoiesis. *Annu Rev Genet.* 2005;39:481-501.
61. Liao EC, Paw BH, Oates AC, Pratt SJ, Postlethwait JH, Zon LI. SCL/Tal-1 transcription factor acts downstream of cloche to specify hematopoietic and vascular progenitors in zebrafish. *Genes Dev.* 1998;12(5):621-626.
62. Detrich HW, Kieran MW, Chan FY, et al. Intraembryonic hematopoietic cell migration during vertebrate development. *Proc Natl Acad Sci U S A.* 1995;92(23):10713-10717.
63. Thompson MA, Ransom DG, Pratt SJ, et al. The cloche and spadetail genes differentially affect hematopoiesis and vasculogenesis. *Dev Biol.* 1998;197(2):248-269.
64. Sumanas S, Gomez G, Zhao Y, Park C, Choi K, Lin S. Interplay among Etsrp/ER71, Scl, and Alk8 signaling controls endothelial and myeloid cell formation. *Blood.* 2008;111(9):4500-4510.
65. Patterson LJ, Gering M, Eckfeldt CE, et al. The transcription factors Scl and Lmo2 act together during development of the hemangioblast in zebrafish. *Blood.* 2007;109(6):2389-2398.
66. Paik EJ, Zon LI. Hematopoietic development in the zebrafish. *Int J Dev Biol.* 2010;54(6-7):1127-1137.
67. Cantor AB, Orkin SH. Transcriptional regulation of erythropoiesis: an affair involving multiple partners. *Oncogene.* 2002;21(21):3368-3376.
68. Scott EW, Simon MC, Anastasi J, Singh H. Requirement of transcription factor PU.1 in the development of multiple hematopoietic lineages. *Science.* 1994;265(5178):1573-1577.
69. Okuda T, van Deursen J, Hiebert SW, Grosveld G, Downing JR. AML1, the target of multiple chromosomal translocations in human leukemia, is essential for normal fetal liver hematopoiesis. *Cell.* 1996;84(2):321-330.
70. Yokomizo T, Hasegawa K, Ishitobi H, et al. Runx1 is involved in primitive erythropoiesis in the mouse. *Blood.* 2008;111(8):4075-4080.
71. Kalev-Zylinska ML, Horsfield JA, Flores MV, et al. Runx1 is required for zebrafish blood and vessel development and expression of a human RUNX1-CBF2T1 transgene advances a model for studies of leukemogenesis. *Development.* 2002;129(8):2015-2030.
72. Chen MJ, Yokomizo T, Zeigler BM, Dzierzak E, Speck NA. Runx1 is required for the endothelial to haematopoietic cell transition but not thereafter. *Nature.* 2009;457(7231):887-891.
73. de Bruijn M, Dzierzak E. Runx transcription factors in the development and function of the definitive hematopoietic system. *Blood.* 2017;129(15):2061-2069.

74. Soza-Ried C, Hess I, Netuschil N, Schorpp M, Boehm T. Essential role of c-myb in definitive hematopoiesis is evolutionarily conserved. *Proc Natl Acad Sci U S A*. 2010;107(40):17304-17308.
75. Kumar A, D'Souza SS, Thakur AS. Understanding the Journey of Human Hematopoietic Stem Cell Development. *Stem Cells Int*. 2019;2019:2141475.
76. Konantz M, Alghisi E, Müller JS, et al. Evi1 regulates Notch activation to induce zebrafish hematopoietic stem cell emergence. *EMBO J*. 2016;35(21):2315-2331.
77. Kanz D, Konantz M, Alghisi E, North TE, Lengerke C. Endothelial-to-hematopoietic transition: Notch-ing vessels into blood. *Ann N Y Acad Sci*. 2016;1370(1):97-108.
78. Pruchniak MP, Arazna M, Demkow U. Life of neutrophil: from stem cell to neutrophil extracellular trap. *Respir Physiol Neurobiol*. 2013;187(1):68-73.
79. Cowland JB, Borregaard N. Granulopoiesis and granules of human neutrophils. *Immunol Rev*. 2016;273(1):11-28.
80. Hong CW. Current Understanding in Neutrophil Differentiation and Heterogeneity. *Immune Netw*. 2017;17(5):298-306.
81. da Silva FM, Massart-Leën AM, Burvenich C. Development and maturation of neutrophils. *Vet Q*. 1994;16(4):220-225.
82. Schürch C, Schaefer T, Müller JS, et al. SRP54 mutations induce Congenital Neutropenia via dominant-negative effects on XBP1 splicing. *Blood*. 2020.
83. Roberts AW. G-CSF: a key regulator of neutrophil production, but that's not all! *Growth Factors*. 2005;23(1):33-41.
84. Lieschke GJ, Grail D, Hodgson G, et al. Mice lacking granulocyte colony-stimulating factor have chronic neutropenia, granulocyte and macrophage progenitor cell deficiency, and impaired neutrophil mobilization. *Blood*. 1994;84(6):1737-1746.
85. Seymour JF, Lieschke GJ, Grail D, Quilici C, Hodgson G, Dunn AR. Mice lacking both granulocyte colony-stimulating factor (CSF) and granulocyte-macrophage CSF have impaired reproductive capacity, perturbed neonatal granulopoiesis, lung disease, amyloidosis, and reduced long-term survival. *Blood*. 1997;90(8):3037-3049.
86. Liu F, Wu HY, Wesselschmidt R, Kornaga T, Link DC. Impaired production and increased apoptosis of neutrophils in granulocyte colony-stimulating factor receptor-deficient mice. *Immunity*. 1996;5(5):491-501.
87. Coffelt SB, Wellenstein MD, de Visser KE. Neutrophils in cancer: neutral no more. *Nat Rev Cancer*. 2016;16(7):431-446.
88. Jin H, Li L, Xu J, et al. Runx1 regulates embryonic myeloid fate choice in zebrafish through a negative feedback loop inhibiting Pu.1 expression. *Blood*. 2012;119(22):5239-5249.
89. Gowney JD, Shigematsu H, Li Z, et al. Loss of Runx1 perturbs adult hematopoiesis and is associated with a myeloproliferative phenotype. *Blood*. 2005;106(2):494-504.
90. Zhang DE, Zhang P, Wang ND, Hetherington CJ, Darlington GJ, Tenen DG. Absence of granulocyte colony-stimulating factor signaling and neutrophil development in CCAAT enhancer binding protein alpha-deficient mice. *Proc Natl Acad Sci U S A*. 1997;94(2):569-574.
91. Yamanaka R, Barlow C, Lekstrom-Himes J, et al. Impaired granulopoiesis, myelodysplasia, and early lethality in CCAAT/enhancer binding protein epsilon-deficient mice. *Proc Natl Acad Sci U S A*. 1997;94(24):13187-13192.

92. Hock H, Hamblen MJ, Rooke HM, et al. Intrinsic requirement for zinc finger transcription factor Gfi-1 in neutrophil differentiation. *Immunity*. 2003;18(1):109-120.
93. Ward AC, Loeb DM, Soede-Bobok AA, Touw IP, Friedman AD. Regulation of granulopoiesis by transcription factors and cytokine signals. *Leukemia*. 2000;14(6):973-990.
94. Rosales C. Neutrophil: A Cell with Many Roles in Inflammation or Several Cell Types? *Front Physiol*. 2018;9:113.
95. Semerad CL, Liu F, Gregory AD, Stumpf K, Link DC. G-CSF is an essential regulator of neutrophil trafficking from the bone marrow to the blood. *Immunity*. 2002;17(4):413-423.
96. Ma Q, Jones D, Springer TA. The chemokine receptor CXCR4 is required for the retention of B lineage and granulocytic precursors within the bone marrow microenvironment. *Immunity*. 1999;10(4):463-471.
97. Köhler A, De Filippo K, Hasenberg M, et al. G-CSF-mediated thrombopoietin release triggers neutrophil motility and mobilization from bone marrow via induction of Cxcr2 ligands. *Blood*. 2011;117(16):4349-4357.
98. Kim HK, De La Luz Sierra M, Williams CK, Gulino AV, Tosato G. G-CSF down-regulation of CXCR4 expression identified as a mechanism for mobilization of myeloid cells. *Blood*. 2006;108(3):812-820.
99. Chavakis E, Choi EY, Chavakis T. Novel aspects in the regulation of the leukocyte adhesion cascade. *Thromb Haemost*. 2009;102(2):191-197.
100. Ley K, Laudanna C, Cybulsky MI, Nourshargh S. Getting to the site of inflammation: the leukocyte adhesion cascade updated. *Nat Rev Immunol*. 2007;7(9):678-689.
101. Phillipson M, Heit B, Colarusso P, Liu L, Ballantyne CM, Kubes P. Intraluminal crawling of neutrophils to emigration sites: a molecularly distinct process from adhesion in the recruitment cascade. *J Exp Med*. 2006;203(12):2569-2575.
102. Dincey JT, Deubelbeiss KA, Harker LA, Finch CA. Neutrophil kinetics in man. *J Clin Invest*. 1976;58(3):705-715.
103. Ng LG, Ostuni R, Hidalgo A. Heterogeneity of neutrophils. *Nat Rev Immunol*. 2019;19(4):255-265.
104. Zhang D, Chen G, Manwani D, et al. Neutrophil ageing is regulated by the microbiome. *Nature*. 2015;525(7570):528-532.
105. Whyte MK, Meagher LC, MacDermot J, Haslett C. Impairment of function in aging neutrophils is associated with apoptosis. *J Immunol*. 1993;150(11):5124-5134.
106. Adrover JM, Aroca-Crevillén A, Crainiciuc G, et al. Programmed 'disarming' of the neutrophil proteome reduces the magnitude of inflammation. *Nat Immunol*. 2020;21(2):135-144.
107. Adrover JM, Nicolás-Ávila JA, Hidalgo A. Aging: A Temporal Dimension for Neutrophils. *Trends Immunol*. 2016;37(5):334-345.
108. Mayadas TN, Cullere X, Lowell CA. The multifaceted functions of neutrophils. *Annu Rev Pathol*. 2014;9:181-218.
109. Boulay F, Naik N, Giannini E, Tardif M, Brouchon L. Phagocyte chemoattractant receptors. *Ann N Y Acad Sci*. 1997;832:69-84.
110. Migeotte I, Communi D, Parmentier M. Formyl peptide receptors: a promiscuous subfamily of G protein-coupled receptors controlling immune responses. *Cytokine Growth Factor Rev*. 2006;17(6):501-519.

111. Futosi K, Fodor S, Mócsai A. Neutrophil cell surface receptors and their intracellular signal transduction pathways. *Int Immunopharmacol.* 2013;17(3):638-650.
112. Wang Y, Jönsson F. Expression, Role, and Regulation of Neutrophil Fcγ Receptors. *Front Immunol.* 2019;10:1958.
113. Segal AW, Dorling J, Coade S. Kinetics of fusion of the cytoplasmic granules with phagocytic vacuoles in human polymorphonuclear leukocytes. Biochemical and morphological studies. *J Cell Biol.* 1980;85(1):42-59.
114. Nordenfelt P, Tapper H. Phagosome dynamics during phagocytosis by neutrophils. *J Leukoc Biol.* 2011;90(2):271-284.
115. Lee WL, Harrison RE, Grinstein S. Phagocytosis by neutrophils. *Microbes Infect.* 2003;5(14):1299-1306.
116. Borregaard N, Cowland JB. Granules of the human neutrophilic polymorphonuclear leukocyte. *Blood.* 1997;89(10):3503-3521.
117. Faurschou M, Borregaard N. Neutrophil granules and secretory vesicles in inflammation. *Microbes Infect.* 2003;5(14):1317-1327.
118. Bainton DF, Farquhar MG. Differences in enzyme content of azurophil and specific granules of polymorphonuclear leukocytes. II. Cytochemistry and electron microscopy of bone marrow cells. *J Cell Biol.* 1968;39(2):299-317.
119. Dewald B, Bretz U, Baggiolini M. Release of gelatinase from a novel secretory compartment of human neutrophils. *J Clin Invest.* 1982;70(3):518-525.
120. Borregaard N, Miller LJ, Springer TA. Chemoattractant-regulated mobilization of a novel intracellular compartment in human neutrophils. *Science.* 1987;237(4819):1204-1206.
121. Uriarte SM, Powell DW, Luerman GC, et al. Comparison of proteins expressed on secretory vesicle membranes and plasma membranes of human neutrophils. *J Immunol.* 2008;180(8):5575-5581.
122. Calafat J, Kuijpers TW, Janssen H, Borregaard N, Verhoeven AJ, Roos D. Evidence for small intracellular vesicles in human blood phagocytes containing cytochrome b558 and the adhesion molecule CD11b/CD18. *Blood.* 1993;81(11):3122-3129.
123. Sheshachalam A, Srivastava N, Mitchell T, Lacy P, Eitzen G. Granule protein processing and regulated secretion in neutrophils. *Front Immunol.* 2014;5:448.
124. Roos D, van Bruggen R, Meischl C. Oxidative killing of microbes by neutrophils. *Microbes Infect.* 2003;5(14):1307-1315.
125. Robinson JM. Phagocytic leukocytes and reactive oxygen species. *Histochem Cell Biol.* 2009;131(4):465-469.
126. Brinkmann V, Reichard U, Goosmann C, et al. Neutrophil extracellular traps kill bacteria. *Science.* 2004;303(5663):1532-1535.
127. Takei H, Araki A, Watanabe H, Ichinose A, Sendo F. Rapid killing of human neutrophils by the potent activator phorbol 12-myristate 13-acetate (PMA) accompanied by changes different from typical apoptosis or necrosis. *J Leukoc Biol.* 1996;59(2):229-240.
128. Yipp BG, Kubes P. NETosis: how vital is it? *Blood.* 2013;122(16):2784-2794.
129. Thiam HR, Wong SL, Wagner DD, Waterman CM. Cellular Mechanisms of NETosis. *Annu Rev Cell Dev Biol.* 2020;36:191-218.

130. Thiam HR, Wong SL, Qiu R, et al. NETosis proceeds by cytoskeleton and endomembrane disassembly and PAD4-mediated chromatin decondensation and nuclear envelope rupture. *Proc Natl Acad Sci U S A*. 2020;117(13):7326-7337.
131. Wang Y, Li M, Stadler S, et al. Histone hypercitrullination mediates chromatin decondensation and neutrophil extracellular trap formation. *J Cell Biol*. 2009;184(2):205-213.
132. Guiducci E, Lemberg C, Küng N, Schraner E, Theodorides APA, LeibundGut-Landmann S. -Induced NETosis Is Independent of Peptidylarginine Deiminase 4. *Front Immunol*. 2018;9:1573.
133. Kenny EF, Herzig A, Krüger R, et al. Diverse stimuli engage different neutrophil extracellular trap pathways. *Elife*. 2017;6.
134. Tsourouktsoglou TD, Warnatsch A, Ioannou M, Hoving D, Wang Q, Papayannopoulos V. Histones, DNA, and Citrullination Promote Neutrophil Extracellular Trap Inflammation by Regulating the Localization and Activation of TLR4. *Cell Rep*. 2020;31(5):107602.
135. Fuchs TA, Abed U, Goosmann C, et al. Novel cell death program leads to neutrophil extracellular traps. *J Cell Biol*. 2007;176(2):231-241.
136. Neubert E, Meyer D, Rocca F, et al. Chromatin swelling drives neutrophil extracellular trap release. *Nat Commun*. 2018;9(1):3767.
137. Espín-Palazón R, Stachura DL, Campbell CA, et al. Proinflammatory signaling regulates hematopoietic stem cell emergence. *Cell*. 2014;159(5):1070-1085.
138. Kwak HJ, Liu P, Bajrami B, et al. Myeloid cell-derived reactive oxygen species externally regulate the proliferation of myeloid progenitors in emergency granulopoiesis. *Immunity*. 2015;42(1):159-171.
139. Kawano Y, Fukui C, Shinohara M, et al. G-CSF-induced sympathetic tone provokes fever and primes antimobilizing functions of neutrophils via PGE2. *Blood*. 2017;129(5):587-597.
140. Bowers E, Slaughter A, Frenette PS, Kuick R, Pello OM, Lucas D. Granulocyte-derived TNF α promotes vascular and hematopoietic regeneration in the bone marrow. *Nat Med*. 2018;24(1):95-102.
141. Cossío I, Lucas D, Hidalgo A. Neutrophils as regulators of the hematopoietic niche. *Blood*. 2019;133(20):2140-2148.
142. Scapini P, Laudanna C, Pinardi C, et al. Neutrophils produce biologically active macrophage inflammatory protein-3 α (MIP-3 α)/CCL20 and MIP-3 β /CCL19. *Eur J Immunol*. 2001;31(7):1981-1988.
143. Soehnlein O, Zernecke A, Eriksson EE, et al. Neutrophil secretion products pave the way for inflammatory monocytes. *Blood*. 2008;112(4):1461-1471.
144. Soehnlein O, Weber C, Lindbom L. Neutrophil granule proteins tune monocytic cell function. *Trends Immunol*. 2009;30(11):538-546.
145. Filardy AA, Pires DR, Nunes MP, et al. Proinflammatory clearance of apoptotic neutrophils induces an IL-12(low)IL-10(high) regulatory phenotype in macrophages. *J Immunol*. 2010;185(4):2044-2050.
146. Costantini C, Calzetti F, Perbellini O, et al. Human neutrophils interact with both 6-sulfo LacNAc⁺ DC and NK cells to amplify NK-derived IFN γ : role of CD18, ICAM-1, and ICAM-3. *Blood*. 2011;117(5):1677-1686.

147. Costantini C, Cassatella MA. The defensive alliance between neutrophils and NK cells as a novel arm of innate immunity. *J Leukoc Biol.* 2011;89(2):221-233.
148. Pelletier M, Maggi L, Micheletti A, et al. Evidence for a cross-talk between human neutrophils and Th17 cells. *Blood.* 2010;115(2):335-343.
149. Müller I, Munder M, Kropf P, Hänsch GM. Polymorphonuclear neutrophils and T lymphocytes: strange bedfellows or brothers in arms? *Trends Immunol.* 2009;30(11):522-530.
150. Tateda K, Moore TA, Deng JC, et al. Early recruitment of neutrophils determines subsequent T1/T2 host responses in a murine model of *Legionella pneumophila* pneumonia. *J Immunol.* 2001;166(5):3355-3361.
151. Huard B, McKee T, Bosshard C, et al. APRIL secreted by neutrophils binds to heparan sulfate proteoglycans to create plasma cell niches in human mucosa. *J Clin Invest.* 2008;118(8):2887-2895.
152. Scapini P, Bazzoni F, Cassatella MA. Regulation of B-cell-activating factor (BAFF)/B lymphocyte stimulator (BLyS) expression in human neutrophils. *Immunol Lett.* 2008;116(1):1-6.
153. Amulic B, Cazalet C, Hayes GL, Metzler KD, Zychlinsky A. Neutrophil function: from mechanisms to disease. *Annu Rev Immunol.* 2012;30:459-489.
154. Ellis TN, Beaman BL. Interferon-gamma activation of polymorphonuclear neutrophil function. *Immunology.* 2004;112(1):2-12.
155. Gosselin EJ, Wardwell K, Rigby WF, Guyre PM. Induction of MHC class II on human polymorphonuclear neutrophils by granulocyte/macrophage colony-stimulating factor, IFN-gamma, and IL-3. *J Immunol.* 1993;151(3):1482-1490.
156. Mudzinski SP, Christian TP, Guo TL, Cirenza E, Hazlett KR, Gosselin EJ. Expression of HLA-DR (major histocompatibility complex class II) on neutrophils from patients treated with granulocyte-macrophage colony-stimulating factor for mobilization of stem cells. *Blood.* 1995;86(6):2452-2453.
157. Reinisch W, Lichtenberger C, Steger G, et al. Donor dependent, interferon-gamma induced HLA-DR expression on human neutrophils in vivo. *Clin Exp Immunol.* 2003;133(3):476-484.
158. Enciso J, Mendoza L, Pelayo R. Normal vs. Malignant hematopoiesis: the complexity of acute leukemia through systems biology. *Front Genet.* 2015;6:290.
159. Bates I, Barbara B. Approach to the diagnosis and classification of blood diseases. *Dacie and Lewis Practical Haematology.* Vol. 10; 2006:609-624.
160. Downing JR, Shannon KM. Acute leukemia: a pediatric perspective. *Cancer Cell.* 2002;2(6):437-445.
161. Siegel RL, Miller KD, Jemal A. Cancer statistics, 2020. *CA Cancer J Clin.* 2020;70(1):7-30.
162. De Kouchkovsky I, Abdul-Hay M. 'Acute myeloid leukemia: a comprehensive review and 2016 update'. *Blood Cancer J.* 2016;6(7):e441.
163. Ferrara F, Schiffer CA. Acute myeloid leukaemia in adults. *Lancet.* 2013;381(9865):484-495.
164. Arnone M, Konantz M, Hanns P, et al. Acute Myeloid Leukemia Stem Cells: The Challenges of Phenotypic Heterogeneity. *Cancers (Basel).* 2020;12(12).

165. Rowley JD. Letter: A new consistent chromosomal abnormality in chronic myelogenous leukaemia identified by quinacrine fluorescence and Giemsa staining. *Nature*. 1973;243(5405):290-293.
166. Mitelman F, Johansson B, Mertens F. The impact of translocations and gene fusions on cancer causation. *Nat Rev Cancer*. 2007;7(4):233-245.
167. Mitelman F, Mertens F, Johansson B. Prevalence estimates of recurrent balanced cytogenetic aberrations and gene fusions in unselected patients with neoplastic disorders. *Genes Chromosomes Cancer*. 2005;43(4):350-366.
168. Gilliland DG. Molecular genetics of human leukemias: new insights into therapy. *Semin Hematol*. 2002;39(4 Suppl 3):6-11.
169. Dash A, Gilliland DG. Molecular genetics of acute myeloid leukaemia. *Best Pract Res Clin Haematol*. 2001;14(1):49-64.
170. Gilliland DG, Griffin JD. The roles of FLT3 in hematopoiesis and leukemia. *Blood*. 2002;100(5):1532-1542.
171. Kitamura T, Inoue D, Okochi-Watanabe N, et al. The molecular basis of myeloid malignancies. *Proc Jpn Acad Ser B Phys Biol Sci*. 2014;90(10):389-404.
172. Steensma DP, Bejar R, Jaiswal S, et al. Clonal hematopoiesis of indeterminate potential and its distinction from myelodysplastic syndromes. *Blood*. 2015;126(1):9-16.
173. Heuser M, Thol F, Ganser A. Clonal Hematopoiesis of Indeterminate Potential. *Dtsch Arztebl Int*. 2016;113(18):317-322.
174. Meyer SC, Levine RL. Translational implications of somatic genomics in acute myeloid leukaemia. *Lancet Oncol*. 2014;15(9):e382-394.
175. Gregory TK, Wald D, Chen Y, Vermaat JM, Xiong Y, Tse W. Molecular prognostic markers for adult acute myeloid leukemia with normal cytogenetics. *J Hematol Oncol*. 2009;2:23.
176. Ley TJ, Miller C, Ding L, et al. Genomic and epigenomic landscapes of adult de novo acute myeloid leukemia. *N Engl J Med*. 2013;368(22):2059-2074.
177. Patel JP, Gönen M, Figueroa ME, et al. Prognostic relevance of integrated genetic profiling in acute myeloid leukemia. *N Engl J Med*. 2012;366(12):1079-1089.
178. Ohyashiki K, Ohyashiki JH, Iwabuchi H, Tauchi T, Iwabuchi A, Toyama K. Philadelphia chromosome-positive chronic myelogenous leukemia with deleted fusion of BCR and ABL genes. *Jpn J Cancer Res*. 1990;81(1):35-42.
179. Apperley JF. Chronic myeloid leukaemia. *Lancet*. 2015;385(9976):1447-1459.
180. Man LM, Morris AL, Keng M. New Therapeutic Strategies in Acute Lymphocytic Leukemia. *Curr Hematol Malig Rep*. 2017;12(3):197-206.
181. Hunger SP, Mullighan CG. Acute Lymphoblastic Leukemia in Children. *N Engl J Med*. 2015;373(16):1541-1552.
182. Hallek M, Shanafelt TD, Eichhorst B. Chronic lymphocytic leukaemia. *Lancet*. 2018;391(10129):1524-1537.
183. Reed D. On the pathological changes in Hodgkin's disease with special reference to its relation to tuberculosis. *John Hopkins Hospital Reports*. Vol. 10; 1902:133-193.
184. Sternberg C. Über eine eigenartige unter dem Bilde der Pseudoleukämie verlaufende Tuberkulose des lymphatischen Apparates. *Zeitschrift für Heilkunde*. Vol. 19; 1898:21-90.

185. Küppers R, Rajewsky K. The origin of Hodgkin and Reed/Sternberg cells in Hodgkin's disease. *Annu Rev Immunol*. 1998;16:471-493.
186. Küppers R, Hansmann ML. The Hodgkin and Reed/Sternberg cell. *Int J Biochem Cell Biol*. 2005;37(3):511-517.
187. Armitage JO, Gascoyne RD, Lunning MA, Cavalli F. Non-Hodgkin lymphoma. *Lancet*. 2017;390(10091):298-310.
188. Hasserjian RP. Myelodysplastic Syndrome Updated. *Pathobiology*. 2019;86(1):7-13.
189. Ogawa S. Genetics of MDS. *Blood*. 2019;133(10):1049-1059.
190. Kralovics R, Passamonti F, Buser AS, et al. A gain-of-function mutation of JAK2 in myeloproliferative disorders. *N Engl J Med*. 2005;352(17):1779-1790.
191. Skoda RC, Duek A, Grisouard J. Pathogenesis of myeloproliferative neoplasms. *Exp Hematol*. 2015;43(8):599-608.
192. Nangalia J, Green AR. Myeloproliferative neoplasms: from origins to outcomes. *Hematology Am Soc Hematol Educ Program*. 2017;2017(1):470-479.
193. Chinen J, Shearer WT. Secondary immunodeficiencies, including HIV infection. *J Allergy Clin Immunol*. 2010;125(2 Suppl 2):S195-203.
194. Duraisingham SS, Buckland M, Dempster J, Lorenzo L, Grigoriadou S, Longhurst HJ. Primary vs. secondary antibody deficiency: clinical features and infection outcomes of immunoglobulin replacement. *PLoS One*. 2014;9(6):e100324.
195. Notarangelo LD. Primary immunodeficiencies. *J Allergy Clin Immunol*. 2010;125(2 Suppl 2):S182-194.
196. McCusker C, Upton J, Warrington R. Primary immunodeficiency. *Allergy Asthma Clin Immunol*. 2018;14(Suppl 2):61.
197. Bucciol G, Meyts I. Recent advances in primary immunodeficiency: from molecular diagnosis to treatment. *F1000Res*. 2020;9.
198. Sholzberg M. Malignant benign hematology. *Res Pract Thromb Haemost*. 2019;3(1):15-17.
199. Boxer LA. How to approach neutropenia. *Hematology Am Soc Hematol Educ Program*. 2012;2012:174-182.
200. Hauck F, Klein C. Pathogenic mechanisms and clinical implications of congenital neutropenia syndromes. *Curr Opin Allergy Clin Immunol*. 2013;13(6):596-606.
201. Spoor J, Farajifard H, Rezaei N. Congenital neutropenia and primary immunodeficiency diseases. *Crit Rev Oncol Hematol*. 2019;133:149-162.
202. Boxer L, Dale DC. Neutropenia: causes and consequences. *Semin Hematol*. 2002;39(2):75-81.
203. Moore DC. Drug-Induced Neutropenia: A Focus on Rituximab-Induced Late-Onset Neutropenia. *P T*. 2016;41(12):765-768.
204. Boztug K, Welte K, Zeidler C, Klein C. Congenital neutropenia syndromes. *Immunol Allergy Clin North Am*. 2008;28(2):259-275, vii-viii.
205. KOSTMANN R. Infantile genetic agranulocytosis; agranulocytosis infantilis hereditaria. *Acta Paediatr Suppl*. 1956;45(Suppl 105):1-78.
206. Welte K, Zeidler C. Severe congenital neutropenia. *Hematol Oncol Clin North Am*. 2009;23(2):307-320.

207. Skokowa J, Dale DC, Touw IP, Zeidler C, Welte K. Severe congenital neutropenias. *Nat Rev Dis Primers*. 2017;3:17032.
208. Skokowa J, Germeshausen M, Zeidler C, Welte K. Severe congenital neutropenia: inheritance and pathophysiology. *Curr Opin Hematol*. 2007;14(1):22-28.
209. Welte K, Platzer E, Lu L, et al. Purification and biochemical characterization of human pluripotent hematopoietic colony-stimulating factor. *Proc Natl Acad Sci U S A*. 1985;82(5):1526-1530.
210. Souza LM, Boone TC, Gabilove J, et al. Recombinant human granulocyte colony-stimulating factor: effects on normal and leukemic myeloid cells. *Science*. 1986;232(4746):61-65.
211. Welte K, Zeidler C, Reiter A, et al. Differential effects of granulocyte-macrophage colony-stimulating factor and granulocyte colony-stimulating factor in children with severe congenital neutropenia. *Blood*. 1990;75(5):1056-1063.
212. Rosenberg PS, Alter BP, Bolyard AA, et al. The incidence of leukemia and mortality from sepsis in patients with severe congenital neutropenia receiving long-term G-CSF therapy. *Blood*. 2006;107(12):4628-4635.
213. Rosenberg PS, Zeidler C, Bolyard AA, et al. Stable long-term risk of leukaemia in patients with severe congenital neutropenia maintained on G-CSF therapy. *Br J Haematol*. 2010;150(2):196-199.
214. Dale DC, Person RE, Bolyard AA, et al. Mutations in the gene encoding neutrophil elastase in congenital and cyclic neutropenia. *Blood*. 2000;96(7):2317-2322.
215. Nayak RC, Trump LR, Aronow BJ, et al. Pathogenesis of ELANE-mutant severe neutropenia revealed by induced pluripotent stem cells. *J Clin Invest*. 2015;125(8):3103-3116.
216. Horwitz MS, Duan Z, Korkmaz B, Lee HH, Mealiffe ME, Salipante SJ. Neutrophil elastase in cyclic and severe congenital neutropenia. *Blood*. 2007;109(5):1817-1824.
217. Horwitz MS, Corey SJ, Grimes HL, Tidwell T. ELANE mutations in cyclic and severe congenital neutropenia: genetics and pathophysiology. *Hematol Oncol Clin North Am*. 2013;27(1):19-41, vii.
218. Benson KF, Li FQ, Person RE, et al. Mutations associated with neutropenia in dogs and humans disrupt intracellular transport of neutrophil elastase. *Nat Genet*. 2003;35(1):90-96.
219. Köllner I, Sodeik B, Schreek S, et al. Mutations in neutrophil elastase causing congenital neutropenia lead to cytoplasmic protein accumulation and induction of the unfolded protein response. *Blood*. 2006;108(2):493-500.
220. Xia J, Link DC. Severe congenital neutropenia and the unfolded protein response. *Curr Opin Hematol*. 2008;15(1):1-7.
221. Grenda DS, Murakami M, Ghatak J, et al. Mutations of the ELA2 gene found in patients with severe congenital neutropenia induce the unfolded protein response and cellular apoptosis. *Blood*. 2007;110(13):4179-4187.
222. Makaryan V, Zeidler C, Bolyard AA, et al. The diversity of mutations and clinical outcomes for ELANE-associated neutropenia. *Curr Opin Hematol*. 2015;22(1):3-11.
223. Dale DC, Bolyard AA, Aprikyan A. Cyclic neutropenia. *Semin Hematol*. 2002;39(2):89-94.

224. Dale DC, Welte K. Cyclic and chronic neutropenia. *Cancer Treat Res.* 2011;157:97-108.
225. Nustede R, Klimiankou M, Klimenkova O, et al. ELANE mutant-specific activation of different UPR pathways in congenital neutropenia. *Br J Haematol.* 2016;172(2):219-227.
226. Germeshausen M, Deerberg S, Peter Y, Reimer C, Kratz CP, Ballmaier M. The spectrum of ELANE mutations and their implications in severe congenital and cyclic neutropenia. *Hum Mutat.* 2013;34(6):905-914.
227. Germeshausen M, Grudzien M, Zeidler C, et al. Novel HAX1 mutations in patients with severe congenital neutropenia reveal isoform-dependent genotype-phenotype associations. *Blood.* 2008;111(10):4954-4957.
228. Klein C, Grudzien M, Appaswamy G, et al. HAX1 deficiency causes autosomal recessive severe congenital neutropenia (Kostmann disease). *Nat Genet.* 2007;39(1):86-92.
229. Doll L, Aghaallaei N, Dick AM, Welte K, Skokowa J, Bajoghli B. A zebrafish model for HAX1-associated congenital neutropenia. *Haematologica.* 2020.
230. Person RE, Li FQ, Duan Z, et al. Mutations in proto-oncogene GFI1 cause human neutropenia and target ELA2. *Nat Genet.* 2003;34(3):308-312.
231. Boztug K, Appaswamy G, Ashikov A, et al. A syndrome with congenital neutropenia and mutations in G6PC3. *N Engl J Med.* 2009;360(1):32-43.
232. Boztug K, Rosenberg PS, Dorda M, et al. Extended spectrum of human glucose-6-phosphatase catalytic subunit 3 deficiency: novel genotypes and phenotypic variability in severe congenital neutropenia. *J Pediatr.* 2012;160(4):679-683.e672.
233. Gatti S, Boztug K, Pedini A, et al. A case of syndromic neutropenia and mutation in G6PC3. *J Pediatr Hematol Oncol.* 2011;33(2):138-140.
234. Kiykim A, Baris S, Karakoc-Aydiner E, et al. G6PC3 Deficiency: Primary Immune Deficiency Beyond Just Neutropenia. *J Pediatr Hematol Oncol.* 2015;37(8):616-622.
235. McDermott DH, De Ravin SS, Jun HS, et al. Severe congenital neutropenia resulting from G6PC3 deficiency with increased neutrophil CXCR4 expression and myelokathexis. *Blood.* 2010;116(15):2793-2802.
236. Notarangelo LD, Savoldi G, Cavagnini S, et al. Severe congenital neutropenia due to G6PC3 deficiency: early and delayed phenotype in two patients with two novel mutations. *Ital J Pediatr.* 2014;40:80.
237. Goldberg L, Simon AJ, Rechavi G, et al. Congenital neutropenia with variable clinical presentation in novel mutation of the SRP54 gene. *Pediatr Blood Cancer.* 2020;67(6):e28237.
238. Carden MA, Connelly JA, Weinzierl EP, Kobrynski LJ, Chandrakasan S. Severe Congenital Neutropenia associated with SRP54 mutation in 22q11.2 Deletion Syndrome: Hematopoietic Stem Cell Transplantation Results in Correction of Neutropenia with Adequate Immune Reconstitution. *J Clin Immunol.* 2018;38(5):546-549.
239. Saettini F, Cattoni A, D'Angio' M, et al. Intermittent granulocyte maturation arrest, hypocellular bone marrow, and episodic normal neutrophil count can be associated with SRP54 mutations causing Shwachman-Diamond-like syndrome. *Br J Haematol.* 2020;189(4):e171-e174.
240. NEZELOF C, WATCHI M. [Lipomatous congenital hypoplasia of the exocrine pancreas in children. (2 cases and review of the literature)]. *Arch Fr Pediatr.* 1961;18:1135-1172.

241. SHWACHMAN H, DIAMOND LK, OSKI FA, KHAW KT. THE SYNDROME OF PANCREATIC INSUFFICIENCY AND BONE MARROW DYSFUNCTION. *J Pediatr*. 1964;65:645-663.
242. Mack DR, Forstner GG, Wilschanski M, Freedman MH, Durie PR. Shwachman syndrome: exocrine pancreatic dysfunction and variable phenotypic expression. *Gastroenterology*. 1996;111(6):1593-1602.
243. Dror Y, Freedman MH. Shwachman-diamond syndrome. *Br J Haematol*. 2002;118(3):701-713.
244. Nelson AS, Myers KC. Diagnosis, Treatment, and Molecular Pathology of Shwachman-Diamond Syndrome. *Hematol Oncol Clin North Am*. 2018;32(4):687-700.
245. Burroughs L, Woolfrey A, Shimamura A. Shwachman-Diamond syndrome: a review of the clinical presentation, molecular pathogenesis, diagnosis, and treatment. *Hematol Oncol Clin North Am*. 2009;23(2):233-248.
246. Boocock GR, Morrison JA, Popovic M, et al. Mutations in SBDS are associated with Shwachman-Diamond syndrome. *Nat Genet*. 2003;33(1):97-101.
247. Mäkitie O, Ellis L, Durie PR, et al. Skeletal phenotype in patients with Shwachman-Diamond syndrome and mutations in SBDS. *Clin Genet*. 2004;65(2):101-112.
248. Nicolis E, Bonizzato A, Assael BM, Cipolli M. Identification of novel mutations in patients with Shwachman-Diamond syndrome. *Hum Mutat*. 2005;25(4):410.
249. Shamma C, Menne TF, Hilcenko C, et al. Structural and mutational analysis of the SBDS protein family. Insight into the leukemia-associated Shwachman-Diamond Syndrome. *J Biol Chem*. 2005;280(19):19221-19229.
250. Austin KM, Leary RJ, Shimamura A. The Shwachman-Diamond SBDS protein localizes to the nucleolus. *Blood*. 2005;106(4):1253-1258.
251. Ganapathi KA, Austin KM, Lee CS, et al. The human Shwachman-Diamond syndrome protein, SBDS, associates with ribosomal RNA. *Blood*. 2007;110(5):1458-1465.
252. Shimamura A. Shwachman-Diamond syndrome. *Semin Hematol*. 2006;43(3):178-188.
253. Savchenko A, Krogan N, Cort JR, et al. The Shwachman-Bodian-Diamond syndrome protein family is involved in RNA metabolism. *J Biol Chem*. 2005;280(19):19213-19220.
254. Bezzerri V, Cipolli M. Shwachman-Diamond Syndrome: Molecular Mechanisms and Current Perspectives. *Mol Diagn Ther*. 2019;23(2):281-290.
255. Austin KM, Gupta ML, Coats SA, et al. Mitotic spindle destabilization and genomic instability in Shwachman-Diamond syndrome. *J Clin Invest*. 2008;118(4):1511-1518.
256. Orelia C, Verkuijlen P, Geissler J, van den Berg TK, Kuijpers TW. SBDS expression and localization at the mitotic spindle in human myeloid progenitors. *PLoS One*. 2009;4(9):e7084.
257. Hashmi SK, Allen C, Klaassen R, et al. Comparative analysis of Shwachman-Diamond syndrome to other inherited bone marrow failure syndromes and genotype-phenotype correlation. *Clin Genet*. 2011;79(5):448-458.
258. Dhanraj S, Matveev A, Li H, et al. Biallelic mutations in. *Blood*. 2017;129(11):1557-1562.

259. Stepensky P, Chacón-Flores M, Kim KH, et al. Mutations in. *J Med Genet*. 2017;54(8):558-566.
260. Lo KY, Li Z, Bussiere C, Bresson S, Marcotte EM, Johnson AW. Defining the pathway of cytoplasmic maturation of the 60S ribosomal subunit. *Mol Cell*. 2010;39(2):196-208.
261. Weis F, Giudice E, Churcher M, et al. Mechanism of eIF6 release from the nascent 60S ribosomal subunit. *Nat Struct Mol Biol*. 2015;22(11):914-919.
262. Tan S, Kermasson L, Hoslin A, et al. EFL1 mutations impair eIF6 release to cause Shwachman-Diamond syndrome. *Blood*. 2019;134(3):277-290.
263. D'Amours G, Lopes F, Gauthier J, et al. Refining the phenotype associated with biallelic DNAJC21 mutations. *Clin Genet*. 2018;94(2):252-258.
264. Koh AL, Bonnard C, Lim JY, et al. Heterozygous missense variant in EIF6 gene: A novel form of Shwachman-Diamond syndrome? *Am J Med Genet A*. 2020;182(9):2010-2020.
265. Bradford YM, Toro S, Ramachandran S, et al. Zebrafish Models of Human Disease: Gaining Insight into Human Disease at ZFIN. *ILAR J*. 2017;58(1):4-16.
266. Streisinger G, Walker C, Dower N, Knauber D, Singer F. Production of clones of homozygous diploid zebra fish (*Brachydanio rerio*). *Nature*. 1981;291(5813):293-296.
267. Carroll KJ, North TE. Oceans of opportunity: exploring vertebrate hematopoiesis in zebrafish. *Exp Hematol*. 2014;42(8):684-696.
268. Akopian D, Shen K, Zhang X, Shan SO. Signal recognition particle: an essential protein-targeting machine. *Annu Rev Biochem*. 2013;82:693-721.
269. Pool MR. Signal recognition particles in chloroplasts, bacteria, yeast and mammals (review). *Mol Membr Biol*. 2005;22(1-2):3-15.
270. Cross BC, Sinning I, Luirink J, High S. Delivering proteins for export from the cytosol. *Nat Rev Mol Cell Biol*. 2009;10(4):255-264.
271. Zopf D, Bernstein HD, Johnson AE, Walter P. The methionine-rich domain of the 54 kd protein subunit of the signal recognition particle contains an RNA binding site and can be crosslinked to a signal sequence. *EMBO J*. 1990;9(13):4511-4517.
272. Janda CY, Li J, Oubridge C, Hernández H, Robinson CV, Nagai K. Recognition of a signal peptide by the signal recognition particle. *Nature*. 2010;465(7297):507-510.
273. Halic M, Gartmann M, Schlenker O, et al. Signal recognition particle receptor exposes the ribosomal translocon binding site. *Science*. 2006;312(5774):745-747.
274. Newitt JA, Bernstein HD. The N-domain of the signal recognition particle 54-kDa subunit promotes efficient signal sequence binding. *Eur J Biochem*. 1997;245(3):720-729.
275. Althoff SM, Stevens SW, Wise JA. The Srp54 GTPase is essential for protein export in the fission yeast *Schizosaccharomyces pombe*. *Mol Cell Biol*. 1994;14(12):7839-7854.
276. Juaira KD, Lapouge K, Becker MMM, et al. Structural and Functional Impact of SRP54 Mutations Causing Severe Congenital Neutropenia. *Structure*. 2021;29(1):15-28.e17.
277. Schröder M, Kaufman RJ. ER stress and the unfolded protein response. *Mutat Res*. 2005;569(1-2):29-63.
278. Lin JH, Walter P, Yen TS. Endoplasmic reticulum stress in disease pathogenesis. *Annu Rev Pathol*. 2008;3:399-425.

279. Araki K, Nagata K. Protein folding and quality control in the ER. *Cold Spring Harb Perspect Biol.* 2012;4(8):a015438.
280. Ellgaard L, Helenius A. Quality control in the endoplasmic reticulum. *Nat Rev Mol Cell Biol.* 2003;4(3):181-191.
281. Navid F, Colbert RA. Causes and consequences of endoplasmic reticulum stress in rheumatic disease. *Nat Rev Rheumatol.* 2017;13(1):25-40.
282. Bravo R, Parra V, Gatica D, et al. Endoplasmic reticulum and the unfolded protein response: dynamics and metabolic integration. *Int Rev Cell Mol Biol.* 2013;301:215-290.
283. Bertolotti A, Zhang Y, Hendershot LM, Harding HP, Ron D. Dynamic interaction of BiP and ER stress transducers in the unfolded-protein response. *Nat Cell Biol.* 2000;2(6):326-332.
284. Shen J, Chen X, Hendershot L, Prywes R. ER stress regulation of ATF6 localization by dissociation of BiP/GRP78 binding and unmasking of Golgi localization signals. *Dev Cell.* 2002;3(1):99-111.
285. Calton M, Zeng H, Urano F, et al. IRE1 couples endoplasmic reticulum load to secretory capacity by processing the XBP-1 mRNA. *Nature.* 2002;415(6867):92-96.
286. Lee AH, Iwakoshi NN, Glimcher LH. XBP-1 regulates a subset of endoplasmic reticulum resident chaperone genes in the unfolded protein response. *Mol Cell Biol.* 2003;23(21):7448-7459.
287. Hollien J, Weissman JS. Decay of endoplasmic reticulum-localized mRNAs during the unfolded protein response. *Science.* 2006;313(5783):104-107.
288. Rozpedek W, Pytel D, Mucha B, Leszczynska H, Diehl JA, Majsterek I. The Role of the PERK/eIF2 α /ATF4/CHOP Signaling Pathway in Tumor Progression During Endoplasmic Reticulum Stress. *Curr Mol Med.* 2016;16(6):533-544.
289. Haze K, Yoshida H, Yanagi H, Yura T, Mori K. Mammalian transcription factor ATF6 is synthesized as a transmembrane protein and activated by proteolysis in response to endoplasmic reticulum stress. *Mol Biol Cell.* 1999;10(11):3787-3799.
290. Adachi Y, Yamamoto K, Okada T, Yoshida H, Harada A, Mori K. ATF6 is a transcription factor specializing in the regulation of quality control proteins in the endoplasmic reticulum. *Cell Struct Funct.* 2008;33(1):75-89.
291. Yoshida H, Okada T, Haze K, et al. ATF6 activated by proteolysis binds in the presence of NF-Y (CBF) directly to the cis-acting element responsible for the mammalian unfolded protein response. *Mol Cell Biol.* 2000;20(18):6755-6767.
292. Tsuru A, Imai Y, Saito M, Kohno K. Novel mechanism of enhancing IRE1 α -XBP1 signalling via the PERK-ATF4 pathway. *Sci Rep.* 2016;6:24217.
293. Schaefer T, Ramadoss A, Leu S, et al. Regulation of glioma cell invasion by 3q26 gene products PIK3CA, SOX2 and OPA1. *Brain Pathol.* 2018.
294. Henry KM, Loynes CA, Whyte MK, Renshaw SA. Zebrafish as a model for the study of neutrophil biology. *J Leukoc Biol.* 2013;94(4):633-642.
295. Farnsworth DR, Saunders LM, Miller AC. A single-cell transcriptome atlas for zebrafish development. *Dev Biol.* 2020;459(2):100-108.
296. Borrello MT, Santofimia-Castaño P, Bocchio M, et al. NUPR1 interacts with eIF2 α and is required for resolution of the ER stress response in pancreatic tissue. *FEBS J.* 2021.

297. Santofimia-Castaño P, Lan W, Bintz J, et al. Inactivation of NUPR1 promotes cell death by coupling ER-stress responses with necrosis. *Sci Rep*. 2018;8(1):16999.
298. Dahm R, Nüsslein-Volhard C. Zebrafish: A practical approach. New York: Oxford University Press; 2002.
299. Warga RM, Kimmel CB. Cell movements during epiboly and gastrulation in zebrafish. *Development*. 1990;108(4):569-580.
300. Renshaw SA, Loynes CA, Trushell DM, Elworthy S, Ingham PW, Whyte MK. A transgenic zebrafish model of neutrophilic inflammation. *Blood*. 2006;108(13):3976-3978.
301. Picelli S, Björklund Å, Faridani OR, Sagasser S, Winberg G, Sandberg R. Smart-seq2 for sensitive full-length transcriptome profiling in single cells. *Nat Methods*. 2013;10(11):1096-1098.
302. Picelli S, Faridani OR, Björklund AK, Winberg G, Sagasser S, Sandberg R. Full-length RNA-seq from single cells using Smart-seq2. *Nat Protoc*. 2014;9(1):171-181.
303. Yoon SB, Park YH, Choi SA, et al. Real-time PCR quantification of spliced X-box binding protein 1 (XBP1) using a universal primer method. *PLoS One*. 2019;14(7):e0219978.
304. Bettigole SE, Lis R, Adoro S, et al. The transcription factor XBP1 is selectively required for eosinophil differentiation. *Nat Immunol*. 2015;16(8):829-837.
305. Tanimura A, Miyoshi K, Horiguchi T, Hagita H, Fujisawa K, Noma T. Mitochondrial Activity and Unfolded Protein Response are Required for Neutrophil Differentiation. *Cell Physiol Biochem*. 2018;47(5):1936-1950.
306. Kwok I, Becht E, Xia Y, et al. Combinatorial Single-Cell Analyses of Granulocyte-Monocyte Progenitor Heterogeneity Reveals an Early Uni-potent Neutrophil Progenitor. *Immunity*. 2020;53(2):303-318.e305.
307. Kanda S, Yanagitani K, Yokota Y, Esaki Y, Kohno K. Autonomous translational pausing is required for XBP1u mRNA recruitment to the ER via the SRP pathway. *Proc Natl Acad Sci U S A*. 2016;113(40):E5886-E5895.
308. Wang Y, Xing P, Cui W, et al. Acute Endoplasmic Reticulum Stress-Independent Unconventional Splicing of XBP1 mRNA in the Nucleus of Mammalian Cells. *Int J Mol Sci*. 2015;16(6):13302-13321.
309. Uemura A, Oku M, Mori K, Yoshida H. Unconventional splicing of XBP1 mRNA occurs in the cytoplasm during the mammalian unfolded protein response. *J Cell Sci*. 2009;122(Pt 16):2877-2886.
310. Steed E, Rodrigues NT, Balda MS, Matter K. Identification of MarvelD3 as a tight junction-associated transmembrane protein of the occludin family. *BMC Cell Biol*. 2009;10:95.
311. Sánchez-Pulido L, Martín-Belmonte F, Valencia A, Alonso MA. MARVEL: a conserved domain involved in membrane apposition events. *Trends Biochem Sci*. 2002;27(12):599-601.
312. Raleigh DR, Marchiando AM, Zhang Y, et al. Tight junction-associated MARVEL proteins marveld3, tricellulin, and occludin have distinct but overlapping functions. *Mol Biol Cell*. 2010;21(7):1200-1213.
313. Zhou T, Lu Y, Xu C, Wang R, Zhang L, Lu P. Occludin protects secretory cells from ER stress by facilitating SNARE-dependent apical protein exocytosis. *Proc Natl Acad Sci U S A*. 2020;117(9):4758-4769.

314. Song Z. Roles of the nucleotide sugar transporters (SLC35 family) in health and disease. *Mol Aspects Med.* 2013;34(2-3):590-600.
315. Hadley B, Litfin T, Day CJ, Haselhorst T, Zhou Y, Tiralongo J. Nucleotide Sugar Transporter SLC35 Family Structure and Function. *Comput Struct Biotechnol J.* 2019;17:1123-1134.
316. Wong MY, Chen K, Antonopoulos A, et al. XBP1s activation can globally remodel N-glycan structure distribution patterns. *Proc Natl Acad Sci U S A.* 2018;115(43):E10089-E10098.
317. Liu T, Jiang W, Han D, Yu L. DNAJC25 is downregulated in hepatocellular carcinoma and is a novel tumor suppressor gene. *Oncol Lett.* 2012;4(6):1274-1280.
318. Shen Y, Meunier L, Hendershot LM. Identification and characterization of a novel endoplasmic reticulum (ER) DnaJ homologue, which stimulates ATPase activity of BiP in vitro and is induced by ER stress. *J Biol Chem.* 2002;277(18):15947-15956.
319. Shen Y, Hendershot LM. ERdj3, a stress-inducible endoplasmic reticulum DnaJ homologue, serves as a cofactor for BiP's interactions with unfolded substrates. *Mol Biol Cell.* 2005;16(1):40-50.
320. Pattwell SS, Arora S, Cimino PJ, et al. A kinase-deficient NTRK2 splice variant predominates in glioma and amplifies several oncogenic signaling pathways. *Nat Commun.* 2020;11(1):2977.
321. Nakagawara A, Liu XG, Ikegaki N, et al. Cloning and chromosomal localization of the human TRK-B tyrosine kinase receptor gene (NTRK2). *Genomics.* 1995;25(2):538-546.
322. Adams JH, Wigg KG, King N, et al. Association study of neurotrophic tyrosine kinase receptor type 2 (NTRK2) and childhood-onset mood disorders. *Am J Med Genet B Neuropsychiatr Genet.* 2005;132B(1):90-95.
323. Lim W, Bae H, Bazer FW, Song G. Brain-derived neurotrophic factor improves proliferation of endometrial epithelial cells by inhibition of endoplasmic reticulum stress during early pregnancy. *J Cell Physiol.* 2017;232(12):3641-3651.
324. Chowdhury UR, Samant RS, Fodstad O, Shevde LA. Emerging role of nuclear protein 1 (NUPR1) in cancer biology. *Cancer Metastasis Rev.* 2009;28(1-2):225-232.
325. Adomavicius T, Guaita M, Zhou Y, et al. The structural basis of translational control by eIF2 phosphorylation. *Nat Commun.* 2019;10(1):2136.
326. Wek RC. eIF-2 kinases: regulators of general and gene-specific translation initiation. *Trends Biochem Sci.* 1994;19(11):491-496.
327. Sinha NK, Ordureau A, Best K, et al. EDF1 coordinates cellular responses to ribosome collisions. *Elife.* 2020;9.
328. Marten LM, Brinkert F, Smith DEC, Prokisch H, Hempel M, Santer R. Recurrent acute liver failure in alanyl-tRNA synthetase-1 (AARS1) deficiency. *Mol Genet Metab Rep.* 2020;25:100681.
329. Stijf-Bultsma Y, Sommer L, Tauber M, et al. The basal transcription complex component TAF3 transduces changes in nuclear phosphoinositides into transcriptional output. *Mol Cell.* 2015;58(3):453-467.
330. Livneh I, Cohen-Kaplan V, Cohen-Rosenzweig C, Avni N, Ciechanover A. The life cycle of the 26S proteasome: from birth, through regulation and function, and onto its death. *Cell Res.* 2016;26(8):869-885.

331. Iio E, Matsuura K, Nishida N, et al. Genome-wide association study identifies a PSMD3 variant associated with neutropenia in interferon-based therapy for chronic hepatitis C. *Hum Genet.* 2015;134(3):279-289.
332. Ning S, Pagano JS, Barber GN. IRF7: activation, regulation, modification and function. *Genes Immun.* 2011;12(6):399-414.
333. Martín-Martín B, Nabokina SM, Blasi J, Lazo PA, Mollinedo F. Involvement of SNAP-23 and syntaxin 6 in human neutrophil exocytosis. *Blood.* 2000;96(7):2574-2583.
334. Konantz M, Balci TB, Hartwig UF, et al. Zebrafish xenografts as a tool for in vivo studies on human cancer. *Ann N Y Acad Sci.* 2012;1266:124-137.
335. Schindelin J, Arganda-Carreras I, Frise E, et al. Fiji: an open-source platform for biological-image analysis. *Nat Methods.* 2012;9(7):676-682.

List of Genes and Abbreviations

<i>aars1</i>	<i>Alanyl-tRNA synthetase 1</i>
<i>ABL</i>	<i>Abelson tyrosine-protein kinase 1</i>
<i>AKT</i>	<i>RAC-alpha serine/threonine protein kinase</i>
<i>ASXL1</i>	<i>Additional sex combs like 1</i>
<i>ATF4</i>	<i>Activating transcription factor 4</i>
<i>ATF6a</i>	<i>Activating transcription factor 6 alpha</i>
<i>ATP</i>	<i>Adenosine triphosphate</i>
<i>BCR</i>	<i>Breakpoint cluster region protein</i>
<i>BiP</i>	<i>Binding immunoglobulin protein</i>
<i>BMP-4</i>	<i>Bone morphogenetic protein 4</i>
<i>C/EBP</i>	<i>CCAAT/enhancer binding protein</i>
<i>CHOP</i>	<i>C/EBP homologous protein</i>
<i>C-MYB</i>	<i>Cellular Myb-like DNA-binding domain</i>
<i>CXCL</i>	<i>Chemokine CXC ligand</i>
<i>CXCR</i>	<i>CXC chemokine receptor</i>
<i>dnajc25</i>	<i>DnaJ homolog subfamily C member 25</i>
<i>DNMT3A</i>	<i>DNA methyltransferase 3A</i>
<i>edf1</i>	<i>Endothelial differentiation-related factor 1</i>
<i>ERK</i>	<i>Extracellular signal-regulated kinase</i>
<i>ETSRP</i>	<i>ETS1-related protein</i>
<i>FLI1</i>	<i>Friend leukemia integration factor 1</i>
<i>GATA1</i>	<i>GATA-binding factor 1</i>
<i>GFI-1</i>	<i>Growth factor independent 1</i>
<i>GFP</i>	<i>Green fluorescent protein</i>
<i>G-CSF</i>	<i>Granulocyte colony stimulating factor</i>
<i>GM-CSF</i>	<i>Granulocyte-macrophage colony stimulating factor</i>
<i>HSP40</i>	<i>Heat shock protein 40</i>
<i>eIF2</i>	<i>Eukaryotic translation initiation factor 2</i>
<i>IFN-γ</i>	<i>Interferon-γ</i>
<i>IgG</i>	<i>Immunoglobulin G</i>
<i>IL-6</i>	<i>Interleukin-6</i>
<i>IRE1α</i>	<i>Inositol-requiring enzyme alpha</i>
<i>irf7</i>	<i>Interferon regulatory factor 7</i>
<i>JAK</i>	<i>Janus kinase</i>

<i>KITL</i>	<i>KIT-ligand</i>
<i>KRAS</i>	<i>Kirsten rat sarcoma viral oncogene homolog</i>
<i>LMO2</i>	<i>LIM domain only 2</i>
<i>MEK</i>	<i>Mitogen-activated protein kinase kinase (MAP2K)</i>
<i>MFN1</i>	<i>Mitofusin-1</i>
<i>mgst1.1</i>	<i>Microsomal glutathione S-transferase 1</i>
<i>MPO</i>	<i>Myeloperoxidase</i>
<i>NADPH</i>	<i>Nicotinamide adenine dinucleotide phosphate</i>
<i>NFAT</i>	<i>Nuclear factor of activated T-cells</i>
<i>NF-κB</i>	<i>Nuclear factor kappa-light-chain-enhancer of activated B-cells</i>
<i>NLRP3</i>	<i>NLR family pyrin domain containing 3</i>
<i>nupr1</i>	<i>Nuclear protein 1</i>
<i>ntkr2a</i>	<i>Neurotrophic receptor tyrosine kinase 2a</i>
<i>OPA1</i>	<i>Dominant optic atrophy 1</i>
<i>P53</i>	<i>Tumor protein 53</i>
<i>PAD4</i>	<i>Protein arginine deiminase 4</i>
<i>PERK</i>	<i>PKR-like ER kinase</i>
<i>PIK3CA</i>	<i>Phosphatidylinositol-4,5-bisphosphate 3-kinase catalytic subunit alpha</i>
<i>ppp1r26</i>	<i>Protein phosphatase 1 regulatory subunit 26</i>
<i>PU1</i>	<i>PU-binding protein 1 (encoded by SPI1)</i>
<i>RUNX1</i>	<i>Runt-related transcription factor 1</i>
<i>psmd3</i>	<i>26S proteasome non-ATPase regulatory subunit 3</i>
<i>SCF</i>	<i>Stem cell factor</i>
<i>SCL</i>	<i>Stem cell leukemia</i>
<i>scl35e</i>	<i>Solute carrier family 35 member e</i>
<i>snap23.1</i>	<i>Synaptosomal-associated protein 23.1</i>
<i>SNARE</i>	<i>SNAP receptor</i>
<i>SOX2</i>	<i>SRY (sex determining region Y)-box 2</i>
<i>STAT</i>	<i>Signal transducer and activator of transcription</i>
<i>taf13</i>	<i>Transcription initiation factor TFIID subunit 13</i>
<i>TAL</i>	<i>T-cell acute lymphocytic leukemia protein 1</i>
<i>TET2</i>	<i>Tet methylcytosine dioxygenase 2</i>
<i>TNF</i>	<i>Tumor necrosis factor</i>
<i>mTORC</i>	<i>Mechanistic Target of rapamycin complex</i>
<i>TLR</i>	<i>Toll-like receptor</i>
<i>TrkB</i>	<i>Tropomyosin receptor kinase B</i>

<i>VEGF</i>	<i>Vascular-endothelial growth factor</i>
<i>WNT</i>	<i>Wingless and Int-1 signalling</i>
<i>XPB1</i>	<i>X-box binding protein 1</i>

Appendix

Curriculum Vitae



Christoph Schürch

Independent and resourceful scientist with a strong background in hematology, oncology, stem cells and rare blood disorders.

Professional Experience

- **Medical Affairs Associate**
SFL Regulatory Affairs & Scientific Communication GmbH, Basel (Switzerland)
09/2021 – Present
 - Prepared high-quality scientific and regulatory documents with operational, strategic and/or educational content.
 - Supported Swiss Market Access projects such as reimbursement applications.
- **Post-Doctoral Researcher**
University of Basel and University Hospital Basel, Basel (Switzerland)
05/2021 - Present
 - Studied the transcriptome of neutropenic zebrafish and unraveled novel disease-driving mechanisms.
 - Independently planned, managed and performed multiple ***RNA-sequencing*** experiments (bulk sequencing and single-cell sequencing).
- **PhD Student**
University of Basel and University Hospital Basel, Basel (Switzerland)
01/2018 – 04/2021
 - Obtained a wealth of experience in the field of ***hematology*** and ***rare blood diseases***, from *in vivo* zebrafish models and cell culture to protein analyses, FACS and RNA-sequencing preparation.
 - Studied a novel driver mutation associated with ***Congenital Neutropenia*** and ***Shwachman-Diamond Syndrome***.
 - Presented own work and won awards at national and international conferences.
 - Involved in several collaboration projects with leading international research groups.
 - Published work in high impact scientific journals

Education

- **PhD in Molecular Biology**
University of Basel, Basel (Switzerland),
01/2018 – 04/2021
Thesis title: “*SRP54* mutations induce Congenital Neutropenia via dominant-negative effects on *XBP1* splicing”.
Grade: Summa Cum Laude
- **MSc in Cell Biology**
University of Basel, Basel (Switzerland),
09/2016 – 12/2017
- **BSc in Molecular Biology**
University of Basel, Basel (Switzerland),
08/2013 – 08/2016

Courses & Training List Highlights

- **Essentials in Drug Development & Clinical Trials**
Swiss Tropical & Public Health Institute, Basel (Switzerland), 2019
- **Good Clinical Practice for Investigators and Study Teams**
Swiss Tropical & Public Health Institute, Basel (Switzerland), 2019
- **LTK M.1: Introductory Course in Laboratory Animal Science – non-rodents**
University of Zurich, Basel (Switzerland), 2018

Email

chris.schuerch@gmail.com

Address

Welschmattstrasse 41,
4055 Basel, Switzerland

Phone

+41791743909

Nationality

Swiss

Link

www.linkedin.com/in/christoph-schuerch

Languages

German

Native proficiency

English

Professional working
proficiency

French

Advanced proficiency

Catalan

Basic proficiency

IT Skills

Microsoft office
Affinity designer
Adobe Illustrator
GraphPad Prism
FlowJo
ImageJ -Fiji
Javascript
Python
EndNote

Soft Skills

Communication
Teamwork
Problem-Solving
Conflict-handling
Pressure management
Collaboration

Interests

Like to play tennis, football and hiking.
Vice President of 1. FC Rickenbach 2008.
Used to work as junior tennis coach.

Conference & Award List Highlights

- **American Society of Hematology (ASH) conference**, Orlando, USA, 2019: ASH Abstract Achievement Award and Oral Presentation.
- **European Hematology Association conference**, Amsterdam, NL, 2019.
- **Jahrestagung der Deutschen, Österreichischen und Schweizerischen Gesellschaften für Hämatologie und Medizinische Onkologie (DGHO)**, Vienna, AT 2018: Poster Award.
- **Zebrafish Disease Models Conference**, Leiden, NL 2018: Poster Flash Talk, Oral Presentation and Poster Award.

Publications

- **SRP54 mutations induce Congenital Neutropenia via dominant-negative effects on XBP1 splicing.** Christoph Schürch, Thorsten Schaefer, Joëlle Seraina Müller, Pauline Hanns, Marlon Arnone, Alain Dumlin, Jonas Schärer, Irmgard Sinning, Klemens Wild, Julia Skokowa, Karl Welte, Raphael Carapito, Seiamak Bahram, Martina Konantz, Claudia Lengerke; *SRP54 mutations induce Congenital Neutropenia via dominant-negative effects on XBP1 splicing. Blood* 2020; blood.2020008115. doi: <https://doi.org/10.1182/blood.2020008115>
- **Modeling hematopoietic disorders in zebrafish.** Konantz M*, Schürch C*, Hanns P, Müller JS, Sauteur L, Lengerke C. *Dis Model Mech.* 2019 Sep 6;12(9):dmm040360. doi: 10.1242/dmm.040360. PMID: 31519693; PMCID: PMC6765189.
- **Oncogenic Kras^{G12D} causes myeloproliferation via NLRP3 inflammasome activation.** Shaima'a Hamarsheh, Lena Osswald, Benedikt S. Saller, Susanne Unger, Donatella De Feo, Janaki Manoja Vinnakota, Martina Konantz, Franziska M. Uhl, Heiko Becker, Michael Lübbert, Khalid Shoumariyeh, Christoph Schürch, Geoffroy Andrieux, Nils Venhoff, Annette Schmitt-Graeff, Sandra Duquesne, Dietmar Pfeifer, Matthew A. Cooper, Claudia Lengerke, Melanie Boerries, Justus Duyster, Charlotte M. Niemeyer, Miriam Erlacher, Bruce R. Blazar, Burkard Becher, Olaf Groß, Tilman Brummer & Robert Zeiser. *Nat Commun* 11, 1659 (2020). <https://doi.org/10.1038/s41467-020-15497-1>
- **Targeting Chronic NFAT Activation with Calcineurin Inhibitors in Diffuse Large B-Cell Lymphoma.** Philip Bucher, Tabea Erdmann, Paula Grondona, Wendan Xu, Anja Schmitt, Christoph Schürch, Myroslav Zapukhlyak, Caroline Schönfeld, Edgar Serfling, Daniela Kramer, Michael Grau, Pavel Klener, Claudia Lengerke, Klaus Schulze-Osthoff, Georg Lenz, Stephan Hailfinger; *Blood* 2020; 135 (2): 121–132. doi: <https://doi.org/10.1182/blood.2019001866>
- **Regulation of glioma cell invasion by 3q26 gene products PIK3CA, SOX2 and OPA1.** Schaefer, T., Ramadoss, A., Leu, S., Tintignac, L., Tostado, C., Bink, A., Schürch, C., Müller, J., Schärer, J., Moffa, G., Demougin, P., Moes, S., Stippich, C., Falbo, S., Neddersen, H., Bucher, H., Frank, S., Jenö, P., Lengerke, C., Ritz, M.-F., Mariani, L. and Boulay, J.-L. (2019). *Brain Pathol*, 29: 336-350. <https://doi.org/10.1111/bpa.12670>

References

Prof. Dr. med. Claudia Lengerke, Medical director of Internal Medicine II and Principal Investigator, Universitätsklinikum Tübingen (Germany)
Email: Claudia.Lengerke@med.uni-tuebingen.de

Dr. Martina Konantz, Post-doctoral fellow of the Stem Cells and Hematopoiesis research group, University Hospital Basel (Switzerland)
Email: martina.konantz@unibas.ch, +41 61 328 55 87